Nouveaux dérivés d'antibiotique pour l'éradication de bactéries tolérantes et résistantes aux antibiotiques

Melina Cyrenne

THÈSE DE DOCTORAT

NNT : 2022UPASL049

Novel Antibiotic Derivatives for Killing Multidrug Tolerant and Resistant Bacteria

Nouveaux dérivés d'antibiotiques pour l'éradication de bactéries tolérantes et résistantes aux antibiotiques

Thèse de doctorat de l'université Paris-Saclay

École doctorale n°577 : structure et dynamique des systèmes vivants (SDSV)
Spécialité de doctorat : Sciences de la vie et de la santé
Graduate School : Life Sciences and Health. Référent : Faculté des sciences d'Orsay

Thèse préparée dans l'unité de recherche **LBPA (Université Paris-Saclay, ENS Paris-Saclay, CNRS)** sous la direction de **Dominique FOURMY**, directeur de recherche

Thèse soutenue à Paris-Saclay, le 31 août 2022, par

Melina CYRENNE

Composition du Jury

Jean-Luc PERNODET Professeur, CNRS, Université de Paris-Saclay	Président
Sabine SZUNERITS Professeure, Université de Lille	Rapporteur & Examinatrice
Sandra DA RE Chargée de recherche, HDR, Université de Limoges	Rapporteur & Examinatrice
Fany REFFUVEILLE Maître de conférences, Université de Reims Champagne-Ardenne	Examinatrice
Christophe BELOIN Professeur associé, Institut Pasteur	Examinateur
Dominique FOURMY Directeur de recherche, CNRS, Université Paris-Saclay	Directeur de thèse

université PARIS-SACLAY

ÉCOLE DOCTORALE
Structure et dynamique des systèmes vivants (SDSV)

Titre : Nouveaux dérivés d'antibiotiques pour l'éradication de bactéries tolérantes et résistantes aux antibiotiques

Mots clés : photocatalyseurs, thérapie photodynamique, aminoglycoside, bactéries persistantes, résistance aux antibiotiques

Résumé : L'augmentation de la résistance aux antibiotiques chez les bactéries est une menace à la médecine moderne. Un rapport publié le 26 janvier 2022 fait la mention de 670 000 infections causées par des bactéries résistantes aux antibiotiques dans l'Union Européenne. De ce chiffre, environ 33 000 patients sont décédés. Dans cette optique, la communauté scientifique recherche des alternatives de traitements pour les infections microbiennes. L'une de ces stratégies prometteuses est l'utilisation de la thérapie photodynamique antibactérienne (aPDT) ou de l'inactivation photodynamique (aPDI). Cependant, la technique présente certaines limites. Par exemple, la plus forte tolérance des bactéries Gram-négatives à l'aPDT seule et le manque de connaissances entourant l'application de l'aPDT aux cellules persistantes, soient des sous-populations bactériennes hautement tolérantes aux antibiotiques. Grâce à l'utilisation d'aminoglycosides liés à des photocatalyseurs, nous avons réussi à démontrer un effet bactéricide important contre des bactéries Gram-positives et Gram-négatives, des espèces bactériennes multirésistantes, des biofilms et des cellules persistantes. Les composés ont un effet synergique contre des espèces nosocomiales telles que *P. aeruginosa* et *S. aureus* lorsqu'on compare à l'utilisation des aminoglycosides et des photocatalyseurs seuls. L'aPDT a également entraîné l'éradication des cellules persistantes chez *S. aureus* Newman et *S. aureus* USA300, deux bactéries pathogènes de référence. De plus, la faible survie des espèces résistantes aux aminoglycosides démontre que le développement d'une résistance contre les composés créés est peu probable. Leur utilisation pour tuer les bactéries résistantes et tolérantes aux médicaments grâce à l'aPDT est prometteuse dans la lutte contre la résistance aux antibiotiques, en particulier en milieu hospitalier où ils pourraient être appliqués à la stérilisation du matériel et au traitement des infections topiques.

université PARIS-SACLAY

ÉCOLE DOCTORALE
Structure et dynamique des systèmes vivants (SDSV)

Title : Novel antibiotic derivatives for killing multidrug tolerant and resistant bacteria

Keywords : photosensitizers, photodynamic therapy, aminoglycoside, persister cells, antibiotic resistance

Abstract : The rise of antibiotic resistance in bacteria is a threat to modern medicine. A report published on January 26th 2022 declares 670 000 infections caused by antibiotic-resistant bacteria in the European Union. Of this number, approximately 33 000 patients died. With this in mind, the scientific community is looking for alternative treatments for microbial infections. One such promising strategy is the use of antibacterial photodynamic therapy (aPDT) or photodynamic inactivation (aPDI). However, the technique has limitations. For example, the higher tolerance of Gram-negative bacteria to aPDT alone and the lack of knowledge surrounding the application of aPDT to persister cells, a drug-tolerant bacterial subpopulation. Thanks to the use of aminoglycosides linked to photosensitizers, we have succeeded in demonstrating a significant bactericidal effect against Gram-positive and Gram-negative bacteria, multidrug resistant bacterial species, biofilms and persister cells. The compounds have a synergistic effect against nosocomial species such as *P. aeruginosa* and *S. aureus* when compared to the use of aminoglycosides and photosensitizers alone. aPDT also resulted in the eradication of persister cells in *S. aureus* Newman and *S. aureus* USA300, two reference bacterial pathogens. Moreover, the low survival of species resistant to aminoglycosides following aPDT demonstrates that the development of resistance against the compounds created is unlikely. Their use in aPDT to kill drug-resistant and tolerant bacteria is promising, especially in hospital settings where they could be applied to sterilizing equipment and treating topical infections.

SUMMARY

Bacterial resistance to antibiotics is a growing complication that has led to the infection of a little under 700 000 Europeans in 2015. Of this number, about 30 000 died from consequences of these bacterial infections (Cassini *et al*., 2019). Nosocomial bacteria from the ESKAPE group (*Enterococcus faecium, Staphylococcus aureus, Klebsiella pneumoniae, Acinetobacter baumannii, Pseudomonas aeruginosa* and *Enterobacter* sp.) are known for their multidrug resistance and are heavily supervised in the medical field (Laxminarayan et al., 2016; Renwick et al., 2016). However, other issues may be linked to these pathogens, like biofilm production and the presence of a bacterial subpopulation called persister cells. Those persister cells are not genetically different from the rest of the population but their metabolisms are slowed down and they show tolerance to antibiotics. As an example, persister cells could be killed by aminoglycosides once their proton motor force (PMF) was stimulated, suggesting PMF was low to begin with (Allison *et al.*, 2011). Some of these cells, once the antibiotic treatment is ended, may shift to a normal phenotype and regrow a sensitive population. Consequently, persister cells are linked to chronic infections and may simplify adaptive evolutions in the strain and lead to genetic resistance (Cohen et al., 2013). Therefore, it becomes urgent to find ways to counter and eradicate persister cells.

The goal of this project was to combine aminoglycosides with photosensitizers (PSs), molecules which produce reactive oxygen species (ROS) when excited with certain wavelengths. Those ROS, mostly singlet oxygen, are particularly toxic for bacteria. PSs are commonly studied to treat cancerous cells and are becoming popular in the field of microbiology. From what is known, they have not been studied when grafted to an antibiotic, though they are being used after or before an antibiotic treatment (Yin and Hamblin, 2015). Here, the conjugates would be used to kill persister cells as well as biofilms, normal bacterial populations and antibiotic-resistant bacteria.

Aminoglycosides are known for their high penetration capacities, even in biofilms (Lebeaux *et al.*, 2015; Singh *et al.*, 2010; Walters *et al.* 2003). Plus, the Fourmy team has obtained preliminary data suggesting that their neomycin-cyanine 5 (Neo-Cy5) complex did interact and/or accumulate in the periplasm of *Escherichia coli* MG1655 persister cells. The neomycin could therefore be used as a Trojan horse to bring the PS on and/or in bacteria. We also chose to try tobramycin as well. The main target of the singlet oxygen produced by the linked PS is found in bacterial membranes, so the adhesion of our complexes to the bacterial surface could suffice to eradicate bacterial populations in their entirety.

We have chosen two PSs: methylene blue (MB) and chlorin E6 (Ce6). To be further investigated, compounds needed to check three conditions:

1. Singlet oxygen production similar to the PS alone;
2. Increased penetration and/or adhesion to bacterial cells;
3. Significant survival drop when used in antimicrobial photodynamic therapy (aPDT) against selected strains.

The first compound, neomycin linked to MB (Neo-MB), was only used a few times as the singlet oxygen production was too low when compared to MB alone. Neomycin linked to Ce6 (Neo-Ce6) and tobramycin linked to Ce6 (Tobra-Ce6) showed sufficient singlet oxygen production and were used in aPDT.

Neo-Ce6 significantly lowered survival in most of the tested strains, completely eradicating some strains like *A. baummannii* DSM30011. Minimal inhibition concentration (MIC) tests revealed synergy against Gram-positive strains and some Gram-negative strains when compared to neomycin and the Ce6 alone. Fluorescence microscopy showed heightened penetration and/or adhesion to tested cells, further confirming that the link between neomycin and Ce6 has a synergistic effect on both molecules.

Tobra-Ce6 was not as effective as Neo-Ce6 when it came to MICs, only showing additive effect against some strains. However, as Neo-Ce6, it showed great results when used against persister cells from clinically relevant species like *S. aureus* Newman and *S. aureus* USA300.

Biofilms cells proved to be harder to eradicate, even in species where the survival was highly affected in aPDT on planktonic cells. A few factors may be at play in such a discrepancy, such as lack of oxygen in the biofilm and adhesion of our compounds to the surrounding matrix.

To summarize, both Neo-Ce6 and Tobra-Ce6 showed potential against a list of ESKAPE pathogens, some being multidrug resistant (MDR) species, and their persister cells. The use of such compounds also allowed us to study their mechanism of action through fluorescence microscopy and aPDT. After being further studied with other compounds, this method of chemically linking PSs and antibiotics could therefore result in a new antibacterial technique.

Key words: antibacterial photodynamic therapy (aPDT), persister cells, photosensitizers, aminoglycoside, neomycin, tobramycin, biofilm, ESKAPE.

ACKNOWLEDGMENTS

I would like to thank everyone who supported me through this thesis, mainly Mahnaz, Marie, Clara and Romane who were the greatest colleagues and made it easier for me to adjust to this new life. I thank my partner, Mathias, who always understood what I was going through, and our daughter Mira for being such a wonder. I also wish to thank the communication team at the University Paris-Saclay, mainly Gaëlle Degrez who gave me the chance to discover the world of science journalism. Plus, I want to show my appreciation to Sandrine Le Bihan from the doctorate school who helped me navigate the complex French administration more than once.

I also give thanks to Dominique Fourmy and Satoko Yoshizawa who believed in me when I was a stranger living thousands of miles away in Canada. They gave me the opportunity to discover science elsewhere. They always did their best to provide the environment, the equipment and the backing I needed, while trusting me as a human and as a scientist.

TABLE OF CONTENTS

ACRONYMS

Complete word	Acronym
Aminoglycoside	AG
Aminoglycoside-modifying enzyme	AME
Antimicrobial photodynamic therapy	aPDT
Cation-adjusted Mueller-Hinton broth	MHB-CA
Chlorin E6	Ce6
Colony forming unit	CFU
Fractional inhibitory concentration	FIC
Luria-Bertani	LB
Methicillin-resistant *Staphylococcus aureus*	MRSA
Methylene blue	MB
Multidrug resistant	MDR
Optical density	OD
Photodynamic therapy	PDT
Photosensitizer	PS
Proton motive force	PMF
Reactive oxygen species	ROS
Relative fluorescence unit	RFU
Relative light unit	RLU
Toxin/antitoxin	TAT
Tryptic-soy broth	TSB
Wild-type	WT

TABLE LIST

FIGURE LIST

CHAPTER 1

INTRODUCTION

1.1 Photosensitizers and photodynamic therapy

PSs are defined as molecules capable of absorbing light to be activated and induce chemical changes to adjacent molecules (Roelandts, 2002). These chemical changes can be cytotoxic, for instance, when ROS are generated. They're used in some therapies like photochemical therapy and PDT. Photochemical therapy is defined as the use of a PS in combination with UVA light (300 to 400 nm) and is used to treat topical health conditions like psoriasis, eczema, vitiligo and other skin diseases (Ledo and Ledo, 2000). PDT is similar, but the light used is from a wider range of wavelengths and oxygen is needed for the energy transfer (Ledo and Ledo, 2000).

Phototherapy has been around since 1400 AD. Ancient Egyptians would use sunlight and herbs containing a natural PS called psoralen to treat leprosy lesions (Ackroyd *et al.*, 2001). Yet, PDT is only studied since the 90s and has only been approved by the FDA (Food and Drug Administration) in 1990 with the arrival of Photofrin, a porphyrin used in the treatment of some cancer types (Macdonald and Dougherty, 2001).

The ideal characteristics of a good PS are as follows according to Pushpan *et al.*;

a) Available in pure form with a known chemical composition;

b) Easily replicated and synthesizable from accessible precursors;
c) High singlet oxygen quantum yield;
d) Strong absorption in the wavelengths between 680 to 800 nm, with a high extinction coefficient (εmax) (50 000 to 100 000 $M^{-1}cm^{-1}$);
e) Important accumulation in tumorous tissues with a low dark toxicity for both the PS and its metabolites;
f) Stability and solubility in the body's fluids while being easy to administer;
g) Easily excreted from the body after the treatment.

As noted, those characteristics are specific to the use of PSs in the case of cancer treatment and should be slightly modified to cover both topical and deep-tissue infections by bacteria, in addition to the use of PSs to disinfect surfaces and medical instruments. A review by Cieplik in 2018 defines the "perfect" aPDT system as follows:

a) Cationic charge of the PS for optimal binding to the negatively charged cell walls;
b) Low-molecular weight to allow penetration in the biofilm matrix;
c) High singlet oxygen yield;
d) Photostability during irradiation;
e) No toxicity and mutagenicity towards eukaryotic cells and microorganisms when there's no irradiation;
f) An effective concentration range where targeted microorganisms are killed but not eukaryotic cells.

Antibacterial or antimicrobial photodynamic therapy (aPDT) is being investigated since the 1990s. Most studies show promising results with a mean drop of 5 log10 CFUs, which is known as a disinfecting effect (Boyce and Pittet, 2002). However, these studies have mostly been done on planktonic cells which are more convenient to work on. Biofilms are known to be more resistant and to this date, no articles have been published on the use of aPDT against persister cells.

Antibacterial PDT is a favorable alternative to some antibiotherapies. What gives rise to drug resistance within bacterial communities is the nature of antibiotics. Their target is specific,

in a key-lock manner, while the oxidative damage of aPDT is unselective. This randomness makes the development of genetic resistance against aPDT unlikely (Wainwright *et al.,* 2017).

1.1.1 Photodynamic therapy

PDT requires the use of a PS, light capable of activating the said PS and the presence of oxygen. The exposition to a certain wavelength triggers the PS, exciting it from a normal state (S_0) to the first level of excitation (S_1). In order to reach a longer excitation period, the PS must be stable enough to undergo an intersystem conversion, leading to a triplet state (T_1). Two types of reactions may then occur.

In the type I reaction, an electron is transferred between adjacent PS molecules which results in the production of a radical ion. This radical ion may then interact with oxygen ($^3O_2$) to produce ROS like superoxide anion ($O_2^{-\bullet}$), hydrogen peroxide (H_2O_2) and the radical hydroxyl (OH•) (Zimcik and Miletin, 2008). In the type II reaction shown in Figure 1, the energy from type 1 is directly transferred to the $^3O_2$ molecule, transforming it in singlet oxygen ($^1O_2$) (Zimcik and Miletin, 2008). Although the two types of reactions occur simultaneously, type II is dominant when the reacting species have a triplet state multiplicity (Macdonald et Dougherty, 2001).

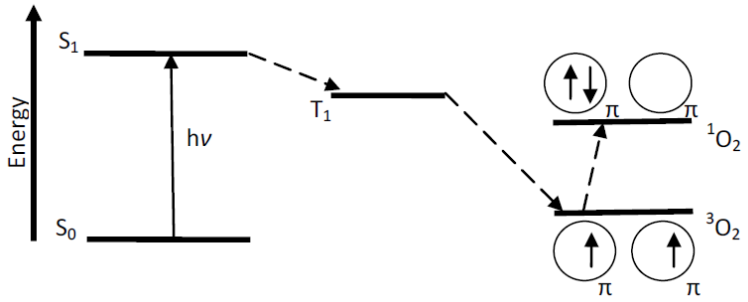

Figure 1: Modified Jablonski's diagram showing the type II reaction (figure from Ormond and Freeman, 2013).

As for the activation of the PS, three main light sources have been described in the field of aPDT literature: lasers, light-emitting diodes (LEDs) and gas-discharge lamps (Nagata et al., 2012; Wilson and Patterson 2008).

1.1.2 Photosensitizers used in medicine

PSs are divided in two classes: first- and second-generation PSs. Photofrin® is a first-generation PS because it is a monomer, dimer and oligomer mixture with a ε_{max} of about 3000 $M^{-1}cm^{-1}$ when excited at 630 nm. This PS is far from satisfying all the characteristics proposed by Pushpan *et al.* (page 19). In addition, Photofrin® is known for its lasting phototoxicity, estimated around 6 to 10 weeks post-treatment (Ormond and Freeman, 2013). However, the excited PS yields a lot of singlet oxygen, so it is still used to treat cancerous cells in many countries (Usuda *et al.*, 2006; Pushpan *et al.*, 2002). Photogem® and Photosan-3®, like

Photofrin®, are other hematoporphyrin-derived PSs and are considered a first-generation PS (Hage *et al.*, 2012).

Second-generation PSs are defined by lower toxicity and absorption in red wavelengths (680-800 nm), characteristics suggested by Pushpan *et al.* (page 15) (Ormond and Freeman, 2013).

1.1.2.1 Tetrapyrrole structures

Many PSs have tetrapyrrole structures, like porphyrins, chlorins, bacteriochlorins and phthalocyanines. Their structures are connected to biological molecules like heme, chlorophyll and bacteriochlorophyll (Battersby, 2000). These PSs are mainly used and researched for treating cancerous cells, and most of them result in type II reactions, with the exception of bacteriochlorins (Fernandez et al., 1997). Their absorption spectra show a few peaks, including one at around 400 nm called the Soret band and Q bands situated at 500 nm and above (Gouterman 1961)

Figure 2 shows how slight variations in their structures affect both tissue penetration and absorption in those PSs.

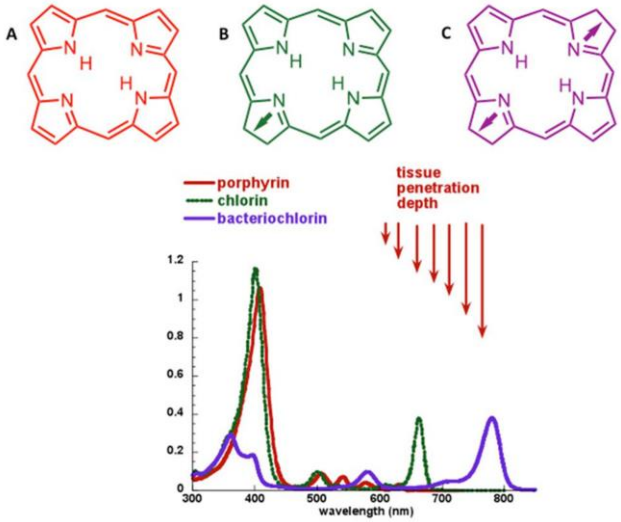

Figure 2: Structure, tissue penetration and absorption in tetrapyrrole structured PSs (Abrahamse and Hamblin, 2016).

Porphyrins are perhaps the most studied PSs due to the use of Photofrin®. Molecules of this class are mostly excited around 400 nm but several peaks are present up to 630 nm (Allison and Sibata, 2010).

Chlorins are also well known and have peaks around 650 to 700 nm. A variety of molecules like Foscan (also known as Temoporfin), Verteporfin and Bremachlorin are used as PSs to treat cancerous cells and macular degeneration (Wagner *et al.*, 2015; Chan *et al.*, 2010). One chlorine does stand out for its promising use in antimicrobial PDT: chlorin E6, which has been chosen as a candidate for this project.

Bacteriochlorins are excited further in the spectrum, around 700 to 800 nm, which makes them useful to treat pigmented tumours like melanomas (Mroz *et al.*, 2010). Known bacteriochlorins, like TOOKAD and its new formula, TOOKAD Soluble, and LUZ11, are presently used in clinical trials to treat prostate cancer, and cancers affecting the head and the neck (Azzouzi *et al.*, 2015; Saavedra *et al.*, 2014).

Phthalocyanines, which are also considered as synthetic dyes, are activated around 670 nm. Most have been tested against cancerous cells, but RLP068 has been tested against bacteria found in foot ulcers in diabetic patients. In addition to effectively lowering the CFU counts in the treated area, only a few side effects were observed (Mannucci *et al.*, 2014). They are however hydrophobic and uncharged, requiring methods of solubilisation to be used in aPDT (Ribeiro et al., 2015).

1.1.2.2 Synthetic dyes

Several synthetic dyes can be PSs, like phenothiazinium salts, rose Bengal, squaraines, BODIPY dyes and transition metal compounds.

Methylene blue (MB) and toluidine blue are two popular phenothiazinium salts, known for their antibacterial proprieties (Tseng *et al.*, 2017; Wainwright and Crossley, 2002). In 2017, toluidine blue was tested against 32 methicillin-resistant *Staphylococcus aureus* (MRSA) strains and was able to significantly reduce CFU when used in PDT. Strains sampled from hospital environments and patients showed higher sensitivity to the dye than community strains. In addition to lowering CFU counts, sub-lethal concentrations of the dye caused a drop in the production of virulence factors, proteases, lipases, hemolysin α and enterotoxins in the tested strains (Tseng *et al.*, 2017). MB is detailed later as it is a dye used in this study (page 25).

Rose Bengal is an interesting PS as the insertion of halogenic atoms in its structure increases its stability and allows for a longer triplet state phase (Fig. 3 a). The PS is studied for applications in tumour treatment and antimicrobial PDT (Panzarini *et al.*, 2014; Costa *et al.*, 2012). The dye has shown an effect against *Candida albicans*, both on planktonic cells and

biofilms (Costa *et al.*, 2012). Rose Bengal was also tested against nosocomial species like *Enterococcus faecalis* and *Fusobacterium nucleatum* (Manoil *et al.*, 2016). Interestingly, the dye is also activated by electromagnetic waves, which could result in other applications (Nakonechny *et al.*, 2019).

Like Rose Bengal, squaraines have improved stability due to the presence of heavy atoms in their structures (Fig. 3 a). This leads to a longer triplet state with increased production of singlet oxygen. These dyes are used in biomedical imagery and in PDT as they have significant photocytotoxicity (Ilina *et al.*, 2019; Ramaiah *et al.*, 2004).

BODIPY (boron-dypyrromethene) dyes, known for their use as fluorophores, also have stable structures like rose Bengal and squaraines (Fig. 3 c). The DIMPy-BODIPY has been tested against strains of bacteria, viruses and some fungi (Carpenter *et al.*, 2015). Molecules from this class also have a high εmax and low toxicity in the absence of light. They also show high accumulation in cells in addition to low photobleaching (Kamkaew *et al.*, 2013). BODIPY dyes require the insertion of halogenic atoms in their structures in order to reach the triplet state (Hinkeldey *et al.*, 2008).

Phenalenones were studied for their high production of singlet oxygen in a variety of solvents (Segado and Reguero, 2011). Due to its potential as a PS for antibacterial PDT, a German team modified a phenalene-1-one molecule in 2-((4-pyridinyl)methyl)-1H-phenalen-1-one chloride (SAPYR) (Fig. 3 d) and tested it against biofilms produced by bacterial species linked to periodontitis like *E. faecalis, Actinomyces naeslundii* and *F. nucleatum*. They showed that SAPYR could weaken biofilms without light and successfully inactivate bacteria in polymicrobial biofilms once it was irradiated (Cieplik *et al.*, 2013).

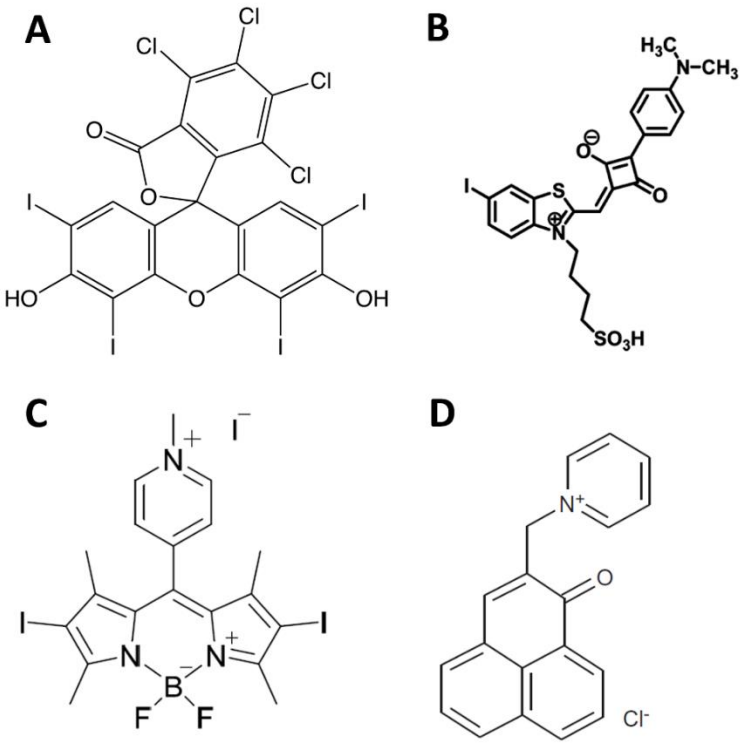

Figure 3: Chemical structure of (A) rose Bengal, (B) an asymmetrical squaraine (Shafeekh *et al.*, 2014), (C) DIMPy-BODIPY (Carpenter *et al.*, 2015) and (D) SAPYR (Cieplik *et al.*, 2013).

Transition metal compounds like ruthenium(II) form a new class of PSs. These metals can reach a triplet state for longer times than other PSs (more than 1 µs) and some metals like gold(III) and platinum(II) are now being tested in PDT (To *et al.*, 2013).

1.1.2.3 Natural compounds

Several molecules from natural origins have photosensitizing potential, like hypericin, riboflavin and curcumin.

Hypericin comes from a flowering plant known as the St. John's wort which has been used as a medicinal plant for around 2 400 years. The molecule, classified as a perylenequinone, absorbs around 590 nm with a ε_{max} around 44 000 $M^{-1}cm^{-1}$ (Ormond and Freeman, 2013). Being hydrophobic, the molecule does need a hydrophilic vehicle to enter the cells. Hypericin's main mechanism is causing stress in the endoplasmic reticulum where it collects. It has been studied in cancerous cells, but does show toxicity in absence of light and accumulation in healthy cells, making hypericin a bad candidate for lack of specificity (Huntosova and Stroffekova, 2016). Its use in antibacterial PDT is recent, but it showed efficacity against planktonic cells and biofilms produced by *Staphylococcus saprophyticus* subsp. *bovis*. CFUs were around 2.6 to 4.1 log lower depending on the hydrophilic vehicle used (Plenagl *et al.*, 2019).

Riboflavin, also known as vitamin B2, has several medical applications. It has been used as an antimicrobial and a natural disinfectant for blood-based products (Ettinger *et al.*, 2012). The molecule's absorption peak is around 360 to 440 nm. A cationic version has been studied as a PS against bacteria and showed promising results against MRSA, enterohemorrhagic *E. coli*, *P. aeruginosa* and *A. baumannii*. In some strains, the CFUs were 6 logs lower after just a few seconds of illumination, while showing no impact on human keratinocytes (Maisch *et al.*, 2014).

Curcumin, the main pigment in curcuma (*Curcuma longa*), is a known anti-inflammatory molecule (Satoskar *et al.*, 1986). Like hypericin, it's a hydrophobic molecule requiring a hydrophilic vehicle to be used as a PS. Trials include using it as a mouthwash in combination with light to lower CFU counts for bacteria linked to periodontitis. At 455 nm for 5 minutes, CFUs in the saliva of tested patients were significantly lower, although they did increase two hours later (Leite *et al.*, 2014).

1.1.3 Photosensitizers used in this project

For this project, we used MB and Ce6 and conjugated them with aminoglycosides. We selected those two PS because past studies showed they had an effect on bacteria when used in aPDT. MB and Ce6 also have a high yield of singlet oxygen.

1.1.3.1 Methylene blue

As described earlier, MB is a phenothiazinium salt and a synthetic dye (Figure 4). The PS absorbs at 666 nm with a ε_{max} around 82 000 $M^{-1}cm^{-1}$ (Ormond and Freeman, 2013). It has mostly been tested against melanomas but trials also include basal cell carcinomas and Kaposi's sarcoma (Chen *et al.*, 2008).

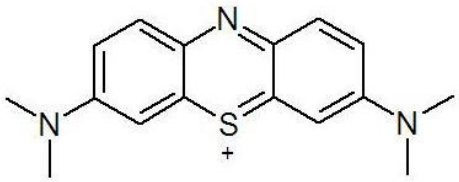

Figure 4: Chemical structure of methylene blue.

MB has also been tested in antibacterial PDT. It's efficient against bacteria causing chronic periodontitis (Balata *et al.*, 2013). The dye was also tested against *E. coli, S. aureus* and *Clostridium perfringens*, three pathogens commonly found in Fournier's gangrene. The team

observed a complete eradication of *S. aureus* and *C. perfringens* with a significant drop in *E. coli*'s CFUs when using 1 mg/L of MB with 5, 10 and 15 minutes of illumination at 660 nm (Pereira *et al.*, 2018). Generally, *E. coli* is less sensitive to treatments with MB, showing the dye acts differently with Gram-positive and Gram-negative bacteria. This is clearly shown in an experiment done with eosin-MB on *S. aureus* and *E. coli*. The aPDT worked on *S. aureus,* but the PS concentration and the illumination time had to be increased for it to have the same effect on *E. coli* (Caires *et al.,* 2017). Conjugating MB with carbon nanotubes increased the efficiency of the PDT against *E. coli* without yielding the same results as when it was tested against *S. aureus* (Parasuraman *et al.*, 2019).

MB is also tested against other microbes in PDT. It reduced *Leishmania major* and *Leishmania braziliensis* promastigotes vitality by 70 % and could be used to treat dermatitis caused by a fungus named *Trichophyton mentagrophytes* (Pinto *et al.*, 2017; López-Chicón *et al.*, 2016). The dye has also been tested to sterilise medical instruments and surfaces. A Brazilian team even filed a patent for a photodynamic inactivation box that they used to disinfect orthodontic equipment. To show their creation worked, they first inoculated the instruments with 3 x 10^8 CFU/mL of *S. aureus, Streptococcus mutans* and *E. coli* and incubated them for 20 minutes in 100 µM MB solution. They then placed the equipment in the box and illuminated it for 20 minutes at 660 nm. They completely eradicated *E. coli* and *S. mutans* while observing a significant drop in the CFU of *S. aureus* (Foggiato *et al.*, 2018).

1.1.3.2 Chlorin E6

Ce6 is a dye with a tetrapyrrole structure (Figure 5). It absorbs around 660 nm with a ε_{max} of 40 000 $M^{-1}cm^{-1}$ (Ormond and Freeman, 2013). Like MB and most of the other PSs, Ce6

was mostly tested on cancer cells. Many derivatives are available to treat tumours, like Laserphyrin in Japan (Usuda *et al.*, 2006) but some derivatives can be used in aPDT, like Photodithazine (Dovigo et al., 2013). Ce6 is an ideal PS for antibacterial PDT. In addition, the dye is biodegradable, easily extracted from spirulina and is selective for bacterial cells and yeast (Maisch *et al.*, 2004).

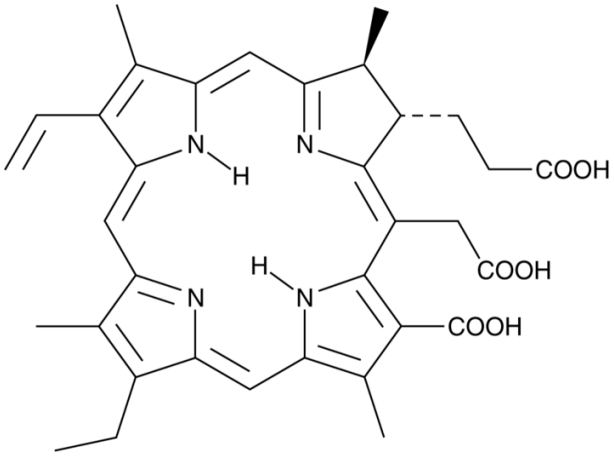

Figure 5: Chemical structure of chlorin E6.

Ce6 has been tested on topical infections and mouth problems. The dye works against polymicrobial biofilms found in severe cases of periodontitis. On oral biofilms harvested from patients, Ce6 killed 90 % of the bacteria when used at a 100 µg/ml concentration with a 5-minute illumination using a combination of infrared A and visible light (Karygianni *et al.*, 2014). Nanocomposite derivatives of Ce6 showed similar effects *in vitro*, reducing CFUs and polysaccharide production in the biofilms of several species: *Porphyromonas gingivalis, Prevotella intermedia, Streptococcus sanguinis* and *F. nucleatum* (Sun *et al.*, 2019; Zhang *et al.*, 2019). In addition to helping against periodontitis, the PS may be useful against acne. When used in PDT, the dye reduced the bacterial load of *Propionibacterium acnes* and reduced inflammation witnessed in acne phases by inhibiting cytokines induced by the bacteria (Wang *et al.*, 2017; Jeon *et al.*, 2015).

The PS was also tested against the multidrug-resistant (MDR) strain *P. aeruginosa* (PA54) in a keratitis model done on mice. Although the team first witnessed a drop in CFU, the bacteria were not all eradicated and the bacterial load increased a few hours after the treatment, suggesting that PDT should be repeated a few times to completely remove *P. aeruginosa* (Wu *et al.*, 2017). Another team tested this keratitis model with 12 MRSA strains. The CFUs were reduced by 5 logs for all strains after a 30-minute incubation with concentrations over 128 µM followed by a 10-minute irradiation at 670 nm (Winkler *et al.*, 2016).

The use of Ce6 combined with nanoparticles is a popular subject. Ce6 combined to silicon nanoparticles showed an inhibiting effect against *S. aureus* and MRSA. This compound also favored healing in a *S. aureus* contaminated wound model in mice (Lin *et al.*, 2019). A team also built a compound with chitosan and magnetic Ce6, demonstrating how it captured and killed MRSA strains in a mice abscess model (Lu *et al.*, 2019).

1.1.4 Effect of singlet oxygen on bacteria

ROS are known for their noxious effect on both bacteria and eukaryotic cells. Many proteins are produced to reduce the impact of ROS, like SodA, SodB, SodC, AhpCF, KatG, and KatE (Zhao and Drlica, 2014). Yet, in bacteria, there are no known enzymes capable of defending the cell against singlet oxygen (Cieplik et al., 2018). Singlet oxygen, when produced, is present for around 10 to 40 nanoseconds and travels about 10 to 50 nanometers inside cells. Damages caused by the ROS are therefore in the area where the PS is excited (Alves et al., 2014; Kuimova *et al.*, 2009; Moan *et al.*, 2007; Dysart et Patterson, 2005). When using a PS capable of producing singlet oxygen, the impact on the bacteria is therefore directly linked to the localization of the PS (Moan *et al.*, 2007; Dysart and Patterson, 2005). Damages depend on

the PS used and the type of bacteria. Plus, as oxygen is required, bacterial density also impacts singlet oxygen production (Maisch *et al.*, 2007).

In 1987, a team created a set-up to investigate the effect of singlet oxygen alone on bacterial cells. To do so, they needed to create space between a fixed PS and the cells (Dahl *et al.*, 1987). Using this model, rose Bengal was tested on *Streptococcus faecium*. Following 7 minutes of exposition, survival was significantly lower in the tested group (Valduga *et al.*, 1993). To have the same results with *E. coli*, the membranes needed to be treated with Tris-EDTA before the experiment, indicating that singlet oxygen has a more potent effect on Gram-positive bacteria. When using a *Salmonella typhimurium* mutant lacking parts of its external membrane, they showed it was more affected by singlet oxygen than the wild-type strain (Dahl *et al.*, 1989). It was suggested that this may be due to the quenching effect of several polysaccharide groups found on Gram-negative bacteria surfaces (Valduga *et al.*, 1993; Foote *et al.*, 1976). Singlet oxygen may also have an effect on the unsaturated lipids and proteins found in the external membrane without impacting the cell survival, as Gram-negative can survive without an external membrane (Dahl *et al.*, 1989; Straight and Spikes, 1985).

As for all molecules, PS accumulation is also different between Gram-positive and Gram-negative bacteria, which affects the impact of the produced singlet oxygen (Malik *et al.*, 1992; Nitzan *et al.*, 1992). Photofrin accumulates easily in *S. aureus* but not in *E. coli* (Maisch *et al.*, 2007). In *E. coli*, porphyrin will only bind the inner membrane if it is exposed (Ehrenberg et al., 1985; Boye and Moan, 1980). This is simply explained by the fact that Gram-negative bacteria, due to the nature of their membranes, have a lower permeability for small lipophilic molecules. It is therefore recommended, as Cieplik has mentioned, to use cationic molecules in aPDT against Gram-negative species (Cieplik et al., 2018). For example, highly cationic molecules, such as water-soluble zinc pyridinium phthalocyanine, led to successful aPDT against *E. coli* and *P. aeruginosa* (Minnock *et al.*, 1996).

The effect of singlet oxygen may also be modified by the presence of carotenoids. *Sarcina lutea*, which can survive ROS production in leukocytes by producing pigments, and *S. aureus* strains capable of producing a carotenoid called staphyloxanthine both showed less

sensitivity to singlet oxygen (Krinsky, 1974). Using a *S. aureus* strain which was mutated in a gene linked to staphyloxanthine, a team showed it was more sensitive to PDT with Ce6 than its wild-type counterpart (Winkler *et al.*, 2016).

Singlet oxygen may also impact other cell functions. In Valduga's study, they showed a 30-40 % drop in the activity of NADH dehydrogenase. The ROS could act on cholesterol molecules and amino acids containing nitrogen and sulfur atoms found in the bacterial membrane, resulting in increased permeability which could in turn affect membrane transport (Hamblin and Hasan, 2004). It also greatly impacts proteins as demonstrated by a study on *Vibrio haemolyticus* and *Vibrio parahaemolyticus*. The team showed all proteins, except those around 38 kDa, were degraded following PDT with curcumin and MB (Deng *et al.*, 2016; Wu *et al.*, 2016).

As for the general impact on the cells, Valduga's team witnessed the formation of mesosomes, linked to increased membrane production in *S. faecium* following exposition to singlet oxygen (Figure 6). They also noted compact packaged nucleic acid. Their theory is that even though singlet oxygen acts directly on the cytoplasmic membrane, the chain of reactions leads to the production of free radicals and peroxide which may penetrate further into the cells to impact nucleic acids and chromatin (Valduga *et al.*, 1993; Vaca *et al.*, 1988). An old study analyzed the effects of singlet oxygen produced by MB on *S. typhimurium* and found base modifications, in guanine residues in particular (Luksiene, 2003; Epe *et al.*, 1989; Friedmann and Brown, 1978). It seems this effect is specific to MB as it has high affinity for DNA (OhUigin *et al.*, 1987). Most conclude that although the main target of singlet oxygen is not DNA, the chain reaction of a PS yielding high amounts of singlet oxygen may lead to damages in nucleic acids (Epe *et al.*, 1989; Dahl *et al.*, 1987). Testing was also done on *Deinococcus radiodurans*, an extremophile species known for surviving high amounts of ionization radiation. The bacteria was shown to be sensitive to aPDT, even with an efficient DNA repair system, meaning damage was done elsewhere within the cell (Nitzan and Ashkenazi, 1999). Though these conclusions do not mean that singlet oxygen cannot affect DNA. Other studies showed singlet oxygen could cause DNA damages in *V. parahaemolyticus, E. coli, P. aeruginosa* and *L. monocytogenes* (Wu

et al., 2016). The effect of singlet oxygen on DNA was also assessed on eukaryotic cells, where the damages were great but temporary: impact on the replication fork, drop in dNTP reserves, ribonucleotide reductase oxidation and inhibition of replication activation (origin firing) (Graindorge *et al.*, 2015).

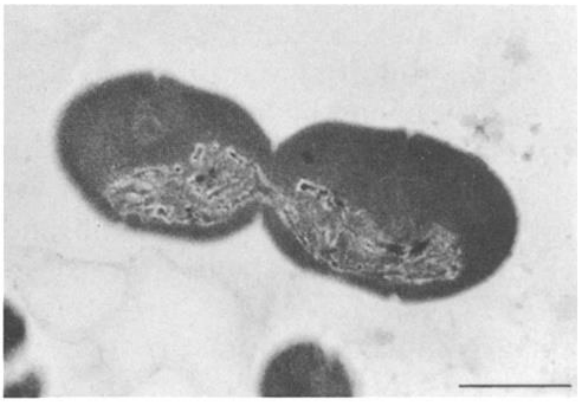

Figure 6: *S. faecium* following exposition to singlet oxygen for 7 minutes. White spots are nucleic acid bundles.

As it has been shown several times, Gram-negative are less sensitive to PDT than Gram-positive bacteria. To overcome this problem, scientists suggest combining antibiotic treatments with PDT, either using the antibiotic before or after PDT. *E. coli* CFUs were lowered for ciprofloxacin and colistin when cells were first treated in PDT with Ce6 (Tichaczek-Goska *et al.*, 2019). Treating *E. coli* and *Salmonella enterica* serovar *Typhimurium* with colistin before a PDT with chlorophyllin allowed for permeabilization of the bacteria and a greater impact of the PS with and without light (Richter *et al.*, 2019). This technique also works on antibiotic-resistant strains. A team took an ampicillin-resistant strain, *P. aeruginosa* PAO1, and pre-treated it with ampicillin. They then incubated the cells in hypericin and illuminated them, successfully reducing the bacterial load by 3.4 logs (Alam *et al.*, 2019).

With the increased interest in aPDT, the scientific community has also created several compounds that are promising in the treatment of Gram-negative infections (Sperandio *et al.*, 2013). Examples include new MB and di methyl MB (Gollmer *et al.*, 2015), zinc phtalocyanine (Minnock *et al.,* 1996) and PSs linked to chitosan (Calixto *et al.*, 2019).

1.2 Bacterial persistence

Persister cells form subpopulations within bacterial communities. These cells are genetically identical to the rest of the community but differ in their metabolism. Due to this slow metabolism, often described as dormancy, persister cells are tolerant to antibiotics. In fact, most of the cells are killed efficiently when treated with an antibiotic, but after a certain time/concentration, a plateau of persister cells is formed. Eradicating the whole population is therefore impossible (Lewis, 2010). If the persister cells resulting in this plateau are collected and treated with another antibiotic, they remain tolerant (Wiuff *et al.*, 2005). Once the stress of the antibiotic is removed, persister cells become active and reform a sensitive community (Figure 7). This phenomenon may be the key to chronic infections. In addition, this tolerance may become genetic resistance (Cohen *et al.*, 2013).

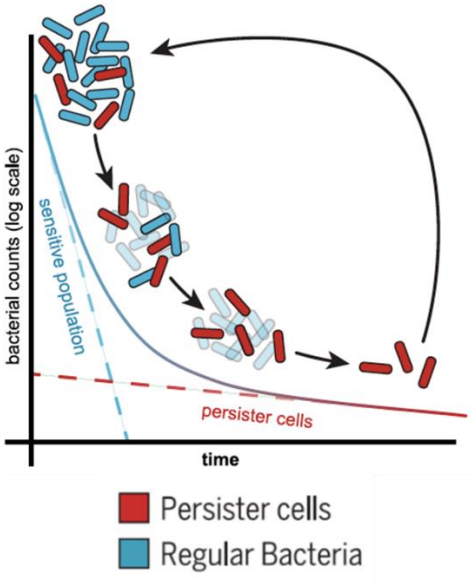

Figure 7: Killing curves of sensitive populations with persister cells (from Harms *et al.*, 2016).

The existence of persister cell populations has first been observed in the 1940s. In 1944, Joseph Bigger noted that one cell in a million survived treatment with penicillin when he treated a staphylococcus community (Bigger, 1944). He called them “persisters”. Two years earlier, a

similar result had been observed with streptococcus (Hobby *et al.*, 1942). However, the matter of persistence has gone largely unnoticed over the years because it is a transient condition touching a small fraction of bacterial populations, while the problem of antibiotic resistance was well defined and recognized as a research priority (Verstraeten *et al.*, 2016). In the 1980s, the study of persistence resurfaced when a team created 3 mutants of *E. coli* producing 10 to 10 000 times more persistent bacteria, thus facilitating the study of these tolerant cells (Moyed and Bertrand, 1983). The mutations affected the hipA locus, linked to a toxin-antitoxin (TAT) system, and would become a central subject in the understanding of persistence.

It is hard to describe exactly what are persister cells and how regular bacteria shift towards persistence. Many believed the bacteria first needed to be in dormancy to acquire this phenotype, but studies showed persistence could occur to bacteria without them having to go through dormancy first (Orman and Brynildsen, 2013). Transcriptomic studies did show that expression in persister cells was different, with lower expression of genes linked to biosynthesis and higher expression of genes linked to stress response and TAT systems (Alkasir *et al.*, 2018; Shah *et al.*, 2006; Keren *et al.*, 2004). This has also been shown with the use of a ribosomal RNA promoter coupled to GFP, demonstrating inferior protein synthesis in persistent bacteria, which could also explain their tolerance to antibiotics targeting these systems (Shah *et al.*, 2006). Several examples of how the SOS response may lead to heightened persister prevalence have been shown in *E. coli*. One of them is TisB, a peptide toxin, which is upregulated when the stress response is strongly induced. This toxin then creates pores in *E. coli*'s outer membrane, which interferes with the PMF and results in a persister state (Dörr et al., 2010).

Several transition pathways are possible. For example, an overproduction of RelE, a mRNA endonuclease part of a chromosomal TAT module, increases the number of persistent cells in *E. coli*. This enzyme inhibits protein synthesis and leads to a state of dormancy, and consequently to a state of tolerance to antibiotics (Keren *et al.*, 2004; Christensen *et al.*, 2001). HipA, part of a TAT module as well, also affects protein synthesis, which increases the fraction of persistent cells (Correia et al., 2006). The inhibition of protein synthesis and the state of dormancy seem to be the first steps in understanding the formation of persistent cells. However,

it is important to note that mutant libraries were created, 3985 mutants of *E. coli* and 5000 of *P. aeruginosa,* and that none of these mutants lacked a complete persister cell subpopulation (De Groote et al., 2009; Hansen et al., 2008). Thus, there is more than one way to reach a persistence status. Nevertheless, several studies showed that the stress response, called the SOS regulatory pathway, is the main candidate for the production of persistent cells since deletions in genes of this system affect the prevalence of persistence (Dörr *et al.*, 2009; Dörr *et al.*, 2010).

In *E. coli*, the formation of persister cells has also been attributed to the OxyR and SoxRS regulons involved in oxidative stress response (Wu *et al.*, 2012). Oxidative stress is, after all, one of several paths towards the activation of an SOS response. Indole, a molecule also induced during oxidative stress, was also linked to persister formation in *E. coli*. Contact with antibiotics and exposure to oxidative stress led to an upregulation of the *tnaA* gene which is responsible for indole synthesis in some cells. This resulted in the transcriptional changes in nearby cells. These changes were linked to the upregulation of efflux pumps and oxidative stress protection mechanisms. Antibiotic tolerance in a larger population then ensued (Lee *et al.*, 2010). Indole has also been said to be a stationary phase "marker", which could also explain why persister prevalence is higher in stationary cultures (Gaimster and Summers, 2015).

Most of the studies concerning persister transition have been done on *E. coli*. Some would even say it is an unknown pathway in Gram-positive bacteria. A team sought to understand the transition mechanism in *S. aureus,* a species known to have a subpopulation called small-colony variants (SCV) that share lots of similarities with persister cells. SCV have an altered electron chain, which results in a slow metabolism and diminished virulence (Proctor *et al.*, 2006). They first studied TAT knock-out strains of *S. aureus*, with no success. They moved on to the stress response which is mostly regulated by CodY in *S. aureus*. Persister levels were unchanged for *codY* and *rsh* mutants (mutant that does not produce an increase in (p)ppGpp) (Conlon *et al.*, 2016). Other studies had demonstrated that *S. aureus* shows tolerance to many antibiotics in the stationary phase, which led them to investigate stationary markers in the bacteria (Shan *et al.*, 2015). Their experiments led to the understanding that some *S. aureus* cells enter early stationary phase throughout exponential phase, increasing in correlation to

bacterial density. It is a heterogenous process rather than a homogenous one. Moreover, they determined these early stationary phase cells were persister cells. Finally, they linked this process to ATP depletion by mimicking a stationary phase ATP level in an exponential phase community using arsenate. This resulted in a 325-fold increase in persister prevalence (Conlon et al., 2016).

Joseph Bigger said that some bacteria "are in the persister phase when inoculated into fresh medium, but the condition is induced in others by their new environment". Later on, Balaban would write about two types of persister cells. Type I persister cells form a non-growing subpopulation (growth rate ≈ 0). These cells are already present in the stationary phase, originating from the exponential phase, and show a negligible conversion rate. If these type I persister cells are inoculated in fresh medium, they demonstrate a long lag time before shifting to a regular phenotype. Type II persister cells tend to form slowly growing communities (growth rate $\neq 0$) and are formed when a culture approaches stationary phase (Balaban *et al.*, 2004; Keren *et al.*, 2004).

1.2.1 Toxin/antitoxin systems and their link with persistence

TAT systems have been an important target in the study of persistence since the discovery of the famous *hip* mutation which resulted in a 10 to 10 000-fold increase in the prevalence of persister cells in *E. coli* (Moyed and Bertrand, 1983). In 2011, 10 TAT systems had been linked to persistence in *E. coli* (Yamaguchi and Inouye, 2011). When bacteria are placed in normal growth conditions, antitoxins inhibit the activities of their counterpart: the toxins. However, in stressful conditions, antitoxins are degraded and the toxins are free to play their part. Toxins then inhibit cellular processes such as DNA replication and protein translation, which results in sudden growth arrest (Hayes et al., 2011). TAT modules have been classified

in 6 groups which essentially differ on the mechanism used by the antitoxin to inhibit the toxin. The antitoxin can either be a non-coding RNA (groups I and III) or a protein with a low molecular weight (groups II, IV, V and VI) (Page and Peti, 2016).

In the study of persistence, TAT systems from the group II seem to be under the spotlight (Page and Peti, 2016; Balaban, 2011; Moyed and Bertrand, 1983). Group II TAT systems are the most studied TAT system and loci from this group have been identified in most bacteria (Pandey and Gerdes, 2005). Antitoxins from these systems are proteins. They generally have two domains; one that binds DNA and the second that binds and prevents the activity of their toxin (Afif *et al*., 2001; Bernard *et al.*, 1993). These antitoxins are sensitive to proteolysis while their toxins are significantly more stable, which simplifies the degradation of antitoxins in stress conditions (Page and Peti, 2016). Toxins from this group inhibit replication (i.e., inhibition of the DNA gyrase) or translation (i.e., cleaving mRNA) (Pedersen *et al.*, 2003; Bernard *et al.*, 1993).

The *hipA* (high persister protein A) gene investigated in *E. coli* is from the type II group and codes for a kinase that inactivates glutamyl-tRNA synthetase. The mutant, called *hipA7* has two mutations, G22S and D291A, and increases persister cell subpopulations due to the destabilization of high-order oligomers formed when HipAB complexes bind the *hipAB* operator (Moyed and Bertrand, 1983). The toxin activity is increased because the HipA active site becomes exposed in the process (Schumacher *et al*., 2015). Another study then revealed that the HipA activity rather leads to the ppGpp-mediated activation of the type II RNase toxins, which then leads to persistence (Germain *et al.*, 2015). This mechanism seems to be generalized to a majority of type II TAT module toxins, especially RNase toxins. They have been shown to be highly upregulated in persister cells when compared to the regular non-persistent population (Shah *et al.*, 2006; Keren *et al.*, 2004).

Although type II TAT systems were widely investigated for their role in persistence, type I systems have also been linked to persistence. A universally conserved GTPase known as Obg induces the transcription of the type I *hokB* toxin which, in turn, promotes persistence

through membrane depolarization (Verstraeten *et al.*, 2015). This GTPase's function also relies on ppGpp to which it binds, creating a common ground between type I and type II TAT-linked persister induction.

Through mathematical modeling, scientists demonstrated how TAT systems, and the balance between toxins and their antitoxins, are directly linked to regular growing populations and their persister subpopulations (Rotem *et al.,* 2010). Briefly, it seems an unbalance in toxins and antitoxins leads to cells entering a persister state, a transition induced by toxins exceeding a set threshold. This could be linked to the apparition of stressful microenvironments within a growing population. A consequence of this stress is a rise in the levels of (p)ppGpp alarmone, which triggers the Lon protease and results in the degradation of the antitoxin (Germain *et al.,* 2015; Maisonneuve and Gerdes, 2014). The toxin, now free to roam the cells, exceeds the said threshold and this allows the bacteria to switch to a persister state.

But, how do persister cells revert back to a normal state? Studies point towards a type II TAT system phenomenon called conditional cooperativity (Garcia-Pino *et al.,* 2010; Overgaard *et al.,* 2008). Type II TAT loci are transcriptionally autoregulated. Like mentioned earlier, the type II antitoxins have two domains: one that binds to DNA and the other that binds their toxins. In a majority of cases, the toxins bind the antitoxins which enhances the first domain's binding to DNA, which in turn further represses transcription of the toxin (Garcia-Pino *et al.,* 2010; Overgaard *et al.,* 2008).

Conditional cooperativity is also linked to the fact that most toxin-binding domains found on antitoxins are intrinsically disordered proteins (IDP) in the absence of said toxin (Schureck *et al.,* 2014; Dienemann *et al.,* 2011). How are conditional cooperativity, the persister state and IDP linked to one another? A few hypotheses exist, the first being that the IDP domain of antitoxins allows for an easier proteolytic degradation (van der Lee *et al.,* 2014). The IDP domain is also crucial in TAT regulation, even more in TAT systems regulated by conditional cooperativity (Garcia-Pino *et al.,* 2010; De Jonge *et al.,* 2009).

Conditional cooperativity was defined by a discovery made in the Doc/Phd TAT system: large quantities of toxins derepressed transcription instead of repressing it (Garcia-Pino *et al.*, 2010; Magnuson and Yarmolinsky, 1998). Afterwards, this switch from repression to derepression was linked to a change in the oligomerization state of the TAT system. This was observed in the CcdB/CcdA system in which the protein A is the antitoxin and protein B inhibits the DNA gyrase. The antitoxin had a maximal DNA binding, therefore an optimal repression, when a ratio of CcdB to CcdA of 1:1 was observed. When the ratio shifted to something higher than 1:1, DNA binding was suppressed, resulting in enhanced transcription rather than inhibition of transcription. This can be easily explained by a clash between toxins that link their antitoxins. This has been illustrated for RelB and Phd (Garcia-Pino *et al.*, 2010; Overgaard *et al.*, 2008). It was then hypothesized that this cycle and the surplus of toxin would lead to augmentation of transcription for both CcdA and CcdB and, ultimately, to a ratio which would allow the cells to exit persister state (Afif et al., 2001).

Conditional cooperativity has been found in other TAT systems, while mostly in the type II TAT group (Page and Peti, 2016). Although the process of transition between persistence and regular state may be linked to other factors, mathematical models support that this phenomenon can create a balance between the two states, regular growth and persistence, within a single culture (Cataudella *et al.*, 2013; Gelens *et al.*, 2013).

1.2.2 Problems linked to persistence

1.2.2.1 Medical complications and clinical significance

In vitro, persister cells can withstand and survive high antibiotic concentrations. In fact, to isolate them, one technique is to treat cells with a concentration at least 10 times the minimal inhibitory concentration (MIC) for more than 5 hours (Michiels and Fauvart, 2016). In the human body however, antibiotics must be used in precise doses to avoid toxicity. The chosen dose may suffice to kill the sensitive population of a bacteria, but persister cells can survive both the antibiotic and, for some, the immune system. These infections can be asymptomatic for a while and undergo reactivation after some time, leading to a relapse. Chronic illnesses caused by asymptomatic persistence have been observed in tuberculosis, syphilis, salmonellosis, and other diseases (Grant and Hung, 2013).

In the case of tuberculosis, the immune system often suffices to contain *Mycobacterium tuberculosis*. In 95 % of patients, macrophages, monocytes and T cells are called to the lungs and create structures called granulomas which encapsulate the live bacteria. However, the immune system cannot completely sterilize the lungs, leading to the creation of a bacterial reservoir. Most individuals infected with *M. tuberculosis* will not relapse, but in 10 % of cases, the infection can switch to an active and symptomatic status years later (Gomez and McKinney, 2004). Another asymptomatic infection linked to persister cells is caused by *Helicobacter pylori*, a Gram-negative bacteria which colonizes the gastric epithelium. It is most known for its role in gastritis and ulcerations in the stomach. Through its evasion of the host's immune system and capacity to enter a persister state, *H. pylori* remains active for decades and can be linked to an increase in the risk of gastric adenocarcinoma and gastric lymphoma (Monack *et al.*, 2004; Nomura *et al.*, 1994; Wotherspoon *et al.*, 1991).

Symptomatic persistent infections are less subtle and are associated with apparent symptoms, either at the time of the infection or occasionally during the infection. One of the most common symptomatic persistent infections is caused by the insertion of external devices

in the host. More than 50 % of these infections are acquired in the hospital because of infected medical devices like contaminated prosthetic joints, prosthetic heart valves and central venous catheters (Bryers, 2008). Another problematic infection caused by a reactivation of persister cells is pneumonia and lung diseases in cystic fibrosis patients. The lung mucus from these patients is thicker than normal due to a mutation in the cystic fibrosis transmembrane regulator (CFTR), which creates an ideal niche for bacteria. Two of those frequent colonizers are *P. aeruginosa* and *S. aureus*, dangerous nosocomial species which are known to switch to a persister state when treated with antibiotics, if they are not already resistant to the drugs used to begin with. *S. aureus* is also known to have a high prevalence of persister cells within its communities and *hip* strains, mutants producing more persister cells, of *P. aeruginosa* are commonly isolated from cystic fibrosis patients (Möker *et al.*, 2010; Mulcahy *et al.*, 2010). Ultimately, because they are so hard to eradicate from cystic fibrosis patients, 80 to 95 % of patients die from respiratory failure due to secondary infections by these pathogens (Lyczak et al., 2002).

Some symptomatic persister diseases are not necessarily linked to changes within the host or due to genetic conditions. Chronic cystitis are common consequences of repeated acute urinary tract infections (UTIs), mostly linked to *E. coli* colonization of the urinary tract through fecal contamination (Hunstad and Justice, 2010). Most women will suffer from at least one UTI in their lifetime and 10 % suffer from it on a yearly basis (Salvatore et al., 2011). Some women do suffer from a chronic form of cystitis. One study showed that 30 % of women experienced at least one relapse within six months of their primary infection (Foxman, 1990). This might be explained by the presence of *hipA7 E. coli* mutants found in chronic UTI, a mutant known to produce a 1000-fold more persister cells than the wild-type strain (Schumacher *et al.*, 2015).

A hypothesis to explain how bacterial cells survive within a host is the presence of protective niches where the immune system is rarer (joints, sinuses, etc.) and even environments created by the immune system itself, like the granulomas in the case of tuberculosis (Grant and Hung, 2013). Although granulomas were first thought to interfere with antibiotic diffusion, it was also demonstrated that antibiotics can reach within the granulomas (Barclay, 1953). In sum,

the argument of protective niches is not sufficient to explain bacterial survival, which leads to the next answer: persister cells.

A team mimicked drug serum concentration by gradually increasing the concentration of kanamycin and ciprofloxacin *in vitro*, which increased 10-fold the prevalence of persister cells in *K. pneumoniae*, in addition to favoring the emergence of resistant genotypes (Ren *et al.*, 2015). Those resistant genotypes could be favored when the antibiotic concentration is sublethal or through repeated oxidative stress (Kohanski *et al.*, 2010). Another team mimicked clinical high-dose extended therapy by treating ESKAPE pathogens with aminoglycosides. They cycled killing and cell regrowth, and although they did not observe the emergence of genotypic resistance, they found a 37- to 213-fold increase in persister prevalence, showing how medical care could, unfortunately, lead to heightened persister formation (Michiels *et al.*, 2016).

In sum, many diseases thought to be caused by drug-resistant bacteria may be linked to persister cells. However, symptomatic and asymptomatic persister infections lead to extended antibiotic therapies, increasing the risk for the emergence of antibiotic-resistant strains (Levin and Rozen, 2006).

1.2.2.2 Studying persistence

As persistence is a transitional phase touching small fractions of a bacterial community, many problems arise when trying to study persister cells. Single-cell study and microscopy become harder when trying to find these cells and even though high persister prevalence mutants exist, like *hip* mutants, they do not mimick the “natural” state of these cells. In addition, persister cells may revert to a regular phenotype which can affect results.

For selecting persister cells, the most common technique is treatment with high doses of antibiotics for long periods of time. Once a plateau is obtained, it is assumed that these surviving cells are in a persistent state. Persister selection has also been done using fluorescent-activated cell sorting (FACS). Based on the observation that persister cells are dormant cells with low levels of protein synthesis and, therefore, low levels of rRNA transcription, a team sorted *E. coli* persister using a *rrnB* promoter linked to a gene encoding an unstable fluorescent protein. They were then able to separate the dimly lighted persister cells from the highly fluorescent regular cells (Shah *et al.,* 2006).

Selection through the use of antibiotics has been combined with transparent microfluidics devices, which allows for microscopic observations. This way, scientists can monitor single cells for extended periods of time while testing growth conditions. By adding antibiotics, they can select for persister cells. The technique has been used several times to study pre-existing persister cell populations, to characterize the dormant state of cells and to assess persister formation through the addition of indole (Vega *et al.,* 2012; Gefen *et al.,* 2008; Balaban *et al.,* 2004). Single-cell studies are useful to understand the transition from regular bacteria to persister cells but limit the number of cells that can be analysed. This is why flow cytometry is often used in parallel. Through the sorting of millions of cells, the kinetics of persister awakening has been studied (Jõers *et al.,* 2010).

1.2.3 Anti-persister strategies

As persister cells are tolerant to antibiotics, and that the repeated use of antibiotics to treat these populations can lead to the emergence of resistant mutants, new strategies must be established. Many studies have found possible alternatives, from fast-freezing cells to metabolite potentiation. Defraine and colleagues mention three main antipersister strategies.

The first is direct eradication of persister cells, the second is sensitization of persister cells to treat them with traditional antibiotics and the last encompasses molecules able to affect persister formation, completely or partially (Defraine *et al.*, 2018).

As antibiotics already exist and are approved to treat certain diseases, the first tactic is to use them in a wiser and different way to treat persister cells (O'Neill, 2018; Coates et al., 2002). In the case of aminoglycosides (AG), studies have found that certain metabolites like glucose, mannitol and alanine, increase the AG uptake and make the antibiotic more potent against tolerant and resistant pathogens (Su *et al.*, 2018; Peng *et al.*, 2015; Allison et al., 2011). These metabolites wake the persister, therefore making them sensitive to the antibiotic, as the effect was specific to AGs and not to antibiotics affecting bacterial division. This phenomenon is linked to the PMF, which seems to be activated by the metabolites and allows the antibiotic to enter the persister cells. By adding CCCP, a PMF inhibitor, to the medium, the killing effect of AGs was lost (Allison *et al.*, 2011). Fumarate was also tested to eradicate *P. aeruginosa* persister cells and successfully increased by up to 6 times the killing effect of tobramycin on a selection of cystic fibrosis isolates (Koeva *et al.*, 2017). Silver-ions are known to affect membrane permeability, which allows for antibiotic penetration in both dormant and regular cell populations (Morones-Ramirez *et al.*, 2013).

Other strategies include stress-inducing tactics like hypoionic shocks or fast-freezing of cells. Treatment with an ion-free solution increased the potency of AGs against stationary-phase *E. coli* persister cells while 10-second freezing in liquid nitrogen pre-treatment increased the effect of AGs against persister cells from diverse species, mostly affecting *E. coli* and *P. aeruginosa* (Zhao *et al.*, 2020; Jiafeng *et al.*, 2015). Anti-persister effect of traditional antibiotics has also been increased by changing the pH, by using membrane-active macromolecules, and other osmotic compounds (Falghoush *et al.*, 2017; Uppu *et al.*, 2017). A team succeeded in killing 99 % of planktonic and biofilm cells with a combination of L-arginine and gentamicin in *S. aureus, E. coli* and *P. aeruginosa*. Using this blend, they demonstrated enduring eradication of *S. aureus* and *E. coli* biofilms in a catheter infection model in rats (Lebeaux *et al.*, 2014).

Sensitization is not the only way to kill persister cells, direct killing is another option. Persister cells can be killed directly, but this requires molecules that target alternative processes like depolarization or destruction of the membrane, generation of ROS, DNA cross-linking, activation/inhibition of some enzymes, etc. Defraine listed over 50 molecules and techniques in her 2018 review. Here are a few.

Amphiphilic macromolecules (Qn-prAP and QCybuAP) killed *E. coli* persister cells through non-specific targeting of bacterial membranes (Upu *et al.,* 2017). Other compounds target the membrane, like the fluoroquinolone-derived HT61 which kills both persister and regular populations in *S. aureus* and SPI009 which kills persister cells in Gram-positive and Gram-negative bacteria by causing widespread membrane damage (Liebens *et al.,* 2017; Hu *et al.,* 2010). In *P. aeruginosa*, an intracellular peak in ROS caused by an electrochemical treatment led to persister eradication and heightened synergy with tobramycin (Sultana *et al.,* 2016). Low levels of electrical currents resulted in the loss of membrane integrity and a drop in persister cell populations in the same organism. This technique also showed synergy with tobramycin (Niepa *et al.,* 2012). Enzyme interference is another tactic to eradicate persister subpopulations. In *S. aureus*, the acyldepsipeptide antibiotic ADEP4 activates the ClpP protease which leads to the death of growing cells but also to the eradication of persister cells. In addition to those interesting results, by combining ADEP4 with rifampicin, the team was able to kill persisters, stationnary and biofilm populations *in vitro* and in a deep-tissue murine infection model (Conlon *et al.,* 2013). Lassomycin, which also activates the ClpP protease has been successfully used against *M. tuberculosis* persister cells (Gavrish *et al.,* 2014).

Anticancer drugs are also promising in the persister fight. Mitomycin C, a DNA cross-linking compound, killed persister cell subpopulations in clinically relevant pathogens like *E. coli, P. aeruginosa, S. aureus* and *A. baumannii* (Cruz-Muñiz *et al.,* 2016; Kwan *et al.,* 2015). Cisplatin, which is also a DNA cross-linking agent used in cancer therapy, was also capable of killing *E. coli, P. aeruginosa* and *S. aureus* persister cells (Chowdhury *et al.,* 2016).

Finally, it is also possible to interfere with or inhibit persister formation. As knowledge about persister formation continues expanding, so are the ways to play with these pathways. In *P. aeruginosa*, inhibition of the pro-persistence QS molecule MfvR led to a drop in persister prevalence (Starkey *et al.*, 2014). Some other molecules interfere with (p)ppGpp alarmone accumulation in Gram-positive species, which in turn interferes with the phenotypical switch to the persister state (Wexselblatt *et al.*, 2012). Nitric oxide has also been shown to reduce the formation of *E. coli* persister in the stationary phase (Orman and Brynildsen, 2016).

1.3 Biofilms

Biofilms are characterized by two main components: an extracellular matrice and the bacteria that produced it. Microorganisms can form polymicrobial biofilms that are extremely dangerous for human health, like *S. aureus* and *Candida albicans* biofilms for instance (Harriott and Noverr, 2009). In addition, because biofilms can form on exposed or mucosal host tissues, they are often composed of bacteria from the host microbiota and nocosomial pathogens (Harriott and Noverr, 2011). However, even biofilms produced by one strain, although rare, can pose a threat as they are known to be resistant to both antibiotics and the host's immune system (Stewart and Costerton, 2001). In addition to this natural resistance, close bacterial communities within those structures facilitate possible horizontal gene transfer, and therefore, potential drug resistance (Madsen et al., 2012; Burmølle et al., 2006). Biofilms are medically relevant as they are linked to many diseases like burn infections and can contaminate medical equipment such as catheters and prosthetics (Azevedo *et al.,* 2020; Donlan, 2001). Planktonic cells that settle to form biofilms change their metabolisms. This has led to the observation that persister cells are found at the core of biofilms, adding yet another challenge to biofilm eradication (Waters *et al.,* 2016).

1.3.1 Description and composition of biofilms

Biofilm production is an ability available to all known bacteria. The mechanisms may differ from one species to another and change according to environmental conditions, but the concept remains the same. Biofilms are bacterial constructs composed of an extracellular matrice and the microorganisms that produce it. This matrice is made of extracellular polymeric

substances (EPS), composed of cell debris like polysaccharides, proteins, lipids and eDNA (external DNA) which are secreted by the bacteria (López *et al.*, 2010).

Biofilm production is cyclical and begins with the adherence of bacteria to a surface (Figure 8). This initial contact with a surface is usually reversible. It is a weak link through van der Waals forces or hydrophobic effects (Briandet *et al.,* 2001). The bacteria can then attach using cell adhesion structures and must produce a monolayer of extracellular matrix for the attachment to become irreversible (O'Toole *et al.,* 2000). This layer protects the bacteria while they divide and grow the biofilm. During the first steps of biofilm production, the dominating EPS is eDNA. This eDNA has later been found to initiate a metabolism change in planktonic cells, promoting biofilm formation in many bacterial species following a subletal antibiotic treatment. Antibiotics causing cell lysis promoted this phenomenon more than other antibiotics (Ranieri *et al.,* 2018). It is believed to provide structural integrity as the addition of DNase prevents biofilm formation and disrupts mature biofilms (Whitchurch *et al.*, 2002).

As the biofilm matures, polysaccharides and proteins become more abundant. Quorum sensing is crucial to building this three-dimensional structure and as the structure evolves, so do the bacteria (Camilli and Bassler, 2006). In the later stages of biofilm construction, some cells detach and switch to a planktonic state. These cells can potentially start a new biofilm colony elsewhere (O'Toole *et al.,* 2000).

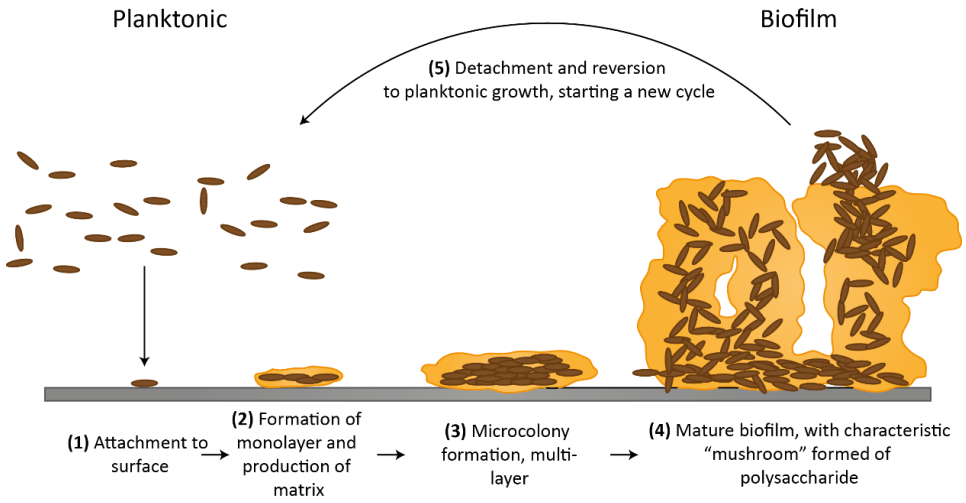

Figure 8: Biofilm cycle. Figure by Hollmann *et al.*.

Many factors can lead to cells forming biofilms: recognition of specific or non-specific attachment sites on organic or inorganic surfaces, nutritional stress, exposure to antibiotics, and others (Ranieri *et al.*, 2018; Karatan and Watnick, 2009). As mentioned earlier, those cues initiate a phenotypic switch within the cell's behavior, leading to biofilm formation.

The composition of the matrix also varies between organisms, environment, and other factors. As an example, *P. aeruginosa* biofilms are constructed with three distinct polysaccharides: alginate, PEL and PSL. In addition, the specific combination of polysaccharides differs from one strain to another. Alginate is dominant in mucoid strains found in cystic fibrosis, while non-mucoid strains rely on PEL and PSL (Colvin *et al.*, 2012; Wozniack *et al.*, 2003). *B. subtilis* produces TasA, the only major protein found in the matrix of its biofilm. Mutants of *tasA* cannot construct a biofilm even though they keep the capacity to produce exopolysaccharides (Branda *et al.*, 2006). That is because TasA seems to be crucial to the architecture of *B. subtilis* biofilms. The proteins form extracellular filaments with properties similar to amyloid (Romero *et al.*, 2010). This amyloid-like structure is also constructed by *E. coli* with the curli proteins, proteins that are crucial to the biofilm integrity (Chapman *et al.*, 2002). *S. aureus* strains use a polymer of N-acetyl glucosamine (PNAG) also called polysaccharide intercellular adhesin (PIA). Although the *ica* operon is crucial in the production of this polymer, not all strains carry it. *S. aureus* relies on many alternate mechanisms to produce

biofilms, like adhesin proteins that allow the pathogen to adhere to many surfaces (O'Gara, 2007). A reknowned example is biofilm-associated proteins (Bap). They are present in the cell-wall of *S. aureus* and hold cells together within the biofilm (Latasa *et al.,* 2006).

Cell-cell attachment and adherence to a designated surface is critical in biofilm formation. That is why many mechanisms have been found in other species. Pili, fimbriae and other cell appendages have been found to be expressed by cells in biofilm. *E. coli* must produce a Type I fimbriae in order to adhere to plastic surfaces and host cells found in the urinary tract (Wright *et al.,* 2007). *P. aeruginosa* mutants that lack type IV pili or the CupA fimbriae genes were unable to form adequate surface-adhered biofilms (Vallet et al., 2001; O'Toole and Kolter, 1998). Other proteins, like lectin-binding proteins, facilitate cell-matrix and cell-cell binding. *P. aeruginosa* has two lectin-binding proteins important for biofilm construction, LecA and LecB (Diggle *et al.,* 2006; Tielker *et al.,* 2005).

In summary, although the basic mechanisms of biofilm formation are the same in all species, the cellular cues and matrix differ greatly. Therefore, it is hard to pinpoint one anti-biofilm strategy focusing on those aspects as each species would require its own technique.

1.3.2 Persister cell contribution to biofilm

Due to all the extracellular components that are found in biofilms, it was believed that cells encapsulated within this matrix were protected from antibiotics. This belief was promoted by the heightened resistance of biofilms to antibiotics and to the immune system when compared to their planktonic counterpart. However, many studies showed that antibiotics do reach the cells within biofilms, but do not kill them all the time (Stewart *et al.,* 2009). Additionally, cells that are released from the biofilm are more tolerant than the planktonic cells that originated the

biofilm. A study done has also shown evidence of "bacterial memory" in persister cells taken from colony-biofilm cultures (formed at an air-solide interface) that remained alive for up to 4 weeks in nutrient-rich antibiotic-containing media. This memory was observed in *E. coli, S. aureus, Acinetobacter radioresistens, S. typhimurium* and *S. epidermidis* (Miyaue *et al.*, 2018). This led many researchers to believe that bacteria found within the biofilm are probably in a persister state (Lewis, 2001). This theory is furthered by the fact that bacteria, like *S. aureus,* are often slow or even non-growing when in a biofilm, a phenotype observed in the stationary phase, which is known for having a higher prevalence of persister cells (Waters *et al.,* 2016; Boles and Horswill, 2008). It was also shown that *E. coli* produces significantly more persister cells in colony-biofilm cultures than in usual liquid cultures, adding to this theory (Miyaue *et al.,* 2018).

The matrix, even though is does not seem to interact with antibiotics, does have an effect on cell metabolism. Oxygen is scarcer in the core of biofilms and so are nutrients. These conditions are similar to stationary phase conditions, perhaps affecting cells in the same way. Due to high cell density, quorum sensing and/or stress induced by lack of nutrients and low oxygen, it has been observed that *S. aureus* has a slowed metabolism (Conlon *et al.,* 2015). This leads to a drop in ATP, which has been known to lead to persister state for *S. aureus* (Conlon *et al.,* 2016). Although biofilm cells and persister cells show similarities, it does not mean they are physiologically identical, but the mechanisms behind their presence are similar and that these issues should be taken in account when treating biofilms (Waters *et al.,* 2016).

Another mechanism that could be linked to antibiotic-tolerance of cells within biofilms is similar to the problem of drug diffusion in patients which may increase *K. pneumoniae* persistence (section 1.2.2.1). Although a said concentration might eradicate the majority of cells in a biofilm, the slow diffusion of the antibiotic through the matrix and cells coming in contact with sub-lethal concentrations of the drug may cause a phenotypic switch towards persistence (Stewart *et al.,* 2009; Zheng and Stewart, 2002). Studies have found that some matrix characteristics in *S. aureus*, like age, cell density and growth condition, influence the way antibiotics like rifampicin, daptomycin, vancomycin, gentamicin and fosfomycin kill biofilm

cells (Hogan *et al.*, 2016; Zapotoczna *et al.*, 2015). The penetration dynamic of the antibiotics used is therefore important in understanding how cells within a biofilm react to a treatment.

Due to their diverse matrix and heterogeneous cell populations, anti-biofilm strategies may have fluctuating outcomes. On the other hand, anti-persister strategies have shown interesting results when used on biofilm. The acyldepsipeptide antibiotic ADEP4 is active against *S. aureus* persisters and also shows an effect against stationary phase and biofilm cells (Conlon *et al.*, 2013). NH125, a histidine kinase inhibitor, has antipersister activity in *S. aureus* and higher concentrations of the molecule have a disruptive effect on biofilms (Kim *et al.*, 2015). In *P. aeruginosa*, the addition of mannitol to a tobramycin treatment increases the killing of persister and biofilm cells (Mlynek *et al.*, 2016). These examples demonstrate how the integrity of a biofilm relies greatly on cells exhibiting persister-like metabolisms.

1.4 Aminoglycosides

AG antibiotics have been used in medicine for almost 80 years. The first AG was discovered in 1944 by Selman Waksman who would win a Nobel prize in 1952 for this breakthrough. Isolated from *Streptomyces griseus*, the molecule was named streptomycin and introduced as a treatment for tuberculosis (Woodruff, 2014; Kresge *et al.*, 2004). Since then, other AGs have been discovered and divided into three groups: the "mycins" like streptomycin, neomycin, kanamycin and others that come from the *Streptomyces* group, the "micins" like gentamicin, sisomicin and others that come from the *Micromonospora* group and finally, the modifications of existing AG like amikacin and plazomicin (Serio *et al.*, 2018).

Although this class holds approximately 15 approved members, the interest in AGs has declined due to the discovery of other antibiotics and the obscurities surrounding its bactericidal mechanism of action. However, with the rise of drug-resistance in bacteria, there is a regain of interest around AGs. In fact, plazomicin, a new AG, was approved by the FDA (Food and Drug Administration) in 2018, which makes it the first new AG in almost 40 years (Serio *et al.*, 2018).

AGs are bactericidal antibiotics with a broad spectrum, affecting both Gram-positive and Gram-negative bacteria and even some multidrug resistant strains. Although they are less potent against *P. aeruginosa* and *Acinetobacter* spp., they are effective against members of the *Enterobacteriaceae* family, like *E. coli, K. pneumoniae, Enterobacter cloacae, Proteus* spp., *Serratia* spp. and others (Krause *et al.*, 2016; Sader *et al.*, 2015; Sorlozano *et al.*, 2014; Landman *et al.*, 2011). As for Gram-positive species, AGs have been used effectively against *S. aureus* and MRSA strains (Aggen *et al.*, 2010). As active electron transport and PMF is required for AG uptake, anaerobic bacteria are intrinsically resistant to the antibiotic (Martin *et al.*, 1972). Species like *Burkholderia, Stenotrophomonas, Streptococcus* and *Enterococcus* are not affected by AG therapy as well (Krause *et al.*, 2016).

Amikacin, gentamicin and tobramycin are the AGs that are the most current today (Serio *et al.*, 2018). They are mostly used to treat urinary tract infections, sepsis, neonatal sepsis and pneumonia (Avent *et al.*, 2011; Xie *et al.*, 2011). Tobramycin is frequently used in the treatment of pneumonia and chronic *P. aeruginosa* infection in cystic fibrosis patients, where it is administered through inhalation (Shteinberg and Elborn, 2015). Other commonly used AGs are neomycin, which is used topically in skin infections and intramuscularly administered spectinomycin to treat gonorrhea. Kanamycin and amikacin can also be used to treat tuberculosis, though kanamycin is less popular due to clinical resistance (Serio *et al.*, 2018; Avent *et al.*, 2011; Xie *et al.*, 2011).

1.4.1 Mechanism and penetration

AGs are polycationic and hydrophobic, weighing generally between 450 to 600 g/mol. Their primary mechanism of action is the inhibition of crucial steps in bacterial protein synthesis (Davis, 1987; Taber *et al.*, 1987). While molecules that inhibit protein synthesis are generally bacteriostatic, like tetracyclines, macrolides and others, AGs are bactericidal. This bactericidal effect is linked to the uptake of the molecules in the cell, as discussed ahead, and an extended postantibiotic effect (Stratton, 2005; Salauze and Davies, 1990; Taber *et al.*, 1987; Bryan and Van den Elzen, 1976).

The AG uptake is a complex process with some gray zones (Figure 9). It is a three-step process beginning with the entry of the antibiotic through electrostatic binding to the bacterial membrane. This step does not require energy as the molecule is polycationic and the membrane is negatively charged. This process is fast, but non-specific and reversible. In Gram-negative

bacteria, this means binding the lipopolysaccharides of the outer membrane while the AGs interacts with the phospholipids and teichoic acid in Gram-positive bacteria. This binding leads to an increase in membrane permeability and the molecules reach the perisplasmic space (Salauze and Davies, 1990; Davis, 1987; Taber *et al.*, 1987).

The two following steps require energy, and are thus called energy-dependent phase I (EDPI) and energy-dependent phase II (EDPII). EDPI is linked to the PMF and leads to a minimal cytoplasmic uptake. It is a slow step that depends on the external antibiotic concentration (Salauze and Davies, 1990; Davis, 1987; Taber *et al.*, 1987). Once inside, the molecules target their site of action, inducing errors in the protein synthesis process which results in misfolded proteins. The hypothesis is that those misshapen proteins cause damage to the cytoplasmic membrane, displacing molecules and forming nonspecific channels that promote the entry of more AG molecules, accelerating this cycle of incorrect protein synthesis and membrane damage (Figure 9c) (Serio *et al.*, 2018). This massive AG entry is labeled as EDPII and results in a rapid bacterial killing (Davis *et al.*, 1986).

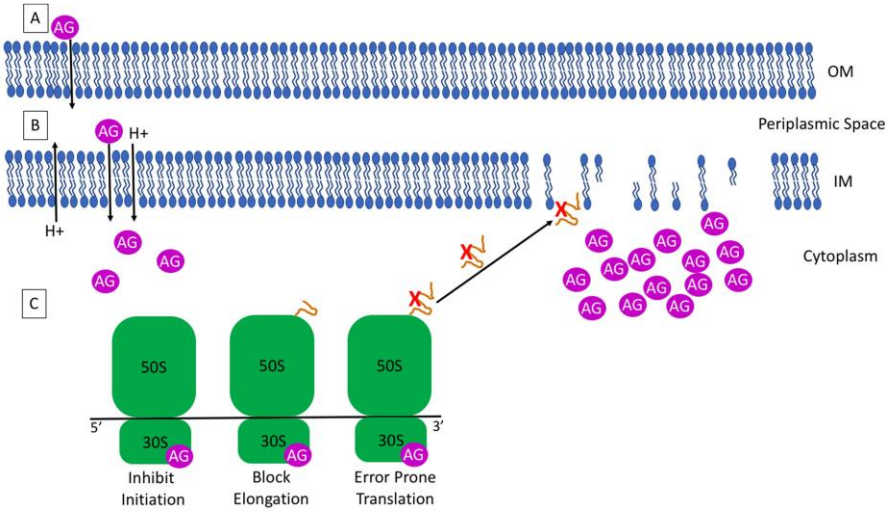

Figure 9: Steps of aminoglycoside uptake in bacterial cells (figure from Serio *et al.*, 2018) (A) The first step of AG uptake is reversible electrostatic binding to the anionic membrane components, which leads to infiltration in the periplasmic space. (B) EDPI begins with AGs

crossing the bacterial membrane with the PMF. (C) The AGs bind the ribosome, resulting in mistranslated proteins which affect the membrane, allowing more molecules to enter the cell.

It seems the uptake isn't only linked to the PMF as some porins and mechanosensitive channels may be involved, but data is limited. Some knock-out *E. coli* mutants lacking the expression of OmpF, a porin, have been shown to be resistant to gentamicin and kanamycin, suggesting a role for this porin as well as OmpC in AG uptake (Bafna *et al.,* 2020; Foulds et Chai, 1978). The mechanosensitive channel MscL has a suspected role in uptake of dihydrostreptomycin across de cytoplasmic membrane of *E. coli* (Wray *et al.,* 2016; Iscla *et al.,* 2014). MscL could also be responsible of potentiation of AG uptake by a freezing-induced mechanism or hypoionic shock (Lv *et al.,* 2022; Zhao *et al.,* 2020).

To inhibit protein synthesis, AGs disturb the translation process in the ribosomes. In bacteria, the ribosome is composed of a 30S and a 50S subunit which are made of rRNA: the 30S contains the 16S rRNA and the 50S contains the 23S and 5S rRNAs. These subunits form the 70S ribosome which binds the mRNA, tRNAs and elongation factors. Protein synthesis, although it requires many components, is divided in four steps: initiation, elongation, termination and ribosome recycling (Laursen *et al.,* 2005). The initiation is helped by the rRNA which acts as a scaffold. For example, the 3' end of 16S rRNA has a sequence which matches the Shine-Dalgarno sequence upstream from the start codon, consequently helping to bind the mRNA to the ribosome (Serio *et al.,* 2018).

The ribosome holds specific tRNA sites that are required for the process. The aminoacyl-tRNA site (site A) accepts the new tRNAs carrying the complementary amino acid, while the peptidyl-tRNA site (site P) houses the growing polypeptide chain and finally, the E-site is where the empty tRNA departs from the ribosome (Figure 10) (Laursen *et al.,* 2005; Green and Noller, 1997).

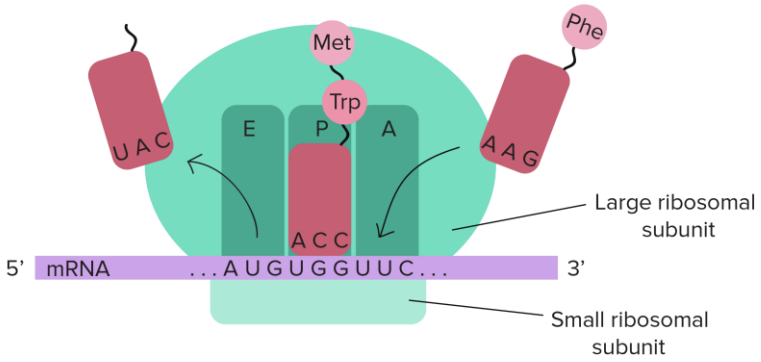

Figure 10: tRNA sites within the ribosome to illustrate the protein synthesis process (figure by Khan University).

Many studies have demonstrated that AGs have a high affinity to the site A on the 16S rRNA, which interferes with the translation process (Fourmy *et al.*, 1998; Fourmy *et al.*, 1996). The affected region differs from one AG to another, but globally, the antibiotic leads to conformation changes in this crucial region. These deviations result in inhibition of initiation, obstruction of the elongation process and misreading which produces misfolded proteins. In turn, those deformed proteins lead to loss of membrane conformity and cell death (Wilson, 2014; Ramirez *et al.*, 2010; Davis, 1987).

1.4.2 Description of neomycin

AGs are classified in four different core structural groups. Three of those four groups are composed of an aminocyclitol 2-deoxystreptamine (DOS) ring which is linked to amino sugars, themselves saturated with amino and hydroxyl substitutions. Neomycin is in the 4,5-disubstituted group (Fig. 11) (Wachino and Arakawa 2012; Magnet and Blanchard 2005).

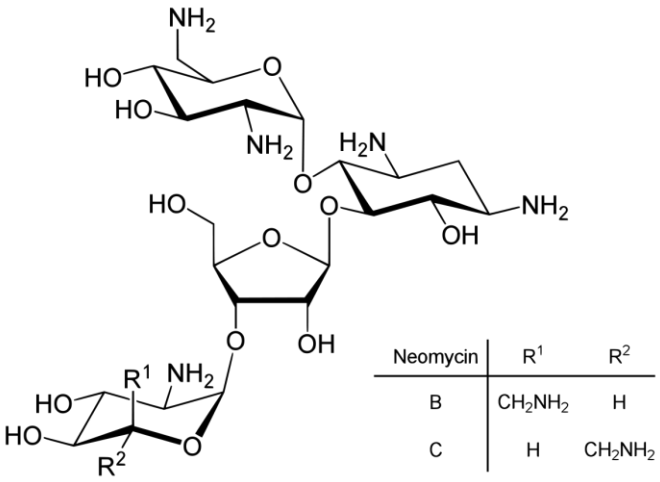

Figure 11: Chemical structure of neomycin.

Neomycin is produced by *Streptomyces fradiae* and was discovered in 1949 (Waksman *et al.,* 1949). It is mostly found in topical medications like ointments and eyedrops, such as Neosporin, but can also be taken orally where it has been used to treat small intestine bacterial overgrowth and tuberculosis (Pimentel *et al.,* 2020; Waksman *et al.,* 1949). The antibiotic is very nephrotoxic and is therefore never given through injections, unless it is in minute concentrations when used as a preservative in some vaccines (Dai *et al.,* 2006; Heidary and Cohen, 2005).

Although neomycin is efficient to kill Gram-negative species and partially effective against Gram-positive species, it is a relatively toxic molecule and many patients have had allergic reactions when treated with neomycin. In fact, on a study conducted on 4500 patients, 10 % had a topical allergic reaction to the molecule, placing it above bacitracin and formaldehyde (Zug *et al.,* 2009). Like most AGs, neomycin displays ototoxicity, toxicity to the ear, in a dose-dependent manner. Neomycin is cochleotoxic, meaning it mainly affects the cochlea, which can result in hearing losses and affect balance. However, this is not specific to neomycin only as studies have shown that AG-induced ototoxicity is observed in around 20 % of patients who received the drug intravenously during several days (Jiang et al., 2017).

In addition to binding the site-A on the 16S ribosome rRNA, neomycin is known to interact with other targets like the *rnpB* component of the RNase P holoenzyme. By binding this enzyme, neomycin prevents it from generating mature tRNA substrates for tRNA synthetases (Blanchard *et al.*, 2016; Mikkelsen *et al.*, 1999).

1.4.3 Description of tobramycin

Tobramycin is derived from *Streptomyces tenebrarius* and has been used to treat several Gram-negative infections since its approval for use in medicine in 1974. Tobramycin is classified in aminoglycosides with a 4,6-di-substituted deoxystreptamine ring, like gentamicin, amikacin and plazomicin (Fig. 12) (Wachino and Arakawa 2012; Magnet and Blanchard 2005).

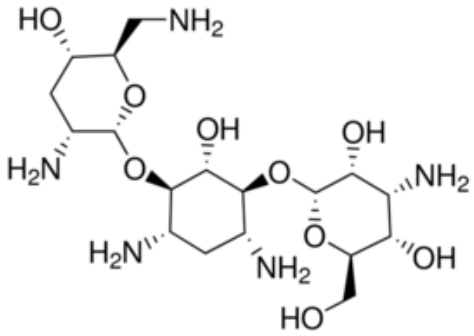

Figure 12: Chemical structure of tobramycin.

Tobramycin is mostly used in inhalation therapy to treat *P. aeruginosa* infections in people suffering from cystic fibrosis (CF). Patients undergoing this kind of therapy are shown to have improved respiratory function and decreased hospitalizations which leads to increased survival (Sawicki et al., 2012; Ramsey et al., 1999). In rare cases of severe infections,

tobramycin can be used intravenously to treat sepsis, meningitis, skin and bone infections, recurrent urinary tract infections, etc. (Neu, 1976). Like neomycin, tobramycin is ototoxic and nephrotoxic (Lerner et al., 1983).

Tobramycin binds to the A site of the 30S bacterial ribosome which leads to miscoding, similarly to other AGs such as neomycin.

1.5 Antibiotic resistance

Antibiotic resistance in bacteria has become increasingly concerning as more and more pathogens develop tactics to survive treatments. The World Health Organization even placed the problematic in the three most important public threats of the 21st century (WHO, 2014). In 2015, about 700 000 Europeans were infected with drug-resistant bacteria and approximately 30 000 died from these infections (Cassini *et al*., 2019). Many believe the world could return to a pre-antibiotic era and it is estimated that more people will die from antibiotic-resistant bacterial infections than cancer in 2050 (Review on Antimicrobial Resistance, 2014). These reservoirs are not only confined to hospital settings and can develop within communities and humans are in an arms race against those pathogens. However, the development or discovery of new antibiotics does not keep up with bacterial resistance evolution, leading scientists to look elsewhere for new antimicrobial compounds (Ventola, 2015).

1.5.1 Global resistance mechanisms

Antimicrobial resistance is not a mechanism developed with the discovery and use of antibiotics in medicine. It is rather an ancient mechanism linked to niche interactions within bacterial ecosystems. As antibiotics are generally produced naturally by microorganisms, nearby residents had to develop resistance mechanisms to survive. This process is called intrinsic resistance while acquired resistance is more clinically linked, meaning a bacteria that was once susceptible to a treatment developed resistance to the compound in a clinical setting. Those acquired resistance may be the result of chromosomal gene mutations or linked to the gain of external genetic determinants (Munita and Arias, 2016).

On a genetic basis, there are two ways to acquire antibiotic resistance: mutations in one or several genes linked to the mechanism of action of the antibiotic, like the target site, or gain of external DNA coding for resistance determinants through horizontal gene transfer (HGT) (Munita and Arias, 2016). Through bacterial division, some subpopulations may develop mutations in genes that interfere with antibacterial activity. These random mutations may not lead to resistance. However, if it does, the sensitive population is eradicated, which leads to the emergence of the resistant mutant. This tactic may lead to several resistance mechanisms exposed later. As for the HGT, the process is different but the results can be the same. HGT is a strategy which led to intrinsic resistance in many species living in the same niches and that is still used to develop acquired resistance. HGT can be done through bacterial transformation, phage-mediated transduction and conjugation (Thomas and Nielsen, 2005).

It is important to note that a resistant strain may use several mechanisms against one antibiotic, and this may result in an additive effect which increases resistance. However, some bacteria seem to prefer some tactics over others. This behavior may be linked to the energy cost of other strategies as antibiotic resistance is generally an expensive aptitude. For example, in the case of β-lactams, Gram-negative bacteria tend to favor the production of enzymes called β-lactamases while Gram-positive bacteria modify their target site, penicillin-binding proteins (Munita and Arias, 2016; Bush, 2013; Chambers and DeLeo, 2009).

Once a genetic resistance is acquired, this can translate in one of four major biochemical pathways. The first is the direct modification or destruction of the compound. The second modifies the access to the target site by interfering with the antibiotic's penetration or by expelling it. The third strategy is modifying the target site. Finally, the fourth path is a resistance acquired through adaptive processes which are reflected on the entire cell.

1.5.1.1 Enzymatic modification or destruction of the antibiotic

Resistance mechanisms falling in the first category are led by enzymes that either modify the antibiotic, which lowers the compound's affinity with the target site or destroy it completely. Modifying enzymes mainly acetylate or adenylate specific sites on the compound's structure. Aminoglycoside-modifying enzymes (AMEs) are good examples of these enzymes and are at the center of aminoglycoside resistance (Ramirez and Tolmasky, 2010). They're further described in section 1.5.2. Destroying the whole molecule is also an ability acquired by some bacteria. Known examples are β-lactamases, which destroy the amine bond of the β-lactam ring. Since the discovery of this enzyme in 1940s, around a thousand β-lactamases have been described in several species (Munita and Arias, 2016; Abraham and Chain, 1940).

1.5.1.2 Modification of the antibiotic uptake

Other described mechanisms are linked to antibiotic uptake, which may be disrupted with efflux pumps and modifications in the membrane permeability (Munita and Arias, 2016). A majority of clinically used antibiotic target intracellular mechanisms and molecules, making penetration a crucial part of their capacity to reach their objective. Thus, the antibiotic must cross the outer and/or cytoplasmic membrane (Nikaido, 2003). Resistance mechanisms can be intrinsic, like Gram-negative bacteria which are naturally resistant to vancomycin as it can't penetrate through the outer membrane. In addition, alteration in the outer membrane's permeability also affect other molecules like β-lactams, tetracyclines and some fluoroquinolones which use porins to penetrate the outer membrane (Pagès *et al.*, 2008).

Porins are classified according to their structure, their selectivity and how their expression is regulated. Known porins include *E. coli*'s OmpF, OmpC and PhoE, and *P. aeruginosa*'s OprD (Hancock and Brinkman, 2002). Those channels have been linked to porin-mediated antibiotic resistance, which is achieved through three general processes: gene expression shift leading to the expression of other types of porin, changes in the level expression of already expressed porins, or through the modifications to the porin's function (Munita and Arias, 2016). These porin-mediated mechanisms allow for intermediate antibiotic resistance and must be conjugated with other strategies to make the bacterial population fully resistant. Mutations in the *oprD* gene which usually codes for a porin that manages amino acid and antibiotic uptake in *P. aeruginosa* have been linked to antibiotic resistance (Quinn *et al.,* 1986). In *K. pneumoniae*, a slight shift in porin expression from OmpK35 to OmpK36 led to a 4-8-fold decrease in susceptibility to a wide range of β-lactams (Hasdemir *et al.,* 2004; Doménech-Sánchez *et al.,* 2003).

Antibiotic uptake can also be interrupted by the presence of efflux pumps, complex machineries which expel the molecules. These pumps can either target one or several antibiotics (Poole, 2005). Since the discovery of a tetracycline-expelling system in *E. coli* in the 1980s, many efflux pumps have been described in both Gram-negative and Gram-positive bacteria (McMurry *et al.*, 1980). These diverse systems are structurally different and vary in many other aspects like their energy source, range of substrates and the type of organisms in which they are found. Therefore, they have been classified into 5 major families: major facilitator superfamily, small multidrug resistance family, resistance-nodulation-cell-division family, ATP-binding cassette family and the multidrug and toxic compound extrusion family (Munita and Arias, 2016; Piddock, 2006). A classic example of efflux pumps is the MexAB-OprM system found in *P. aeruginosa*, a pump from the resistance-nodulation-cell-division family which leads to multi-drug resistance in this species (Hancock and Brinkman, 2002).

1.5.1.3 Target site strategies

Species that acquire antibiotic resistance through alteration of the compound's target site can do so through protection of the site or by modifying the site. Both strategies result in a decrease in binding affinity or in the complete absence of binding.

Tetracycline resistance through Tet(M) and Tet(O) proteins is a classic example of target protection (Connell *et al.,* 2003). These proteins release the tetracycline from the target site by interacting with the ribosome in a GTP-dependent manner. Both have their own strategy: TetM removes the molecule by interacting with a domain located on the 16S rRNA, which is a crucial part of the ribosome, while TetO competes for the same niche as tetracycline. The proteins and their interaction with the ribosome result in an alteration of the binding site which prevents the tetracycline from rebinding (Li *et al.,* 2013; Dönhöfer *et al.,* 2012).

As for target modification, it is a common strategy which results in resistance to almost all antibiotics. They occur through mutations in the genes coding for the site, complete replacement or bypass of the target, and changes in the site through enzymatic reactions (Munita and Arias, 2016). An example of mutational resistance has been described in the case of rifampicin resistance. Rifampicin interferes with the DNA-dependent RNA polymerase, which results in the inhibition of transcription. The compound binds to the β subunit of the RNA polymerase, which is a highly conserved structure encoded by *rpoB* (Campbell et al., 2001). It was observed that simple amino-acids substitutions in the *rpoB* gene were sufficient to create antibiotic resistance without disrupting transcription (Floss and Yu, 2005).

Bacteria can also acquire antibiotic resistance by replacing the target with a site which has equivalent functions but to which the compound cannot bind. For example, MRSA strains have acquired a foreign gene named *mecA* which leads to the production of exogenous penicillin-binding sites (PBP2a) instead of native PBP (still produced, but not as much as non-MRSA strains) to which β-lactams and carbapenems do not bind (Hiramatsu *et al.,* 2013). Bypassing the target's pathway by massively producing the antibiotic's binding site and

"overwhelming" the antibiotic is also a tactic that has been observed (Flensburg and Sköld, 1987).

Finally, the *erm* (erythromycin ribosomal methylation) genes are a classic example of enzymatic modification of the target site. They have been observed in more than 30 bacterial genera, but are costly for bacterial fitness (Munita and Arias, 2016). By mono- or dimethylating an adenine residue located on the position A2058 of the domain V found in the 50S ribosome subunit, these enzymes can protect the site from macrolides, lincosamides and streptogramin B (Leclercq, 2002; Weisblum, 1995).

1.5.1.4 Global resistance through adaptation

Antibiotic resistance through global adaptation can be defined as a more subtle kind of resistance, born from intrinsic resistance in competitive bacterial ecosystems. This type of resistance is the foundation of survival and is linked to crucial cellular processes like cell wall synthesis and general homeostasis. In a clinical setting, daptomycin and vancomycin resistance are classic examples of this type of tactic (Munita and Arias, 2016).

Daptomycin is a lipopeptide with a function similar to cationic antimicrobial peptides (CAMPs), which are part of the immune system. Similar to the CAMPs, the process through which daptomycin kills bacteria is complex. Briefly, the process begins with daptomycin binding to calcium, which is positively charged. This results in the antibiotic interacting with the outer leaflet of the cell membrane, leading to oligomerization of the daptomycin. The compound can then reach the inner leaflet and form a pore-like structure leading to cytoplasmic

leaking and major shifts in the cell's general homeostasis which lead to cell death (Taylor and Palmer, 2016).

To survive, bacteria had to develop defense systems against CAMPs and this led to modification in regulatory systems involved in protecting the cell envelope when attacked by those molecules. One of these components is LiaFSR, a regulatory system which coordinates cell-envelope stress in Gram-positive bacteria. LiaFSR contains three proteins: LiaF, a transmembrane protein linked to negative regulation of the system, LiaS, a sensor-histidine kinase that interacts with the response regulator and LiaR, the response regulator of the system. A study showed slight modifications in this pathway led to daptomycin resistance in *E. faecalis*. As an example, deletion of the isoleucine found at position 177 of the LiaF protein increased the daptomycin MIC from 1 to 4 µg/ml (Munita *et al.*, 2014; Munita *et al.*, 2013)

1.5.2 Resistance to aminoglycosides

As described earlier, antibiotic resistance is induced through several mechanisms. Resistance to AGs can be achieved through enzymatic modification, efflux mechanisms and target site modification with the help of an enzyme. Often, several mechanisms are found within the same strain and resistance strategies differ from one antibiotic to another.

Enzymatic modification of antibiotics is a common resistance tactic. Approximately a hundred aminoglycoside-modifying enzymes (AMEs) have been discovered and described. Those enzymes have been classified according to whether they acetylate, phosphorylate or adenylate amino or hydroxyl groups found within the core structure of AGs (Ramirez and Tolmasky 2010). These classes are further divided, depending on which position is modified on

the AG structure. Consequently, those enzymatic modifications result in a decrease in binding affinity for the affected AG molecules and a drop in effectiveness.

The largest family of AMEs is the aminoglycoside acetyltransferases (AACs), part of the GCN5-related N-acetyltransferase (GNAT) superfamily which contains 10,000 described proteins (Ramirez and Tolmasky, 2010). Through an acetyl-CoA-dependent reaction, the enzymes of this family acetylate various amino groups on the AG structure. Since the discovery of the first AAC in 1965, 70 members have been described (Krause *et al.,* 2016; Okamoto and Suzuki 1965). The second most prevalent group of AMEs is the AG phosphotransferases (APHs) which display kinase-like behavior by catalyzing the ATP-dependent phosphorylation of hydroxyl groups found in the AG structure. The 30 APHs placed in this group reduce the binding affinity of AGs to their targets by lowering the hydrogen bonding potential of AG hydroxyl groups with crucial rRNA molecules (Krause *et al.,* 2016). This leads to resistance against kanamycin and neomycin, and for some APHs, to amikacin and gentamicin B resistance (Shaw *et al.,* 1993). Finally, the AG nucleotidyltransferase (ANTs) mostly target kanamycin A, B and C, gentamicin A, amikacin, tobramycin, streptomycin, spectinomycin and neomycin B and C (Ounissi *et al.,* 1990; Hollingshead and Vapnek, 1985; Murphy, 1985).

It has been demonstrated that enzymes, like 16S rRNA methyltransferases (RMTs), can alter defined rRNA nucleotide residues which results in interferences in the AG binding process (Wachino and Arakawa, 2012; Cundliffe, 1989; Beauclerk and Cundliffe, 1987). These enzymes have been classified according to which residues they modify. In 2003, the first clinical case of a pathogen with an RMT resistance mechanism was reported in Japan in a *P. aeruginosa* isolate (Yokoyama *et al.,* 2003). Again, in Japan, an enzyme named NpmA was discovered on a plasmid belonging to an AG-resistant *E. coli* clinical isolate in 2007 (Wachino *et al.,* 2007). Interestingly, this enzyme led to a pan-AG resistance due to its capacity to modify the A_{1408} nucleotide, a residue which seems crucial to 4,6- and 4,5-di-substituted AGs, in addition to the monosubstituted AGs. Since then, only one additional clinical occurrence of this enzyme has been noted (Al Sheikh *et al.,* 2014).

Efflux systems are also linked to AG resistance in several pathogens (Krause *et al.*, 2016; Magnet and Blanchard, 2005). *P. aeruginosa* is known for its efflux pumps, granting the pathogen with some low-level resistance to a few antibiotics like AGs, tetracycline and erythromycin. This efflux system is mediated by the expression of the multiple efflux (Mex) XY-OprM system (Aires *et al.*, 1999). However, this MexXY system is not only found in *P. aeruginosa* as orthologs have been discovered in other bacteria like AcrD, a similar transporter found in *E. coli* and the *Acinetobacter* drug efflux (Ade) known as the ABC efflux system found in *A. baumannii* (Magnet *et al.*, 2001; Rosenberg *et al.*, 2000).

1.6 Thesis project and hypotheses

The goal of this project is to assess the potential use of AG-linked PSs to eradicate persister cells. Persister cells are tolerant to antibiotics in a transient way, exhibiting slow or non-existent metabolisms upon certain quorum sensing cues and/or stress conditions, but they are also a part of all known bacterial communities. They are genotypically identical to the main bacterial population, dubbed "sensitive" or "regular" population, while antibiotic-resistant cells require genetic mutations to acquire this resistance. The two differ by their ability to grow in presence of a given antibiotic (Michiels and Fauvart, 2016; Lewis *et al.,* 2010). Drug-resistant bacteria will divide and grow in presence of said antibiotic, while persister cells remain dormant until the pressure of the antibiotic treatment is taken away. When the stress is withdrawn, persister cells revert to a regular phenotype and rebuild a community. These cells are problematic as they can lead to chronic illnesses and favor the emergence of antibiotic-resistant bacteria (Cohen *et al.,* 2015; Grant and Hung, 2013). In addition to being difficult to eliminate, they are also found in biofilms, threatening bacterial constructions that are found on catheters, non-healing wounds, etc., which makes persister cells medically relevant in several ways (Waters *et al.,* 2016).

The hope is to eradicate regular cells, biofilms and antibiotic-resistant bacteria, in addition to persister cells. The compounds could be used to sterilize hospital surfaces, medical instruments like catheters and topical wounds. While an antibiotic is still used in the process, we hypothesize the main killing effect will come from the singlet oxygen produced by the PSs. If the AG used still keeps a part of its effect, it may also serve as a "back-up", killing remaining cells after illumination.

Our hypotheses are as follows:

1) The link between the PSs and AGs will not disturb the production of singlet oxygen by the PS and the antibiotic effect of the AGs.

To verify this hypothesis, we will compare the MIC of our compounds to the MIC of AG alone and analyse the singlet oxygen production of PSs alone versus our compounds.

2) The link between PSs and AGs will not disturb the cellular penetration of both parties.

To verify this allegation, we will use fluorescence microscopy to observe if our compounds penetrate the selected bacteria and compare data to the PSs alone.

3) The compounds will have a greater effect against persister cells, regular cells, resistant bacteria and biofilm than the AGs and PSs alone.

To validate this proposition, we will assess the CFUs of all listed parties when illuminated in contact with our compounds and compare them to the CFU of AGs and PSs alone. We selected ESKAPE pathogens and other research-related organisms to test this theory.

CHAPTER 2

MATERIAL AND METHODS

2.1 Selected strains

Strains that were used during this project are described in Table 1.

Table 1: Description of the strains used during this project.

Strains	Description	References	Provider
A. baumannii DSM30011	Environmental strain, first isolated in 1944.	Allen et al., 1944	Professor Christiane Forestier, University of Clermont-Ferrand
B. subtilis 168	Strain isolated from soil with endospore production.	Kunst et al., 1997	Doctor Etienne Dervyn, INRA Jouy-en-Josas
C. albicans SC5314	Reference strain.	Jones et al., 2004	Doctor Sophie Bachellier-Bassi, Pasteur Institute
E. coli LF82	Adherent and invasive *E. coli* strain associated with Crohn's disease.	Krause *et al*., 2011	Professor Christophe Beloin, Pasteur Institute
E. coli MG1655	Modified *E. coli* K-12 strain.	Soupene et *al.,* 2003	Doctor Dominique Fourmy, Institute for Integrative

			Biology of the Cell (I2BC)
E. coli MG1655 KanR	MG1655 yefM yoeb::gfp strain. Presence of an AG-3'-phosphotransferase-IIa	Maisonneuve et al., 2013	Professor Kenn Gerdes, University of Copenhagen
E. coli MG1655 pET-29	MG1655 with the pET-29 plasmid (kanamycin resistance through AG-3'-phosphotransferase-Ia)		Doctor Dominique Fourmy, I2BC
E. coli MG1655 *ΔtolC*	*E. coli* mutant lacking the tolC gene coding for a channel involved in the transport of many molecules.	Koronakis, 2003	Professor Christophe Beloin, Pasteur Institute
K. pneumoniae LM21 (serotype K35)		Favre-Bonte et al., 1999	Professor Christophe Beloin, Pasteur Institute
K. pneumoniae LM21 *Δcps*	Capsule defective *K. pneumoniae* mutant with a kanamycin resistance cassette.	Balestrino *et al.,* 2008; Favre-Bonte et al., 1999	Professor Christiane Forestier, University of Clermont-Ferrand
P. aeruginosa PA14	Strain from the most common clonal group of *P. aeruginosa* in the world. It is a highly virulent strain containing two pathogenicity islands.	Wiehlmann *et al.,* 2007 ; He *et al.,* 2004	Doctor Frédéric Boccard, I2BC
P. aeruginosa PAO1	Strain belonging to a rare clonal group. It is a moderately virulent strain isolated from a wound.	Wiehlmann *et al.,* 2007 ; Lee *et al.,* 2006	Doctor Frédéric Boccard, I2BC
P. aeruginosa PAO1 *ΔABM*	MexAB-oprM pump mutation of PAO1		Doctor Isabelle Broutin, University of Paris Cité
P. aeruginosa PAO1 *Δxy*	MexXY pump mutation of PAO1		Doctor Isabelle Broutin, University of Paris Cité

P. aeruginosa PAO1 *ΔABM Δxy*	MexAB-oprM-mexXY double pump mutation of PAO1		Doctor Isabelle Broutin, University of Paris Cité
P. aeruginosa PAO1116 (*Δ6*)	PAO1 strain mutated for MexAB-oprM, MexXY, MexCD-oprJ, MexEF-oprN, MexJK, triABC pumps		Professor Herbert Schweizer, The Pathogen and Microbiome Institute
S. aureus Mu50	MRSA strain with vancomycin resistance.	Kuroda et al., 2001	Doctor Philippe Bouloc, I2BC
S. aureus Newman	Strain isolated from a human infection and possessing four integrated prophages and two large pathogenicity islands.	Baba et al., 2008	Doctor Philippe Bouloc, I2BC
S. aureus USA300	MRSA strain associated with outbreaks of skin and soft tissue infection in the US, Canada and Europe.	Diep et al., 2006	Doctor Philippe Bouloc, I2BC

2.2 Creating the compounds

Atto MB2 NHS-ester was obtained from Merck. Ce6 was purchased from Bertin Bioreagent, dicyclohexylcarbodiimide *N*-hydroxysuccinimide (NHS), neomycin and tobramycin from Sigma.

A derivative of neomycin containing 2-N-trifluoroacetamidoethylthio in place of a hydroxyl group in ring III was used to conjugate neomycin to NHS-ester dye as previously described (Sabeti-Azad *et al.,* 2020). Other amino groups of the neomycin derivative were protected by hexa-N-tert-butyloxycarbonyl groups for selective reactivity at the specific 5" NH_2 position. Selective deprotection of the 5" position was performed in ammonium hydroxide in methanol, and the unique free amino group was reacted with MB2 or Ce6 NHS-ester. The NHS ester of Ce6 was prepared by reacting 1.5 equivalents of dicyclohexylcarbodiimide and 1.5 equivalents of NHS with 1 equivalent of Ce6 in dry dimethyl sulfoxide (DMSO) for 24 hours and was frozen in aliquots for further use following the reported procedure (Khasen *et al.,* 1999). Reactions were monitored by analytical thin-layer chromatography (TLC) on silica gel 60 F254 plates (0.25 mm). The Neo-MB2 and Neo-Ce6 conjugates were purified on TLC plates (Silica gel 60, Merck), eluted in ethanol, and deprotected with trifluoroacetic acid (90%) to remove butyloxycarbonyl groups.

2.2 Evaluating the compounds

2.2.1 Excitation/emission evaluation

Concentrations were obtained using the Beer's law equation (absorption = Ɛ (molar extinction coefficient) x optical path length x concentration). Samples of unknown concentrations were diluted in ethanol and the absorption was obtained using a spectrophotometer. Absorbance was taken from the peak in the 650-670 nm region and converted using the extinction coefficient of Ce6 obtained from Nyman and Hynninen, 2004.

2.2.2 Gaging the singlet oxygen production

Singlet oxygen production was evaluated using the Singlet Oxygen Sensor Green (SOSGR) kit from Molecular Probes. Reagents were prepared as suggested by the company, and a final concentration of 2.5 µM of the SOSGR was used for all experiments. Dilutions of both the compounds, photosensitizers and SOSGR were in cation-adjusted Mueller-Hinton broth (MHB-CA). Irradiation was done at specified wavelengths and for a specified amount of time in darkness on a total volume of 120 µl placed in a transparent 96-well plate (Nunclon Delta Surface, Thermo Scientific). Directly after illumination, 100 µl of the reaction were transferred to a 96-well black plate (Optiplate-96F, Perkin Elmer). Relative light units (RLU)

emitted by the SOSGR were read on a Tecan Infinite 200 or on a Perken Elmer Victor X5 at 485/535 nm. Statistics were done on GraphPad Prism version 8.4.3.

2.2.3 Microscopy observations

All microscopy pictures were taken with an inverted Zeiss Axio Observer Z1 microscope. Fluorescence images were acquired with an EMCCD camera (Photometrics) through a 63X total internal reflection fluorescence (TIRF) objective (Zeiss, NA 1.43). Image acquisition was done with the Metamorph software package (Molecular Devices). MB and Ce6 illumination were performed using a 642-nm laser (0.002 kW/cm^2, Roper Scientific), and a filter set was used for fluorescence excitation and emission (Chroma Technology; ET 532/640 nm Laser Dual Band; excitation filter 530/20 nm and 638/25 nm, dichroic mirror 585/70 nm and 650 nm (long pass), and emission filter 580/70 nm and 700/100 nm). Neo-MB, Neo-Ce6 and Tobra-Ce6 uptake was typically observed with an electron-multiplying gain of 50 and an exposure of 50 to 400 ms.

Cells were grown overnight in MHB-CA and diluted to an OD of 0.0375 the next morning. Samples were then grown to an OD of 0.3 and incubated for 10 minutes at 37°C with the compounds. They were washed with the use of a filtration device and filters that retained the cells while allowing them to be washed gently using MOPS-g. Samples were washed three times, the filters were recovered and divided to recuperate the dyed region where bacteria would collect. This piece of filter was then placed in a tube and washed with 2 µl of MOPS-g. Samples were then pipetted on freshly prepared agar pads. Bright-field pictures were taken and compared with pictures taken with laser excitation (done at 642 nm) to assess bacterial penetration and/or adhesion of the compounds and photosensitizers.

All microscopy analysis were done the same way. Using ImageJ's ROI (region of interest) selection tool, a minimum of a hundred bacteria were analysed on bright field images. The ROI filter was then added to the fluorescence image taken at the same region and RLUs were measured for images taken with a 200 ms exposure. Regions containing no bacteria were also selected to be used as blanks. Statistical analysis was done using GraphPad Prism 8.4.3.

2.3 Bacterial killing

2.3.1 Antibacterial photodynamic therapy on planktonic cells

Cells were brought to stationary phase by incubating them in MHB-CA for at least 18 hours at 37°C with 180 rpm and diluted to an OD of 1.0 just before the experiment. Cells were incubated 20 minutes with either the compounds, PSs alone, or AGs alone. Unless described otherwise, samples were then irradiated for 30 minutes at 660 nm with the Solis-660C from ThorLabs, receiving about 5 J/mm², or kept in the dark.

After irradiation, cells were washed three times with PBS 1X. Dilutions were plated on MH agar and incubated at 37°C. The next day, CFUs were counted and statistics were done using one-way ANOVA to compare all means to the mean of controls in GraphPad Prism 8.4.3.

2.3.2 Minimal inhibitory concentrations

Minimal inhibitory concentrations (MICs) for selected bacteria were investigated according to the EUCAST guidelines. Serial dilutions of the conjugates, PSs and AGs were made in MHB-CA in 384-well plates to reduce the consumption of the molecules. Stationary-phase cells were diluted in MHB-CA to a concentration of 5.5×10^5 CFU/mL and added to the

wells. *C. albicans* SC5314 was grown and tested in yeast extract peptone dextrose (YEPD). Samples were incubated in the dark for 20 minutes at 37°C and either irradiated at 660 nm for 30 minutes or kept in the dark. Irradiated samples therefore received a total of 168 mJ/mm², although some species received 5 J/mm². Plates were then incubated at 37°C for 18 hours. The MIC were established visually in triplicates. The synergy, or fractional inhibitory concentration (FIC), was calculated according to Doern, 2014.

$$FIC = \frac{MIC\ of\ AB}{MIC\ of\ A} + \frac{MIC\ of\ AB}{MIC\ of\ B}$$

2.3.3 Effects on biofilm cells

Stationary-phase cells were grown in MHB-CA and diluted to a concentration of 5.5 x 10^5 CFU/ml. A volume of 100 µl of diluted bacteria were placed in 96-well plates (351172, Falcon) overnight. The next day, the supernatant was removed carefully as to not disturb the biofilm. The biofilm was washed three times using 150 µl of PBS 1X. Compounds and PSs were diluted in MHB-CA and 100 µl was pipetted carefully over the biofilms. After 20 minutes of incubation in darkness, biofilms were irradiated with the Solis-660C lamp from Thor Labs for a total of 30 minutes (alternating 5 minutes of irradiation with 1 minute in darkness). Samples therefore received a total of 5 J/mm².

Biofilms were then aggressively pipetted and scratched off the plaque before being washed three times with 150 µl of PBS 1X. Pellets were then diluted in 96-well plates and placed on MH agar. The next day, CFUs were counted and statistics were done using GraphPad Prism version 8.4.3.

2.3.4 Effects on persister cells

Before doing aPDT on persister cells, we needed to find the persister plateau for selected species. Stationary-phase cells were therefore treated for a maximum of 24 hours with high doses of neomycin or tobramycin. Samples were collected at 0, 2, 4, 6 and 24 hours of incubation, washed three times with PBS 1X, diluted and plated on MH agar. The next day, CFUs were counted and killing curves were analysed on GraphPad Prism 8.4.3. Triplicates were done and concentrations which led to a survival plateau were selected for aPDT.

After static incubation for 6 to 24 hours with the previously selected AG concentration, the compounds, PSs or AGs were added so as to not dilute the cells past a certain limit. 10 µL of 10 times concentrated compound, PS or AG was therefore added to 90 µL of samples. We chose not to wash or dilute the samples before aPDT as this sometimes led to persister cells reverting to a sensible phenotype. Cells were incubated in the dark for 20 minutes before being irradiated for 30 minutes at 660 nm with the Solis-660C lamp from Thor Labs, receiving a total of 5 J/mm². Samples were washed with PBS 1X, diluted and plated on MH agar. The next day, CFUs were counted and statistics were done using one-way ANOVA to compare all means to the mean of controls in GraphPad Prism 8.4.3. If the aminoglycoside alone led to cell death (significantly lower than the persister control), results were considered invalid as the persister plateau was not fully reached.

2.3.5 Cytotoxicity assays

Cells lines were obtained from the American Type Culture Collection (Rockville, MD, USA) and were cultured according to the supplier's instructions. Human MRC-5 cells were grown in DMEM supplemented with 10 % fetal calf serum (FCS) and 1 % glutamine. hTERT-RPE1 cells were cultured in DMEM/F12 medium containing 10 % FCS and 1 % glutamine. Cells were maintained at 37°C in humidified atmosphere containing 5 % CO_2.

Cell viability was determined by a luminescent assay according to the manufacturer's instructions (Promega, Madison, WI, USA). The cells were seeded in 96-well plates (3×10^3 cells/well) containing 100 µL of growth medium. After 24 hours of incubation, the cells were treated with the compounds at different final concentrations. Control cells were incubated in the growth medium only. Plates were incubated in darkness at 37°C for 20 minutes before being irradiated at 665 nm for 30 minutes, receiving a total of 168 mJ/mm². Experiments were performed in triplicates.

After 48 hours of incubation, 100 µL of the CellTiter Glo Reagent was added for 15 minutes before recording luminescence with a spectrophotometric plate reader (PolarStar Omega, BMG, LabTech). The dose-response curves were plotted on GraphPad Prism 8.4.3.

CHAPTER 3

RESULTS

3.1 Description of the created compounds

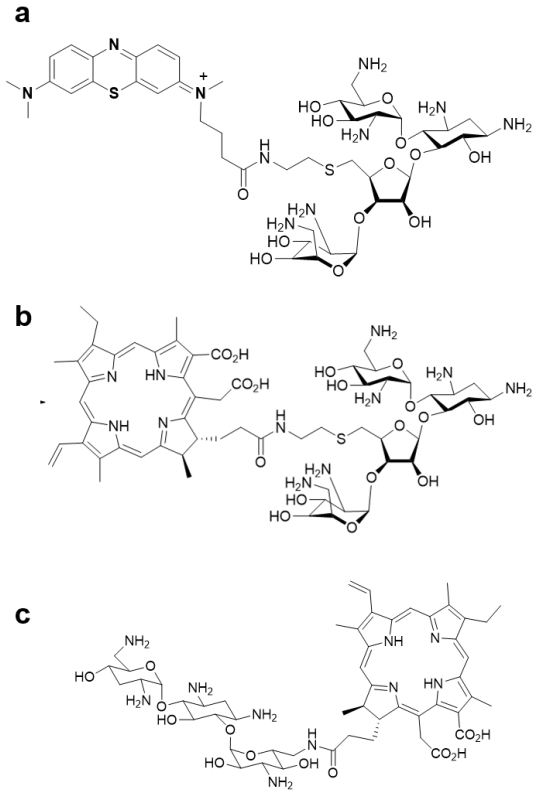

Figure 13: Photosensitizer-aminoglycoside conjugates: a) Neo-MB, b) Neo-Ce6 and c) Tobra-Ce6.

All created compounds were highly soluble in water. Concentration of the final product varied from one synthesis to another. It was determined using the absorption and the extinction coefficient of Ce6 (Nyman and Hynninen, 2004). Absorption spectrums are quite similar with a small shift for Neo-Ce6 (665 nm), while Tobra-Ce6 and Ce6 stand at 662 nm. For Neo-MB and MB, the peak was around 660 nm (Fig. 15).

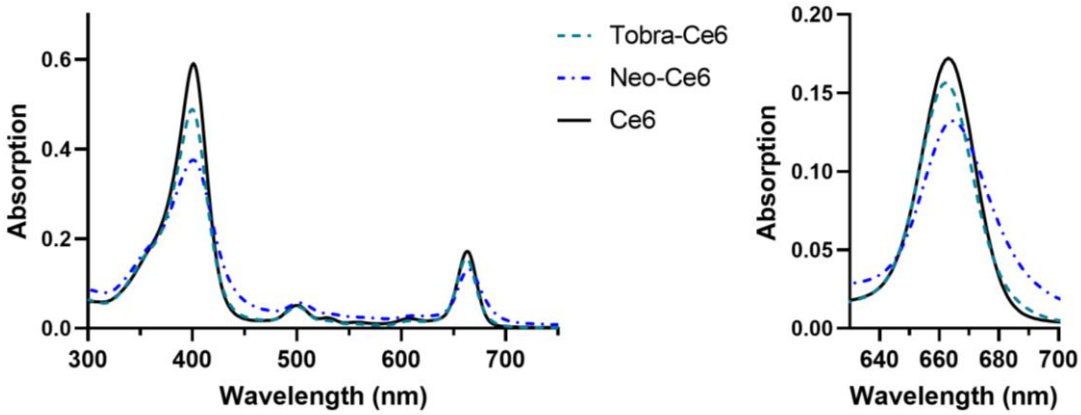

Figure 14: Absorption spectra of Ce6 (3.1 µM), Neo-Ce6 (2.4 µM) and Tobra-Ce6 (2.8 µM).

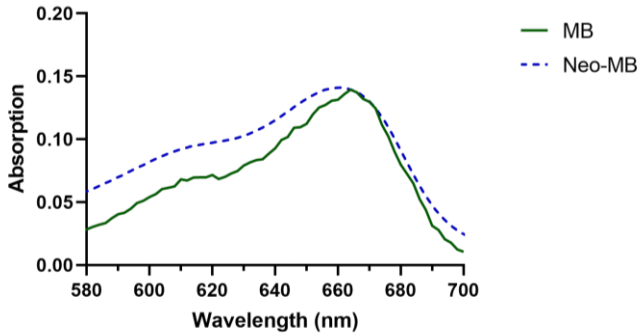

Figure 15: Absorption spectra of MB and Neo-MB at 5 µM.

3.2 Singlet oxygen production

Several light sources were tested in order to select one with a maximum yield of singlet oxygen. At first, a prototype with 5 LED lamps that illuminates approximately 5.6 mJ/minute/mm² was used.

Neo-MB produced less than half the singlet oxygen yielded by MB and ATTO-MB2 alone, while Neo-Ce6 yielded similar quantities of singlet oxygen when compared to Ce6 alone. Tobra-Ce6 on the other hand produced a lot more singlet oxygen than Neo-Ce6 and Ce6 (Fig. 16).

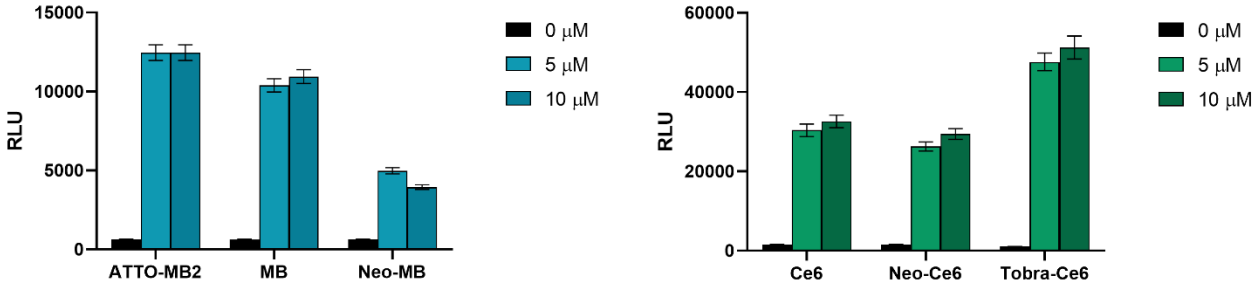

Figure 16: RLU emitted by the SOSGR kit after a 15-minute illumination with the prototype (665 nm). Total energy received: 84 mJ/mm².

Later in the project, we acquired a new light source: the Solis-660C from Thor Labs. This new lamp was mainly used to irradiate biofilms and persister cells as the prototype did not produce sufficient energy. This new lamp was used at a setting allowing for 171 mJ/minute/mm² irradiation. Results show higher singlet oxygen production for both compounds when compared to Ce6 (Fig. 17). As a different plate reader was used to analyse RLUs, prior results could not be compared to the results obtained after using the Solis-660C lamp. However, figure 18 shows

results comparing singlet oxygen production in Neo-Ce6 and Ce6 when comparing the two lamps. After only 5 minutes of irradiation with Solis-660C, singlet oxygen yield was significantly higher for both the PS and the conjugate.

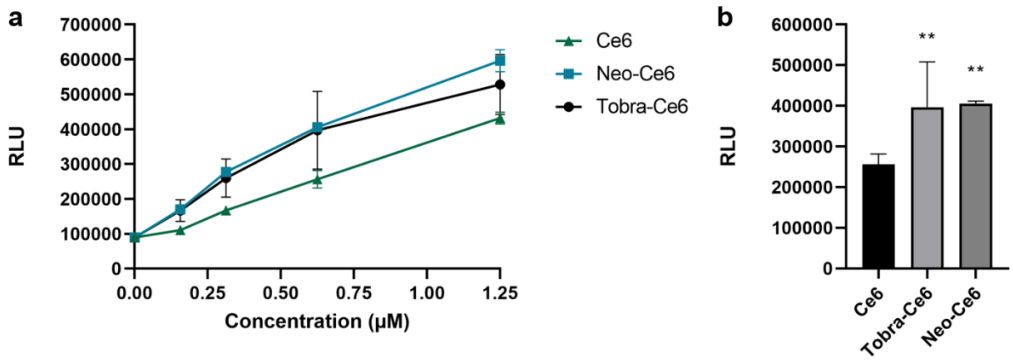

Figure 17: RLU emitted by the SOSGR kit after a 5-minute irradiation with the Solis 660C lamp (660 nm). Energy received: 857 mJ/mm². In a) curve with increasing concentration of Ce6 or compounds. In b) columns for a concentration of 0.6125 µM. Statistics were done using one-way ANOVA against the control (Ce6) on GraphPad Prism 8.4.3.

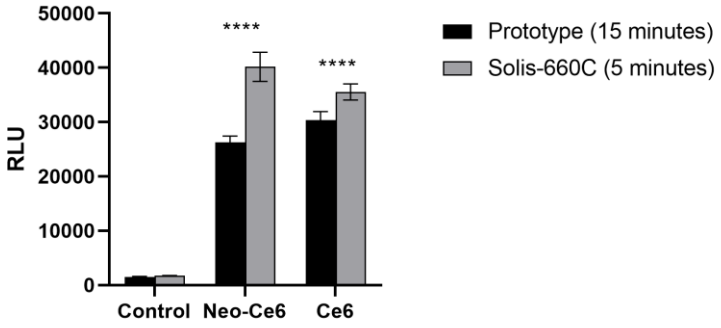

Figure 18: Comparing RLU emission by the SOSGR kit when irradiated with the prototype (84 mJ/mm²) or the Solis-660C lamp (857 mJ/mm²). Done on 5 µM of Neo-Ce6 and Ce6. Statistics were done using two-way ANOVA between the means of each column on GraphPad Prism 8.4.3.

3.3 Fluorescence microscopy observations

Globally, the compounds always showed significantly higher penetration and/or adhesion than PSs alone in all tested strains. We also witnessed some bacterial explosions when taking time-lapse pictures at 642 nm with 10-second intervals in a few species like *P. aeruginosa* PA14 and *B. subtilis* 168. Those explosions usually occurred after 2 minutes of these 200 ms flashes each 10 seconds. Analysis has also shown no correlation between mean RFUs and mean survival following aPDT ($R^2 = 0.41$).

In Gram-positive bacteria, Ce6 showed the highest penetration and/or adhesion in *B. subtilis* 168 cells (Fig. 19), but mean RFUs for cells incubated in Neo-Ce6 remained significantly higher.

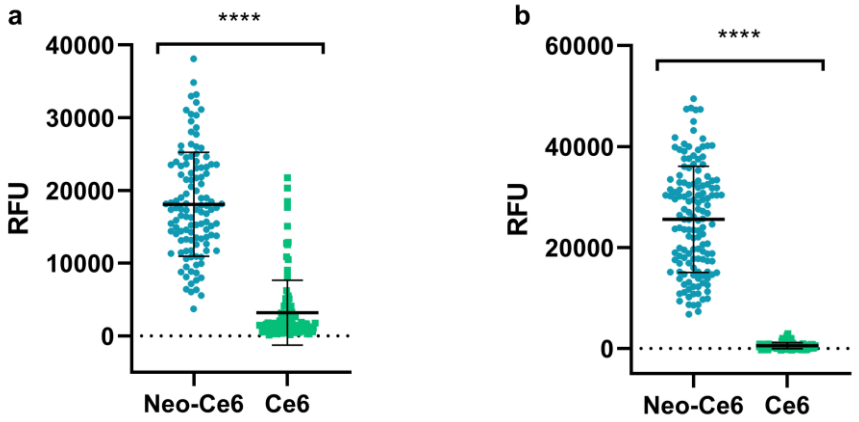

Figure 19: Gram-positive species RFUs with 1 µM of Neo-Ce6 and Ce6 at 200 ms of exposure at 642 nm with *B. subtilis* 168 in a and *S. aureus* USA300 in b. Bars represent mean and standard deviation. Asterisks represent a $p < 0.0001$ obtained through a t-test done on GraphPad Prism 8.4.3.

In *B. subtilis* 168, spores were also stained with Neo-Ce6 (Fig. 20). Although we did not have access to more problematic strains like *Clostridium*, this means Neo-Ce6 could have the capacity to eradicate sporulating pathogens like *C. tetani* and *C. botulinum* as aPDT against *B. subtilis* 168 showed a MIC under 0.125 µM (Section 3.4.1).

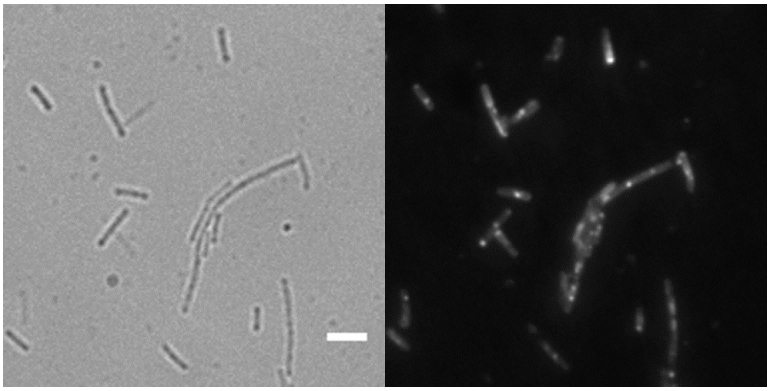

Figure 20: Microscopy images of *B. subtilis* 168 with 1 µM of Neo-Ce6. The fluorescence picture (right) was taken at 642 nm with 200 ms of exposure and a gain set at 50. Scale: 5 µM.

We also tested *E. coli* MG1655 and a few mutant strains. This was meant to study penetration and/or adhesion mechanisms of our compounds (Fig. 21). Statistical analysis is shown in Table 2. To summarize, mean RFU from cells incubated with Neo-Ce6 and Ce6 was always significantly higher in the wild-type strain than in the three mutants. For Neo-Ce6, the *ΔtolC* strain's mean RFU was significantly higher than the means for the KanR and pET-29 strains. Therefore, for Neo-Ce6, *E. coli* MG1655 was the strain showing the highest mean RFU while the KanR strain had significantly the lowest. For Tobra-Ce6, we only tested the wild-type strain and *ΔtolC*, and the latter showed a mean RFU that was significantly higher than the *E. coli* MG1655 strain. For Ce6, only the mean RFU for the wild-type strain is significantly different from the others (Table 2).

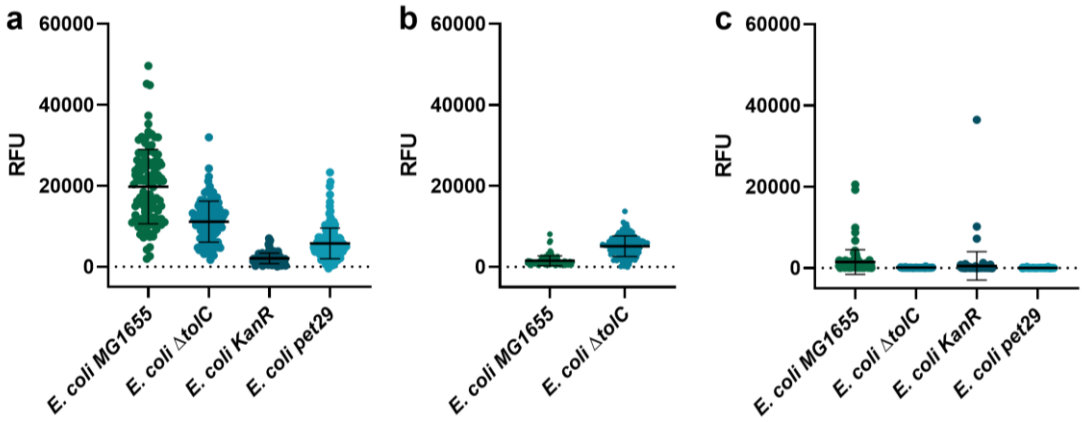

Figure 21: RFUs for *E. coli* MG1655 and mutants with 1 µM of Neo-Ce6 in a, Tobra-Ce6 in b and Ce6 in c, with 200 ms of exposure at 642 nm. Bars represent mean and standard deviation.

Table 2: One-way ANOVA statistical analysis results for RFUs in *E. coli* MG1655 and its mutants. [1]WT: wild-type strain. [2]ns: not significant.

Compound	Comparison	Mean 1	Mean 2	Significance	*P*-value
Neo-Ce6	WT vs. Δ*tolC*	19806	11139	****	<0,0001
	WT vs. KanR	19806	2052	****	<0,0001
	WT vs. pET-29	19806	5754	****	<0,0001
	Δ*tolC* vs. KanR	11139	2052	****	<0,0001
	Δ*tolC* vs. pET-29	11139	5754	****	<0,0001
	KanR vs. pET-29	2052	5754	****	<0,0001
Tobra-Ce6	WT vs. Δ*tolC*	1506	5121	****	<0,0001
Ce6	WT vs. Δ*tolC*	1465	99,66	***	0,0002
	WT vs. KanR	1465	518,4	*	0,0159
	WT vs. pET-29	1465	25,47	***	0,0001
	Δ*tolC* vs. KanR	99,66	518,4	ns	0,5576
	Δ*tolC* vs. pET-29	99,66	25,47	ns	0,9962
	KanR vs. pET-29	518,4	25,47	ns	0,4212

To further explore penetration/adhesion mechanisms, we also tested *K. pneumoniae* LM21 and its capsule deficient mutant *Δcps* (Fig. 22). When comparing Neo-Ce6 penetration

between the wild-type and the mutant, the t-test shows the mean RFU is significantly higher in *Δcps* (*p*-value = 0.0003) while there are no significant differences in the mean RFU for Ce6.

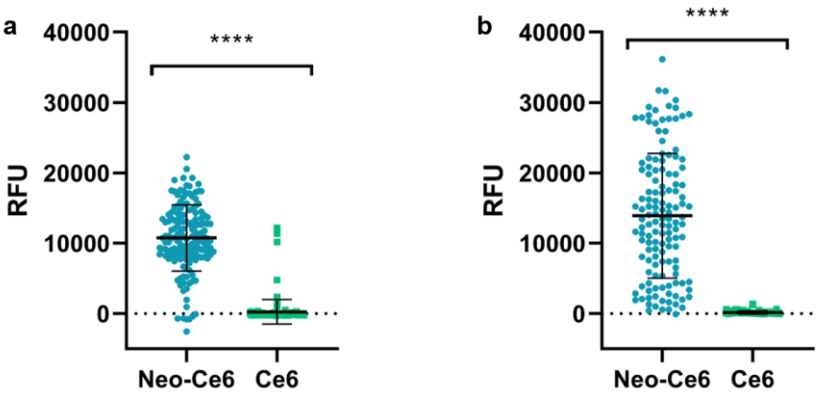

Figure 22: RFUs with 1 µM of Neo-Ce6 and Ce6 at 200 ms of exposure at 642 nm in *K. pneumoniae* LM21 in a and *K. pneumoniae* LM21 *Δcps* in b. Bars represent mean and standard deviation. Asterisks represent a $p < 0.0001$ obtained through a t-test done on GraphPad Prism 8.4.3.

K. pneumoniae LM21 and the capsule-deficient mutant appeared differently in microscopy (Fig. 23). Neo-Ce6 tended to accumulate in a more diffuse way in the wild-type, with a slight build-up at the septum during division, while it seems to gather in the periplasm in the *Δcps* mutant.

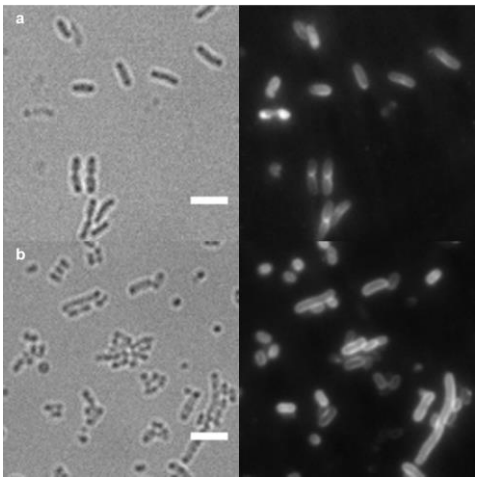

Figure 23: Microscopy images of *K. pneumoniae* LM21 in line a, and *K. pneumoniae* LM21 *Δcps* in line b, with 1 µM of Neo-Ce6. The fluorescence picture (right) was taken at 642 nm with 200 ms of exposure and a gain set at 50. Scale: 5 µm.

A similar periplasmic motif was observed in *A. baumannii* DSM30011 (Fig. 24) with, again, a significantly higher RFU mean with Neo-Ce6 than with Ce6 (Fig. 25).

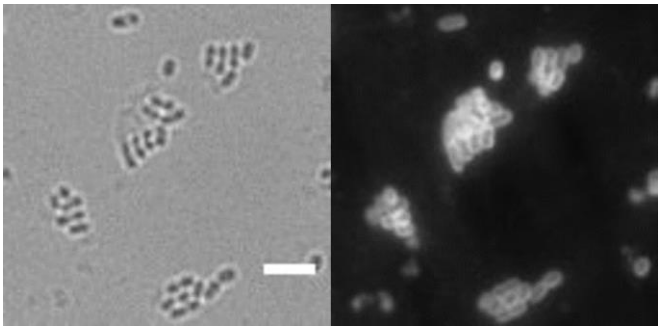

Figure 24: Microscopy images of *A. baumannii* DSM30011 with 1 µM of Neo-Ce6. The fluorescence picture (right) was taken at 642 nm with 200 ms of exposure and a gain set at 50. Scale: 5 µM.

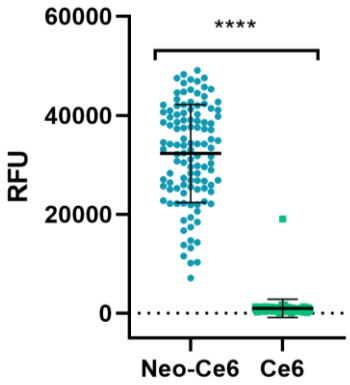

Figure 25: RFUs with 1 µM of Neo-Ce6 and Ce6 at 200 ms of exposure at 642 nm in *A. baumannii* DSM30011. Bars represent mean and standard deviation. Asterisks represent a $p < 0.0001$ obtained through a t-test done on GraphPad Prism 8.4.3.

Several strains of *P. aeruginosa* were also tested, although most were efflux pump mutants of *P. aeruginosa* PAO1 that were investigated to understand how efflux mechanisms could influence the accumulation of Neo-Ce6, Tobra-Ce6 and Neo-MB. In the highly virulent PA14 strain, accumulation of Neo-Ce6 was significant (Fig. 26).

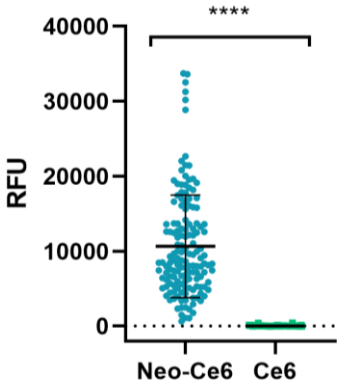

Figure 26: RFUs with 1 µM of Neo-Ce6 and Ce6 at 200 ms of exposure at 642 nm in *P. aeruginosa* PA14. Bars represent mean and standard deviation. Asterisks represent a $p < 0.0001$ obtained through a t-test done on GraphPad Prism 8.4.3.

In *P. aeruginosa* PAO1, accumulation fluctuated between strains and compounds which lead to a lot of analysis being done on this data. Visually, both Neo-Ce6 and Tobra-Ce6 seemed to adhere to some kind of "matrix" around cells. This may be alginate, as *P. aeruginosa* PAO1 is known to show a mucoid state. Statistical analysis is described in depth in Table 3 and mean RFUs are shown in a heatmap to summarize the data (Fig. 27 b).

Globally, as for all other tested strains, mean RFUs for compounds was always significantly higher than for PSs alone ($p < 0.0001$). Within strain analysis showed two profiles. For the wild-type strain PAO1, the *Δ6* and *ΔABMΔxy* mutants, mean RFUs for Neo-MB was significantly higher than the mean RFU of all other compounds and PSs ($p < 0.0001$). Tobra-Ce6 took the second place in those two strains, showing a significantly higher mean RFU than Neo-Ce6 and PSs alone ($p < 0.0001$). In *ΔABM* and *Δxy*, it was rather Tobra-Ce6 which had a significantly higher RFU mean than all other compounds and PSs, with Neo-MB in second place ($p < 0.0001$). Neo-Ce6 was therefore the compound which resulted in the lowest mean RFU for these strains.

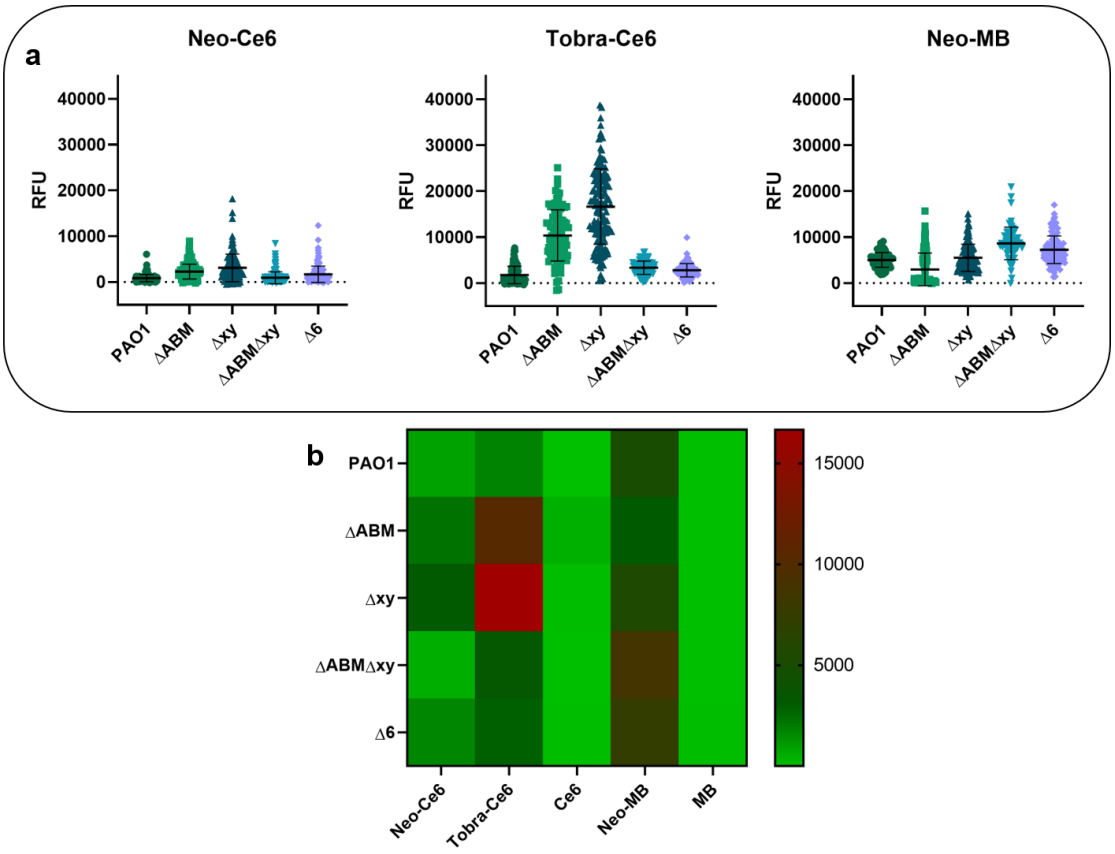

Figure 27: a) RFUs with 1 µM of Neo-Ce6, Tobra-Ce6 and Neo-MB at 200 ms of exposure at 642 nm in *P. aeruginosa* PAO1 and efflux pump mutants. b) Heatmap showing the mean RFU for all compounds and PSs in *P. aeruginosa* PAO1 and its mutants.

When comparing compound accumulation between the strains, Neo-Ce6 and Tobra-Ce6 result in the highest mean RFUs in *Δxy*, while the highest mean RFU is found for *ΔABMΔxy* for Neo-MB (Table 3). For PSs alone, the highest mean RFU for Ce6 is in *ΔABM* and in *Δ6* for MB, although not always significantly higher than other means (Table 3).

Table 3: One-way ANOVA statistical analysis results for RFUs in *P. aeruginosa* PAO1 and its mutants. [1]WT: wild-type strain. [2]ns: not significant.

Compound	Comparison	Mean 1	Mean 2	Significance	*P*-value
Neo-Ce6	WT vs. *ΔABM*	861,8	2281	****	<0,0001
	WT vs. *Δxy*	861,8	3092	****	<0,0001
	WT vs. *ΔABMΔxy*	861,8	931,1	ns	0,9984
	WT vs. *Δ6*	861,8	1692	**	0,0038
	ΔABM vs. *Δxy*	2281	3092	**	0,0016
	ΔABM vs. *ΔABMΔxy*	2281	931,1	****	<0,0001
	ΔABM vs. *Δ6*	2281	1692	*	0,0477
	Δxy vs. *ΔABMΔxy*	3092	931,1	****	<0,0001
	Δxy vs. *Δ6*	3092	1692	****	<0,0001
	ΔABMΔxy vs. *Δ6*	931,1	1692	**	0,0065
Tobra-Ce6	WT vs. *ΔABM*	1789	10372	****	<0,0001
	WT vs. *Δxy*	1789	16661	****	<0,0001
	WT vs. *ΔABMΔxy*	1789	3360	ns	0,1415
	WT vs. *Δ6*	1789	2807	ns	0,5117
	ΔABM vs. *Δxy*	10372	16661	****	<0,0001
	ΔABM vs. *ΔABMΔxy*	10372	3360	****	<0,0001
	ΔABM vs. *Δ6*	10372	2807	****	<0,0001
	Δxy vs. *ΔABMΔxy*	16661	3360	****	<0,0001
	Δxy vs. *Δ6*	16661	2807	****	<0,0001
	ΔABMΔxy vs. *Δ6*	3360	2807	ns	0,9361
Neo-MB	WT vs. *ΔABM*	5039	2991	****	<0,0001
	WT vs. *Δxy*	5039	5515	ns	0,7657
	WT vs. *ΔABMΔxy*	5039	8638	****	<0,0001
	WT vs. *Δ6*	5039	7273	****	<0,0001
	ΔABM vs. *Δxy*	2991	5515	****	<0,0001
	ΔABM vs. *ΔABMΔxy*	2991	8638	****	<0,0001
	ΔABM vs. *Δ6*	2991	7273	****	<0,0001
	Δxy vs. *ΔABMΔxy*	5515	8638	****	<0,0001
	Δxy vs. *Δ6*	5515	7273	****	<0,0001
	ΔABMΔxy vs. *Δ6*	8638	7273	*	0,0265
Ce6	WT vs. *ΔABM*	3,203	467,5	****	<0,0001
	WT vs. *Δxy*	3,203	78,99	ns	0,8240
	WT vs. *ΔABMΔxy*	3,203	20,51	ns	0,9992
	WT vs. *Δ6*	3,203	79,02	ns	0,8158
	ΔABM vs. *Δxy*	467,5	78,99	****	<0,0001
	ΔABM vs. *ΔABMΔxy*	467,5	20,51	****	<0,0001
	ΔABM vs. *Δ6*	467,5	79,02	****	<0,0001
	Δxy vs. *ΔABMΔxy*	78,99	20,51	ns	0,9163
	Δxy vs. *Δ6*	78,99	79,02	ns	>0,9999
	ΔABMΔxy vs. *Δ6*	20,51	79,02	ns	0,9116
MB	WT vs. *ΔABM*	9,809	20,29	ns	0,9590

	WT vs. *Δxy*	9,809	19,79	ns	0,9666
	WT vs. *ΔABMΔxy*	9,809	60,16	*	0,0401
	WT vs. *Δ6*	9,809	60,48	*	0,0214
	ΔABM vs. *Δxy*	20,29	19,79	ns	>0,9999
	ΔABM vs. *ΔABMΔxy*	20,29	60,16	ns	0,0534
	ΔABM vs. *Δ6*	20,29	60,48	*	0,0214
	Δxy vs. *ΔABMΔxy*	19,79	60,16	ns	0,0520
	Δxy vs. *Δ6*	19,79	60,48	*	0,0211
	ΔABMΔxy vs. *Δ6*	60,16	60,48	ns	>0,9999

Finally, we also observed subtle accumulation in *C. albicans* SC5314. Results show significantly higher accumulation and/or adhesion for Neo-Ce6 than Ce6 alone (Fig. 28).

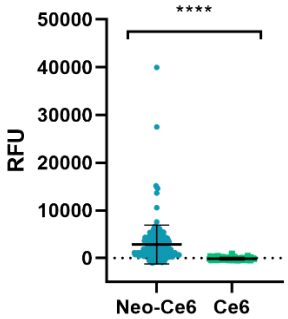

Figure 28: RFUs in *C. albicans* SC5314 with 1 µM of Neo-Ce6 and Ce6 at 200 ms of exposure with 642 nm. Bars represent mean and standard deviation. Asterisks represent a $p < 0.0001$ obtained through a t-test done on GraphPad Prism 8.4.3.

3.4 Antibacterial photodynamic therapy

3.4.1 Antimicrobial photodynamic therapy on planktonic cells

Overall, we observed a drop in survival following aPDT for all strains and all compounds. Disinfecting effect was observed when Neo-Ce6 was used against *S. aureus* Mu50, *S. aureus* USA300, *A. baumannii* DSM30011 and *E. coli* KanR and when Tobra-Ce6 was used against *S. aureus* Mu50. PSs and aminoglycosides alone impacted survival for some strains, but not as much as the compounds. Irradiation by all tested light sources never affected the survival of control samples and samples being incubated with the aminoglycosides alone. In addition, we also tested adding unlinked neomycin and Ce6 to some strains to confirm that Neo-Ce6 acted differently than both molecules separately. Results show survival was not affected by the addition of unlinked neomycin and Ce6 (Fig. 38).

3.4.1.1 Neo-MB and MB

Only a few bacterial species were used in aPDT with Neo-MB as the compound produced significantly less singlet oxygen than MB and ATTO-MB2 alone (Fig. 16). The compound did have a slight effect against a few species, like *E. coli* MG1655 (Fig. 29). Survival dropped 0.9 log10 CFU/mL and 1.8 log10 CFU/mL for Neo-MB at 5 µM and 10 µM

respectively when irradiated. The effect is similar without irradiation, with a drop of 0.9 log10 CFU/mL and 1.5 log10 CFU/mL for Neo-MB at 5 µM and 10 µM respectively.

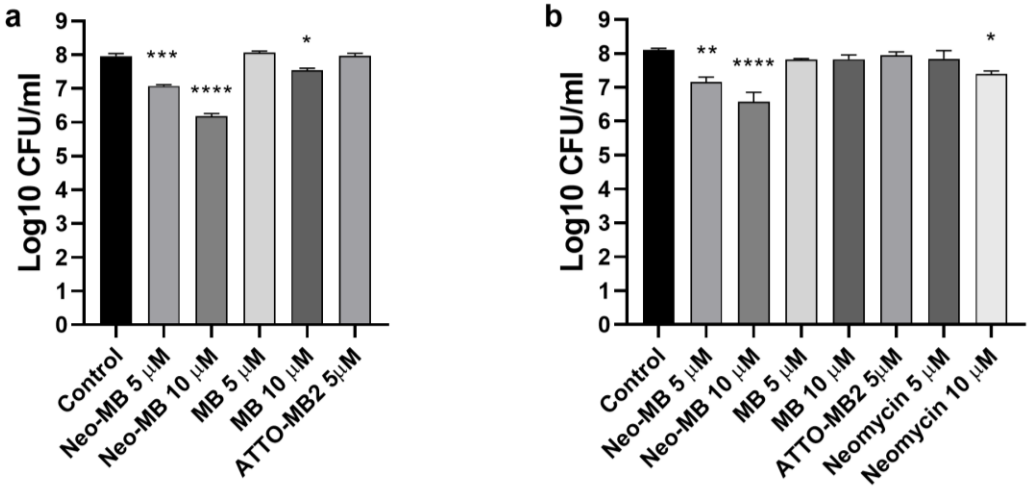

Figure 29: Log10 CFU/mL of *E. coli* MG1655 following aPDT with Neo-MB and MB. In a, with 15 minutes of irradiation and in b, without irradiation. Irradiated samples received a total of 84 mJ/mm².

Killing was also observed in *S. aureus* USA300, although not significant when not irradiated (Fig. 30). When irradiated, survival dropped by about 1 log10 CFU/ml for both 5 µM and 10 µM.

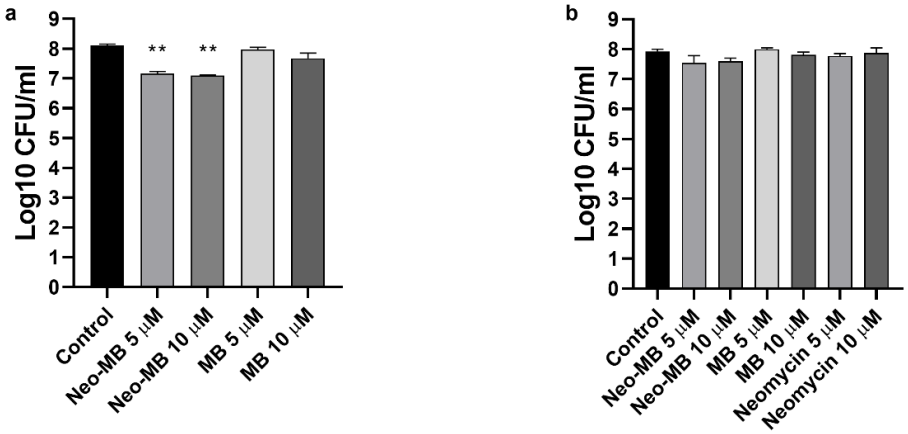

Figure 30: Log10 CFU/mL of *S. aureus* USA300 following aPDT with Neo-MB and MB. In a, with 15 minutes of irradiation and in b, without irradiation. Irradiated samples received a total of 84 mJ/mm².

In *P. aeruginosa* PA14, survival was lowered in both irradiated and non-irradiated samples (Fig. 31). Irradiated samples showed a drop of 1.3 and 1.4 log10 CFU/ml when treated with Neo-MB at 5 µM and 10 µM respectively, while in non-irradiated samples survival dropped 0.8 log10 CFU/ml and 1.3 log10 CFU/ml.

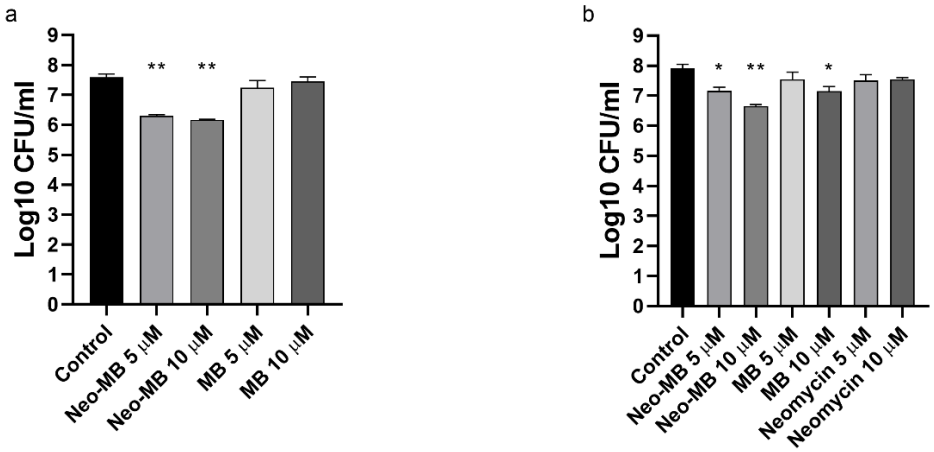

Figure 31: Log10 CFU/mL of *P. aeruginosa* PA14 following aPDT with Neo-MB and MB. In a, with 15 minutes of irradiation and in b, without irradiation. Irradiated samples received a total of 84 mJ/mm².

To further our understanding of the mechanisms involved in the penetration of some of our compounds, we also investigated the use of MB alone against *P. aeruginosa* PAO1 and its efflux pump mutants (Fig. 32).

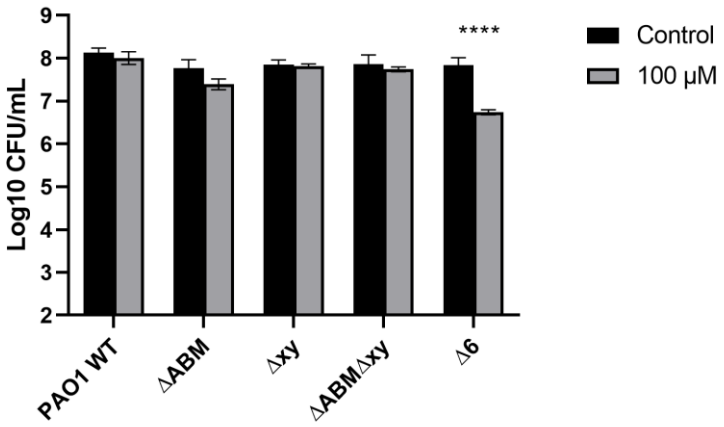

Figure 32: Log10 CFU/mL of *P. aeruginosa* PAO1 and mutants after 30 minutes of irradiation with 100 µM of MB. Irradiated samples received a total of 168 mJ/mm².

3.4.1.2 Neo-Ce6, Tobra-Ce6 and Ce6

Globally, tested strains were more susceptible to treatment with Neo-Ce6 than with Neo-MB. In *S. aureus* species Mu50 (an AG-resistant strain (Table 4) and USA300, survival was often close to or below the detection limit in irradiated samples treated with Neo-Ce6 (Fig. 33 a and e). Tobra-Ce6 did lead to high bacterial death in Mu50 (Fig. 33 a), showing a significant difference ($p = 0.0086$) when compared to Ce6 alone. However, this is the only *S. aureus* species for which Tobra-Ce6 leads to significantly less survival than the PS alone, meaning there is no additive effect to the linking of the AG to Ce6. On the other hand, except in *S. aureus* Newman, Neo-Ce6 leads to significantly more bacterial death than Ce6.

Mean CFU drops for irradiated samples are as follows. In *S. aureus* Mu50, survival dropped by 4.9, 5.4 and 3.2 log10 CFU/mL for Neo-Ce6, Tobra-Ce6 and Ce6 respectively. In

S. aureus Newman, survival was a little bit higher. Survival dropped by about 4.3, 3.9 and 3.6 log10 CFU/mL for Neo-Ce6, Tobra-Ce6 and Ce6 respectively. Finally, in *S. aureus* USA300, survival dropped by 5.6, 3.5 and 3.2 log10 CFU/mL for Neo-Ce6, Tobra-Ce6 and Ce6 respectively.

As shown in figure 33, non-irradiated samples treated with Neo-Ce6 always display a significant drop in CFUs (Fig. 33 b, d and f). Although the *p* is often low, this result has been seen in a few species, indicating the neomycin part of the compound may still have an effect when linked to Ce6. Plus, this effect may be additive as neomycin alone at the same concentration does not lead to significantly less survival, except in *S. aureus* USA300.

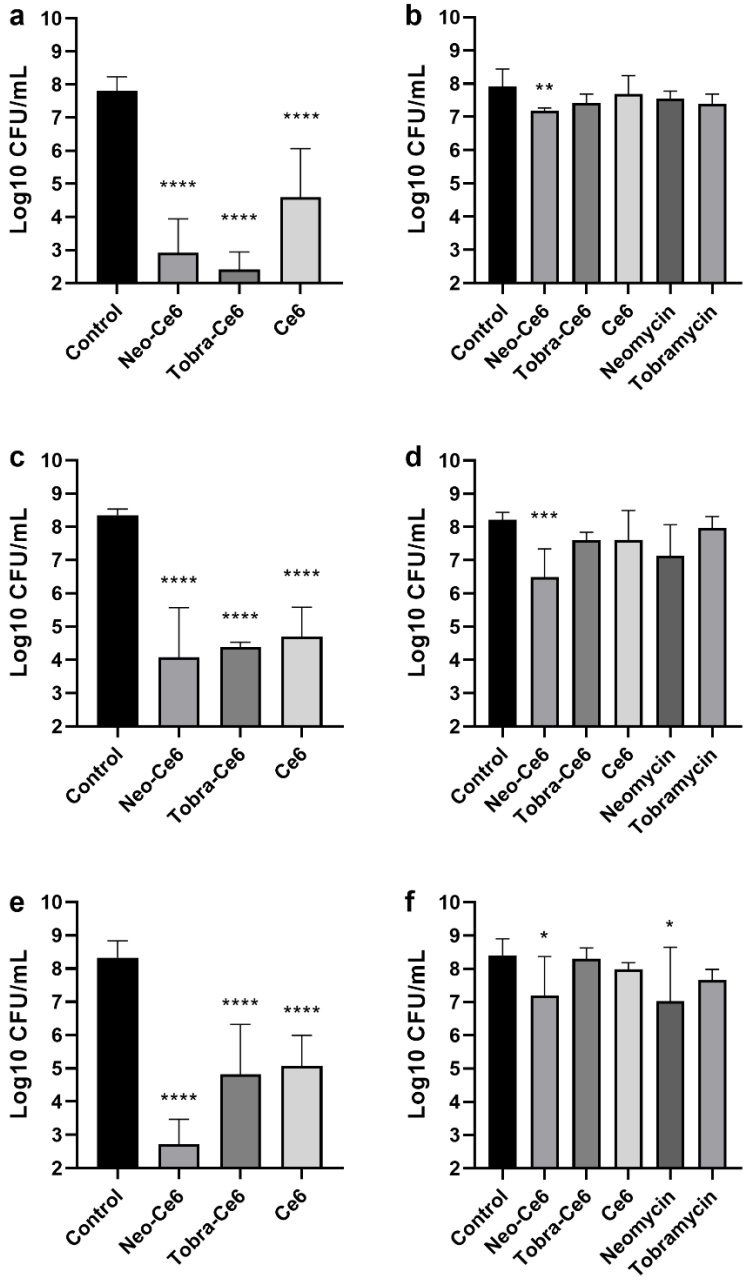

Figure 33: Log10 CFU/mL in *S. aureus* species following aPDT with 10 µM of Neo-Ce6 and Tobra-Ce6. In a and b, *S. aureus* Mu50 with and without irradiation respectively, in c and d, *S. aureus* Newman with and without irradiation respectively and in e and f, *S. aureus* USA300 with and without irradiation respectively. Irradiated samples received a total of 5 J/mm².

As described in the introduction, Gram-negative species are usually more resistant to aPDT than Gram-positive but we did have successful killing in most of our Gram-negative

strains. For example, *A. baumannii* DSM30011 CFUs were under the detection limit in irradiated samples with Neo-Ce6 (Fig. 34 a). Survival was also close to the detection limit for non-irradiated samples (Fig. 34 b). Irradiated samples in *B. subtilis* 168 were also close to the detection limit (Fig. 34 c).

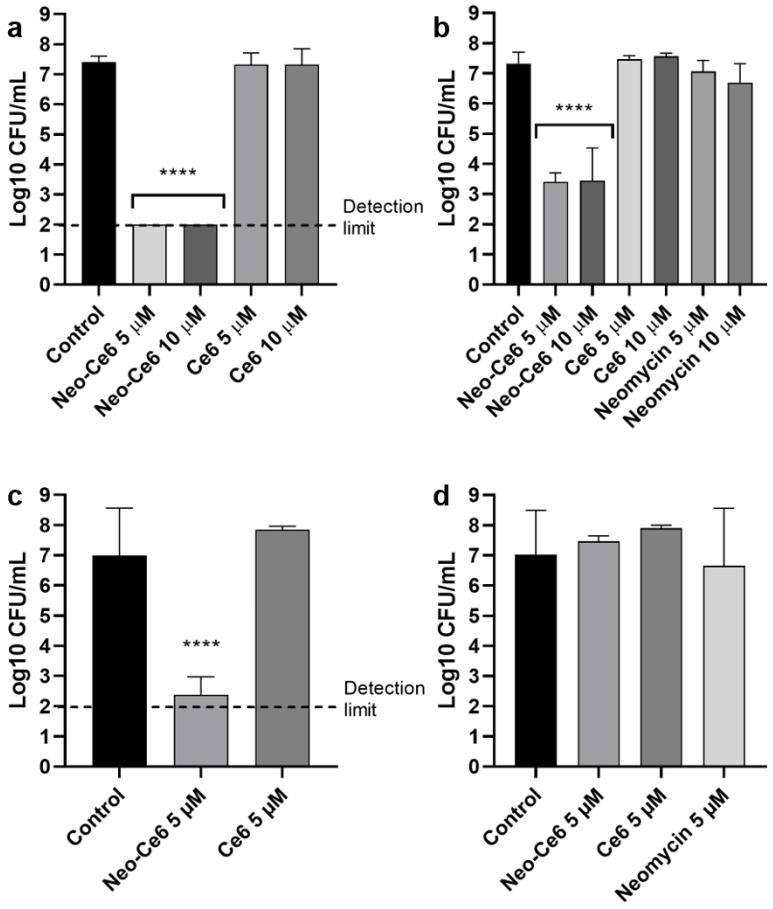

Figure 34: Log10 CFU/ml in Gram-negative and Gram-positive species following aPDT with Neo-Ce6. In a and b, *A. baumannii* DSM3001 with and without irradiation respectively, and in c and d, *B. subtilis* 168 with and without irradiation. Irradiated samples received a total of 168 mJ/mm².

K. pneumoniae LM21 survival was decreased with Neo-Ce6 at both 5 µM and 10 µM, with and without irradiation (Fig. 35 a and b). Capsule-defective mutant *Δcps* also showed less survival when treated with Neo-Ce6, with and without irradiation (Fig. 35 c and d). Similar results for irradiated and non-irradiated samples indicate that the Ce6 part of the compound may not be effective against the wild-type strain (Fig. 35 a and b). However, it adds to the penetrative and/or adhesion synergy as neomycin alone does not lead to bacterial death.

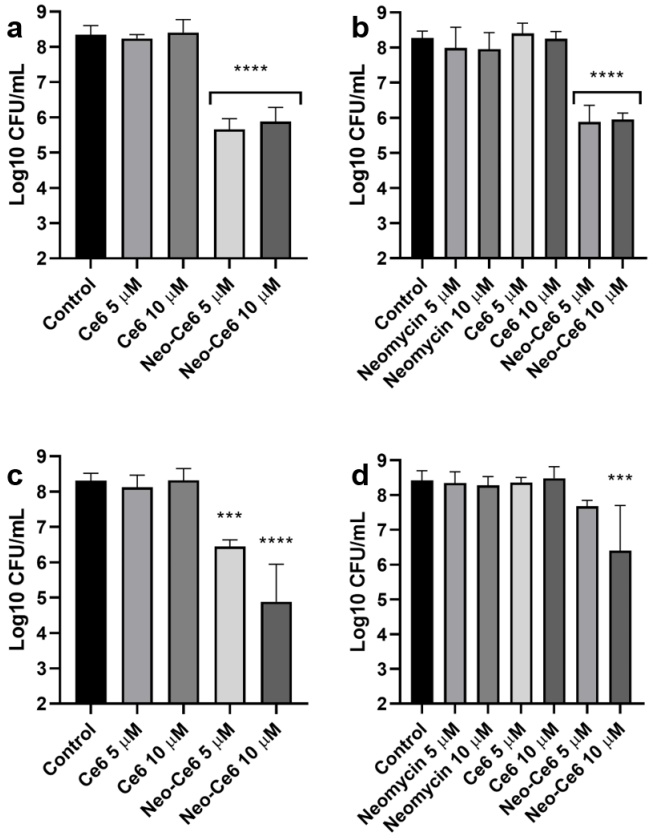

Figure 35: Log10 CFU/ml in *K. pneumoniae* species following aPDT with Neo-Ce6. In a and b, *K. pneumoniae* LM21 wild-type with and without irradiation respectively, and in c and d, *K. pneumoniae* LM21 *Δcps* with and without irradiation. Irradiated samples received a total of 168 mJ/mm².

E. coli MG1655 and a selection of mutants were also tested in order to further the understanding around the mechanisms involved in aPDT using Neo-Ce6 (Fig. 36). As shown in the following figure, survival against Neo-Ce6 at 10 µM was the lowest in the strain containing the kanamycin resistance cassette (nicknamed *E. coli* KanR). Statistical analysis has shown that the bacterial load is significantly lower for all mutants when compared to the wild-type. Two-way ANOVA between irradiated samples and non-irradiated samples also show that there is no significant difference in the survival for the *E. coli ΔtolC* and *E. coli* pET-29 mutants.

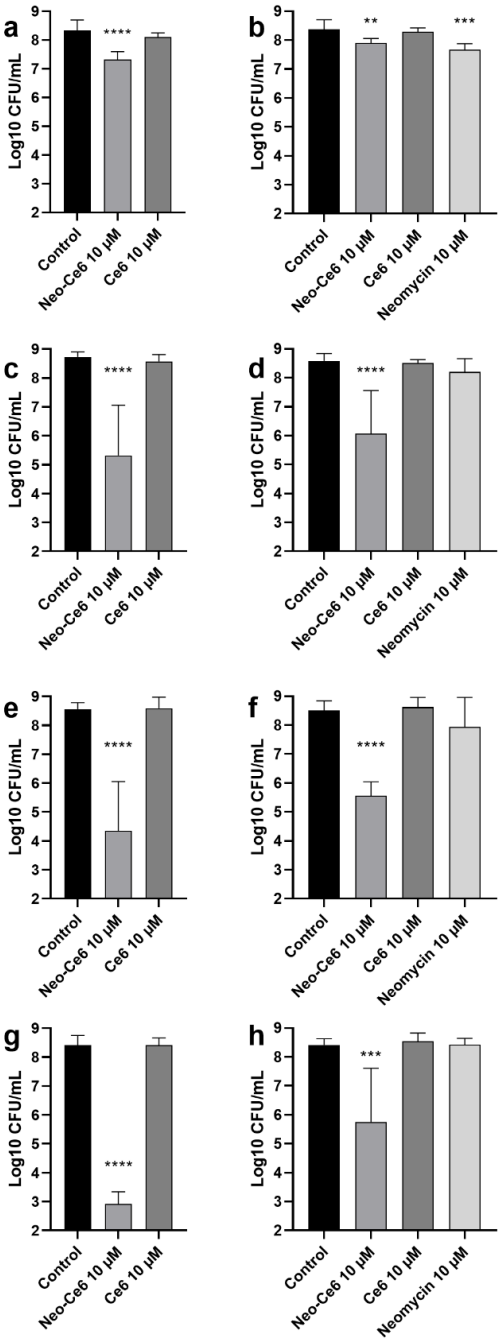

Figure 36: Log10 CFU/ml in *E. coli* and mutants following aPDT with Neo-Ce6. In a and b, *E. coli* MG1655 with and without irradiation respectively, in c and d, *E. coli ΔtolC* with and without irradiation, in e and f, *E. coli* pET-29 with and without irradiation, and in g and h, *E. coli* KanR with and without irradiation. Irradiated samples received a total of 168 mJ/mm².

Survival was also affected in clinically relevant strains from *P. aeruginosa* (Fig. 37). Survival dropped 3.8 and 2.6 log10 CFU/mL for irradiated *P. aeruginosa* PA14 cells treated with 10 µM of Neo-Ce6 and Tobra-Ce6 respectively. In *P. aeruginosa* PAO1, Neo-Ce6 showed a similar drop as in PA14 (3.6 log10 CFU/mL), while Tobra-Ce6 had slightly more effect (3.5 log10 CFU/mL). This is also seen in tobramycin alone, which led to a drop of survival of about 2.3 log10 CFU/mL. Irradiated samples treated with Tobra-Ce6 remain significantly lower than samples incubated with tobramycin however (p = 0.046), showing an additive effect from the addition of Ce6.

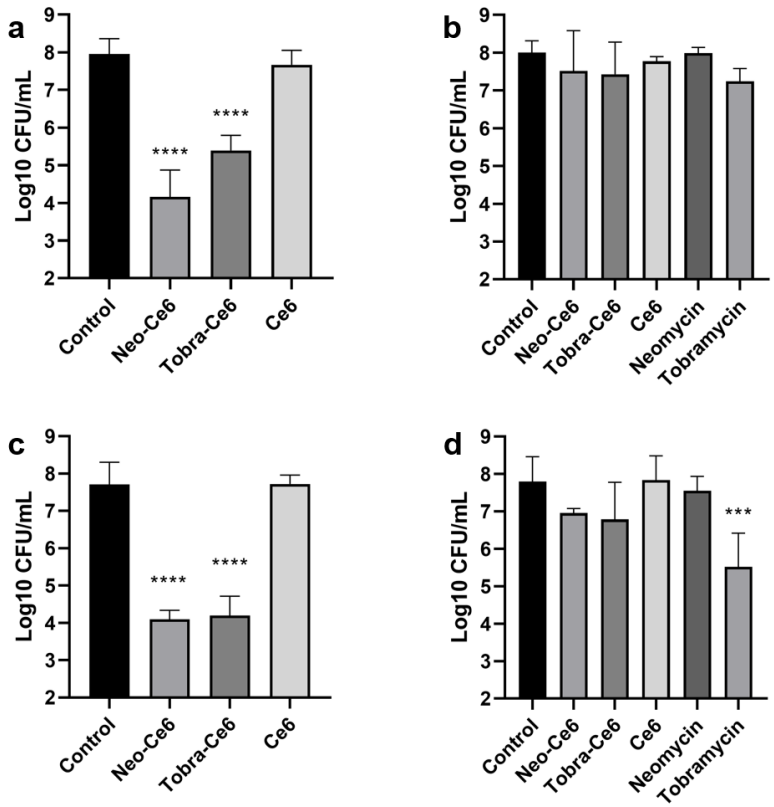

Figure 37: Log10 CFU/mL in *P. aeruginosa* species following aPDT with Neo-Ce6 and Tobra-Ce6. In a and b, *P. aeruginosa* PA14 with and without irradiation respectively, and in c and d, *P. aeruginosa* PAO1 with and without irradiation respectively. Irradiated samples received 5 J/mm². Concentrations are all 10 µM.

Controls were done to compare the addition of unlinked neomycin and Ce6 and the Neo-Ce6 compound. Survival rates were always significantly lower or equivalent when using the compound with irradiation than when using a mix of neomycin and Ce6 as seen in the examples in Figure 38.

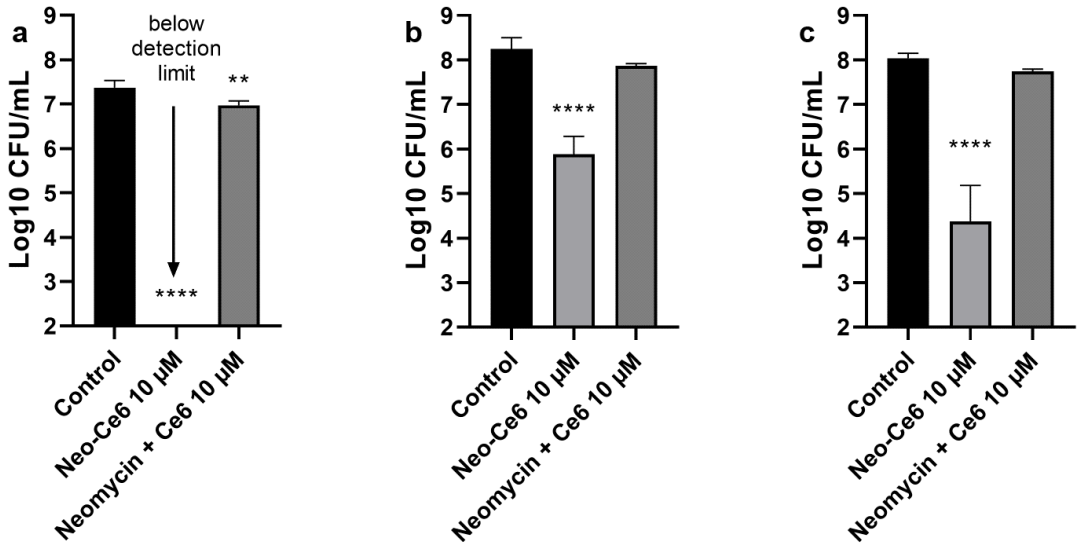

Figure 38: Comparison between aPDT with Neo-Ce6 and unlinked neomycin and Ce6 in a selection of species. With *A. baumannii* DSM3011 (a), *K. pneumoniae* LM21 (b) and *P. aeruginosa* PA14 (c). Irradiated samples only. Received 168 mJ/mm².

3.4.2 Minimal inhibitory concentrations

MICs were assessed visually as triplicates and are shown in Table 4. Synergy was calculated according to the fractional inhibitory concentration (FIC) for irradiated samples only (Doern, 2014).

The combination of neomycin and Ce6 in the Neo-Ce6 compound had a synergistic effect against *A. baumannii* DSM30011, *B. subtilis* 168, *C. albicans* SC5314, *S. aureus* USA300, *S. aureus* Mu50 and *S. aureus* Newman. On the other hand, the compound had an antagonistic effect against *E. coli* MG1655 and *K. pneumoniae* LM21, while having no negative or positive effect against *E. coli ΔtolC*, *P. aeruginosa* PA14 and *P. aeruginosa* PAO1.

Tobra-Ce6 on the other hand was only tested on a few species as results were not as promising. It showed an additive effect against *A. baumannii* DSM30011 and *S. aureus* Newman, but no synergy. We also tested some strains with the Solis-660C lamp without increasing synergy.

Table 4: MICs (µM) for neomycin, tobramycin, Ce6, Neo-Ce6 and Tobra-Ce6 with (+) or without (-) irradiation. FICs are expressed as follows: ++: synergy; +: additive; =: no difference; -: antagonistic. Bold species were irradiated with 5 J/mm², while other species were irradiated with 168 mJ/mm².

	Neo	Neo-Ce6		Synergy	Tob	Tobra-Ce6		Synergy	Ce6	
		+	-			+	-		+	-
A. baumannii DSM30011	8	0.5-1	16-32	++	4-8	2-4	> 16	+	> 64	> 64
B. subtilis 168	0.4	< 0.125	0.5-0.8	++					> 64	> 64
C. albicans SC5314	> 512	< 0.5	> 16	++					32	> 64
E. coli MG1655	4	16	8-16	-					> 64	> 64
E. coli tolC	4	4-8	8	=					> 64	> 64
E. coli KanR	> 512	> 16	> 16	ND					> 64	> 64
E. coli pET-29	128-256	> 16	> 16	ND					> 64	> 64
K. pneumoniae LM21	2	4-8	16	-					> 64	> 64
K. pneumoniae Δcps	256	> 16	> 16	ND					> 64	> 64
P. aeruginosa PA14	4	8	16	=	1-2	> 16	> 16	-	> 64	> 64
***P. aeruginosa* PAO1**	16	8-16	> 16	=	0.5-1	4-8	> 16	-	> 64	> 64
***S. aureus* USA300**	4	0.5	4-8	++	4	2-4	> 16	=	16-32	> 64
S. aureus Mu50	> 512	1-2	4-8	+	> 512	2-4	16	=	4	> 64
***S. aureus* Newman**	8	0.5	4-8	++	4	2	> 16	+	64	> 64

3.4.3 Antimicrobial photodynamic therapy on biofilms

As expected, biofilm cells were more resistant to aPDT than planktonic cells. A good example is *A. baumannii* DSM30011. Planktonic cells were under the detection limit (Fig. 34) while the cells found in the biofilm survived aPDT with both Neo-Ce6 and Tobra-Ce6. Survival dropped 2.6 and 4.1 log10 CFU/mL for Neo-Ce6 and Tobra-Ce6 respectively (Fig. 39).

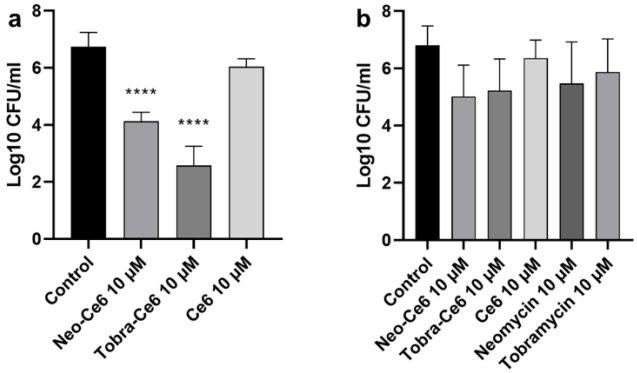

Figure 39: Log10 CFU/mL in *A. baumannii* DSM30011 biofilm cells following aPDT with Neo-Ce6 and Tobra-Ce6. With (a) or without (b) irradiation. Irradiated samples received 168 mJ/mm².

For *P. aeruginosa* species, biofilm cells also showed higher survival than planktonic cells. In irradiated samples, survival dropped 1.9 and 1.3 log10 CFU/mL when treated with 10 µM of Neo-Ce6 and Tobra-Ce6 respectively in *P. aeruginosa* PAO1 (Fig. 40 a). For *P. aeruginosa* PA14, results showed CFUs were lowered by 1.4 and 1.7 log10 CFU/mL for Neo-Ce6 and Tobra-Ce6 respectively (Fig. 40 c). Except in *P. aeruginosa* PAO1 treated with Neo-Ce6, statistical analysis comparing irradiated to non-irradiated samples led to no significant difference in survival. Therefore, the singlet oxygen must not be linked to the bacterial killing.

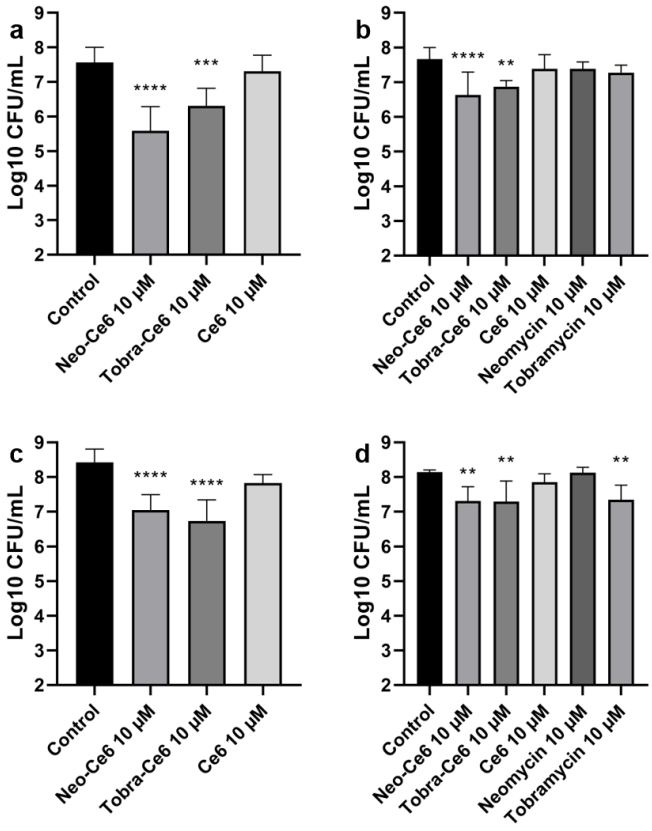

Figure 40: Log10 CFU/mL in *P. aeruginosa* biofilm cells following aPDT with Neo-Ce6 and Tobra-Ce6. In *P. aeruginosa* PAO1, with (a) or without (b) irradiation and in *P. aeruginosa* PA14, with (c) or without (d) irradiation. Irradiated samples received 5 J/mm².

In *S. aureus* species, Neo-Ce6 showed more effect against *S. aureus* Mu50 biofilm cells, reducing bacterial load by about 1.9 log10 CFU/mL, while only dropping by 1.1 in Newman and 0.8 in USA300. Tobra-Ce6 led to a drop of around 1.3 log10 CFU/mL in both Mu50 and Newman, while reducing bacterial load by 0.1 in USA300 (Fig. 41). No significant difference is seen between irradiated and non-irradiated samples for Newman. In Mu50, a *p*-value of 0.0012 and 0.019 is obtained through 2way ANOVA for samples treated with Neo-Ce6 and Tobra-Ce6 respectively. In USA300, a slight difference (*p*-value = 0.01) is observed for Neo-Ce6.

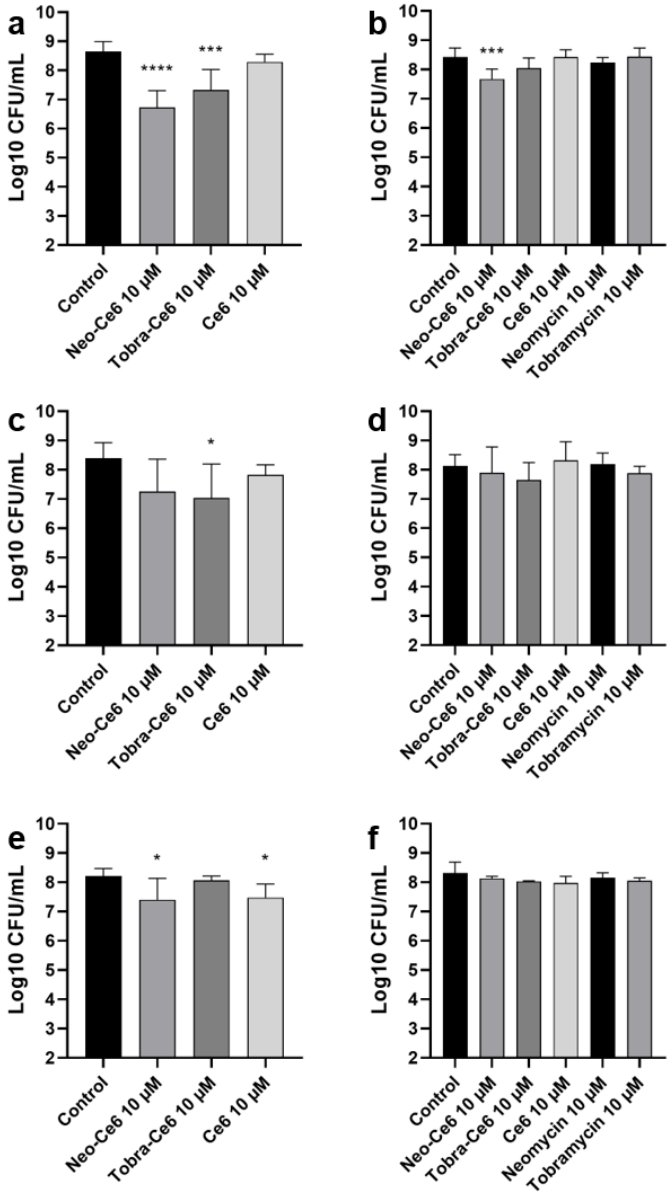

Figure 41: Log10 CFU/ml of biofilm cells in *S. aureus* species following aPDT with Neo-Ce6 and Tobra-Ce6. In *S. aureus* Mu50, with (a) or without (b) irradiation, in *S. aureus* Newman, with (c) or without (d) irradiation, and in S. aureus USA300 with (e) or without (f) irradiation. Irradiated samples received 5 J/mm².

3.4.4 Antimicrobial photodynamic therapy on persister cells

Antibacterial PDT did lead to persister death in most tested species. Some species, like *P. aeruginosa* PAO1 showed no drop in survival, while aPDT against PA14 persister cells did show slight killing. In Gram-negative *A. baumannii* DSM30011 and Gram-positive species *S. aureus* USA300 and Newman, aPDT against persister cells often led to CFU being under the detection limit.

Persister plateau and AG concentration varied from one species to another. In *S. aureus* USA300, a stable plateau was obtained following 6 hours of incubation with 2 mM of neomycin. The resulting persister cells were close to or under detection limit after aPDT with Neo-Ce6 and Tobra-Ce6 at 10 µM (Fig. 42 a). Ce6 alone also resulted in some killing as shown in Figure 42 a and statistical analysis show no significant difference in survival when comparing CFUs between Ce6 and Neo-Ce6. Neomycin alone resulted in no significant drop in survival, as expected. This control is crucial to make sure that a persister state has been achieved. CFUs were also lowered in samples that were not irradiated, showing that the synergistic penetration of the compounds may lead to an effect of neomycin even in cells in a persister state. As there are no significant differences between irradiated and non-irradiated samples however, the production of singlet oxygen may not be the factor leading to cell death.

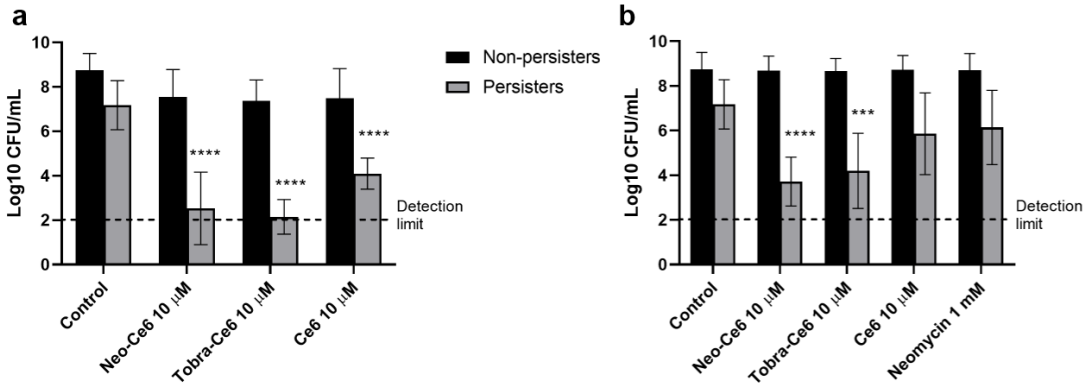

Figure 42: Log10 CFU/mL in *S. aureus* USA300 persister cells following aPDT with Neo-Ce6 and Tobra-Ce6. With (a) or without (b) irradiation. Samples received a total of 5 J/mm². Statistics were done using 2way ANOVA, comparing the mean of each column to the mean of the control for individual categories.

In *S. aureus* Newman, cells were treated for 24 hours with 1 mM of neomycin. Survival for irradiated persister cells treated with Neo-Ce6 and Tobra-Ce6 is significantly lower than in cells treated with Ce6 alone (Fig. 43). Although this synergy does exist, like in *S. aureus* USA300, there are no significant difference in survival for irradiated and non-irradiated samples, except for Ce6.

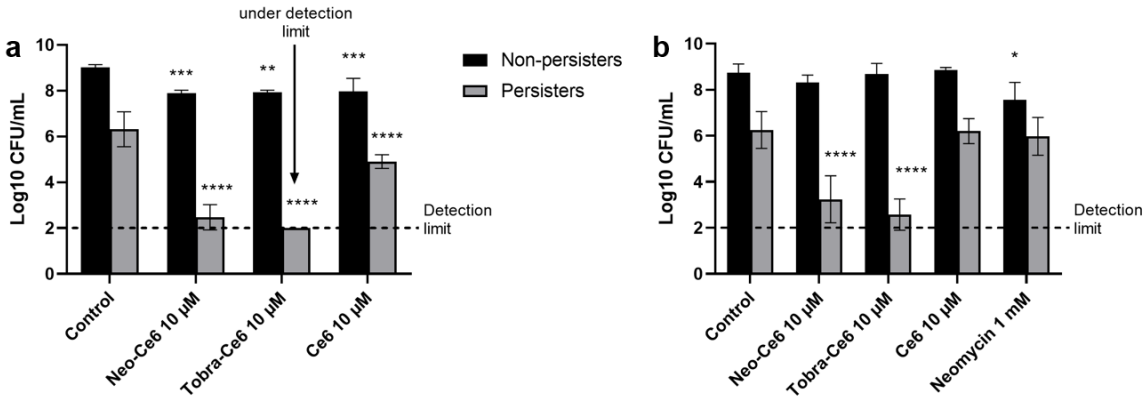

Figure 43: Log10 CFU/mL in *S. aureus* Newman persister cells following aPDT with Neo-Ce6 and Tobra-Ce6. With (a) or without (b) irradiation. Samples received a total of 5 J/mm². Statistics were done using 2way ANOVA, comparing the mean of each column to the mean of the control for individual categories.

Difference in irradiated and non-irradiated samples is found in Gram-negative bacteria *A. baumannii* DSM30011 where Neo-Ce6 leads to CFUs close to the detection limit (Fig. 44 c). Persister cells were obtained after incubation with 200 µM of neomycin for 24 hours. Treatment

in aPDT led to a drop of 3.5 and 1.8 log10 CFU/mL for Neo-Ce6 and Tobra-Ce6, while non-irradiated samples incubated with Neo-Ce6 only show a 1.4 log10 CFU/mL difference with the control (Fig. 44 c and d).

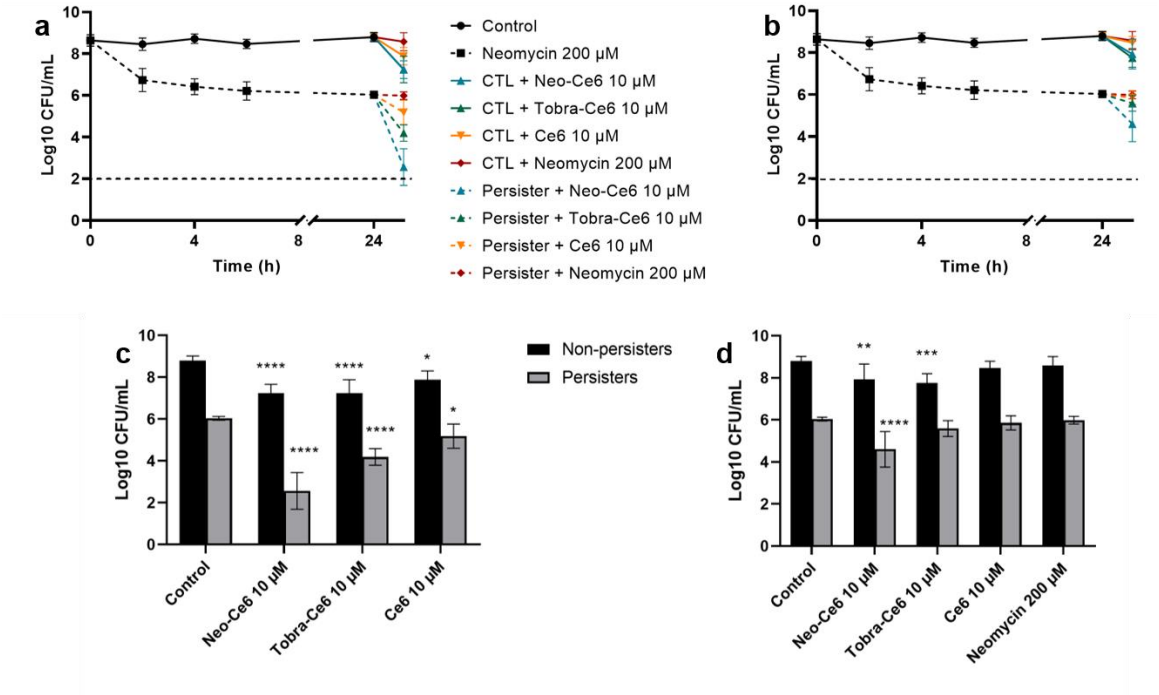

Figure 44: Log10 CFU/mL in *A. baumannii* DSM30011 persister cells following aPDT with Neo-Ce6 and Tobra-Ce6. Curves represent the persister plateau and results of the following aPDT, with irradiation (a) and without irradiation (b). The dashed line represents the limit of detection. Focus on aPDT results for persister and non-persisters cells, with irradiation (c) and without irradiation (d). Samples received a total of 5 J/mm². Statistics were done using 2way ANOVA, comparing the mean of each column to the mean of the control for individual categories.

In *P. aeruginosa* PA14, persister cells were obtained by treating with 1 mM of tobramycin for 24 hours. The effect of aPDT was not as impactful (Fig. 45 c and d), but there is a slight drop of 1.6 and 1.1 log10 CFU/mL for Neo-Ce6 and Tobra-Ce6 respectively.

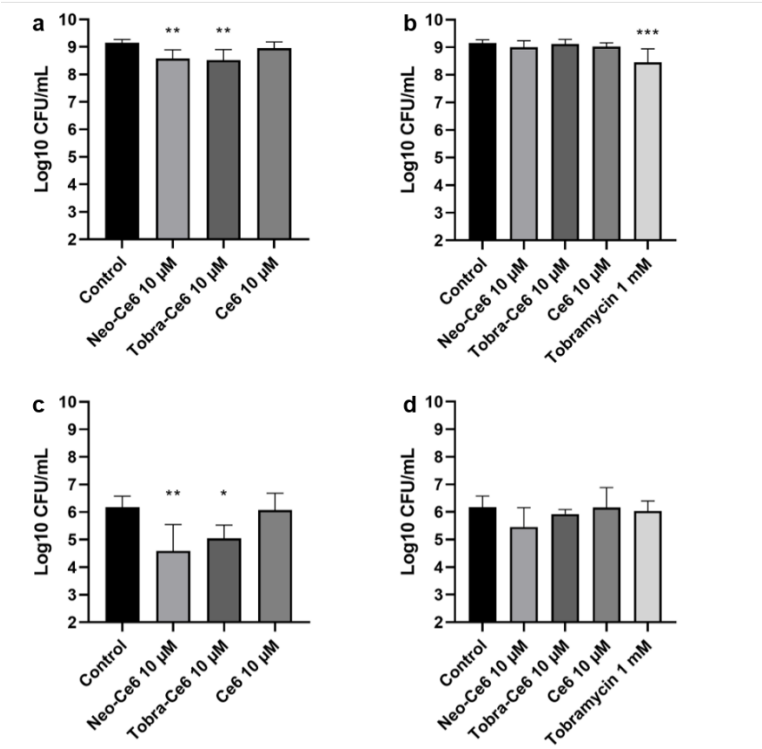

Figure 45: Log10 CFU/mL in *P. aeruginosa* PA14 non-persister cells with (a) or without irradiation (b) and in *P. aeruginosa* PA14 persister cells with (c) and without irradiation (d). Irradiated samples received 5 J/mm².

3.5 Cytotoxicity assays

Viability tests were done on MRC5 cells with increasing concentrations of Neo-Ce6. As shown in Figure 46, controls (0 µM) were not affected by the irradiation. Viability was non-existent for irradiated samples treated with Neo-Ce6 48 hours after the experiment. As for non-irradiated samples, the impact on viability was proportional to the concentration of Neo-Ce6.

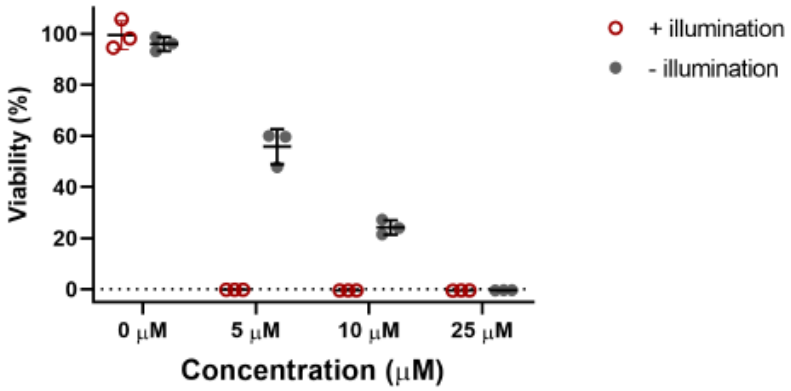

Figure 46: Viability of human MRC5 cells following aPDT with Neo-Ce6. Viability tests were done 48 hours after irradiation.

Cytotoxicity observations were later done on REL1 cells (retina cells) with doses ranging from 2.5 µM to 10 µM. We started by observing the cells 24 hours after the irradiation and noted total eradication at all concentrations, with and without irradiation. As we suspected cell aspiration during the wash, the experiment was done a second time and cells were observed after each step.

After 10 minutes of incubation with Neo-Ce6, most cells were already in a state of death. Observation after irradiation showed that killing was higher at small doses in non-irradiated samples, and that killing was the same in all irradiated samples. Post-wash observations on the

control wells revealed no aspiration of cells. After 24 hours, controls were still in a good state, indicating irradiation alone did not affect the cell survival, but all cells were dead in irradiated and non-irradiated wells treated with Neo-Ce6. We decided to not go one with viability tests as no cells were observed under the microscope.

CHAPTER 4

DISCUSSION AND CONCLUSION

The rise of drug-resistance in microbes puts the health system at risk worldwide and many scientists are worried we could go back to the pre-antibiotic era (Laxminarayan *et al.*, 2016; Renwick *et al.*, 2016). Many alternatives are being investigated like antibodies, bacteriophages, probiotics and others. Antibacterial photodynamic therapy (aPDT) is one of those alternatives, although less investigated. A review done on this subject by Czaplewski in 2016 covers 2287 citations from PubMed without mentioning aPDT. Although its use is limited due to the need of both a light source and oxygen, promising results, the reduction of virulence factors in surviving bacteria and the low risk for generating resistance within bacteria have increased interest in aPDT (Tseng *et al.*, 2017; Wainwright *et al.*, 2017).

For this project, we conjugated aminoglycosides (AGs) to photosensitizers (PSs) to evaluate their combined effect on several ESKAPE pathogens with a focus on biofilms and persister cells. AGs were chosen as they are known to penetrate biofilms and preliminary results from the laboratory had shown interaction of a neomycin-cyanine 5 (Neo-Cy5) conjugate with persister cells from *E. coli* MG1655 (Lebeaux *et al.*, 2015; Singh *et al.*, 2010; Walters *et al.* 2003).

We have chosen two PSs: methylene blue (MB) and chlorin E6 (Ce6). To be of interest, conjugates needed to check three conditions:

1. Singlet oxygen production similar to the PS alone;
2. Increased penetration and/or adhesion to bacterial cells;

3. Significant survival drop when used in aPDT against selected strains.

Three compounds were created: Neo-MB, Neo-Ce6 and Tobra-Ce6. All three were highly soluble and showed absorbance spectra that were very similar to the spectrum of the PS alone (Fig. 14). Analysis of the singlet oxygen production showed that the conjugation of neomycin and MB led to a decrease in yield (Fig. 16). This could be due to structural perturbation of MB which may have led to decreased excitability or a drop in type II reactions. Thus, Neo-MB was not studied as much as Neo-Ce6 and Tobra-Ce6.

For Neo-Ce6 and Tobra-Ce6, singlet oxygen production was higher than that of Ce6 alone (Fig. 17). Ce6 is poorly soluble in water which can lead to self-quenching and sub-optimal therapeutic efficacy (Jeong *et al.*, 2011). Thanks to the AG moiety, Neo-Ce6 and Tobra-Ce6 are highly soluble which could positively influence singlet oxygen formation by preventing aggregation. Stabilizing PSs to create more singlet oxygen is already explored in literature, although most of the methods include adding heavy atoms in the structure, like in Rose Bengal and squaraines (Fig. 3) or using a molecular symmetry-controlling strategy to fine-tune the excited state dynamics (Wang *et al.*, 2020). Sugar-aromatic interactions have been observed and play an important role in sugar recognition by proteins or nucleic acids (Fourmy et al. 1996; Quiocho, 1986). Whether such interactions would affect the photochemistry of Ce6 in our conjugates remains to be investigated. Although this possibility is unlikely because of the short length of the linker between the AG and Ce6.

The conjugation of an AG with a PS led to increased fluorescence when observing cells in fluorescence microscopy suggesting an increased accumulation. On the contrary, Ce6 and MB alone showed little to no fluorescence in tested species, even in Gram-positive species where PSs are known to penetrate more easily than in Gram-negative species (Malik *et al.*, 1992). This could be explained by the low concentration (1 µM) used for these experiments as we did not want to generate cell death while taking fluorescence imagery. This synergistic penetration and/or adhesion to cells is intriguing. First, by connecting Ce6 to neomycin or tobramycin one carboxylic group is engaged in the covalent linkage, leaving two carboxylic

groups free. This results in a decrease of the global cationic charge of neomycin. Second, the molecular mass of the AG more than doubles. O'Shea and Moser, while studying physichochemical properties that govern the entry of antimicrobials in bacteria, found that 95% of the compounds active against Gram-negative bacteria have a molecular weight below 600 Daltons (O'Shea and Moser, 2008). This suggests that the properties of Neo-Ce6 and Tobra-Ce6 are interesting as they seem to be well adapted to penetrate membranes of Gram-negative pathogens.

In addition to this heightened uptake, we witnessed bacterial explosions in some species (*P. aeruginosa* PA14 and *B. subtilis* 168) due to the laser excitation when taking time-lapse pictures. In these videos, killing occurred around 2 minutes and shows expulsion of Neo-Ce6 through bursts of fluorescence emerging from cells. In *B. subtilis* 168, spores were also fluorescent, indicating that sporulating pathogens could be affected by aPDT with Neo-Ce6 (Fig. 20). Destruction of *Bacillus* spores by aPDT has been shown for phenothiazinium salts, like MB and toluidine blue O. However, dyes like Rose Bengal and polylysine-Ce6 were shown to kill vegetative cells only (Demidova and Hamblin, 2005).

As for the third condition, aPDT on different types of cells from diverse species led to mixed observations. Globally, aPDT with the compounds did result in a significant drop in survival for some species. Disinfecting effect was even observed against *S. aureus* Mu50, *S. aureus* USA, *A. baumannii* DSM30011 and *E. coli* KanR for Neo-Ce6 and against *S. aureus* Mu50 for Tobra-Ce6. These results are explored in depth in the next section.

4.1 Antibacterial effect of aPDT with compounds

4.1.1 *S. aureus* species

Neo-Ce6 and Tobra-Ce6 were tested on a few species of *S. aureus*. Both *S. aureus* Mu50 and *S. aureus* USA300 are MRSA strains (Diep *et al.*, 2006; Kuroda *et al.*, 2001). *S. aureus* Mu50 is also known to be a vancomycin-intermediate strain (VISA) and it did show resistance towards neomycin and tobramycin (Table 4). *S. aureus* Newman on the other hand is known as being highly virulent but does not express any known marker of antibiotic resistance (Baba *et al.*, 2008).

Results were quite interesting for *S. aureus* Mu50. The survival in this strain was the lowest of all *S. aureus* species when testing against planktonic cells, with a disinfecting effect for both Neo-Ce6 and Tobra-Ce6 (Fig. 33 a). Neo-Ce6 did slightly reduce survival in non-irradiated samples, but there is a clear difference between irradiated and non-irradiated samples. Singlet oxygen is therefore involved in the effect of both compounds. Although Ce6 does reduce significantly the survival in *S. aureus* Mu50, survival is significantly lower in both compounds. Therefore, there is an additive effect of conjugating both molecules. Overall, these results are consistent with MIC values being lower for both conjugates when compared to Ce6 alone, with and without irradiation.

As for planktonic cells, *S. aureus* Mu50 biofilm cells showed lower survival than the two other strains, with a clear difference between irradiated and non-irradiated samples suggesting a clear effect from singlet oxygen (Fig. 41 a and b). CFUs are also significantly lower in irradiated samples treated with the conjugates than the samples incubated with Ce6

alone, suggesting an additive effect from linking both molecules. Slight killing in non-irradiated samples for Neo-Ce6 also suggests that the conjugate uptake was promoted in bacterial cells when comparing to neomycin alone.

Since *S. aureus* Mu50 is resistant to both neomycin and tobramycin (Table 4), it could be argued that the strain is more sensitive than other *S. aureus* strains to singlet oxygen and ROS. This could be linked to a reduced production of staphyloxanthin when compared to other *S. aureus* strains, as staphyloxanthin is a carotenoid molecule that protects *S. aureus* against ROS. When sensor proteins are oxidized, the AirSR regulator induces biosynthesis of staphyloxanthin (Hall *et al.*, 2017). Although results do not indicate clearly whether one strain produces more or less staphyloxanthin, a study done in 2018 shows similar survival in strains undergoing a H_2O_2 killing assay, with survival around 40% for both *S. aureus* Mu50 and *S. aureus* Newman, and survival around 50% in *S. aureus* USA300 (Ni *et al.*, 2018). Plus, *airSR* genes are involved in vancomycin resistance, meaning this regulator is present in *S. aureus* Mu50 and does promote staphyloxanthin production (Sun *et al.*, 2013). Thus, higher uptake could also be argued, but being a VISA, this strain is known to have a thicker cell wall than vancomycin-susceptible counterparts (Katayama *et al.*, 2016).

As antibiotic resistance does come at a cost, this susceptibility to singlet oxygen could be linked to reduced fitness within *S. aureus* Mu50. Planktonic cells in *S. aureus* Newman, which has no known genetic markers of antibiotic resistance, did show higher survival than both *S. aureus* Mu50 (ns) and *S. aureus* USA300 (p-value = 0.04) when treated with Neo-Ce6, and higher survival than *S. aureus* Mu50 when treated with Tobra-Ce6 (p-value = 0.04).

In *S. aureus* Newman, both compounds and Ce6 alone led to similar survival (Fig. 33 c). Those results suggest the AG part of the conjugate does not add to the bactericidal effect, but non-irradiated samples showed a slight drop in CFUs when incubated with Neo-Ce6. Although not significant, neomycin also did reduce CFUs by 1 log10 CFU/mL. In aPDT against biofilm cells (Fig. 41 c and d), there is almost no bactericidal effect but persister cells were close/under the detection limit for both compounds (Fig. 43 a and b). In the latter, there are no

significant difference between the survival of irradiated and non-irradiated samples. Therefore, the singlet oxygen does not seem to result in killing.

As for *S. aureus* USA300, the strain shows more sensitivity towards Neo-Ce6 than Tobra-Ce6. In irradiated samples, survival is similar when comparing Tobra-Ce6 and Ce6 (Fig. 33 e). In non-irradiated samples, Neo-Ce6 and neomycin do lead to a slight drop in survival with low significance (Fig. 33 f). Like *S. aureus* Newman, biofilm cells showed heightened resistance. Neo-Ce6 did succeed in killing 0.8 log10 CFU/mL with a slight significant difference with control cells (Fig. 41 e). Persister cells were around or below the detection limit for both Neo-Ce6 and Tobra-Ce6 in irradiated and non-irradiated samples (Fig. 42). Statistics do not show any significant difference in survival between irradiated cells treated with Ce6 and those treated with Neo-Ce6.

In sum, aPDT against planktonic, biofilm and persister cells in *S. aureus* species gave mixed results. The MICs resulted in Neo-Ce6 synergy against *S. aureus* Newman and *S. aureus* USA300 and an additive effect against *S. aureus* Mu50. Tobra-Ce6 only showed an additive effect against *S. aureus* Newman. In planktonic cells, the killing was likely linked to singlet oxygen production as survival in irradiated samples for the three strains was always lower than survival in non-irradiated samples. The addition of an AG molecule seemed to increase uptake and therefore the impact of singlet oxygen in *S. aureus* Mu50 for both molecules and for Neo-Ce6 in *S. aureus* USA300. Neo-Ce6 also led to slight killing in non-irradiated samples, showing there could be an increased uptake for this conjugate leading to an increase in neomycin reaching its target.

Almost no killing was observed for biofilm cells except in *S. aureus* Mu50. As mentioned earlier, this phenomenon could be explained by the attachment of the conjugate to the matrix around cells or to the lack of oxygen in the biofilm core. In addition, for the *S. aureus* Newman and the *S. aureus* Mu50 strains, this resilience cannot be linked to a persister state in the biofilm cells as results show high killing in persister cells pre-treated with high doses of neomycin.

As results for aPDT on persister cells were always close or below the detection limit. In *S. aureus* Newman, irradiated samples treated with Ce6 show higher survival than cells treated with the compounds, while both conjugates and Ce6 do not show significantly different results in *S. aureus* USA300. For both species, non-irradiated and irradiated samples show similar survival, meaning the singlet oxygen may not be the main cause of death, but a higher uptake in the linked AG results in lower survival.

4.1.2 *P. aeruginosa* species

Two main species of *P. aeruginosa* were used (Table 1), *P. aeruginosa* PA14 and *P. aeruginosa* PAO1.

Planktonic cells from both strains were susceptible to aPDT with our compounds (Fig. 37). Survival was similar for Neo-Ce6 in both strains while *P. aeruginosa* PA14 seemed to be more resistant to Tobra-Ce6 and tobramycin than *P. aeruginosa* PAO1. MIC values obtained during this project and those found in the literature do show that *P. aeruginosa* PAO1 is more susceptible to tobramycin than *P. aeruginosa* PA14 (Chen *et al.*, 2012; Tré-Hardy *et al.*, 2010). Difference in survival is significant for our compounds when comparing to non-irradiated samples and to irradiated Ce6. This clear difference in survival can be linked to an increased uptake of the PS part of the compound due to the AG and, therefore, to amplified oxidative damage from the singlet oxygen. In non-irradiated samples of *P. aeruginosa* PAO1, both compounds led to a slight and non-significant decrease in survival, indicating a probable increased penetration leading to the AG reaching its target.

Like *S. aureus* species, biofilm cells from both strains proved to be more resistant to aPDT. Statistics also show no clear difference between the survival of irradiated samples and the survival of non-irradiated samples (Fig. 40). This means the effect on biofilm cells is linked to the AG and not to Ce6. These results may indicate that the lack of oxygen is interfering with proper aPDT.

When aPDT was done on persister cells, *P. aeruginosa* PAO1 proved to be problematic. The cells were incubated with 2 mM of neomycin for 24 hours. During the first 6 hours, a plateau would form. The next day, a sample was taken at 24 hours and aPDT was done on both control cells and what were considered to be persister cells. Results showed that the strain seemed to go through adaptative resistance as controls from the "persister cells" group had almost the same CFUs as controls from the normal group. This is a technical obstacle that prevents assessing the conjugates efficiency in aPDT on persisters of *P. aeruginosa* PAO1. In *P. aeruginosa* PA14, a stable plateau was obtained after incubating cells with 1 mM of tobramycin for 24 hours and Neo-Ce6 and Tobra-Ce6 led to a drop of 1.6 and 1.1 log10 CFU/mL respectively (Fig. 45 c).

4.1.3 Other species

Many other species were tested, such as *E. coli* and *K. pneumoniae*. These species were mostly investigated with the goal of understanding the mechanism of action of our compounds and are explored in depth in the next section.

Briefly, WT strains from both species turned out to be quite resilient to aPDT. MICs for both species show an antagonistic effect from linking both the Ce6 and the AGs (Table 4). *K.*

pneumoniae LM21 did show a little bit over 2 log10 CFU/mL drop in survival in both irradiated and non-irradiated samples. *E. coli* MG1655 turned out to be quite resilient to aPDT with a mere 1 log10 CFU/mL drop in survival in irradiated samples treated with Neo-Ce6. Surprisingly, the strain was more susceptible to Neo-MB (Fig. 35).

Other species included *A. baumannii* DSM30011, *B. subtilis* 13517 and pathogenic yeast *C. albicans* SC5314. MICs against those species showed high synergy for linking neomycin to Ce6. The FIC for *C. albicans* SC5314 was very low, showing that the compound was highly efficient compared to neomycin and Ce6 alone. Interestingly, although fluorescence microscopy did show higher RFUs for Neo-Ce6 than Ce6 in the yeast, the mean value was not that striking when compared to bacterial strains (Fig. 28). Unfortunately, we could not explore aPDT against *C. albicans* SC5314 due to lab restrictions but literature does show that *C. albicans* is sensible to aPDT with Ce6 linked to "vessels" such as graphene and liposomes (Rodriguez-Cerdeira *et al.*, 2021).

aPDT against planktonic cells from *A. baumannii* DSM30011 and *B. subtilis* 13517 showed very low survival (Fig. 34). In *A. baumannii* DSM30011, CFU counts were under the detection limit for irradiated samples and close to this threshold in non-irradiated samples (Fig. 34 a and b). Due to these results, it is hard to say if there is a significant difference in survival. As Ce6 and neomycin alone led to no reduction in survival, results clearly suggest an increased uptake for Neo-Ce6 at 5 and 10 µM. In *B. subtilis* 13517, the effect is clearly linked to singlet oxygen production as survival is not lowered in non-irradiated samples incubated with 5 µM of Neo-Ce6.

Further tests were done against *A. baumannii* DSM30011. Biofilm cells, like in *S. aureus* and *P. aeruginosa*, were more resilient to aPDT. Like in planktonic cells, Neo-Ce6 did not lead to a significant difference in survival when comparing irradiated and non-irradiated samples. Tobra-Ce6 did lead to significantly lower survival in irradiated biofilms. Persister cells from this strain were also investigated following a 24-hour long incubation with 200 µM of neomycin. Irradiated persister cells treated with Neo-Ce6 were often close or below the

detection limit and results show a clear difference between irradiated and non-irradiated persister cells. Interestingly, non-persister cells (Fig. 44 c) do not show the same susceptibility in this experiment when compared to planktonic cells (Fig. 34 a). This may be linked to the cell density which is in turn linked to oxygen availability (Maisch *et al.*, 2007).

4.1.4 Summary of aPDT results

Interesting results were obtained for both Neo-Ce6 and Tobra-Ce6 against most of the selected species, although some were slightly unclear. For example, even though it is clear that our compounds show increased uptake and that death is mainly linked to singlet oxygen production in both planktonic and biofilm cells in *S. aureus* Mu50, the compounds barely affected biofilm cells in *S. aureus* USA300 and showed no increased uptake in *S. aureus* Newman planktonic cells. What is clear is that biofilm cells were more resistant to aPDT with the conjugates.

We speculate that a few factors may lead to reduced killing when comparing to planktonic cells. First, the lack of oxygen at the core of biofilms may inhibit singlet oxygen production (Gad *et al.*, 2004; Walters *et al.*, 2003). This was witnessed in a few species where irradiated planktonic cells showed lower survival than non-irradiated samples, while biofilm cell CFUs were the same for irradiated and non-irradiated samples. Literature also shows that low pH leads to Ce6 aggregation and then to reduced singlet oxygen yield (Datta *et al.*, 2002; Čunderlíková *et al.*, 1999). This could also explain some results as biofilms produced by some species have a lower pH than the surrounding environment (Hollmann *et al.*, 2021). In *S. aureus* however, this pH hypothesis is difficult to evaluate as acidity leads to thinner biofilms in those species which would favor accessibility of conjugates (Nostro *et al.*, 2012).

Then, the conjugates may adhere to the matrix, which lowers the concentration of conjugate which truly reaches the cells imbedded in the biofilm. Such behavior was witnessed when doing fluorescence microscopy of mucoid strain *P. aeruginosa* PAO1 where "clouds" of fluorescence surrounded bacterial cells as the conjugates adhered to the secreted alginate. Poor uptake in biofilms and difficulties reaching lower matrix layers are problems that have been reported in literature (Gad *et al.*, 2004). These limitations seem to be less of a concern when using cationic PSs-conjugates though, which is the case for poly-lysin-Ce6 (Zanin *et al.*, 2005) Lastly, as explored in the introduction, it is hypothesized that biofilm cells are in a persister state (Waters *et al.*, 2016; Lewis, 2001). However, results against a few species, including *S. aureus* Newman and *S. aureus* USA300 do show that the compounds are efficient against persister cells while biofilm cells are resilient to aPDT.

The reduced effect of our compounds on biofilms therefore seems to be mainly linked to oxygen deprivation. Although not shown, we did switch to a "pulsing" method after a period of testing on biofilms. When aPDT was done by using "pulsing" (Section 2.3.3), where 5 minutes of irradiation would be followed by 60 seconds of darkness, survival was slightly lower although not significant. Usually, this technique is used when lasers are the source of light and are meant to allow oxygen renewal between each pulse.

As for persister cells, results were interesting in *A. baumannii* DSM30011, *S. aureus* Newman and *S. aureus* USA300. When comparing to the survival of planktonic cells and biofilm cells of the same species, those results lead to a few questions. Obviously, as cell density is lowered in persister samples due to the presence of a high concentration of AG, this could positively impact aPDT efficiency as the oxygen supply is high (Maisch *et al.*, 2007). However, most of the strains show mortality in their non-irradiated samples as well (Fig. 42 and 43). Due to these results, it seems the persister death is rather linked to synergy in uptake and a double-effect from linked molecules than singlet oxygen alone.

There is also a discrepancy between planktonic and persister cells in the *P. aeruginosa* species. As mentioned earlier, *P. aeruginosa* PAO1 seemed to gain resistance to neomycin, showing regrowth at 24 hours and preventing to reach a stable plateau. As a consequence, cells incubated with neomycin were resisting aPDT with both Neo-Ce6 and Tobra-Ce6. Therefore, this technical obstacle prevented testing the efficiency of the conjugates on these persisters. Plus, although *P. aeruginosa* PA14 reached a stable plateau at 24 hours, aPDT had almost no effect against the persister cells. In 2016, a team did find *P. aeruginosa* subpopulations that showed a persister state following aPDT with MB (Forte Giacobone *et al.*, 2016). Their results suggest that *P. aeruginosa* could produce aPDT-specific persisters with no cross-tolerance to antibiotics. However, a 2018 study by the same team does show that the experiment is also applicable in the other way, meaning that treatment with ofloxacin followed by aPDT with MB did lead to decreased survival (Oppezzo and Forte Giacobone, 2018). Another way to explain this increased resilience in *P. aeruginosa* PA14 could be that environmental stress (here AG stress) promotes a reduction of non-specific porin proteins in exchange for more nutrient specific porins (Tamber and Hancock, 2003). As for regrowth in *P. aeruginosa* PAO1, it could be adaptive resistance, a transient state caused by environmental stress and antibiotic pressure in which *P. aeruginosa* becomes temporarily resistant to some antibiotics, including panaminoglycoside resistance (Poole, 2005; Karlowsky *et al.*, 1997; Gilleland *et al.*, 1989). This description is similar to the definition of persistence, but the nuance is that persister cells do not or barely duplicate (Balaban *et al.*, 2004).

4.2 Analyzing the mechanism of action

The use of mutant strains allowed us to study and to theorize the mechanisms of action involved in the aPDT process with the compounds. Some of our data was obtained using bacteria containing resistance cassettes and some lacking efflux pumps.

Fluorescence microscopy allowed us to evaluate adhesion and/or uptake of our conjugates and PSs alone. However, this data is partly challenged by the fact that literature indicates for eukaryotic cells that pharmaceutical drugs are estimated to have around six protein binding targets within cells, including transporters (Kell *et al.*, 2013; Mestres *et al.*, 2009). On the other hand, the "Phospholipid Bilayer diffusion is Negligible" movement, referred to as "PBIN", contests the fact that xenobiotic elements simply move through the cellular membrane (Jindal *et al.*, 2019; Kell, 2015; Kell and Oliver, 2014). This means that transporters, influxers like effluxers, are an important variable to study to understand the uptake mechanisms of the conjugates. AG uptake remains largely unknown and is supposed to mostly rely on a self-promoted uptake mechanism via the lipopolysaccharides (Hancock and Bell, 1988). Recent work also suggests that porins could have a role in AG uptake (Prajapati *et al.*, 2021; Bafna *et al.*, 2020). It is important to note that most bacteria have multiple efflux systems and that a knock-out for one efflux system does not necessarily lack the capacity to export tested molecules, and this knock-out is not necessarily more susceptible (Ma *et al.*, 1994).

4.2.1 *E. coli, K. pneumoniae* and mutant strains

In *E. coli*, three mutants were tested: *E. coli ΔtolC*, *E. coli* KanR and *E. coli* pET-29 (Table 1). Because of the lack of the outer membrane domain of an important transport channel, it was expected that RFUs would be higher in the *E. coli ΔtolC* mutant when compared to the WT strain due to absence of efflux (Korokanis, 2003; Fralick, 1996). Tobra-Ce6 did show significantly higher RFUs in *E. coli ΔtolC* than in the WT strain, but it wasn't the case for Neo-Ce6 and Ce6 alone (Fig. 21). Visually, fluorescence was periplasmic in *E. coli ΔtolC* while being more diffuse in *E. coli* MG1655 with Neo-Ce6 and Tobra-Ce6.

These results may seem contradictory, but disruption of the tolC gene does not lead to increased cytoplasmic uptake and to AG susceptibility (Rosenberg *et al.,* 2000). In fact, the periplasmic accumulation may be explained by this mutation. According to a 2005 study, AcrD, a transporter from the resistance-nodulation-division family, promotes the efflux of AGs from both the periplasm and cytoplasm with the help of TolC (Aires and Nikaido, 2005). However, due to their hydrophilic and cationic nature, AGs do not easily cross into the cytoplasm (Rosenberg *et al.,* 2000). Therefore, due to the lack of TolC, the Neo-Ce6 possibly accumulates in the periplasm.

Although RFUs were higher in the WT strain, *E. coli ΔtolC* was slightly more sensitive than *E. coli* MG1655 with an irradiated MIC of 4-8 µM versus 16 µM for Neo-Ce6. In aPDT, *E. coli ΔtolC* showed lower survival than *E. coli* MG1655 and survival was also affected in non-irradiated samples. Treatment with 10 µM of Neo-Ce6 led to a drop of 3.4 and 2.5 log10 CFU/mL for irradiated and non-irradiated samples in *E. coli ΔtolC*. As there are no significant difference between survival in those samples, it is fair to say that Ce6 is not linked to heightened killing. Still, it may promote uptake as neomycin alone does not lead to any drop in survival in non-irradiated samples.

The two kanamycin-resistant strains, *E. coli* KanR and *E. coli* harboring pET-29, also showed different visual profiles. *E. coli* KanR was hardly fluorescent when incubated with Neo-Ce6 while the compound seemed to gather in the periplasm of *E. coli* pET-29. If such periplasmic accumulation is expected for a short exposition to a low concentration of conjugate, a difference in fluorescence levels is expected (Sabeti-Azad *et al.*, 2020). This could be explained by the fact that it is believed that the AG modifying enzymes (AMEs) found in *E. coli* KanR is periplasmic while it is cytoplasmic in *E. coli* pET-29. It is also important to note that both AMEs, although they both add phosphate group on the 3' position, are not exactly the same. In *E. coli* pET-29, it is an aminoglycoside-phosphotransferase-(3')-Ia (APH-(3')-Ia), while it is an APH-(3')-IIa in *E. coli* KanR, and those form two distinct groups. The APH-(3')-I subclass is found widely in Gram-negative species, on plasmids and transposons, and shows resistance to kanamycin, neomycin, paromomycin, ribostamycin and lividomycin (Ramirez and Tolmasky, 2010). The APH-(3')-II subclass shows resistance to kanamycin, neomycin, butirosin, paromomycin and ribostamycin (Ramirez and Tolmasky, 2010).

Some of these observations reflect on the MICs and aPDT results. In *E. coli* KanR and *E. coli* pET-29, the inhibitory concentrations were higher than the set threshold of 16 µM for Neo-Ce6 and both strains showed resistance towards neomycin alone. Since the WT strain showed more susceptibility to Neo-Ce6, these results suggest that both AMEs can still modify the 3' site on the neomycin part of the conjugate. Since the Ce6 is linked on the 5'' on the third cycle, it is highly probable, although hard to verify as we do not have a confirmed 3-dimensional structure (Fig. 13). As aPDT on planktonic cells does show bacterial killing, perhaps that Neo-Ce6 accumulates in the periplasm of *E. coli* pET-29 during the MIC assays and that the random oxidative damages of singlet oxygen target molecules that are less valuable to survival of the strain, making it possible for the bacteria to duplicate after irradiation. For example, it may have an effect on the outer membrane, which is not crucial to Gram-negative survival (Dahl *et al.*, 1989; Straight and Spikes, 1985). However, even if the AMEs can impact the AG part of the compound, this should not affect the Ce6 as seen for aPDT with Neo-Ce6 on the strain *E. coli* KanR and, to a weaker extent, on *E. coli* pET-29.

In *E. coli* KanR planktonic cells, aPDT with 10 µM of Neo-Ce6 led to a drop of 5.5 log10 CFU/mL. In *E. coli* pET-29, Neo-Ce6 led to a drop of 4.2 log10 CFU/mL. The neomycin moity of the conjugate was able to reach its target as Neo-Ce6 resulted in a survival drop of 2.7 and 2.9 log10 CFU/mL in non-irradiated samples. In comparison, neomycin alone led to no killing in *E. coli* KanR and a mere 0.5 log10 CFU/mL drop in *E. coli* pET-29. Maybe the AMEs cannot interact efficiently with the neomycin molecule while it is linked to Ce6 and/or the synergy between both molecules allow for a higher uptake which "overwhelms" the AMEs. It is also interesting to note that at 10 µM of Neo-Ce6, survival of *E. coli* KanR and *E. coli* pET-29 was significantly lower than the survival of the WT strain ($p < 0.0001$ for *E. coli* KanR and $p = 0.005$ for *E. coli* pET-29). These results are also at the opposite of what is seen in fluorescence microscopy where mean RFUs for Neo-Ce6 were significantly higher in the WT than in the three other strains (Table 2). In fact, when comparing the mean survival following aPDT with the mean RFUs, a linear correlation with a R^2 of 0.99 is obtained. These results could mean that the RFUs in the WT strain are linked to adhesion rather than uptake as visually, some cells do present periplasmic fluorescence while others show more diffuse fluorescence. Another WT strain, *E. coli* LF82, was also briefly studied and also showed higher resilience. For example, MICs for Neo-Ce6 and Ce6 were over 16 µM and 64 µM respectively while having a MIC of 4 µM when tested with neomycin.

K. pneumoniae LM21 and the capsule-deficient mutant *Δcps* were also analyzed. RFUs for Neo-Ce6 were significantly higher in the *Δcps* strain than in the WT. Visually, fluorescence in *K. pneumoniae* LM21 was more diffuse while Neo-Ce6 seemed to gather in the periplasm of *Δcps*. MICs were lower in the WT strain. This is explained by the presence of a kanamycin resistance cassette (expressing a APH(3')-II enzyme) used to induce the deficiency in the *Δcps* strain (Balestrino et al., 2008). Consequently, the MIC for neomycin was at 256 µM for the mutant while it was at 2 µM for the WT strain. The MIC for Neo-Ce6 in irradiated samples was higher than 16 for the mutant, like for *E. coli* KanR and *E. coli* pET-29, and at 4-8 µM for the WT strain. After aPDT on planktonic cells, Neo-Ce6 led to a drop of around 2.5 log10 CFU/mL for both concentration in *K. pneumoniae* LM21 while it killed 1.9 and 3.4 log10 CFU/mL at 5 and 10 µM respectively in *Δcps*. The major difference between strains was observed in non-

irradiated samples. The WT strain was more affected by unexcited Neo-Ce6 than *Δcps* and, consequently, survival in irradiated samples was not significantly different from survival in non-irradiated samples. This result is consistent with some levels of cytoplasmic uptake for the WT strain as suggested by the diffused signals in fluorescence microscopy. In *Δcps*, there was a slightly significant difference. Since survival was higher in non-irradiated samples from this mutant when compared with the WT, we can suppose this is linked to the presence of the APH(3')-II AME. We note that aPDT in *Δcps* was efficient for the highest concentration of Neo-Ce6 indicating that this strategy allows killing AG-resistant strains as observed for *E. coli* pET-29 and KanR strains.

Although the lack of capsule could have been an interesting variable to observe, the fact that there is a kanamycin resistance cassette and a clear neomycin resistance makes it difficult to see what is due to the deficient capsule or linked to the resistance.

Results for *E. coli* and *K. pneumoniae* suggest two things. First of all, since neomycin alone does not lead to any significant reduction in CFUs while Neo-Ce6 in non-irradiated samples does reduce survival, this confirms that the neomycin portion of the compound is still functional and that uptake is promoted by the linking of Ce6. This synergy also applies to the neomycin portion promoting the uptake of Ce6 as Neo-Ce6 always leads to significantly lower survival than Ce6 alone.

4.2.2 *P. aeruginosa* PAO1 and efflux pump mutants

We decided to further the understanding of the compounds by studying other transport mechanisms through the use of *P. aeruginosa* and four efflux pump mutants. Efflux pumps in

bacteria contribute to their resistance by expulsing a wide variety of substrates like antimicrobials, organic solvents, detergents, dyes and much more (Fruci and Poole, 2018). In *P. aeruginosa*, the tripartite pumps from the resistance-nodulation-cell-division (RND) family are determinants of drug resistance within isolates. Some examples include AG resistance being linked to the MexXY efflux system while triclosan resistance is recognized as being caused by the TriABC pump (Morita et al., 2012; Mima et al., 2007). These pumps are composed of three domains: an antiporter driven by the PMF (MexB, MexD, MexF and MexY), a periplasmic fusion protein (MexA, MexC, MexF and MexX) and an outer membrane portion (OprM, OprJ and OprN) (Lister et al., 2009). These pumps are more or less expressed depending on conditions and antibiotic pressure.

As mentioned in Table 1, we have four mutants. One for the MexAB-OprM pump (*ΔABM*) and one for MexXY (*Δxy*). We also tested a mutant for those two systems (*ΔABMΔxy*) and one lacking all crucial efflux systems nicknamed *Δ6* that is mutated for MexAB-OprM, MexXY, MexCD-OprJ, MexEF-OprN, MexJK and triABC pumps.

Following what is known from literature, here is what was expected of fluorescence microscopy analysis. We hypothesized better penetration of all compounds in the mutants than in the WT strain. We had no speculation concerning Ce6 as it has not been described as a substrate for one of these pumps at the moment. However, we did think MB would accumulate better in *ΔABM, ΔABMΔxy* and *Δ6* than in *Δxy* and the WT strain as phenothiazinium PSs (like MB and toluidine blue O) are substrates of the MexAB pump in *P. aeruginosa* (Tegos and Hamblin, 2006). We also kept in mind that MexXY is linked to AG efflux and expected conjugates to be expulsed from the WT and *ΔABM* strains while resulting in higher mean RFUs for mutants lack the MexXY pump (Morita et al., 2012).

As shown on the heatmap (Fig. 27 b), it is clear that PSs alone show little to no adhesion and/or penetration in all tested strains. We should see higher penetration of MB in *ΔABM, ΔABMΔxy* and *Δ6* mutants, but this is barely the case, with a very slight increase in the mean

RFU when compared to the WT strain (from 9.8 to 20.29, 60.16 and 80.48 respectively), being only merely significant in the case of *ΔABMΔxy* and *Δ6* (Table 3).

Globally, Neo-Ce6 is the compound that showed the lowest RFUs for the three compounds, in agreement with what is described in the literature: better activity of tobramycin when compared to neomycin and MB being a substrate of the MexAB pump for Neo-MB (Tegos and Hamblin, 2006). Although not always significant, mean RFUs are generally higher in all mutant strains for the three compounds when compared to the WT, except for Neo-MB which shows higher penetration/adhesion in the WT than in *ΔABM* (Table 3).

With Neo-Ce6, we observed a slightly higher level of accumulation in *ΔABM* in agreement with a drop of the MIC compared to the WT that has been reported previously (Li et al., 2003; Westbrock-Wadman et al., 1999). With Tobra-Ce6, we observed a much stronger accumulation in this mutant strain (Fig. 27) which could be somewhat contradictory when the absence of an effect on the MIC in MHB-CA has been previously reported (Li et al., 2003; Westbrock-Wadman et al., 1999). However, Li et al., 2003 observed a 2-fold drop of the MIC in LB and in NB (low ionic strength). As mentioned in the Material and Methods section 2.2.3, cells were cultured and incubated with Tobra-Ce6 in MHB-CA and washed in MOPS-G before observation on the agar pad.

For the *Δxy* mutant, results are similar to what we observed for the *ΔABM* strain for the Ce6 conjugates. However, RFUs were of stronger intensity for both conjugates (Fig. 27). Results are in agreement with the drop of the MIC for neomycin measured by Fruci and Poole, 2018 and the 4-fold drop of the MIC measured for tobramycin by Aires J.L. et al., 1999 in this efflux mutant. In our case, the increase of Tobra-Ce6 accumulation in the mutant is impressive. Results are also consistent with previous data showing that exponentially growing PAO1 shows steady accumulation of the dihydrostreptomycin which is 2.5-fold lower than that of the mutant strain when the *mexX* gene is disrupted (Aires *et al.*, 1999).

For both *ΔABMΔxy* and *Δ6* mutants, stimulating effects observed for the Ce6 conjugates accumulation were almost canceled out (Fig. 27 a). This is quite impressive with Tobra-Ce6, especially when compared to single mutants. However, this trend is reversed when testing out Neo-MB as both mutants show significantly higher mean RFUs than all the other strains. This is also observed with MB alone where, although not always significant, both strains have higher mean RFUs (Table 3). In fact, RFUs for Neo-MB are significantly higher in both strains than the RFUs of Neo-Ce6 and Tobra-Ce6. As MB efflux is linked to the MexAB pump, these results do make sense but the effect is not witnessed in single mutant *ΔABM* (Tegos and Hamblin, 2006).

This could mean that both molecules, neomycin and MB, are capable of being recognized by their respective efflux system. Neomycin isn't being expulsed in *Δxy*, MB is not being expulsed in *ΔABM*, and both molecules are not being expulsed in the *ΔABMΔxy* and *Δ6* mutants which leads to higher mean RFUs (Fig. 27 a). In addition, mortality was indeed observed in the *Δ6* mutant using 100 µM of MB while the WT strain remained unscathed (Fig. 32). As for single mutants *ΔABM* and *Δxy*, uptake seems to be linked to the tobramycin part of the conjugate as RFUs remain quite low for Neo-Ce6 and Neo-MB (Fig. 27 a).

Overall, because the stronger accumulation of Neo-Ce6 and Tobra-Ce6 by the *ΔABM* the *Δxy* strains correlates with previously known data, this suggests that the AG conjugates may be valid compounds to monitor drug uptake levels in mutant strains. It would be interesting to evaluate with a functional test if Neo-Ce6, Neo-MB and Tobra-Ce6 are indeed substrates of the mexXY-OprM and mexAB-OprM pumps.

4.3 Conclusion and Perspectives

The goal of this project was to create a light-activated conjugate capable of eradicating multidrug-tolerant and multidrug-resistant bacteria. Results were mixed, but an important factor which makes these compound stand out is the synergy between Ce6 and the linked AG, as seen in results obtain from fluorescence microscopy and a few of the MICs. Even the singlet oxygen yield was significantly higher in the compounds when compared to Ce6 alone. Plus, there is the "double-effect" witnessed in some species where both the singlet oxygen and the AG led to bacterial death. In addition, the Ce6 compounds have been found to reduce survival in planktonic cells from a selection of Gram-positive and Gram-negative species, including a disinfecting effect against *A. baumannii* DSM30011, *E. coli* KanR, *S. aureus* Mu50 and *S. aureus* USA. Persister cells from *A. baumannii* DSM3001, *S. aureus* Newman and *S. aureus* USA300 were also found to often be below the detection limit, suggesting results close to total eradication. Although biofilm cells survived aPDT with the conjugates, persister cells from some clinically relevant strains were partly or totally eradicated.

In sum, these results suggest that the idea of linking PSs to AGs, or to other antibiotics, is an interesting one. This method has been tried before for kanamycin and Rose Bengal and has shown great results (Cahan et al., 2009). Plus, linking PSs to other vehicles is definitely not a new technique, but here we showed that MDR species and persister cells could be killed with our conjugates in a one-step process, without the use of antibiotics pre- or post-aPDT (Sperandio *et al.*, 2013). However, it goes without saying that bacterial behavior *in vitro* and *in vivo* is quite different and that further testing is required to perfect this method.

Obviously, these compounds are not perfect. Cytotoxicity assays showed that toxicity was quite high for Neo-Ce6, even without irradiation in both MRC5 and REL1 cells (Fig. 46). As mentioned, in REL1 cells we observed cellular death a few minutes after irradiation. This compound is therefore highly cytotoxic. This means it cannot be used for topical wounds or

periodontitis like predicted. However, Neo-Ce6 could be used to disinfect equipment, or possibly to eradicate cancerous cells if a precise method of delivery can be found with no systemic dispersion. As both neomycin and Ce6 are known to penetrate eucaryotic cells, these results are logical (Zug et al., 2009; Usuda et al., 2006). Other PSs and linkers are currently being investigated in order to create a compound capable of killing Gram-positive and Gram-negative bacteria without affecting eucaryotic cells. Metal ions such as ruthenium, gold and platinum have been suggested or the use of other antibiotics with less cytotoxicity (To et al., 2013).

ANNEXES

RÉSUMÉ POUR L'ÉCOLE DOCTORALE STRUCTURE ET DYNAMIQUE DES SYSTÈMES VIVANTS

L'augmentation de la résistance aux antibiotiques chez les bactéries est une menace à la médecine moderne. Un rapport publié le 26 janvier 2022 fait la mention de 670 000 infections causées par des bactéries résistantes aux antibiotiques dans l'Union Européenne. De ce chiffre, environ 33 000 patients sont décédés. Dans cette optique, la communauté scientifique recherche des alternatives de traitements pour les infections microbiennes. L'une de ces stratégies prometteuses est l'utilisation de la thérapie photodynamique antibactérienne (aPDT) ou de l'inactivation photodynamique (aPDI). Cependant, la technique présente certaines limites. Par exemple, la plus forte tolérance des bactéries Gram-négatives à l'aPDT seule et le manque de connaissances entourant l'application de l'aPDT aux cellules persistantes, soient des sous-populations bactériennes hautement tolérantes aux antibiotiques. Grâce à l'utilisation d'aminoglycosides liés à des photocatalyseurs, nous avons réussi à démontrer un effet bactéricide important contre des bactéries Gram-positives et Gram-négatives, des espèces bactériennes multirésistantes, des biofilms et des cellules persistantes. Les composés ont un effet synergique contre des espèces nosocomiales telles que *P. aeruginosa* et *S. aureus* lorsqu'on compare à l'utilisation des aminoglycosides et des photocatalyseurs seuls. L'aPDT a également entraîné l'éradication des cellules persistantes chez *S. aureus* Newman et *S. aureus* USA300, deux bactéries pathogènes de référence. De plus, la faible survie des espèces résistantes aux aminoglycosides démontre que le développement d'une résistance contre nos composés est peu probable. Leur utilisation pour tuer les bactéries résistantes et tolérantes aux médicaments grâce à l'aPDT est prometteuse dans la lutte contre la résistance aux antibiotiques, en particulier en milieu hospitalier où ils pourraient être appliqués à la stérilisation du matériel et au traitement des infections topiques.

1. Introduction

1.1 Photocatalyseurs

Les photocatalyseurs (PCs) sont des molécules capables d'absorber l'énergie lumineuse et d'induire des changements chimiques chez les molécules adjacentes. Ces changements chimiques se produisent suite à la production d'espèces réactives d'oxygène (ROS) après un transfert d'énergie depuis le PC vers l'oxygène. Parmi ces espèces, l'oxygène singulet est particulièrement réactif. Les PCs sont plus couramment utilisés en thérapie photodynamique (PDT), un procédé popularisé depuis l'approbation de l'utilisation de la Photofrin par la Foods and Drugs Association (FDA) en 1990 dans le cadre du traitement de certains types de cancers (MacDonald et Dougherty, 2001). L'étude de l'utilisation de photocatalyseurs en thérapie photodynamique antibactérienne (aPDT) est plus récente et les molécules utilisées diffèrent de celles généralement étudiées dans l'éradication de cellules cancéreuses. Cieplik s'est inspiré d'une liste de caractéristiques associées au système de PDT antitumorale idéale écrite par Pushpan en 2002 pour établir une liste de critères pour un système d'aPDT dit « parfait » (Cieplik et al., 2018 ; Pushpan et al., 2002). La liste va comme suit :

a. Charge cationique du PC pour une meilleure adhésion aux membranes bactériennes ;
b. Petit poids moléculaire pour pouvoir pénétrer la matrice des biofilms ;
c. Haute production d'oxygène singulet ;
d. Photostabilité durant le processus d'irradiation ;
e. Aucun effet toxique ou mutagène sur les cellules eucaryotes et les microorganismes lorsqu'il n'y a pas d'irradiation ;
f. Une gamme de concentration qui permet de tuer les microorganismes sans affecter les cellules eucaryotes.

L'oxygène singulet est particulièrement recherché en aPDT car bien que les bactéries aient des systèmes de défense contre la plupart des ROS (SodA, SodB, SodC, etc.), à ce jour, aucune enzyme bactérienne n'a été liée à la protection contre l'oxygène singulet (Cieplik et al., 2018, Zhao et Drlica, 2014). Ce type de ROS est très toxique pour les bactéries, mais a un temps

de vie très court (10 à 320 nanosecondes). Son effet est donc localisé et étroitement lié à la position du PC lors de l'aPDT.

Malgré la toxicité de l'oxygène singulet, il a été remarqué que les bactéries Gram-négatives étaient plus résistantes à l'aPDT que les bactéries Gram-positives. Cette différence peut être liée à l'accumulation des PCs qui ont tendance à mieux traverser la membrane des bactéries Gram-positives que celle des Gram-négatives (Malik *et al.*, 1992; Nitzan *et al.*, 1992). De plus, même si de l'oxygène singulet est produit à l'extérieur de la cellule, il est théorisé que des groupements polysaccharides à la surface des bactéries Gram-négatives pourraient temporiser (« quench ») l'oxygène singulet (Valduga *et al.*, 1993; Foote *et al.*, 1976). Finalement, même si le ROS réussissait à causer des dommages à la capsule bactérienne, il a été remarqué que les bactéries Gram-négatives peuvent survivre sans celle-ci (Dahl *et al.*, 1989; Straight and Spikes, 1985).

Pour ce projet, nous avons utilisé deux PCs : le bleu de méthylène (MB) et la chlorine E6 (Ce6). Ces deux molécules ont fait leurs preuves dans plusieurs études antérieures.

Le MB est un dérivé de phénothiazine qui absorbe autour de 666 nm. Le PC est prometteur dans son utilisation en aPDT contre les bactéries qui causent la périodontite et la gangrène de Fournier (Pereira et al., 2018 ; Balata et al., 2013). Le MB a aussi fait ses preuves contre des parasites comme *Leishmania major* et *Leishmania braziliensis* et des dermatites causées par le champignon *Trichophyton mentagrophytes* (Pinto *et al.*, 2017; López-Chicón *et al.*, 2016).

La Ce6 absorbe plutôt autour de 660 nm. C'est une molécule idéale pour son utilisation en aPDT puisqu'elle produit beaucoup d'oxygène singulet. De plus, elle est biodégradable et facilement extraite de la spiruline (Maisch et al., 2004). Tout comme le MB, la Ce6 a été beaucoup étudiée pour son utilisation contre des bactéries causant la périodontite (Karygianni et al., 2014). Le PC pourrait aussi aider à soigner l'acné. Des études ont démontré son effet en

aPDT contre *Propionibacterium acnes* et les cytokines produites par cette bactérie, réduisant ainsi l'inflammation associée à l'acné (Wang *et al.*, 2017; Jeon *et al.*, 2015).

1.2 Les aminoglycosides

Les aminoglycosides (AGs) sont des antibiotiques bactéricides à large spectre qui affectent les bactéries Gram-positives et Gram-négatives. L'amikacine, la gentamicine et la tobramycine sont les AGs les plus couramment utilisés aujourd'hui (Serio et al., 2018). Ils sont principalement utilisés pour traiter les infections des voies urinaires, les septicémies et les pneumonies (Avent et al., 2011 ; Xie et al., 2011).

Les AGs sont polycationiques, d'une masse entre 450 et 600 g/mol. Leur principal mécanisme d'action est l'inhibition d'étapes cruciales dans la synthèse des protéines bactériennes (Davis, 1987 ; Taber et al., 1987). Pour faire cela, les AGs interfèrent avec le processus ribosomal en se liant au site A situé sur la sous-unité ribosomale 30S (Fourmy *et al.*, 1998; Fourmy *et al.*, 1996). Les changements de conformation induits dans le ribosome mènent à plusieurs effets comme une inhibition de l'initiation, des obstructions du processus d'élongation et des erreurs de lectures qui résultent en la production de protéines difformes. Ce sont ces protéines mal repliées qui mènent à des altérations de la membrane puis à la mort cellulaire (Wilson, 2014; Ramirez *et al.*, 2010; Davis, 1987).

1.3 Les cellules persistantes

Les cellules persistantes forment des sous-populations au sein des communautés bactériennes. Ces cellules sont génétiquement identiques au reste de la communauté mais diffèrent par leur métabolisme. En raison de ce métabolisme lent, souvent décrit comme en dormance, les cellules persistantes sont tolérantes aux antibiotiques. Il a été observé que la

plupart des cellules sont tuées efficacement lorsqu'elles sont traitées avec un antibiotique, mais après un certain temps, un plateau de cellules persistantes se forme (Lewis, 2010). Si les cellules persistantes de ce plateau sont collectées et traitées avec un autre antibiotique, elles demeurent tolérantes (Wiuff et al., 2005). Une fois le stress du traitement éliminé, les cellules persistantes s'activent et reforment une communauté dites « sensible ». Ce phénomène est lié à la chronicité de certaines infections comme la tuberculose et la salmonellose (Grant et Hung, 2013).

Le mécanisme de persistance est complexe car c'est un état transitoire chez les cellules. Cependant, on le croit principalement lié au métabolisme cellulaire et au système toxine/antitoxine (TAT). Des études de transcriptomiques ont effectivement démontré une chute de transcrits liés à la biosynthèse et une augmentation d'expression de gènes liés à des voies de réponse au stress chez les cellules persistantes (Alkasir et al., 2018; Shah et al., 2006; Keren et al., 2004).

2. Résumé des résultats et des méthodes

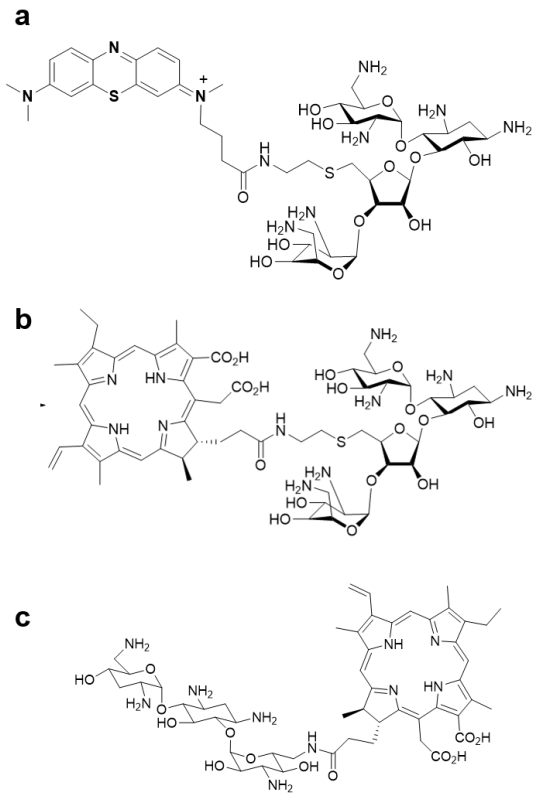

Figure 1 : Structure moléculaire de la Neo-MB (a), de la Neo-Ce6 (b) et de la Tobra-Ce6 (c).

Trois molécules ont été produites par une technique de « Click chemistry » : la néomycine liée au MB (Neo-MB), la néomycine liée à la Ce6 (Neo-Ce6) et la tobramycine liée à la Ce6 (Tobra-Ce6) (Fig. 1). La Neo-MB a été peu étudiée puisqu'elle produisait moitié moins d'oxygène singulet que le MB seul. La Neo-Ce6 et la Tobra-Ce6 produisait significativement plus d'oxygène singulet que la Ce6 seule (Fig. 2). Ces résultats ont été obtenus grâce à l'utilisation d'une trousse appelée Singlet Oxygen Sensor Green (SOSGR).

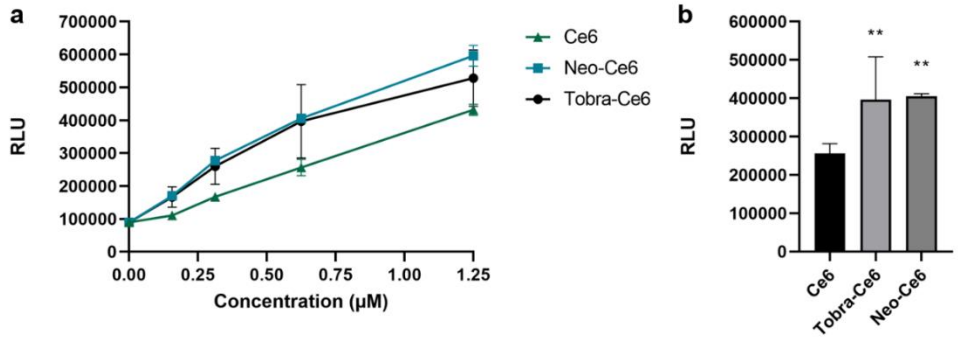

Figure 2 : Unités de lumière relative (RLU) émises par la trousse SOSGR après 5 minutes d'irradiation à 660 nm avec la lampe Solis-660C de Thorlabs. En a, différentes concentrations des composés et de la Ce6. En b, focus sur une concentration de 0,6 µM.

En microscopie, les composés entraient et/ou adhéraient significativement plus aux bactéries que la Ce6 seule. Nous avons aussi pu observer des explosions cellulaires chez *P. aeruginosa* PA14 et *B. subtilis* 168 lors de prises de photos consécutives avec le laser à 642 nm. De plus, il était possible d'observer des motifs de pénétration/adhésion qui différaient d'une bactérie à l'autre, et même chez des mutants d'une même espèce. Ces observations nous ont permis d'émettre des hypothèses sur le fonctionnement des conjugués.

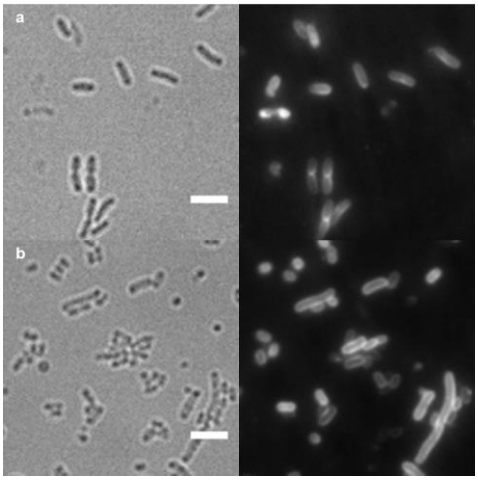

Figure 3 : Dans la ligne a, la souche sauvage *K. pneumoniae* LM21. Dans la ligne b, la souche mutante *K. pneumoniae* LM21 *Δcps*. La photo en fluorescence est prise avec un laser de 642 nm et un temps d'exposition de 200 ms. L'échelle est à 5 µm.

Par exemple, chez *K. pneumoniae* LM21 et son mutant *Δcps* qui a une capsule altérée, la fluorescence différait visuellement et statistiquement. En image (Fig. 3), la souche sauvage démontre un profil de fluorescence diffus avec une accumulation aux septums tandis que la souche *Δcps* a un profile d'accumulation périplasmique plus marqué, suggérant que la Neo-Ce6 pénettre facilement dans cette région. En accord avec cette observation, les statistiques démontrent une plus forte adhésion/pénétration de la Neo-Ce6 dans le mutant que chez la souche sauvage (p = 0,003). De plus, comme chez toutes les autres espèces testées, la Neo-Ce6 démontre une moyenne d'unités de fluorescence relative (RFU) significativement plus élevé que chez la Ce6 seule (Fig. 4).

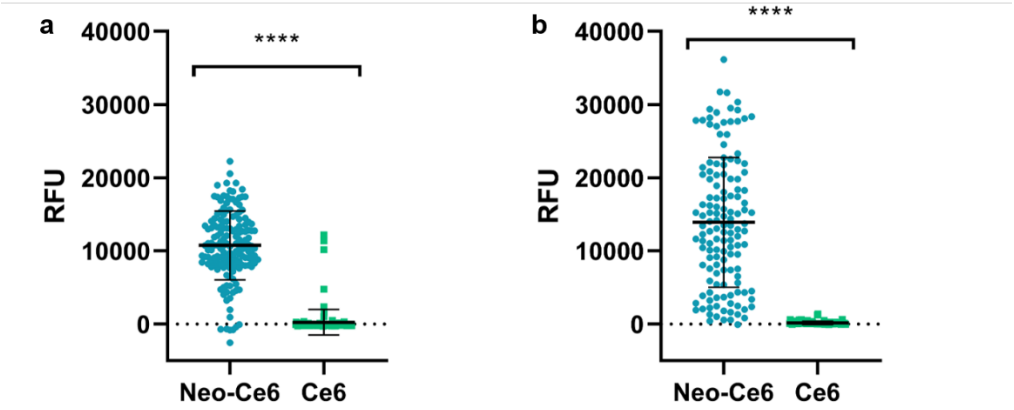

Figure 4 : RFU obtenu avec 1 µM de Neo-Ce6 et de Ce6 avec 200 ms d'exposition à 642 nm chez *K. pneumoniae* LM21 (a) et son mutant *K. pneumoniae* LM21 *Δcps* (b).

Il nous a aussi été possible d'étudier des mutants de pompes à efflux chez *P. aeruginosa* PAO1. Cette heatmap permet ainsi de voir que, comme la Neo-Ce6, la moyenne de RFU pour la Tobra-Ce6 et la Neo-MB est plus grande que le PC seul (Fig. 5).

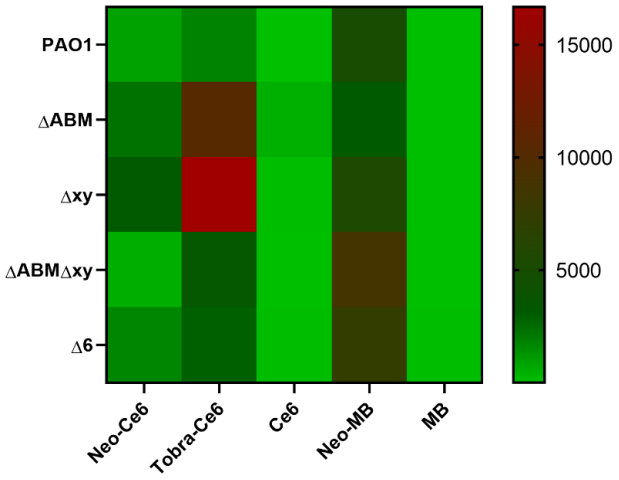

Figure 5 : Heatmap démontrant la moyenne de RFU des composés chez *P. aeruginosa* PAO1 et ses mutants.

Ces analyses démontrent que la liaison à la néomycine et à la tobramycine résulte en une meilleure pénétration/adhésion de la Ce6 et du MB. Cette synergie est aussi observée lorsqu'on évalue les concentrations minimales inhibitrices (CMIs).

Pour les CMI, une concentration de 5,5 x 10^5 CFU/mL de bactéries a été incubée 20 minutes avec des dilutions en série des composés, des aminoglycosides ou de la Ce6. Les échantillons ont ensuite été irradiés 30 minutes puis incubés pendant un minimum de 18 heures à 37°C. La présence d'une synergie a été calculée pour les échantillons irradiés grâce à une équation fournie par Doern, 2014 et les résultats sont présentés sur la table 1.

La liaison entre la néomycine et la Ce6 démontre un effet synergique contre *A. baumannii* DSM30011, *B. subtilis* 168, *C. albicans* SC5314, *S. aureus* USA300, *S. aureus* Mu50 et *S. aureus* Newman. Cependant, cette liaison avait un effet antagoniste lorsque le conjugué était utilisé contre *E. coli* MG1655, *E. coli* LF82 et *K. pneumoniae* LM21. La Tobra-Ce6 avait peu d'effet hormis un léger effet additif contre *A. baumannii* DSM30011 et *S. aureus* Newman.

Table 1 : CMI pour la néomycine, la tobramycine, la Ce6, la Neo-Ce6 et la Tobra-Ce6 avec (+) ou sans (-) irradiation. La synergie est exprimée ainsi : ++: synergie; +: effet additif; =: aucune différence; -: antagoniste. Les espèces en gras ont été irradiées avec 5 J/mm² tandis que les autres ont reçues 168 mJ/mm².

	Neo	Neo-Ce6		Synergie	Tob	Tobra-Ce6		Synergie	Ce6	
		+	-			+	-		+	-
A. baumannii DSM30011	8	0.5-1	16-32	++	4-8	2-4	> 16	+	> 64	> 64
B. subtilis 15317	0.4	< 0.125	0.5-0.8	++					> 64	> 64
C. albicans SC5314	> 512	< 0.5	> 16	++					32	> 64
E. coli MG1655	4	16	8-16	-					> 64	> 64
E. coli LF82	4	> 16	> 16	-					> 64	> 64
E. coli ΔtolC	4	4-8	8	=					> 64	> 64
E. coli KanR	> 512	> 16	> 16	ND					> 64	> 64
E. coli pET-29	128-256	> 16	> 16	ND					> 64	> 64
K. pneumoniae LM21	2	4-8	16	-					> 64	> 64
K. pneumoniae Δcps	256	> 16	> 16	ND					> 64	> 64
P. aeruginosa PA14	4	8	16	=	1-2	> 16	> 16	-	> 64	> 64
***P. aeruginosa* PAO1**	16	8-16	> 16	=	0.5-1	4-8	> 16	-	> 64	> 64
***S. aureus* USA300**	4	0.5	4-8	++	4	2-4	> 16	=	16-32	> 64
S. aureus Mu50	> 512	1-2	4-8	+	> 512	2-4	16	=	4	> 64
***S. aureus* Newman**	8	0.5	4-8	++	4	2	> 16	+	64	> 64

Cette synergie a aussi été observée lors des tests d'aPDT sur des cellules planctoniques. Un effet désinfectant, soit une différence de 5 log10 CFU/mL entre le contrôle et les échantillons irradiés, a été observé lorsque la Neo-Ce6 a été utilisée contre *S. aureus* Mu50, *S. aureus* USA300, *A. baumannii* DSM30011 et *E. coli* KanR, et lorsque la Tobra-Ce6 était utilisée contre *S. aureus* Mu50. Bien que la Ce6 et les aminoglycosides avaient parfois un effet contre certaines souches, la survie était toujours plus basse chez les échantillons traités avec les conjugués et irradiés. Il est important de noter que des contrôles ont été faits en utilisant, en combinaison, de la néomycine et de la Ce6 non-liées chimiquement et que la survie n'était pas affectée de la même façon qu'en utilisant le conjugué.

Chez les espèces de *S. aureus*, voici les résultats obtenus pour les échantillons irradiés (Fig. 6a). Chez *S. aureus* Mu50, le compte bactérien a été réduit de 4,9, 5,4 and 3,2 log10 CFU/mL pour la Neo-Ce6, la Tobra-Ce6 et la Ce6 respectivement. Chez *S. aureus* Newman, le compte bactérien a été réduit de 4,3, 3,9 and 3,6 log10 CFU/mL pour la Neo-Ce6, la Tobra-Ce6 et la Ce6 respectivement. Finalement, chez *S. aureus* USA300, le compte bactérien a été réduit de 5,6, 3,5 and 3,2 log10 CFU/mL pour la Neo-Ce6, la Tobra-Ce6 et la Ce6 respectivement.

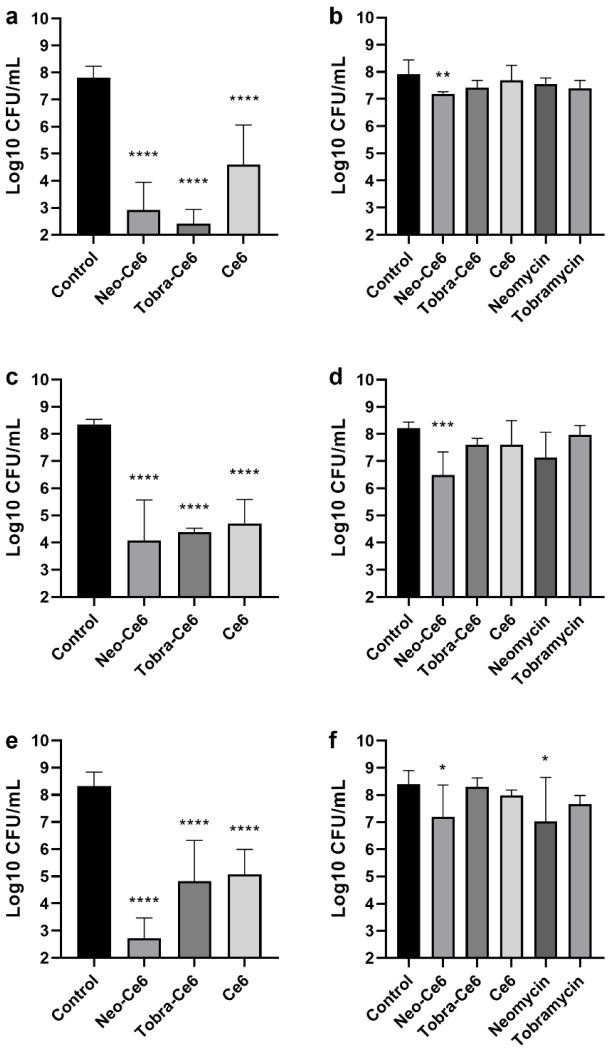

Figure 6 : Log10 CFU/mL suite à une aPDT chez les espèces *S. aureus*. Chez *S. aureus* Mu50 avec (a) et sans (b) irradiation. Chez S. aureus Newman avec (c) et sans (d) irradiation. Chez S. aureus USA300 avec (e) et sans (f) irradiation. Les échantillons irradiés ont reçu un total de 5 J/mm². Toutes les molécules ont été utilisées à une concentration de 10 µM.

Cependant, cet effet n'est pas aussi prononcé lorsque l'aPDT est appliqué à des biofilms. Cette différence est visible lorsqu'on compare la survie de cellules planctoniques chez *S. aureus* à la survie de cellules extraites du biofilm. Par exemple, dans les biofilms irradiés de *S. aureus* Mu50, la Neo-Ce6 et la Tobra-Ce6 résulte en une baisse de 1,9 et de 1,3 log10 CFU/mL (Fig. 7a), soit cent fois moins que la mortalité observée dans les cellules planctoniques.

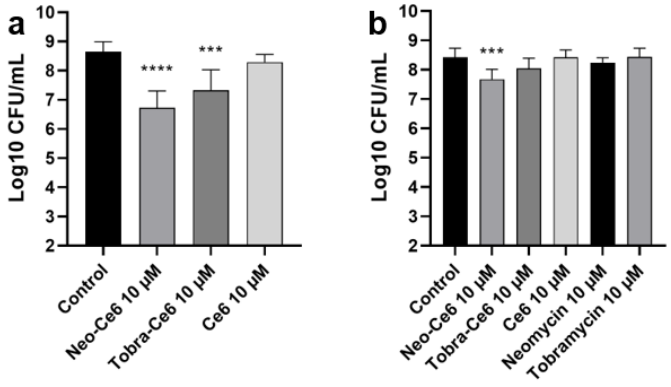

Figure 7 : Log10 CFU/mL des cellules extraites du biofilm de *S. aureus* Mu50 avec (a) ou sans (b) irradiation.

Les conjugués ont finalement été testés en aPDT contre des cellules persistantes de certaines espèces. Pour sélectionner les bactéries persistantes, les échantillons ont été traités avec de fortes doses d'aminoglycosides pendant 6 à 24 heures minimum. Ce traitement a été suivi d'une aPDT. Chez plusieurs espèces, comme *A. baumannii* DSM30011, *S. aureus* Newman et *S. aureus* USA300, la survie des cellules traitées avec les conjugués était sous le seuil ou proche du seuil de détection suite à une irradiation de 30 minutes.

Par exemple, chez *S. aureus* Newman, les cellules ont été traitées avec 1 mM de néomycine pendant 24 heures avant de subir une aPDT. Suite à l'irradiation, les CFU pour les cellules incubées avec la Tobra-Ce6 étaient sous le seuil de détection tandis que cellules traitées avec la Neo-Ce6 s'en rapprochaient (Fig. 8a). Comme il n'existe pas de différence significative entre la survie des échantillons irradiés et des échantillons non-irradiés, sauf chez les cellules traitées avec de la Ce6, l'effet de l'oxygène singulet n'est probablement pas ce qui est le plus délétère pour ces cellules. Cependant, comme la néomycine seule ne mène pas à cette chute de survie, il existe certainement une synergie entre les deux molécules qui accentuent la pénétration de l'aminoglycoside dans les cellules persistantes.

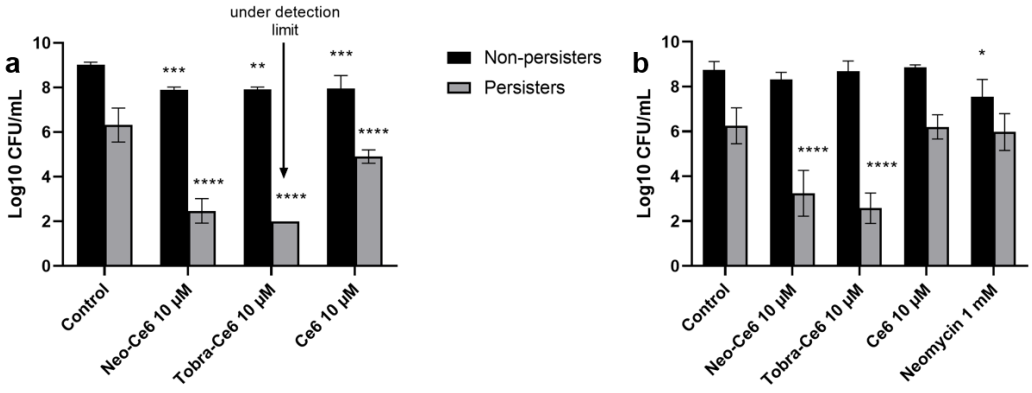

Figure 8 : Log10 CFU/mL chez les cellules persistantes de *S. aureus* Newman avec (a) et sans (b) irradiation. Les échantillons irradiés ont reçu 5 J/mm². Les statistiques ont été faites en utilisant le 2way ANOVA pour comparer la moyenne des colonnes à la moyenne du contrôle pour chaque catégorie.

3. Discussion et conclusion

Globalement, les conjugués semblent prometteurs dans leur utilisation pour stériliser des surfaces ou de l'équipement médical. Pour les conjugués de Ce6, la production de l'oxygène singulet n'a pas été modifiée négativement par la liaison avec la néomycine et la tobramycine (Fig. 2). De plus, les conjugués montrent une bonne pénétration et/ou adhésion aux bactéries sélectionnées en microscopie à fluorescence. Ces résultats démontrent donc qu'il existe une synergie entre les deux molécules une fois qu'elles sont liées.

Cette synergie est aussi détectée pour certaines bactéries lors des tests de CMI et lors des aPDT menées sur les cellules planctoniques. De plus, plusieurs résultats qui ne figurent pas dans ce résumé montrent des effets intéressants sur des cellules planctoniques. Par exemple, les CMIs de *S. aureus* Mu50 montrent une résistance à la néomycine et à la tobramycine (Table 1). Pourtant, en aPDT, la Neo-Ce6 et la Tobra-Ce6 induisent une chute de 4,9 log10 CFU/mL et de 5,4 log10 CFU/mL respectivement. Ces chiffres démontrent un effet désinfectant alors que la souche est résistante à la néomycine et à la tobramycine. Ce phénomène a aussi été observé chez

deux souches d'*E. coli* et une souche de *K. pneumoniae* LM21 *Δcps* portant des cassettes de résistance à la kanamycine. Les CMIs indiquent des valeurs hautes pour la néomycine alors que la Neo-Ce6 induit chez ces souches une chute entre 3 et 5 log10 CFU/mL lorsque les échantillons sont irradiés (Table 1).

En comparant l'effet contre les souches d'*E. coli* pET-29 et *E. coli* KanR, il est possible d'étudier une partie du mécanisme de la Neo-Ce6. La souche pET-29 est résistante à la kanamycine via une enzyme cytoplasmique appelée APH-(3')-Ia, une phosphotransférase agissant sur les aminoglycosides. La souche KanR quant à elle a une APH-(3')-IIa avec une localisation supposée dans le périplasme et l'ajout d'un groupement phosphate par APH-(3')-IIa bloquerait le franchissement de la membrane plasmique donnant un niveau élevé de résistance. Ce mécanisme pourrait expliquer des niveaux d'accumulation faibles observés pour la souche KanR. Pour les deux souches, la Neo-Ce6 a un effet sur les échantillons non-irradiés. Cela signifie que l'oxygène singulet produit par la Ce6 n'est pas la seule source de mortalité chez ces bactéries et que la partie néomycine du conjugué, malgré la présence de ces enzymes modificatrices d'aminoglycosides, a toujours un effet. Ces résultats indiquent que les deux enzymes sont incapables de modifier complétement les molécules de Neo-Ce6 accumulées. La présence de la Ce6 ralentie sans doute l'activité enzymatique des deux phosphotransférases, amenuisant le niveau de résistance. Par conséquent, pour la souche KanR, l'activité partielle de l'enzyme expliquerait le franchissement de la membrane plasmique pour la Neo-Ce6, d'où une mortalité en absence d'irradiation. La mortalité chez les échantillons irradiés et non-irradiés de la souche *E. coli* pET-29 n'est pas significativement différente avec la Neo-Ce6 qui a gardé son effet antibiotique. Dans le cas de KanR, les bactéries irradiées survivent significativement moins que les bactéries non-irradiées. L'oxygène singulet a donc un effet dans cette souche qui, pourtant, présente des taux d'accumulation de Neo-Ce6 faible, tandis que l'effet de mortalité chez *E. coli* pET-29 semble plutôt lié à la néomycine, avec des niveaux supérieurs d'accumulation. Cet effet de l'oxygène singulet plus marqué pour la souche KanR reste difficile à expliquer.

Outre les cellules planctoniques, nos conjugués ont démontré un effet contre certains biofilms. Cependant, la mortalité était moindre chez les cellules issues des biofilms et cela peut s'expliquer de plusieurs manières. D'une, comme la matrice du biofilm est globalement de charge négative, les conjugués ont peut-être adhérés à la matrice ce qui a réduit la concentration qui entrait en contact avec les cellules (López *et al.*, 2010). De plus, le cœur des biofilms est un endroit où l'oxygène est peu présent. Or, il a été démontré que la densité bactérienne et la concentration en oxygène sont deux facteurs qui influencent la production d'oxygène singulet (Maisch *et al.*, 2007). Finalement, cette survie pourrait être attribuée au fait que plusieurs études ont démontrées que les cellules présentes dans les biofilms sont certainement en état de persistance (Miyaue *et al.*, 2018 ; Lewis, 2001).

Cependant, nos conjugués ont montrés des effets bactéricides impressionnants contre les cellules persistantes de certaines espèces. Par exemple, 10 µM de Neo-Ce6 a mené à l'éradication de 4,9 log10 CFU/mL chez les cellules planctoniques de *S. aureus* Mu50 (Fig. 6a). Ce chiffre a baissé à 1,9 log10 CFU/mL pour les cellules extraites du biofilm de cette espèce (Fig. 7a). Puis, une aPDT contre les cellules persistantes de cette espèce a démontré des CFUs sur et/ou sous la limite de détection. Il semblerait donc que l'état de persistance des cellules extraites des biofilms ne soit pas la seule explication pour cette résistance plus élevée à l'aPDT.

Somme toute, la Neo-Ce6 et la Tobra-Ce6 ont démontré des résultats prometteurs contre des souches délétères, comme *S. aureus* et *P. aeruginosa*. Une synergie de pénétration/adhésion et d'action a aussi été démontrée, ce qui justifie que les deux molécules soient liées ainsi. De plus, les conjugués ont aussi des effets contre des souches résistantes, des souches mutantes portant des cassettes de résistance, et des cellules persistantes extraites de certaines souches nosocomiales d'importance clinique.

ATP leakage as a signature of bactericidal antibiotic action for drug discovery and antibiotic susceptibility tests.

Marie Ebeyer-Masotta[a,§,#], Julie Charmeaux-Goulot[a,§], Mélina Cyrenne[a,b,§], Sylvie Auxilien[a], Alba Noël[a], Andréas Odorico[a], Sylvie Lautru[a], Jean-Luc Pernodet[a], Satoko Yoshizawa[a,b], and Dominique Fourmy[a,b]*.

[a] Université Paris-Saclay, CEA, CNRS, Institute for Integrative Biology of the Cell (I2BC), 91198, Gif-sur-Yvette, France.

[b] ENS Paris-Saclay, Université Paris-Saclay, CNRS UMR8113, IDA FR3242, Laboratory of Biology and Applied Pharmacology (LBPA), 91190, Gif-sur-Yvette, France.

[§] *M. E-M, J. C-G and M. C. contributed equally to this paper*

[#] Present address: Center for Biomedical Technology, Department for Biomedical Research, Danube University Krems, Dr.-Karl-Dorrek Strasse 30, 3500 Krems, Austria.

* Email: dominique.fourmy@ens-paris-saclay.fr

Competing Interest Statement: D.F., S.Y., M.E-M. and J.L.P. declare the following competing interests. This study has been submitted to the European Patent Office (EPO) as an invention patent application by D.F., S.Y., M.E-M. and J.L.P. on July 31, 2020 (EP20305886). PCT extension was submitted on August 2, 2021.

Keywords: metabolic signature, adenosine triphosphate, antibiotics, bioluminescence drug discovery, antibiotic susceptibility test.

TOC graphic:

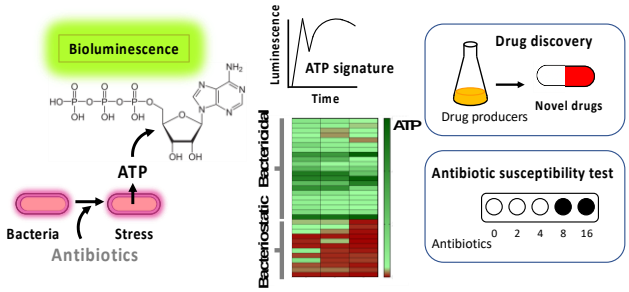

Synopsis:

The release of ATP outside bacteria is a universal signature of the action of bactericidal antibiotics. It can be used for drug discovery from natural products and as a novel rapid and sensitive AST readout.

Abstract

Drug discovery programs and antibiotic susceptibility tests (ASTs) guiding clinical decisions currently rely on time-consuming drug-induced growth inhibition methods. The identification of a novel universal signal reporting more rapidly with increased sensitivity on the bactericidal activity of drugs is in dire need. Here, using real-time bioluminescence profiling of bacteria exposed to various antibiotics, we showed that efflux of adenosine triphosphate (ATP) is a common response of bacteria treated with bactericidal drugs. A similar efflux is not observed for bacteria exposed to bacteriostatic antibiotics, indicating that the bactericidal activity is strongly linked to the leakage of this essential cell metabolite. This chemical readout finely reports, within minutes, on the bactericidal action of the drugs with subminimal inhibitory concentration sensitivity. This observation led us to develop a method to rapidly assess minimum inhibitory concentration in clinical ASTs. Furthermore, the global ATP response finds applications beyond ASTs. The presence of antimicrobial compounds in culture supernatants of drug producers was detected, demonstrating a possible application in drug discovery for screening large libraries of producers/compounds. In this assay, ATP efflux was detected for planktonic cells as well as biofilms of multi-drug-resistant pathogens exposed to effective bactericidal antibiotics, showing that the method can be applied to any medically relevant strain, independently of the type of growth. Overall, ATP response is a universal metabolic signature of the bacterial exposure to bactericidal drugs. It outperforms conventional drug-induced growth-inhibition methods in speed and sensitivity and could be used to accelerate drug discovery and ASTs.

Fluorescent aminoglycoside antibiotics and methods for accurately monitoring uptake by bacteria

Fluorescent aminoglycoside antibiotics and methods for accurately monitoring uptake by bacteria

Mahnaz Sabeti Azad[†], Maho Okuda[†,‡], Mélina Cyrenne[†], Mickael Bourge[†], Marie-Pierre Heck[§], Satoko Yoshizawa[†], and Dominique Fourmy*[,†].

[†] Université Paris-Saclay, CEA, CNRS, Institute for Integrative Biology of the Cell (I2BC), 91198, Gif-sur-Yvette, France.

[§] Université Paris-Saclay, CEA, Service de Chimie Bio-organique et de Marquage, 91191 Gif-sur-Yvette, France.

Email: dominique.fourmy@i2bc.paris-saclay.fr

Characterizing how multidrug-resistant bacteria circumvent the action of clinically used or novel antibiotics requires a detailed understanding of how the antibiotics interact with and cross bacterial membranes to accumulate in the cells and exert their action. When monitoring the interactions of drugs with bacteria it remains challenging to differentiate functionally relevant internalized drug levels from non-specific binding. Fluorescence is a method of choice for observing dynamics of biomolecules. In order to facilitate studies involving aminoglycoside antibiotics, we have generated fluorescently labeled aminoglycoside derivatives with uptake and bactericidal activities similar, albeit with a moderate loss, to those of the parent drug. The method combines fluorescence microscopy with fluorescence-activated cell sorting (FACS) using neomycin coupled to non-permeable cyanine dyes. Fluorescence imaging allowed membrane-bound antibiotic to be distinguished from molecules in the cytoplasm. Patterns of uptake were assigned to different populations in the FACS analysis. Our study illustrates how fluorescent derivatives of an aminoglycoside enable a robust characterization of the three components of uptake: membrane binding, EDPI, and EDPII. Because EDPI levels are weak compared to the two other types of accumulation and critical for the action of these drugs, the three components of uptake must be taken into account separately when drawing conclusions about aminoglycoside function.

Keywords: Fluorescence; antibiotics; aminoglycosides; uptake; flow cytometry; microscopy.

Aminoglycosides are among the oldest antibiotics in clinical use. These broad spectrum antibiotics are used against clinically important bacteria and for treatment of infections caused by multidrug-resistant bacteria.[1,2] In the past decade, novel aminoglycosides have been developed with decreased toxicity and susceptibility to resistance.[2–7] Many widely used aminoglycosides contain a deoxystreptamine ring (2-DOS) that is essential for antimicrobial activity. The 2-DOS aminoglycosides bind both subunits of the ribosome and inhibit protein synthesis.[8–10] These drugs cause miscoding [11] *via* a direct interaction with ribosomal RNA (rRNA) of the small subunit.[10,12–16] Some 2-DOS aminoglycosides also interact at a specific site within the large ribosomal subunit resulting in inhibition of translocation [17,18] or recycling.[19] In addition, aminoglycosides have been reported to inhibit initiation [20,21] and perturb ribosome biogenesis.[22–24]

Aminoglycoside uptake occurs through two energy-dependent phases known as EDPI and EDPII.[25–27] EDPI is known to be dependent on the proton motive force (PMF).[28–30] EDPII requires active protein synthesis by aminoglycoside-sensitive ribosomes and, therefore, is energy dependent. The lethal mode of action of aminoglycosides is thought to occur through induction of ribosomal miscoding, which produces misfolded proteins that when inserted into the inner membrane trigger an increase of permeability and consequently a diffusive entry of the drug in EDPII.[31] Increase in cell killing efficiency is interpreted as an increase in aminoglycoside uptake. Measuring aminoglycoside uptake is important for understanding the basis of aminoglycoside action. This has been often achieved by study of cultured cells treated with radioactively labeled aminoglycosides.[25,26,32] A method has been reported for measuring intracellular levels of kanamycin that relies on an ELISA, but it requires cell lysis.[33] Novel tools making use of fluorescent antibiotics are emerging that enable characterization of the interactions of antibiotics with bacteria at the level of organelles or even whole organisms.[34] For example, gentamicin and tobramycin coupled to Texas Red have been widely used in this type of analysis; however this dye, by itself, penetrates cells, complicating analysis.[35] Recently developed techniques make use of spectrofluorimetry, microspectrofluorimetry and kinetics microspectrofluorimetry for single-cell analysis of naturally fluorescent antibiotics or fluorescently-labeled compounds.[36,37] In addition, mass spectrometry was combined with spectrofluorimetry to provide insights into the efflux mechanisms of fluoroquinolones.[38]

Depending on the analysis, the membrane-bound fraction of a drug may be quantified, biasing the measurement of true internalized drug levels. For aminoglycosides, it is also important to differentiate EDPI and EDPII phases, as only EDPI leads to cell death. EDPII is a consequence of internalization of the drug through the membrane damaged due to EDPI. In addition, because each cell may respond differently to antibiotics, an accurate description of drug uptake requires single-cell analysis. To finely evaluate aminoglycoside uptake, we developed a series of cyanine-modified neomycin

	Neomycin	Neo-Cy5
P. aeruginosa PA14	3.25	150

Measured in minimal medium MOPS-G.

Neo-Cy5 causes misreading during ribosomal decoding. Aminoglycosides cause miscoding *in vitro* at concentrations in the range of 10-100 μM.[5,11,43,44] Since Neo-Cy5 binds the ribosomal decoding site on the small subunit (Figure 2(a)), we tested the capacity of Neo-Cy5 to induce misreading using a dual-luciferase gain-of-function assay. In this assay, misreading restores the enzymatic activity of a mutant firefly luciferase. In the mutant, codon 245, which in the wild-type mRNA is CAC (coding for histidine), is replaced by the near-cognate CGC codon (arginine).[5] Translation activity was analyzed by comparison to the signal due to wild-type *Renilla* luciferase, which served as internal standard. Like neomycin, Neo-Cy5 caused miscoding however effects were attenuated by more than one order of magnitude (Figure 2(b)).

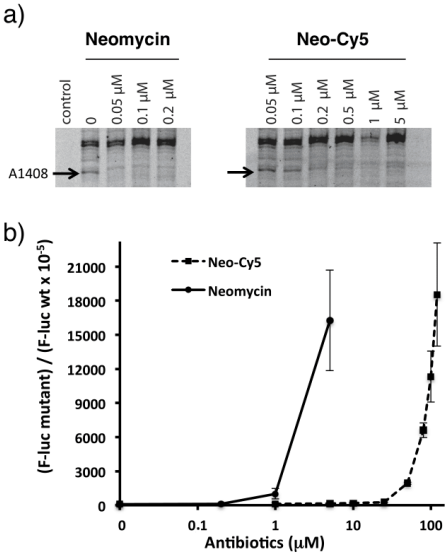

Figure 2. Neo-Cy5 binds ribosomal A site and induces misreading. a) Binding of neomycin (left) and Neo-Cy5 (right) to ribosomes was assayed using DMS chemical probing. Left lane is a control reaction with no DMS added. Right lanes are reactions in the presence of increasing concentrations of neomycin or Neo-Cy5. The protected nucleotide A1408 that belongs to the neomycin binding site (Figure 1(b) is marked with an arrow. b) Mis-incorporation of amino acids was assayed using a gain-of-function assay. Wild-type and mutant firefly luciferase reporters were used for *in vitro* translation reactions together with the *Renilla* luciferase, which served as an internal control. Error bars are s. e. m. for three independent experiments.

Neo-Cy5 has proton motive force-dependent bactericidal activity. Aminoglycoside accumulation in bacterial cells is known to be dependent on PMF.[28] We therefore tested the effect of the protonophore carbonyl cyanide m-chlorophenyl hydrazone (CCCP) on Neo-Cy5-induced bacterial cell death. Addition of CCCP protected cells from the drug-induced killing (Figure 3 and Figure S8), demonstrating that, as for other aminoglycosides, the accumulation of Neo-Cy5 is PMF dependent.

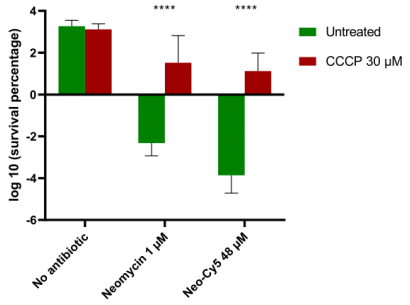

Figure 3. Neo-Cy5-induced cell killing is PMF dependent. Survival of *E. coli* MG1655 cells after a 4.5-h treatment with 1.5 μM neomycin or 48 μM Neo-Cy5 with and without a 2-h pre-incubation with 30 μM CCCP. Plotted are values relative to untreated control culture. Error bars are s. e. m. and were calculated from three independent experiments. Significant differences, calculated by the Mann–Whitney test, are indicated (**** $P < 0.0001$).

FACS and TIRF microscopy reveal drug peripheral accumulation and strong interaction with membranes. Because cationic aminoglycosides can interact with the membranes of the bacterial cell surface, we devised a protocol to measure only tightly-bound or internalized Neo-Cy5. We first removed weakly membrane-bound and not internalized molecules by washing the cells on mixed cellulose ester filters. At least three washes with MOPS-G at 37 °C were necessary to remove non-internalized drug (Figure S9). We measured Neo-Cy5 uptake by *E. coli* MG1655 cells in the exponential phase of growth in the presence of Neo-Cy5 at a concentration three times the MIC. After filtration, cells were recovered and immediately analyzed by FACS. After a short 5-minute exposure to Neo-Cy5, a signal due to the conjugate was clearly distinguished from the background fluorescence (Figure 4(a)). We verified that the signal was dependent on the neomycin moiety: TIRF microscopy showed that the Cy5 dye alone was not incorporated into live bacterial cells and that Cy5 did not interact strongly with membranes (Figure S10 and Figure 4(a)). Because the observed signal for Neo-Cy5 could correspond to molecules tightly bound to the membrane or internalized in the periplasm or cytoplasm, we inspected the localization of the drug by TIRF microscopy (Figure 4(b)). Here, periplasmic accumulation would correspond to the self-promoted mechanism previously proposed where aminoglycoside cross irreversibly the outer membrane *via* the lipopolysaccharides in *E. coli*.[45] After a 5-minute incubation, Neo-Cy5 accumulated at the periphery of the cell and did not overlap with the fluorescence of Spinach-tagged ribosomes[46] (Figure 4(c) and Figure S11)). We conclude that Neo-Cy5 bound at the membrane of a cell or internalized in the periplasm can readily be

derivatives that have antibacterial activity similar to the parent aminoglycoside. When used with adequate protocols, these derivatives allow single-cell analysis of aminoglycoside uptake by fluorescence microscopy and fluorescence-activated cell sorting (FACS).

RESULTS AND DISCUSSION

Generation of Neo-cyanine derivatives. Radioactivity based assays[25,26,32] and ELISA[33] do not report on accumulation at the single cell level. A fluorescent derivative with preserved uptake and bactericidal activities would facilitate analysis of uptake with single-cell resolution. We previously showed that the 5" position of neomycin could be modified with various functional groups without compromising antimicrobial activity (Figure S1). Analysis of the structures of a neomycin-ribosome complex indicated that functional groups introduced at this position are accommodated in the major groove of helix 44 of the 16S rRNA in a conformation that does not interfere with drug binding or induction of miscoding.

We used a derivative of neomycin where the hydroxyl group at the 5" position was substituted with S-$(CH_2)_2$-NH_2 to allow introduction of extra chemical groups by coupling (Supporting information, product 5).[39] Addition of a thyminylacetamidoethylthio or uracil (Neo-U) at the 5" position preserved the antimicrobial activity against *E. coli* as measured using an MIC assay (Figure S1 and Table S1). As expected, Neo-U bound to the A site on the small ribosomal subunit, although affinity was slightly decreased compared to the unmodified neomycin (Figure S2). This result indicated that large chemical modifications can be introduced at the 5" position of ring III without strongly perturbing A-site binding or antimicrobial properties.

We next labeled neomycin with sulfonated cyanines Cy3 and Cy5 (Figures S3,S4,S5 and S6), which are non-membrane permeable dyes suitable for fluorescence microscopy.[40] The spectral properties of Neo-Cy5 conjugate (Figure 1(a)) do not differ from those of the free dye (Figure S7). We verified that the fluorescent probes are accommodated without any steric clash by docking into the crystal structure of *E. coli* ribosomes bound to neomycin (PDB code 4v52). The Cy3 and Cy5 probes, which are bulkier than the uracil base, likely lie in a cavity between helices h27 and h44 of 16S ribosomal RNA (Figure 1(b)).

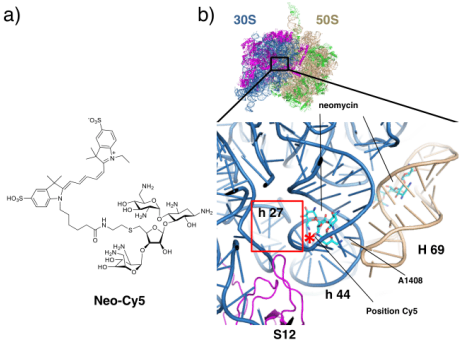

Figure 1. Structure of the Neo-Cy5 conjugate and accommodation at the ribosomal A site. a) Structure of Neo-Cy5 in which Cy5 is coupled to ring III of neomycin. b) Neomycin binding sites in h44 of the small ribosomal subunit (blue) and in H69 of the large ribosomal subunit (beige) (PDB code 4v52). Small and large ribosomal proteins are shown in purple and green, respectively. The red box indicates a cavity near the neomycin binding site in h44 where Cy5 can be accommodated. Nucleotide A1408 that is part of the neomycin binding site is indicated.

Neo-cyanine derivatives are active antibiotics. Next, we verified that Neo-Cy5 binds the decoding site of 16S rRNA in 70S ribosomes. Footprinting analysis of ribosomal particles bound to Neo-Cy5 showed that the conjugate interacts with the decoding site of the small ribosomal subunit in a manner similar to neomycin and Neo-U, and like Neo-U, Neo-Cy5 has slightly lower affinity than the parent antibiotic (Figure 2(a)). We next tested the antimicrobial activity of Neo-Cy5. The measured MIC in minimal medium was slightly higher than that of neomycin (Table 1) and similar to the MICs for Neo-U (Table S1) and closely related aminoglycosides.[41,42] The MIC of Neo-Cy3 was also similar to that of Neo-Cy5 (Table 1).

MIC values were also measured in Mueller-Hinton broth for Gram negative and positive bacteria including ESKAPE pathogens (Table 2). Tested strains included clinically relevant Gram negative pathogens such as *Pseudomonas aeruginosa, A. baumannii, K. pneumoniae, S. typhimurium*, as well as the Gram positive *S. aureus* USA300. MIC values for the parental drug neomycin were higher in rich medium when compared to minimal medium. This effect was stronger for the Neo-Cy5 conjugate as MIC values were increased by factors ranging from 20 to 40 compared to the values measured for neomycin (Table 2). The MIC value was not measurable for *Pseudomonas aeruginosa* in rich medium and found to be 150 µg/ml in MOPS-G (Table 3).

Table 1. MIC values in µg/ml of neomycin-cyanine derivative conjugates against *E. coli* MG1655.

	Neomycin	Neo-Cy5	Neo-Cy3
M9 medium	3.0	13	ND
MOPS medium	1.1	10.4	5.2

Measured in minimal medium MOPS-G. ND: not determined.

Table 2. MIC values of Neo-Cy5 in µg/ml against Gram negative and positive strains.

	Neomycin	Neo-Cy5
E. coli MG1655	2.5	75
P. aeruginosa PA14	2.5	> 150
A. baumannii DSM30011	5.0	75
K. pneumoniae LM21	1.25	25
*S. typhimurium*14028	1.25	50
B. subtilis	0.25	6.25
M. luteus	1.5	6.25
S. aureus USA300	2.5	75

Measured in cation-adjusted Mueller-Hinton broth.

Table 3. MIC values of Neo-Cy5 in µg/ml against *P. aeruginosa* PA14.

detected by FACS and visualized by TIRF fluorescence microscopy.

Neo-Cy5 binding to bacterial membranes is saturable. Binding of Neo-Cy5 to the bacterial membranes was found to be instantaneous as visualized in real time by FACS (Figure S12). Membranes of *E. coli* showed saturability when exposed for 5 minutes to increasing concentrations of Neo-Cy5 (Figure 4(d,e)). At low concentrations, there was strong heterogeneity in fluorescence levels of individual cells (Figure 4(d)). At the highest concentrations, even though the exposure time was short to ensure that only the drug interaction with the membrane was monitored, in a fraction of cells high levels of uptake was observed (Figure 4(d)). Experiments described in the next section demonstrated that this fraction corresponds to cells with cytoplasmic uptake. In cells treated with 64 μM of Neo-Cy5, 2.9% of cells had detectable levels of Neo-Cy5 in the cytoplasm. This value is above the known fraction of 0.3% of cells that are dead in a fast growing bacterial population.[47] Therefore there is rapid cytoplasmic uptake at high concentrations of Neo-Cy5.

Neo-Cy5 is internalized mainly through EDPII. *E. coli* MG1655 cells were treated with 32 μM Neo-Cy5 for 30 minutes, the time period corresponding to the onset of aminoglycoside-induced exponential killing.[48] When cells were imaged using TIRF, we observed that fluorescence signals were distributed over the entire cell volume for most of the cells (time 30 min 88%, n=57), (Figure 5(a)). This clearly indicated cytoplasmic uptake. Most of the cells had low levels of fluorescence corresponding to EDPI uptake. A low percentage of cells had bright Cy5 fluorescence signals suggestive of EDPII accumulation. For 60 min of incubation, 100% of the cells had cytoplasmic uptake (n=119). Cells exposed to Neo-Cy5 overnight showed morphological defects (Figure S13) similar to what has been previously described for cells treated with aminoglycosides,[49,50] in particular foci formation at poles.

Addition of the protein synthesis inhibitor chloramphenicol prior to exposure to aminoglycosides decreases EDPI and abolishes EDPII.[51] We pre-incubated the cells with chloramphenicol before the addition of a lethal concentration of Neo-Cy5 to evaluate the contributions of EDPI and EDPII uptake by FACS (Figure 5(b)). Differences in profiles obtained with or without chloramphenicol were very minor at 30 minutes; TIRF imaging showed that EDPI already occurred for most of the cells (Figure 5(a)). Only a slight shift of the distribution toward stronger levels of fluorescence was observed with time. This result revealed that EDPI uptake is indeed difficult to capture by FACS. The shift of the distribution in absence of chloramphenicol was more pronounced at 60 and 150 minutes in agreement with an EDPII-driven cytoplasmic uptake. We concluded that little Neo-Cy5 accumulates in the cytoplasm *via* EDPI when compared to membrane-bound or cytoplasmic levels that resulted from the EDPII-driven process.

Accumulation of Neo-Cy5 and loss of cell viability. We next performed a detailed kinetic analysis of Neo-Cy5 uptake at the single-cell level. Cell viability was monitored in parallel. Like observed for other aminoglycosides[48], Neo-Cy5 displayed the characteristic lag followed by exponential killing of the cells (Figure 5(c)). The plot of the sum of the fluorescence levels as a function of time calculated from our

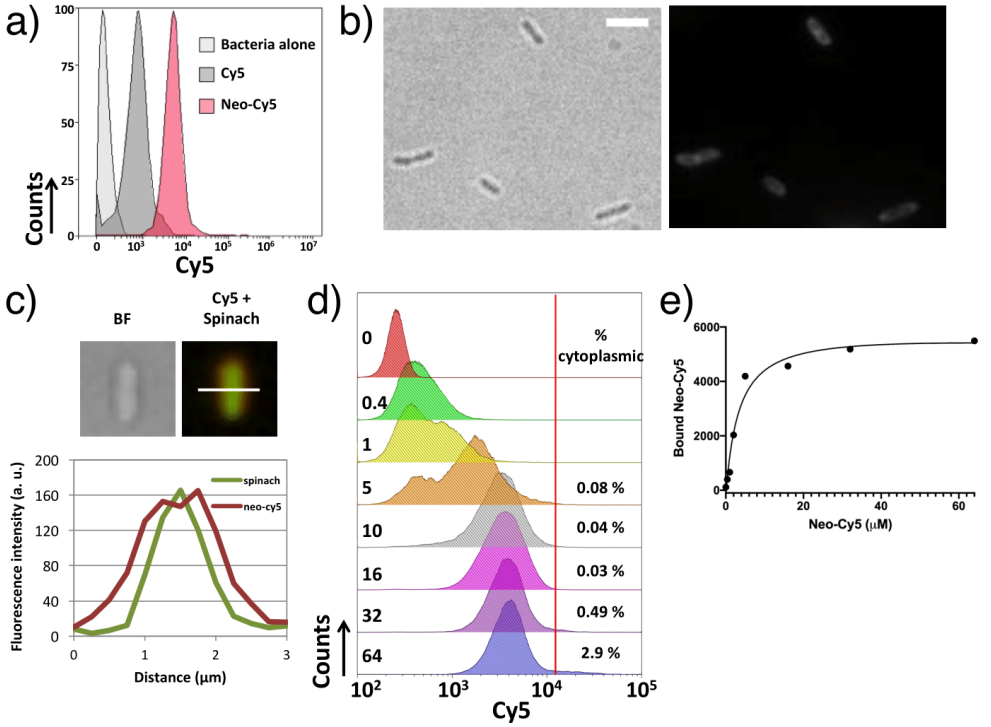

Figure 4. Fluorescence microscopy and FACS enable detection of Neo-Cy5 bound to *E. coli* MG1655 cells. a) FACS analysis of cells exposed to 32 µM Cy5, 32 µM Neo-Cy5, or no dye for 5 min at 37 °C. Cells were washed on a 0.45 µm-pore-size HAWP membrane filter. Binding of Neo-Cy5 was clearly distinct from cellular autofluorescence and residual binding of the free dye. b) Representative brightfield and TIRF microscopy images of cells incubated for 5 min with Neo-Cy5 as in panel "a". Scale bar: 5 µm c) Neo-Cy5 does not localize with ribosomes after a 5-minute incubation. E. coli cells expressing Spinach-tagged ribosomes were exposed to Neo-Cy5 and imaged. Left: Brightfield. Right: Neo-Cy5 (red), Spinach (green). Bottom: plot of a cross section of fluorescence signal for a representative cell with the peripheral pattern. d) Saturability of bacterial membranes to Neo-Cy5 binding. Cells were incubated for 5 min at 37 °C with increasing concentrations of Neo-Cy5, filtered, and analyzed by FACS. The percentage of cells with cytoplasmic uptake was calculated from the number of cell counts with a Cy5 signal higher than the red threshold line divided by the total number of cell counts. e) Binding curve of the membrane-bound Neo-Cy5.

single-cell analysis recapitulated previous data obtained on cell ensembles.[26] During the first 20 minutes of incubation with the drug, fluorescence levels increased slightly while cell survival remained intact. During this period, Neo-Cy5 localized at the cell periphery (Supplementary Figure 13). At 40 minutes, the cytoplasmic pattern became dominant with stronger drug accumulation (Figure 5(c,d) and Figure S14) concomitantly with the onset of the decrease in cell survival rate (Figure 5(c)). This period corresponded to a transition between EDPI and EDPII. The onset of EDPII was previously considered to be the first time point at which uptake becomes linear and rapid.[26] This time point for Neo-Cy5 was around 50 minutes (Figure 5(c)). During the 20-minute transition period (40 to 60-min) 90% of the cells lost viability with a sharp increase in drug uptake. After 80 minutes, 99% of the cells were dead and levels of accumulation continued to increase steeply and linearly during 40 minutes, reaching a factor of approximately 10 of increase taking as a reference the membrane-bound fraction (ratio of medians 120 min/5 min) (Figure 5(c)). Finally, at the beginning of the transition time point (40 minutes), the cytoplasmic drug levels that accumulated during EDPI, accounted for approximately one third of the total levels, the other two thirds corresponded to membrane/periplasmic interaction or accumulation (Figure 5(c)).

CONCLUSIONS

With the purpose of improving methodologies for measuring aminoglycoside uptake by bacteria we used click chemistry to develop fluorescent conjugates of neomycin that have uptake and bactericidal properties similar to the ones of the parent aminoglycoside. We coupled sulfonated cyanine dyes that are not membrane-permeable to neomycin allowing clear visualization of the uptake. The obtained Neo-Cy3 and Neo-Cy5 derivatives exhibited uptake properties strictly

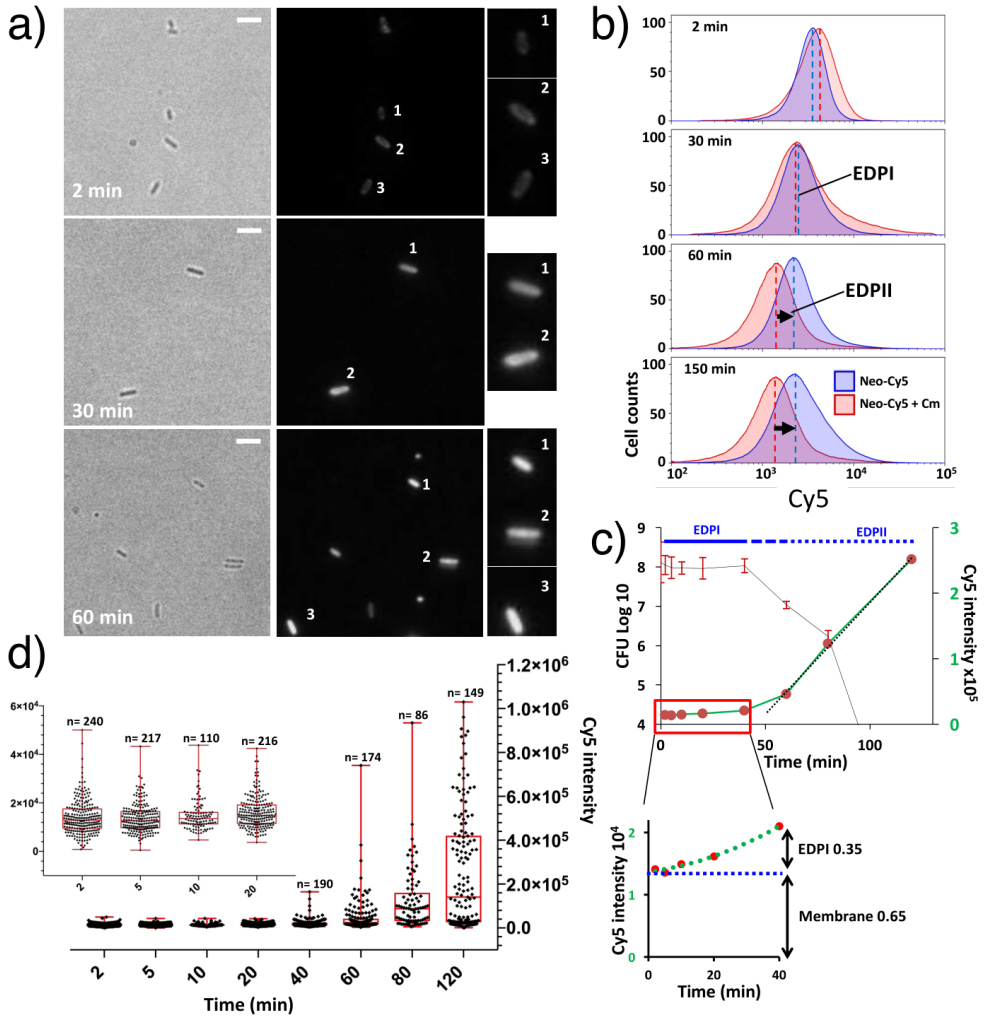

Figure 5. EDPI-mediated uptake can be distinguished from EDPII-mediated uptake. a) Representative brightfield and TIRF microscopy images of cells after 2, 30 and 60 min of exposure to 32 µM Neo-Cy5. Scale bar: 5 µm b) *E. coli* cells treated with 32 µM Neo-Cy5 with or without 25 µg/mL of chloramphenicol were incubated for the times indicated. At each time point, cells were filtered, washed, and analyzed by FACS. Cell counts were normalized to 100%. Weak cytoplasmic uptake, which corresponded to EDPI was detected as an upper shift of the blue population compared to the red population. The stronger shift corresponding to EDPII levels of uptake is highlighted by an arrow. c) Killing curve obtained for *E. coli* with monitoring of Neo-Cy5 uptake. Cells were grown exponentially at 37°C in MOPS medium containing glucose to an OD_{600} of 0.2, diluted 10 times in fresh medium before addition of Neo-Cy5. At different time points, cells were collected and filtered to remove drug excess. Cells were plated on agar pads for fluorescence microscopy (Figure S14) and fluorescence quantification to generate panel d and serial dilutions were made and plated on LB agar for c.f.u. counting. The kinetic of Neo-Cy5 uptake on the cell population is represented by the sum of the single-cell analysis of fluorescence signals displayed in panel d. The rapid and linear EDPII phase is highlighted by a dashed line. d) Single-cell quantification of Neo-Cy5 accumulation as a function of time. Red lines highlight the medians, boxes show 75/25%, and vertical dashed lines indicate 90/10% of the maxima.

dependent on the neomycin moiety demonstrating that this type of conjugate can be widely used to report on aminoglycoside uptake. In addition, these dyes have spectral properties that make them suitable for fluorescence microscopy. The Neo-Cy5 conjugate is active against Gram-positive and negative strains with the exception of *Pseudomonas aeruginosa* in rich medium. This pathogen is known to resist to multiple drugs owing to a membrane of low permeability, the expression of multidrug efflux pumps and its adaptation to the presence of antibiotics. The efflux pump MexX-MexY-OprM plays a role in intrinsic resistance to aminoglycosides.[52–54] The pump has moderate drug specificity as aminoglycosides, macrolides and tetracycline are substrates.[55] Structural data obtained for this type of pumps provided details on their architecture and revealed indeed multiple binding pockets for various drugs.[56–58] It remains to be investigated if the presence of the fluorescent dye will affect the efflux mechanism in *Pseudomonas aeruginosa*.

Using Neo-Cy5 conjugate, we devised a method for accurate monitoring of aminoglycoside uptake. Membrane binding of Neo-Cy5 was found to account for a large fraction of the fluorescence signal. We showed that we could remove the excess of drug and the weakly bound molecules, which otherwise masked the real levels of uptake, by filtration and washing. Using TIRF microscopy we ensured the validity of FACS observations. Using FACS, we monitored drug binding and intracellular accumulation. Neo-sulfonated-cyanine derivatives did not suffer from dye permeability drawbacks observed for dyes such as Texas Red.[35]

Aminoglycosides are bound to the bacterial cell membrane and accumulate in the cytoplasm of bacterial cells through EDPI and EDPII. The membrane-bound and EDPII components accounted for a large fraction of the total levels of Neo-Cy5 tightly associated with *E. coli* cells. Levels of Neo-Cy5 resulting from EDPI-mediated internalization were low even though it is this fraction that results in the deleterious effects of aminoglycosides on cells. The loss of membrane integrity results in the onset of strong diffusive entry of the drug during EDPII.[25,27]

The data reported here illustrate how fluorescent derivatives of an aminoglycoside enable a robust characterization of the three components of uptake: membrane binding, EDPI, and EDPII. EDPII-mediated uptake is a consequence of the miscoding activity of the drug that accumulated *via* EDPI. As miscoding levels can vary between bacterial strains and between mutants of a single strain, EDPII accumulation may only partially reflect EDPI accumulation. Thus, it is critical that the three components of aminoglycoside uptake be evaluated. We expect that the method described here will be applied to characterize aminoglycoside uptake into bacteria to facilitate a better understanding of the mechanisms of action of these drugs and their next generation derivatives. Interestingly, the group of Y. Tor recently investigated the uptake of several aminoglycoside-Cy3 conjugates including neomycin-Cy3 and guanidinoneomycin-Cy3 in Chinese hamster ovarian cells using fluorescence microscopy and FACS.[59] Guanidinoglycosides-Cy3 conjugates entered cells better than their parent aminoglycosides. This work together with our results emphasize the usefulness of Cyanine-aminoglycoside conjugates for further studies of their cellular uptake by eukaryotic and prokaryotic cells. This class of antibiotics, including neomycin, has recently drawn strong attention for the development of novel, potent, and less toxic drugs to address the pressing societal problem of multidrug-resistant (MDR) infectious disease.[60,61] The approach combining fluorescence microscopy and FACS should provide a framework for future antibiotic-cell interaction studies and facilitate the development of novel aminoglycosides.

METHODS

Chemicals. Cy5 and Cy3 NHS-esters were purchased from General Electric Healthcare or Lumiprobe GmbH. 3,5-Difluoro-4-hydroxybenzylidene imidazolinone was purchased from Lucerna Technologies. 2,2,2-trifluoro-N-(2-sulfanylethyl)acetamide was obtained from Merck or prepared following the reported procedure.[62]

Labeling of neomycin with cyanine fluorophores. A derivative of neomycin containing 2-N-trifluoroacetamidoethylthio in place of a hydroxyl group in ring III was used for functionalization. Other amino groups were protected by hexa-N-tert-butyloxycarbonyl groups for selective reactivity at the new 5" NH_2 position. The derivative was used to conjugate neomycin to NHS-ester dyes. Selective deprotection of the 5" position was performed in ammonium hydroxide in methanol, and the unique free amino group was reacted with Cy5 or Cyanine 5 monofunctional NHS-ester. Reactions were monitored by analytical thin-layer chromatography (TLC) on silica gel 60 F254 plates (0.25 mm). The Cy5 and Cyanine 5 conjugates were purified on TLC plates (Silica gel 60, Merck), eluted in ethanol, and deprotected with trifluoroacetic acid (90%) to remove butyloxycarbonyl groups.

Purification of ribosomes. Tightly coupled 70S ribosomes from *E. coli* MRE600 were prepared as described.[63,64] Briefly, cells were grown in exponential phase and when the OD_{600} reached 0.3, cells were collected by centrifugation. Cells were lysed by passage through a module/piston homogenizing system pre-cooled to -80 °C that maintains the material in a frozen state. The piston was actuated with a Carver hydraulic press. Ribosomes were isolated by several centrifugation steps followed by a sucrose gradient (10-40%) fractionation. The fraction containing 70S particles was collected using a density gradient fraction system (Teledyne Isco), pelleted, and resuspended in 50 mM Tris-HCl (pH 7.6), 10 mM $MgCl_2$, 100 mM NH_4Cl, 6 mM 2-mercaptoethanol. Aliquots were stored at -80 °C after flash freezing in liquid nitrogen. The ribosome concentration was obtained by measuring the absorption at 260 nm; we assumed that there are 23 pmol ribosomes per A_{260} unit.

Footprinting of Neo-Cy5 on 70S ribosomes. The concentration of Neo-Cy5 stock solution was estimated from the absorbance at 649 nm measured in 10 mM Tris-HCl, pH 7.5. Chemical probing of Neo-Cy5-ribosome complexes was performed as described.[65] We used the RNA base-specific reagent dimethyl sulfate (DMS) which methylates positions N1 of adenines and N3 of cytidines as well as position N7 of guanines.[66] Modification reactions (100 µl) with 70S particles (10 pmol) were performed in a buffer containing 80 mM potassium cacodylate pH 7.2, 100 mM ammonium chloride, 20 mM magnesium chloride, 1 mM dithiothreitol and 0.5 mM EDTA. In brief, 1 µl of (DMS) (1:10 dilution in 95% ethanol) was added to a 50-µL reaction mixture. After incubation at 37 °C for 10 minute reactions were stopped by addition of 25 µL of 6.7% (v/v) β-mercaptoethanol in 280

mM sodium acetate (pH 5.4) and 150 µL of ethanol followed by rapid mixing. After precipitation, the pellets were resuspended in 10 µL of H_2O.

Sites of modification were analyzed by fluorescent primer extension as previously described.[67] A Cy5-labeled fluorescent DNA primer was purchased from MWG Biotech. Reverse transcription reactions were performed in 10 µL of 50 mM Tris-HCl, pH 8.3, 75 mM KCl, 3 mM $MgCl_2$ 10 mM DTT with 0.25 mM each dNTP. SuperScript II (Invitrogen, 0.5 µL 100 units) was added and reactions were incubated at 45 °C for 40 min. For sequencing samples, 1.25 mM of ddATP, ddCTP, ddGTP, or ddTTP was added to individual reverse transcription reactions of each sample. Reactions were stopped by ethanol precipitation. cDNA samples were dissolved in 10 µL loading solution containing 7 M urea. A small aliquot (1.5 to 3 µL) of each sample was loaded on an 8% polyacrylamide 7 M urea gel for separation of cDNAs. Gels were analyzed on a Typhoon imaging system. Molecular graphics were generated using PyMOL(TM) 2.0.1.

Miscoding assay. Miscoding was assessed in a gain-of-function assay using firefly and *Renilla* luciferases. DNA reporter plasmids pT7 hFluc WT, pT7 hFluc H245R(CGC), and pT7 hRluc WT for *in vitro* translation assay were provided by Erik Böttger and Dimitri Scherbakov (University of Zurich).[5] Wild-type and mutant DNAs were used for *in vitro* translation reactions together with the *Renilla* luciferase DNA, which served as an internal control. *In vitro* translation reactions were performed using the PURExpress system (New England BioLabs). The premix for one reaction contained 2 µL solution A, 1.5 µL solution B, 5 nM DNA templates, and 1 unit/µL of SUPERase·In™ RNase Inhibitor (Invitrogen). The reaction was begun by addition of 4 µL of the premix lacking aminoglycosides to 1 µL of aminoglycoside dilution in 0.2 ml thin-walled tubes on ice. Synthesis was performed at 37 °C for 35 min in a thermocycler (lid temperature 98 °C) and stopped by placing samples on ice. Luciferase activity was measured using the Dual-Luciferase Reporter Assay System (Promega). Luciferase assay reagent (50 µl) was added to each sample, and the samples were mixed and transferred to a white 96-well plate (Greiner, catalog number 655075) for bioluminescence quantification using an Infinite M200 microplate reader (Tecan). Miscoding was quantified by calculating the mutant firefly/*Renilla* luciferase activity compared with the wild-type firefly/*Renilla* luciferase activity.

Minimum inhibitory concentration measurement. The minimum inhibitory concentrations (MICs) were determined using a liquid culture assay according to EUCAST guidelines. Aliquots of an overnight culture of *E. coli* MG1655 were diluted to have an inoculum of $5.5x10^5$ colony-forming units per mL (c.f.u./mL) into the medium containing 2-fold serial dilutions of antibiotics. Growth was measured by turbidity at each concentration during 18 h of incubation at 37 °C. Measurements were performed on 200 µL samples in a 96-well microtiter plate with transparent lid using an Infinite M200PRO (TECAN). For Neo-Cy5, turbidity was measured at 400 nm or 500 nm instead of 600 nm to minimize Cy5 excitation.

Treatment of cells with carbonyl cyanide m-chlorophenyl hydrazone. *E. coli* MG1655 cells from an overnight culture in MOPS supplemented with 0.4 % (w/v) glucose (MOPS-G) were diluted into the same medium. Cells were grown for 2 h at 37 °C with or without 30 µM carbonyl cyanide m-chlorophenyl hydrazone (CCCP). The number of live cells at the time of CCCP addition were estimated as $5x10^7$ c.f.u./mL. After a 4.5-h incubation at 37 °C with neomycin or Neo-Cy5, cell survival was measured in c.f.u./mL.

Neo-Cy5 uptake. For the liquid culture, MOPS-G was used. Overnight cultures were diluted to an OD_{600} of 0.037 with fresh medium and grown until the OD_{600} reached 0.2. Typically, 0.5 µL of Neo-Cy5 dissolved in milliQ water was added to 5 µL of the cell suspension (diluted 10 times). Cells were incubated in a heat block at 37 °C without shaking. To remove Neo-Cy5 not tightly bound or internalized, the samples were filtered through 0.45 µm-pore-size HAWP mixed cellulose ester (MCE) membranes (Merck Millipore) mounted on a micro-sample filtration Minifold II (Schleicher & Schuell) and washed three times with 100 µL MOPS-G prewarmed to 37 °C. Immediately after filtration, the section of the membrane containing cells was placed into an Eppendorf tube containing MOPS-G, and cells were recovered by gentle up and down pipetting. Cells were immediately placed on 1% agarose pad for imaging by fluorescence microscopy or analysis by FACS.

Fluorescence microscopy. Fluorescence images were taken with an EMCCD camera (Photometrics) through a 63X total internal reflection fluorescence (TIRF) objective (Zeiss, NA 1.43) mounted on an inverted Zeiss Axio Observer Z1 microscope. Image acquisition was done with the Metamorph software package (Molecular Devices). Cy5 illumination was performed using a 642-nm laser (0.002 kW/cm^2, Roper Scientific), and a filter set was used for fluorescence excitation and emission (Chroma Technology; ET 532/640 nm Laser Dual Band; excitation filter 530/20 nm and 638/25 nm, dichroic mirror 585/70 nm and 650 nm (long pass), and emission filter 580/70 nm and 700/100 nm). Neo-Cy5 uptake was typically observed with an electron-multiplying gain of 1 or 50 and an exposure of 10 to 100 ms. Spinach aptamer bound to 3,5-difluoro-4-hydroxybenzylidene imidazolinone was excited with a mercury lamp (excitation 470 ± 20 nm, emission 525 ± 25 nm). Image analyses were performed using ImageJ and microbeJ.[68]

FACS analysis. To measure Cy5 fluorescence, cells were analyzed with a BD Accuri C6 flow cytometer (BD Biosciences). For each experiment, more than 100 000 events were recorded. Excitation was performed with a 640-nm diode laser (14.7 mW), and emission was detected through a 675/25 nm band pass filter. Data were analyzed with Kaluza 2.1 (Beckman Coulter) and FlowLogic 7.2. Binding affinity experiments were analyzed with the software GraphPad Prism 8.2.1. Data were fitted to a simple saturation curve.

ASSOCIATED CONTENT

Supporting Information

The Supporting Information is available free of charge on the ACS Publications website.

Supporting methods, 14 figures and one table showing additional results (PDF).

AUTHOR INFORMATION

Corresponding Author

* E-mail: dominique.fourmy@i2bc.paris-saclay.fr.

Present Addresses

† Institute for Environmental and Gender-Specific Medicine, Juntendo University Graduate School of Medicine, Chiba 279-0021, Japan.

Author Contributions

S.Y. and D.F. designed the research strategy. M.S.A., M.O. and D.F performed the microscopy. M.S.A. performed the survival assays. M.S.A. and D.F performed the FACS and M.R. helped with analysis. M.O, S.Y. and D.F. performed the biochemistry. M.C. measured MIC in rich medium on Gram positive and negative strains and in minimal medium on pathogenic strains. M.S.A., M.O. and S. Y. performed other MIC experiments. D.F. performed the chemical synthesis and M.P.H. the NMR and LC-MS. D.F. wrote the manuscript. All authors have given approval to the final version of the manuscript.

ACKNOWLEDGMENTS

We wish to thank Marc Mirande, Soufian Ouchane, Anne-Soisig Steunou, J. Dubois, Stéphanie Bury-Moné for use of equipment. We wish to thank David Buisson for help with the LC-MS. We wish to thank Christophe Beloin, Suzana Salcedo, Frédéric Boccard, Viginia Lioy, Etienne Dervyn, Jean-Luc Pernodet, Philippe Bouloc for strains and Isabelle Broutin for helpful discussions. The authors dedicate this paper to the memory of their colleague Jean-Louis Fourrey. This work was supported by the Centre National de la Recherche Scientifique (CNRS) to D.F. and S.Y. M.O. was supported by JASSO, a fellowship from the French embassy in Japan "Bourse du gouvernement français" and a fellowship from FRM (Fondation pour la recherche Médicale-FDT20140931068). M.S.A. was supported by a PhD fellowship from the French Ministère de l'Enseignement Supérieur et de la Recherche (MESR).

REFERENCES

(1) Jackson, J.; Chen, C.; Buising, K. Aminoglycosides: How Should We Use Them in the 21st Century? *Curr. Opin. Infect. Dis.* **2013**, *26* (6), 516–525.

(2) Takahashi, Y.; Igarashi, M. Destination of Aminoglycoside Antibiotics in the "Post-Antibiotic Era." *J. Antibiot.* **2018**, *71*, 4–14.

(3) Aggen, J. B.; Armstrong, E. S.; Goldblum, A. A.; Dozzo, P.; Linsell, M. S.; Gliedt, M. J.; Hildebrandt, D. J.; Feeney, L. A.; Kubo, A.; Matias, R. D.; Lopez, S.; Gomez, M.; Wlasichuk, K. B.; Diokno, R.; Miller, G. H.; Moser, H. E. Synthesis and Spectrum of the Neoglycoside ACHN-490. *Antimicrob. Agents Chemother.* **2010**, *54* (11), 4636–4642.

(4) Huth, M. E.; Han, K.-H.; Sotoudeh, K.; Hsieh, Y.-J.; Effertz, T.; Vu, A. A.; Verhoeven, S.; Hsieh, M. H.; Greenhouse, R.; Cheng, A. G.; Ricci, A. J. Designer Aminoglycosides Prevent Cochlear Hair Cell Loss and Hearing Loss. *J. Clin. Invest.* **2015**, *125* (2), 583–592.

(5) Matt, T.; Ng, C. L.; Lang, K.; Sha, S.-H.; Akbergenov, R.; Shcherbakov, D.; Meyer, M.; Duscha, S.; Xie, J.; Dubbaka, S. R.; Perez-Fernandez, D.; Vasella, A.; Ramakrishnan, V.; Schacht, J.; Böttger, E. C. Dissociation of Antibacterial Activity and Aminoglycoside Ototoxicity in the 4-Monosubstituted 2-Deoxystreptamine Apramycin. *Proc. Natl. Acad. Sci. U.S.A.* **2012**, *109* (27), 10984–10989.

(6) Sato, R.; Tanigawara, Y.; Kaku, M.; Aikawa, N.; Shimizu, K. Pharmacokinetic-Pharmacodynamic Relationship of Arbekacin for Treatment of Patients Infected with Methicillin-Resistant Staphylococcus Aureus. *Antimicrob. Agents Chemother.* **2006**, *50* (11), 3763–3769.

(7) Zhanel, G. G.; Lawson, C. D.; Zelenitsky, S.; Findlay, B.; Schweizer, F.; Adam, H.; Walkty, A.; Rubinstein, E.; Gin, A. S.; Hoban, D. J.; Lynch, J. P.; Karlowsky, J. A. Comparison of the Next-Generation Aminoglycoside Plazomicin to Gentamicin, Tobramycin and Amikacin. *Expert Rev Anti Infect Ther* **2012**, *10* (4), 459–473.

(8) Borovinskaya, M. A.; Pai, R. D.; Zhang, W.; Schuwirth, B. S.; Holton, J. M.; Hirokawa, G.; Kaji, H.; Kaji, A.; Cate, J. H. Structural Basis for Aminoglycoside Inhibition of Bacterial Ribosome Recycling. *Nat Struct Mol Biol* **2007**, *14* (8), 727–732.

(9) Campuzano, S.; Vazquez, D.; Modolell, J. Functional Interaction of Neomycin B and Related Antibiotics with 30S and 50S Ribosomal Subunits. *Biochem Biophys Res Commun* **1979**, *87* (3), 960–966.

(10) Moazed, D.; Noller, H. F. Interaction of Antibiotics with Functional Sites in 16S Ribosomal RNA. *Nature* **1987**, *327* (6121), 389–394.

(11) Davies, J.; Gorini, L.; Davis, B. D. Misreading of RNA Codewords Induced by Aminoglycoside Antibiotics. *Mol Pharmacol* **1965**, *1* (1), 93–106.

(12) Carter, A. P.; Clemons, W. M.; Brodersen, D. E.; Morgan-Warren, R. J.; Wimberly, B. T.; Ramakrishnan, V. Functional Insights from the Structure of the 30S Ribosomal Subunit and Its Interactions with Antibiotics. *Nature* **2000**, *407* (6802), 340–348.

(13) Demeshkina, N.; Jenner, L.; Westhof, E.; Yusupov, M.; Yusupova, G. A New Understanding of the Decoding Principle on the Ribosome. *Nature* **2012**, *484* (7393), 256–259.

(14) Fourmy, D.; Recht, M. I.; Blanchard, S. C.; Puglisi, J. D. Structure of the A Site of Escherichia Coli 16S Ribosomal RNA Complexed with an Aminoglycoside Antibiotic. *Science* **1996**, *274* (5291), 1367–1371.

(15) Vicens, Q.; Westhof, E. Crystal Structure of Paromomycin Docked into the Eubacterial Ribosomal Decoding A Site. *Structure* **2001**, *9* (8), 647–658.

(16) Yoshizawa, S.; Fourmy, D.; Puglisi, J. D. Structural Origins of Gentamicin Antibiotic Action. *Embo J* **1998**, *17* (22), 6437–6448.

(17) Cabanas, M. J.; Vazquez, D.; Modolell, J. Inhibition of Ribosomal Translocation by Aminoglycoside Antibiotics. *Biochem Biophys Res Commun* **1978**, *83* (3), 991–997.

(18) Misumi, M.; Nishimura, T.; Komai, T.; Tanaka, N. Interaction of Kanamycin and Related Antibiotics with the Large Subunit of Ribosomes and the Inhibition of Translocation. *Biochem Biophys Res Commun* **1978**, *84* (2), 358–365.

(19) Hirokawa, G.; Kiel, M. C.; Muto, A.; Selmer, M.; Raj, V.

S.; Liljas, A.; Igarashi, K.; Kaji, H.; Kaji, A. Post-Termination Complex Disassembly by Ribosome Recycling Factor, a Functional TRNA Mimic. *Embo J* **2002**, *21* (9), 2272–2281.

(20) Hirokawa, G.; Kaji, H.; Kaji, A. Inhibition of Antiassociation Activity of Translation Initiation Factor 3 by Paromomycin. *Antimicrob Agents Chemother* **2007**, *51* (1), 175–180.

(21) Wallace, B. J.; Tai, P. C.; Herzog, E. L.; Davis, B. D. Partial Inhibition of Polysomal Ribosomes of Escherichia Coli by Streptomycin. *Proc Natl Acad Sci U S A* **1973**, *70* (4), 1234–1237.

(22) Foster, C.; Champney, W. S. Characterization of a 30S Ribosomal Subunit Assembly Intermediate Found in Escherichia Coli Cells Growing with Neomycin or Paromomycin. *Arch Microbiol* **2008**, *189* (5), 441–449.

(23) Mehta, R.; Champney, W. S. 30S Ribosomal Subunit Assembly Is a Target for Inhibition by Aminoglycosides in Escherichia Coli. *Antimicrob Agents Chemother* **2002**, *46* (5), 1546–1549.

(24) Sykes, M. T.; Shajani, Z.; Sperling, E.; Beck, A. H.; Williamson, J. R. Quantitative Proteomic Analysis of Ribosome Assembly and Turnover in Vivo. *J Mol Biol* **2010**, *403* (3), 331–345.

(25) Davis, B. D. Mechanism of Bactericidal Action of Aminoglycosides. *Microbiol Rev* **1987**, *51* (3), 341–350.

(26) Hancock, R. E. Aminoglycoside Uptake and Mode of Action-with Special Reference to Streptomycin and Gentamicin. II. Effects of Aminoglycosides on Cells. *J. Antimicrob. Chemother.* **1981**, *8* (6), 429–445.

(27) Taber, H. W.; Mueller, J. P.; Miller, P. F.; Arrow, A. S. Bacterial Uptake of Aminoglycoside Antibiotics. *Microbiol Rev* **1987**, *51* (4), 439–457.

(28) Bryan, L. E.; Kwan, S. Mechanisms of Aminoglycoside Resistance of Anaerobic Bacteria and Facultative Bacteria Grown Anaerobically. *J. Antimicrob. Chemother.* **1981**, *8 Suppl D*, 1–8.

(29) Damper, P. D.; Epstein, W. Role of the Membrane Potential in Bacterial Resistance to Aminoglycoside Antibiotics. *Antimicrob. Agents Chemother.* **1981**, *20* (6), 803–808.

(30) Eisenberg, E. S.; Mandel, L. J.; Kaback, H. R.; Miller, M. H. Quantitative Association between Electrical Potential across the Cytoplasmic Membrane and Early Gentamicin Uptake and Killing in Staphylococcus Aureus. *J. Bacteriol.* **1984**, *157* (3), 863–867.

(31) Davis, B. D.; Chen, L. L.; Tai, P. C. Misread Protein Creates Membrane Channels: An Essential Step in the Bactericidal Action of Aminoglycosides. *Proc Natl Acad Sci U S A* **1986**, *83* (16), 6164–6168.

(32) Hancock, R. E. Aminoglycoside Uptake and Mode of Action with Special Reference to Streptomycin and Gentamicin. I. Antagonists and Mutants. *J. Antimicrob. Chemother.* **1981**, *8* (4), 249–276.

(33) Peng, B.; Su, Y.-B.; Li, H.; Han, Y.; Guo, C.; Tian, Y.-M.; Peng, X.-X. Exogenous Alanine and/or Glucose plus Kanamycin Kills Antibiotic-Resistant Bacteria. *Cell Metab.* **2015**, *21* (2), 249–262.

(34) Stone, M. R. L.; Butler, M. S.; Phetsang, W.; Cooper, M. A.; Blaskovich, M. A. T. Fluorescent Antibiotics: New Research Tools to Fight Antibiotic Resistance. *Trends Biotechnol.* **2018**, *36* (5), 523–536.

(35) Allison, K. R.; Brynildsen, M. P.; Collins, J. J. Metabolite-Enabled Eradication of Bacterial Persisters by Aminoglycosides. *Nature* **2011**, *473* (7346), 216–220.

(36) Cinquin, B.; Maigre, L.; Pinet, E.; Chevalier, J.; Stavenger, R. A.; Mills, S.; Réfrégiers, M.; Pagès, J.-M. Microspectrometric Insights on the Uptake of Antibiotics at the Single Bacterial Cell Level. *Sci Rep* **2015**, *5*, 17968.

(37) Vergalli, J.; Dumont, E.; Pajović, J.; Cinquin, B.; Maigre, L.; Masi, M.; Réfrégiers, M.; Pagés, J.-M. Spectrofluorimetric Quantification of Antibiotic Drug Concentration in Bacterial Cells for the Characterization of Translocation across Bacterial Membranes. *Nat Protoc* **2018**, *13* (6), 1348–1361.

(38) Dumont, E.; Vergalli, J.; Conraux, L.; Taillier, C.; Vassort, A.; Pajovic, J.; Réfrégiers, M.; Mourez, M.; Pagès, J.-M. Antibiotics and Efflux: Combined Spectrofluorimetry and Mass Spectrometry to Evaluate the Involvement of Concentration and Efflux Activity in Antibiotic Intracellular Accumulation. *J. Antimicrob. Chemother.* **2019**, *74* (1), 58–65.

(39) Hernandez Linares, A.; Fourmy, D.; Fourrey, J.-L.; Loukaci, A. Introduction of a Substituent at the 5"-Position of N-Boc Neomycin B under Mitsunobu Reaction Conditions. *Org. Biomol. Chem.* **2005**, *3* (11), 2064–2066.

(40) Dempsey, G. T.; Vaughan, J. C.; Chen, K. H.; Bates, M.; Zhuang, X. Evaluation of Fluorophores for Optimal Performance in Localization-Based Super-Resolution Imaging. *Nat Methods* **2011**, *8* (12), 1027–1036.

(41) Recht, M. I.; Douthwaite, S.; Puglisi, J. D. Basis for Prokaryotic Specificity of Action of Aminoglycoside Antibiotics. *Embo J* **1999**, *18* (11), 3133–3138.

(42) Pfister, P.; Hobbie, S.; Brull, C.; Corti, N.; Vasella, A.; Westhof, E.; Bottger, E. C. Mutagenesis of 16S RRNA C1409-G1491 Base-Pair Differentiates between 6'OH and 6'NH3+ Aminoglycosides. *J Mol Biol* **2005**, *346* (2), 467–475.

(43) Perez-Fernandez, D.; Shcherbakov, D.; Matt, T.; Leong, N. C.; Kudyba, I.; Duscha, S.; Boukari, H.; Patak, R.; Dubbaka, S. R.; Lang, K.; Meyer, M.; Akbergenov, R.; Freihofer, P.; Vaddi, S.; Thommes, P.; Ramakrishnan, V.; Vasella, A.; Böttger, E. C. 4'-O-Substitutions Determine Selectivity of Aminoglycoside Antibiotics. *Nat Commun* **2014**, *5*, 3112.

(44) Perzynski, S.; Cannon, M.; Cundliffe, E.; Chahwala, S. B.; Davies, J. Effects of Apramycin, a Novel Aminoglycoside Antibiotic on Bacterial Protein Synthesis. *Eur. J. Biochem.* **1979**, *99* (3), 623–628.

(45) Hancock, R. E.; Farmer, S. W.; Li, Z. S.; Poole, K. Interaction of Aminoglycosides with the Outer Membranes and Purified Lipopolysaccharide and OmpF Porin of Escherichia Coli. *Antimicrob Agents Chemother* **1991**, *35* (7), 1309–1314.

(46) Okuda, M.; Fourmy, D.; Yoshizawa, S. Use of Baby Spin-

ach and Broccoli for Imaging of Structured Cellular RNAs. *Nucleic Acids Res.* **2017**, *45* (3), 1404–1415.

(47) Jörgensen, F.; Kurland, C. G. Death Rates of Bacterial Mutants. *FEMS Microbiology Letters* **1987**, *40* (1), 43–46.

(48) White, J. R.; White, H. L. Streptomycinoid Antibiotics: Synergism by Puromycin. *Science* **1964**, *146* (3645), 772–774.

(49) Klainer, A. S.; Russell, R. R. Effect of the Inhibition of Protein Synthesis on the Escherichia Coli Cell Envelope. *Antimicrob. Agents Chemother.* **1974**, *6* (2), 216–224.

(50) Ezraty, B.; Vergnes, A.; Banzhaf, M.; Duverger, Y.; Huguenot, A.; Brochado, A. R.; Su, S. Y.; Espinosa, L.; Loiseau, L.; Py, B.; Typas, A.; Barras, F. Fe-S Cluster Biosynthesis Controls Uptake of Aminoglycosides in a ROS-Less Death Pathway. *Science* **2013**, *340* (6140), 1583–1587.

(51) Bryan, L. E.; Elzen, H. M. V. D. Streptomycin Accumulation in Susceptible and Resistant Strains of Escherichia Coli and Pseudomonas Aeruginosa. *Antimicrob. Agents Chemother.* **1976**, *9* (6), 928–938.

(52) Aires, J. R.; Köhler, T.; Nikaido, H.; Plésiat, P. Involvement of an Active Efflux System in the Natural Resistance of Pseudomonas Aeruginosa to Aminoglycosides. *Antimicrob. Agents Chemother.* **1999**, *43* (11), 2624–2628.

(53) Sobel, M. L.; McKay, G. A.; Poole, K. Contribution of the MexXY Multidrug Transporter to Aminoglycoside Resistance in Pseudomonas Aeruginosa Clinical Isolates. *Antimicrob. Agents Chemother.* **2003**, *47* (10), 3202–3207.

(54) Westbrock-Wadman, S.; Sherman, D. R.; Hickey, M. J.; Coulter, S. N.; Zhu, Y. Q.; Warrener, P.; Nguyen, L. Y.; Shawar, R. M.; Folger, K. R.; Stover, C. K. Characterization of a Pseudomonas Aeruginosa Efflux Pump Contributing to Aminoglycoside Impermeability. *Antimicrob. Agents Chemother.* **1999**, *43* (12), 2975–2983.

(55) Li, X.-Z.; Nikaido, H. Efflux-Mediated Drug Resistance in Bacteria. *Drugs* **2004**, *64* (2), 159–204.

(56) Monlezun, L.; Phan, G.; Benabdelhak, H.; Lascombe, M.-B.; Enguéné, V. Y. N.; Picard, M.; Broutin, I. New OprM Structure Highlighting the Nature of the N-Terminal Anchor. *Front Microbiol* **2015**, *6*, 667.

(57) Nakashima, R.; Sakurai, K.; Yamasaki, S.; Nishino, K.; Yamaguchi, A. Structures of the Multidrug Exporter AcrB Reveal a Proximal Multisite Drug-Binding Pocket. *Nature* **2011**, *480* (7378), 565–569.

(58) Murakami, S.; Nakashima, R.; Yamashita, E.; Matsumoto, T.; Yamaguchi, A. Crystal Structures of a Multidrug Transporter Reveal a Functionally Rotating Mechanism. *Nature* **2006**, *443* (7108), 173–179.

(59) Hadidi, K.; Wexselblatt, E.; Esko, J. D.; Tor, Y. Cellular Uptake of Modified Aminoglycosides. *J. Antibiot.* **2018**, *71*, 142–145.

(60) Böttger, E. C.; Crich, D. Aminoglycosides: Time for the Resurrection of a Neglected Class of Antibacterials? *ACS Infect Dis* **2020**, *6* (2), 168-172.

(61) Sati, G. C.; Sarpe, V. A.; Furukawa, T.; Mondal, S.; Mantovani, M.; Hobbie, S. N.; Vasella, A.; Böttger, E. C.; Crich, D. Modification at the 2'-Position of the 4,5-Series of 2-Deoxystreptamine Aminoglycoside Antibiotics To Resist Aminoglycoside Modifying Enzymes and Increase Ribosomal Target Selectivity. *ACS Infect Dis* **2019**, *5* (10), 1718–1730.

(62) Jagt, R. B. C.; Gómez-Biagi, R. F.; Nitz, M. Pattern-Based Recognition of Heparin Contaminants by an Array of Self-Assembling Fluorescent Receptors. *Angew. Chem. Int. Ed. Engl.* **2009**, *48* (11), 1995–1997.

(63) Mazauric, M. H.; Leroy, J. L.; Visscher, K.; Yoshizawa, S.; Fourmy, D. Footprinting Analysis of BWYV Pseudoknot-Ribosome Complexes. *Rna* **2009**, *15* (9), 1775–1786.

(64) Powers, T.; Noller, H. F. A Functional Pseudoknot in 16S Ribosomal RNA. *Embo J* **1991**, *10* (8), 2203–2214.

(65) Yoshizawa, S.; Fourmy, D.; Puglisi, J. D. Recognition of the Codon-Anticodon Helix by Ribosomal RNA. *Science* **1999**, *285* (5434), 1722–1725.

(66) Fourmy, D.; Yoshizawa, S. Protein-RNA Footprinting: An Evolving Tool. *Wiley Interdiscip Rev RNA* **2012**, *3* (4), 557–566.

(67) Ying, B. W.; Fourmy, D.; Yoshizawa, S. Substitution of the Use of Radioactivity by Fluorescence for Biochemical Studies of RNA. *Rna* **2007**, *13* (11), 2042–2050.

(68) Ducret, A.; Quardokus, E. M.; Brun, Y. V. MicrobeJ, a Tool for High Throughput Bacterial Cell Detection and Quantitative Analysis. *Nat Microbiol* **2016**, *1* (7), 16077.

Chlorine E6-Linked Aminoglycosides and Their Use in Photodynamic Therapy Against Persister Cells and Multidrug Resistant Bacteria

Melina Cyrenne[1]*, Marie-Pierre Heck[2], Satoko Yoshizawa[1], Dominique Fourmy[1]*

[1] ENS Paris-Saclay, Université Paris-Saclay, CNRS UMR8113, IDA FR3242, Laboratory of Biology and Applied Pharmacology (LBPA), 91190, Gif-sur-Yvette, France.
[2] Université Paris-Saclay, CEA, Service de Chimie Bio-organique et de Marquage, 91191 Gif-sur-Yvette, France.

*** Correspondence:**
Melina Cyrenne and Dominique Fourmy

melina.cyrenne@gmail.com; dominique.fourmy@ens-paris-saclay.fr

Keywords: persister cells, aPDT (antimicrobial photodynamic therapy), chlorine E6, aminoglycosides, photosensitizer, ESKAPE pathogens

Abstract

It is a known fact that the rise in antibiotic resistance is a global threat to modern medicine. With this in mind, the scientific community is experimenting alternative ways to treat bacterial infections. One of these promising strategies is the use of antibacterial photodynamic therapy (aPDT) or photodynamic inactivation (aPDI). However, the technique has some limitations, including the struggle to kill Gram-negative bacteria through aPDT alone and the lack of knowledge surrounding the application of aPDT to multi-drug tolerant subpopulations called persister cells. Through the use of photosensitizer-linked aminoglycosides, we have successfully shown synergistic killing of Gram-positive and Gram-negative ESKAPE pathogens planktonic and persister cells. Compounds have a synergistic effect against clinically relevant species like *P. aeruginosa* and *S. aureus* when compared to the aminoglycoside and the photosensitizer alone. aPDT also resulted in eradication of persister cells in ESKAPE pathogens *S. aureus* Newman and methicillin resistant *S. aureus* USA300. In addition, the low survival of aminoglycoside-resistant species demonstrates that the development of resistance against our compounds is not likely. Their use in killing drug-resistant and drug-tolerant bacteria through aPDT is promising in the fight against antibiotic resistance, particularly in hospital settings where they could be applied to sterilizing equipment.

1. Introduction

Excessive use and misuse of antibiotics have led to the spread of multi-drug resistant (MDR) bacteria in the last years and the threat of returning to the "pre-antibiotic era" has brought the scientific community to look out for new ways to treat bacterial infections (Cassini *et al.*, 2019; Nordmann *et al.*, 2011). In addition to easily curable diseases becoming a risk to human health, discovery of new antibiotics has been a hard task in the last decades (Martens and Demain, 2017, Miethke *et al*., 2021). Bacterial species from the ESKAPE group (*Enterococcus faecium, Staphylococcus aureus, Klebsiella pneumoniae, Acinetobacter baumannii*, *Pseudomonas aeruginosa* and *Enterobacter* spp.) are known to be quite problematic in hospital settings and are defined by their virulence and antibiotic-resistance (Rice, 2008). Promoting this increase in drug resistance are bacterial "powers" like the creation of

biofilms and antibiotic-tolerant subpopulations called persister cells which are linked to chronic infections like recurring urinary tract infections, salmonellosis and tuberculosis (Grant and Hung, 2013). Additionally, a common occurrence of infection with persister cells is through the insertion of contaminated external medical devices in the patient (prosthetic joints, prosthetic heart valves, central venous catheters, etc.) (Bryers, 2008).

Although first observed in the 1940s, the matter of persistence has gone largely unnoticed over the years because it is a transient condition touching a small fraction of bacterial populations, while the problem of antibiotic resistance was well defined and recognized as a research priority (Verstraeten *et al.*, 2016; Bigger, 1944; Hobby *et al.*, 1942). As it is phenotypic and not genetic resistance, persister cells are also harder to study (Lewis, 2010). Nevertheless, persister cells are as threatening as drug-resistant bacteria. Through their state of slowed metabolism, they acquire multidrug tolerance and form niches that can promote eventual genetic resistance (Alkasir *et al.*, 2018; Cohen *et al.*, 2013; Shah *et al.*, 2006). In addition to showing multidrug tolerance, they also have the capacity to survive within the host and hide inside macrophages (Helaine *et al.*, 2014; Grant and Hung, 2013). Finding strategies to eradicate persisters is a challenge which was mostly addressed for Gram-positive pathogens (Allison *et al.*, 2011, Conlon *et al.*, 2013, Kim *et al*., 2018).

Alternatives to antibiotherapy have been explored and reviewed in depth by Czaplewski in 2016. From the 142 citations covered by the authors, none mentions the use of photodynamic therapy, a technique where light-activated molecules called photosensitizers (PS) are used to produce reactive oxygen species (ROS) to kill bacteria. This is probably due to the fact that those molecules were mostly known for their use in treating cancerous cells. For example, Photofrin is a well-studied porphyrin used in patients suffering from early or late-stage lung cancer, digestive tract cancer and genitourinary tract cancer in Canada, the Netherlands, France, Germany, Japan, and the United States (Macdonald and Dougherty, 2001; Dougherty *et al.*, 1998). In the last few years, the use of photosensitizers in the field of microbiology has gained interest as a new antibacterial tool. In combination with light, in what is called antibacterial photodynamic therapy (aPDT) or antibacterial photoinactivation (aPDI), some photosensitizers have shown great potential in eradicating bacterial communities and biofilms. aPDT is also promising for other reasons. For example, it has been shown that bacteria do not develop resistance to aPDT because of the wide range of cellular components targeted by the produced ROS (Denis *et al.*, 2011). Moreover, activity and/or production of several virulence factors is affected by some of the produced ROS, which leads to reduced pathogenicity in treated cells that survive the initial aPDT (Wozniack and Grinholc, 2018; Fila *et al.*, 2017).

However, even though the use of PSs in aPDT is quite promising, some limitations have been observed. Gram-negative species are known to be harder to kill through aPDT than their Gram-positive counterparts. Their outer membrane, in addition to the underlying peptidoglycan layer, play an important role in Gram-negative resistance to antibiotics that normally affect Gram-positive species (macrolides, novobiocin, rifamycin, lincomycin, clindamycin, fusidic acid) (Sperandio et al., 2013; Nikaido and Vaara, 1985). The morphological configuration of their membrane makes it difficult for photosensitizers to reach the periplasmic space and cytoplasm. Plus, even though ROS production near the outer membrane may generate loss of structural integrity for this layer, Gram-negative bacteria can survive without their capsule (Dahl et al., 1989; Straight and Spikes, 1985). Overall, it is more challenging to find potent photosensitizers to kill Gram-negative species (Sperandio *et al.*, 2013; Bertoloni *et al.*, 1990). “Vehicles” can be linked to promote uptake, like chitosan and polylysin, but most solutions consist in

the use of membrane-disorganizing agents like detergents and antibiotics prior to or after aPDT (Calixto *et al.,* 2019; Sperandio *et al.,* 2013; Soukos *et al.,* 1997; Nitzan *et al.,* 1994).

Here we propose a one-step process consisting in the use of aminoglycosides (AGs) as a "vehicle" linked to photosensitizers. We have tested several PS-linked aminoglycosides and the two Ce6-AG conjugates resulted in high killing not only in Gram-positive but also Gram-negative ESKAPE species. In planktonic cells, a disinfecting effect was witnessed in *A. baumannii* DSM3001, *S. aureus* Mu50 (a strain resistant to AGs) and *S. aureus* USA300 and significant mortality was found in *P. aeruginosa* PA14 and PAO1 strains. The effect was not limited to planktonic cells as some biofilm cells and persister cells of *S. aureus* USA300 and Newman strains were also affected by aPDT with those compounds. We observed a synergistic effect of connecting the aminoglycosides to Ce6 while this outcome was not seen when using both molecules together without being chemically linked. aPDT on aminoglycoside-resistant species also led to low survival, suggesting that singlet oxygen production alone may suffice in killing those bacteria.

2. Material and methods

2.1 Compound production

Atto MB2 NHS-ester was obtained from Sigma-Aldrich. Ce6 was purchased from Bertin Bioreagent, dicyclohexylcarbodiimide *N*-hydroxysuccinimide, neomycin and tobramycin from Sigma.

A derivative of neomycin containing 2-N-trifluoroacetamidoethylthio in place of a hydroxyl group in ring III was used to conjugate neomycin to NHS-ester dye as previously described (Sabeti-Azad *et al.,* 2020). Other amino groups of the neomycin derivative were protected by hexa-N-tert-butyloxycarbonyl groups for selective reactivity at the specific 5" NH_2 position. Selective deprotection of the 5" position was performed in ammonium hydroxide in methanol, and the unique free amino group was reacted with MB2 or Ce6 NHS-ester. The different steps of the synthesis of tobramycin where all amino groups except one were protected by hexa-N-tert-butyloxycarbonyl groups for selective reactivity can be found in the Supplementary material. The NHS ester of Ce6 was prepared by reacting 1.5 equivalents of dicyclohexylcarbodiimide and 1.5 equivalents of NHS with 1 equivalent of Ce6 in dry dimethyl sulfoxide (DMSO) for 24 hours and was frozen in aliquots for further use following the reported procedure (Khadem *et al.,* 1999). All coupling reactions were monitored by analytical thin-layer chromatography (TLC) on silica gel 60 F254 plates (0.25 mm). The Neo-MB2, Neo-Ce6 and Tobra-Ce6 conjugates were dissolved in methanol for purification on TLC plates (Silica gel 60, Merck). For Neo-MB2, the eluent used was chloroform/Ethanol/NH_4OH 5.6/3.8/0.45 and chloroform/Ethanol/NH_4OH 7.8/2/0.16 for Neo-Ce6. For Tobra-Ce6, the purification was performed in two steps. The first step was performed with the eluent chloroform/Ethanol/NH_4OH 7.8/2/0.16 for Tobra-Ce6. The silica gel with the product of lowest migration was recovered and eluted with methanol. The second purification step used the eluent chloroform/Ethanol/NH_4OH 7.8/2/0.39 and the product of fastest migration recovered. For all conjugates, the silica gel was recovered and placed in Eppendorf tubes and the product was eluted in methanol. The resin and the solvent were separated by centrifugation and the elution step was repeated 3 times. The sample was dried and finally, removal of the butyloxycarbonyl groups was performed in trifluoroacetic acid (90%) for 10 minutes at room temperature.

2.2 Evaluating Singlet Oxygen Production in Compounds

Singlet oxygen production was evaluated using the Singlet Oxygen Sensor Green kit from Molecular Probes. Reagents were prepared accordingly to the manufacturer and the final concentration of 2.5 µM of the reagent was used for all experiments. Dilutions of both the compounds, photosensitizers and SOSGR reagent were made in cation-adjusted Mueller-Hinton-II broth (MHB-CA) (Becton, Dickinson and Company, USA) to mimic experimental settings. Irradiation was done at 660 nm for 5 minutes (857 mJ/mm²) with the Solis-660C lamp from ThorLabs on a total volume of 120 µL placed in transparent 96-well plate (Nunclon Delta Surface, Thermo Scientific). Quickly, after illumination, 100 µL of the reaction were transferred to a 96-well black plate (Optiplate-96F, Perkin Elmer). Relative light units (RLU) emitted by the SOSGR were read on a PerkinElmer Victor X5 at 485/535 nm.

2.3 Microorganisms and growth conditions

Acinetobacter baumannii DSM30011, *Bacillus subtilis* 168, *Pseudomonas aeruginosa* PA14, *P. aeruginosa* PAO1, *Staphylococcus aureus* Mu50, *S. aureus* Newman and *S. aureus* USA300 were all grown in MHB-CA at 37°C with an agitation of 180 rpm. *Candida albicans* SC5314 was grown in yeast extract peptone dextrose broth at 35°C with an agitation of 180 rpm.

2.4 Minimal Inhibitory Concentration Evaluation

Minimal inhibitory concentrations (MICs) for selected bacteria were investigated according to the EUCAST guidelines. Serial dilutions of the compounds, photosensitizers and aminoglycosides were made in MHB-CA in 384-well plates. Stationary-phase cells were diluted in MHB-CA to have a final concentration of 5.5 x 10^5 CFU/mL. Samples were incubated in the dark for 20 minutes at 37°C and either irradiated at 660 nm for 30 minutes with a LED device or kept in the dark. Irradiated samples received a total of 168 mJ/mm². Plates were then incubated at 37°C for 18 hours and MICs were evaluated visually. Triplicates were done and the synergy, or fractional inhibitory concentration (FIC), was calculated according to Doern, 2014.

$$FIC = \frac{MIC\ of\ AB}{MIC\ of\ A} + \frac{MIC\ of\ AB}{MIC\ of\ B}$$

2.5 Antibacterial Photodynamic Therapy

2.5.1 Antibacterial photodynamic therapy on planktonic Cells

Cells were brought to stationary phase by incubating them in MHB-CA for at least 18 hours at 37°C with 180 rpm and diluted to an optical density of 1.0 just before the experiment. Cells were incubated for 20 minutes with either the compounds, photosensitizers alone, or aminoglycosides alone. Unless stated otherwise, a concentration of 10 µM was used for all experiments and samples were irradiated for 30 minutes at 660 nm with the Solis-660C lamp from ThorLabs, receiving a total of 5 J/mm².

After illumination, cells were washed with phosphate-buffered saline (PBS) 1X, serially diluted and plated on Mueller-Hinton agar. The next day, colony forming units (CFUs) were counted.

2.5.2 Antibacterial photodynamic therapy on biofilms

Stationary-phase cells were grown in MHB-CA and diluted to a concentration of 5.5 x 10^5 CFU/mL. A volume of 100 µL of diluted bacteria was placed in 96-well plates (Falcon, Cat #351172) overnight. The next day, the supernatant was removed carefully so as to not disturb the biofilm. The biofilms were washed three times using 150 µL of PBS 1X and incubated for 20 minutes in the dark at 37°C with the compounds, photosensitizers alone or aminoglycosides alone. Biofilms were then irradiated with the Solis-660C lamp from Thor Labs for a total 30 minutes (alternating 5 minutes of irradiation with 1 minute in darkness). Samples therefore received a total of 5 J/mm².

Biofilms were then aggressively pipetted and scratched off the plaque before being washed three times with 150 µL of PBS 1X. Pellets were then diluted in 96-well plates (Nunclon Delta Surface, Thermo Scientific) and placed on MH agar. The next day, CFUs were counted.

2.5.3 Antibacterial photodynamic therapy on persister cells

Before doing aPDT on persister cells, the persister plateau was established for selected species. Stationary-phase cells were therefore treated for a maximum of 24 hours with high doses of neomycin or tobramycin. Samples were collected at 0, 2, 4, 6 and 24 hours of incubation, washed with PBS 1X, diluted and placed on MH agar. The next day, CFUs were counted. Triplicates were done and concentrations which led to a survival plateau were selected for aPDT.

After static incubation for 6 to 24 hours with the previously selected aminoglycoside concentration, 10 µL of 100 µM of compounds, photosensitizers or aminoglycosides were added to 90 µL of samples. We chose not to wash or dilute the samples before aPDT as this sometimes led to persister cells reverting to a sensible phenotype. Cells were incubated in the dark for 20 minutes before being irradiated for 30 minutes at 660 nm with the Solis-660C lamp from Thor Labs, receiving a total of 5 J/mm². Samples were washed with PBS 1X, diluted and plated on MH agar. The next day, CFUs were counted. Persister plateau was confirmed by the insensitiveness of the numbers of CFUs to the further addition of aminoglycoside.

3. Statistics

Statistics were done using GraphPad Prism 8.4.3 (San Diego, CA, RRID:SCR_002798).

4. Results

4.1 Singlet Oxygen Production

We created three photosensitizer-AG conjugates and evaluated their capacity to produce singlet oxygen (Figure 1). Photosensitizers were selected according to their charge and effect against pathogenic bacteria. Aminoglycosides were chosen as they are known to bind to bacterial membranes (Sabeti-Azad *et al.*, 2020), penetrate biofilms (Lebeaux *et al.*, 2015; Singh *et al.*, 2010; Walters *et al.* 2003) and interact with persister cells from *E. coli* MG1655 (Sabeti-Azad, 2019). The Solis-660C lamp was used at a setting allowing for 171 mJ/minutes/mm² irradiation. Results show for Ce6-AG conjugates higher singlet oxygen production for both compounds when compared to Ce6 (Figure 1). Ce6 is poorly soluble in water

which can lead to self-quenching and sub-optimal therapeutic efficacy (Jeong *et al.*, 2011). Thanks to the AG moiety, Neo-Ce6 and Tobra-Ce6 are highly soluble which could positively influence singlet oxygen formation by preventing aggregation. Neo-MB produced less than half the singlet oxygen yielded by MB and ATTO-MB2 alone (Supplementary Figure S3) and was therefore not extensively studied in aPDT.

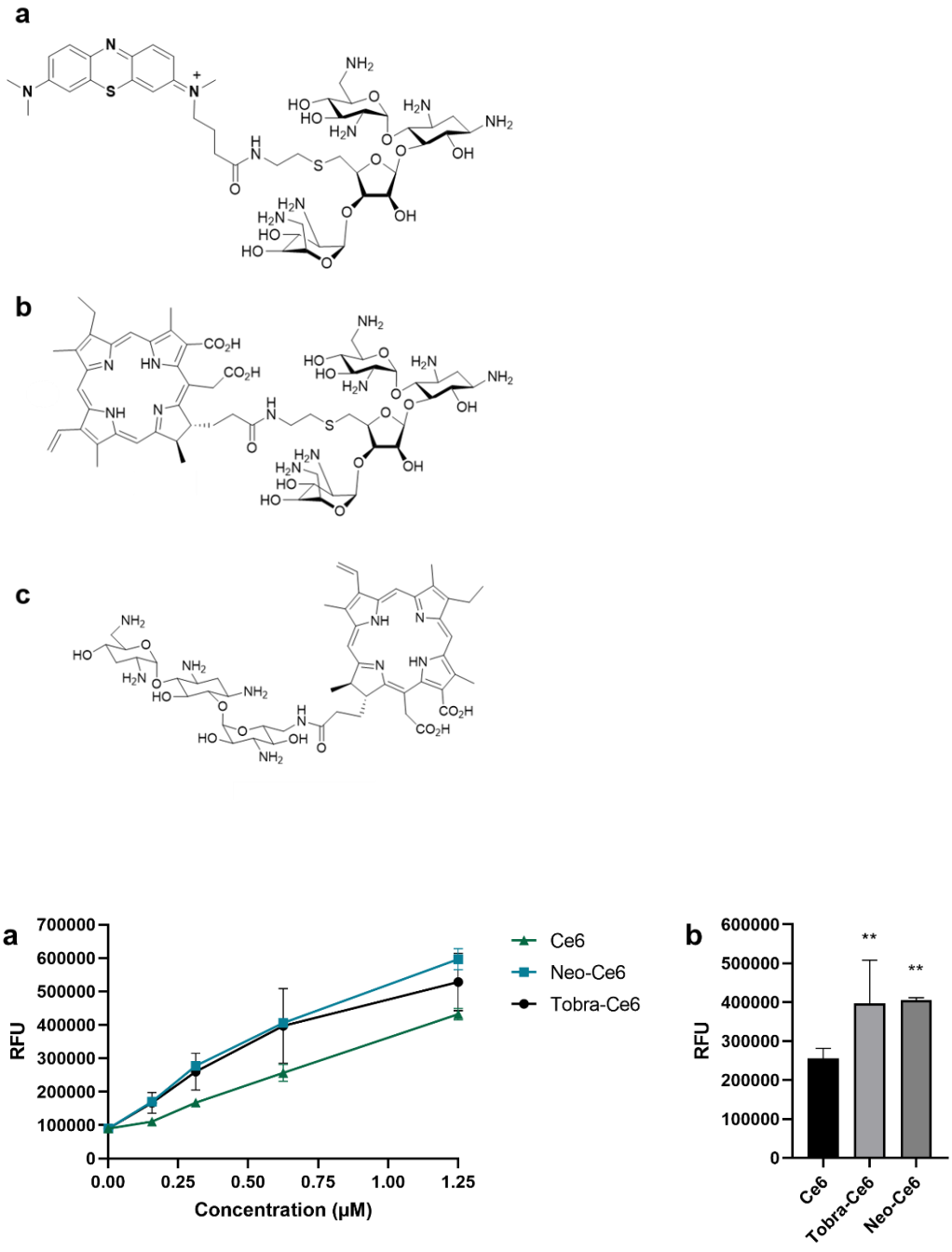

Figure 1: (upper panel) Photosensitizer-aminoglycoside conjugates: A) Neo-MB, B) Neo-Ce6 and C) Tobra-Ce6. (Lower panel) Fluorescence measured using the SOSGR kit (2.5 μM) after 5-minute

irradiation at 660 nm with the Solis 660C lamp. The experiments were performed in MHB-CA. (A) Curve with increasing concentration of Ce6 or compounds are shown. (B) Fluorescence intensity measured for a concentration of 0.6 µM.

4.2 Minimal Inhibitory Concentrations

MICs are shown in Table 1. Synergy was evaluated according to the fractional inhibitory concentration (FIC) for irradiated samples treated with the compounds only (Doern, 2014). The combination of neomycin and Ce6 in a Neo-Ce6 compound had a synergistic effect against *A. baumannii* DSM30011, *B. subtilis* 13517, and *S. aureus* strains USA300, Mu50 and Newman. Neo-Ce6 also demonstrated high inhibition against pathogenic yeast *C. albicans* SC5314. On the other hand, the compound had no synergistic effect against *P. aeruginosa* PA14 and PAO1 strains.

Tobra-Ce6 on the other hand was only tested on a few species as results were not as promising. It showed an additive effect against *A. baumannii* DSM30011 and *S. aureus* Newman, but no synergy.

Table 1: MICs for neomycin, tobramycin, Ce6, Neo-Ce6 and Tobra-Ce6 with (+) or without (-) irradiation. Results are expressed in µM. Synergy was only calculated for conjugates with irradiation (++: synergy; +: additive; =: no difference; -: antagonistic).

	Neomycin	Neo-Ce6			Tobramycin	Tobra-Ce6		
		+	-	Synergy		+	-	Synergy
A. baumannii DSM30011	8	0.5-1	16-32	++	4-8	2-4	> 16	+
B. subtilis 168	0.4	< 0.125	0.5-0.8	++				
C. albicans SC5314	> 512	< 0.5	> 16	++				
E. coli KanR	> 512	> 16	> 16	ND				
E. coli pET-29	128-256	> 16	> 16	ND				
K. pneumoniae LM21	2	4-8	16	-				
P. aeruginosa PA14	4	8	16	=	1-2	> 16	> 16	-
P. aeruginosa PAO1	16	8-16	> 16	=	0.5-1	4-8	> 16	-
S. aureus USA300	4	0.5	4-8	++	4	2-4	> 16	=
S. aureus Mu50	> 512	1-2	4-8	+	> 512	2-4	16	=
S. aureus Newman	8	0.5	4-8	++	4	2	> 16	+

Ce6	
+	-
> 64	> 64
> 64	> 64
32	> 64
> 64	> 64
> 64	> 64
> 64	> 64
> 64	> 64
> 64	> 64
16-32	> 64
4	> 64
64	> 64

4.3 aPDT on Planktonic Cells

Globally, we observed a drop in survival following aPDT for all strains and all compounds. Photosensitizers and aminoglycosides alone impacted survival for some strains, but not as much as the compounds. Irradiation by all tested light sources never affected the survival of control samples and samples being incubated with the aminoglycosides alone. In addition, we also tested adding unlinked neomycin and Ce6 to samples to confirm that Neo-Ce6 acted differently than both molecules separately. Results show survival was not as low in samples containing unlinked neomycin and Ce6 (Figure 2).

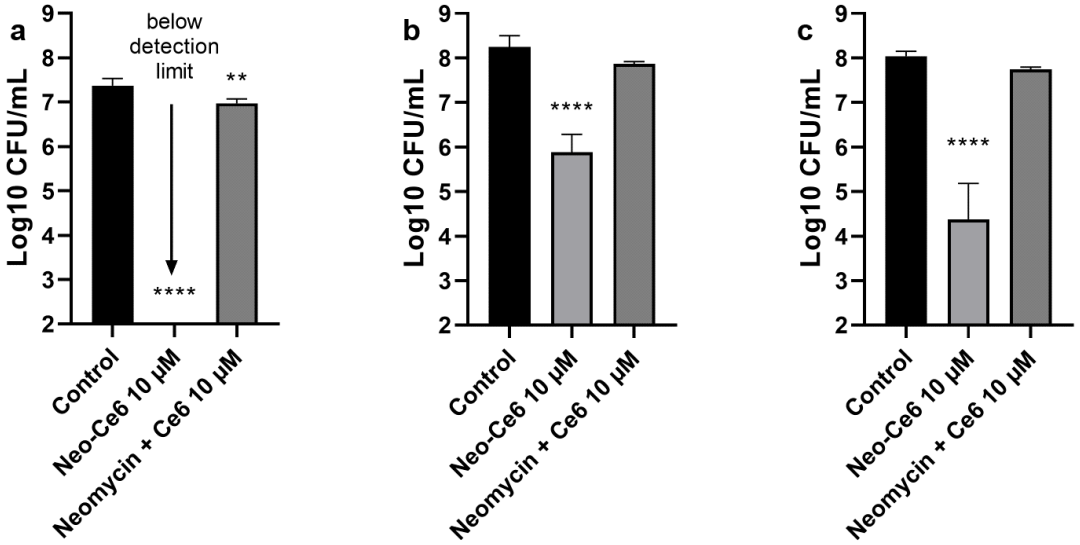

Figure 2: Comparison between aPDT with Neo-Ce6 and unlinked neomycin and Ce6 in a selection of Gram negative species. With *A. baumannii* DSM3011 (A), *K. pneumoniae* LM21 (B) and *P. aeruginosa* PA14 (C). Results are shown for the samples after irradiation (168 mJ/mm^2).

In *S. aureus* species Mu50 and USA300, survival was often close or below the detection limit in irradiated samples treated with Neo-Ce6 (Figures 3A, 3E). Tobra-Ce6 did lead to high bacterial death in Mu50 (Figure 3A), showing a significant difference (p = 0.0086) when compared to Ce6 alone. However, this is the only *S. aureus* strain for which Tobra-Ce6 leads to significantly less survival than Ce6 alone. On the other hand, except in *S. aureus* Newman, Neo-Ce6 leads to significantly more bacterial death than Ce6.

Mean CFU drops for irradiated samples are as follows. In *S. aureus* Mu50, survival dropped by 4.9, 5.4 and 3.2 log10 CFU/mL for Neo-Ce6, Tobra-Ce6 and Ce6, respectively. In *S. aureus* Newman, survival was slightly higher. Survival dropped by about 4.3, 3.9 and 3.6 log10 CFU/mL for Neo-Ce6, Tobra-Ce6 and Ce6, respectively. Finally, in *S. aureus* USA300, survival dropped by 5.6, 3.5 and 3.2 log10 CFU/mL for Neo-Ce6, Tobra-Ce6 and Ce6, respectively.

As shown in Figure 3, non-irradiated samples treated with Neo-Ce6 always display a weak but significant drop in CFUs (Figures 3B, 3D, 3F). Although the *p* is often low, this result has been seen in a few species, indicating the neomycin part of the compound may still have an antibiotic effect when linked to Ce6. Plus, this effect may be additive as neomycin alone at the same concentration does not lead to significantly less survival, except in *S. aureus* USA300.

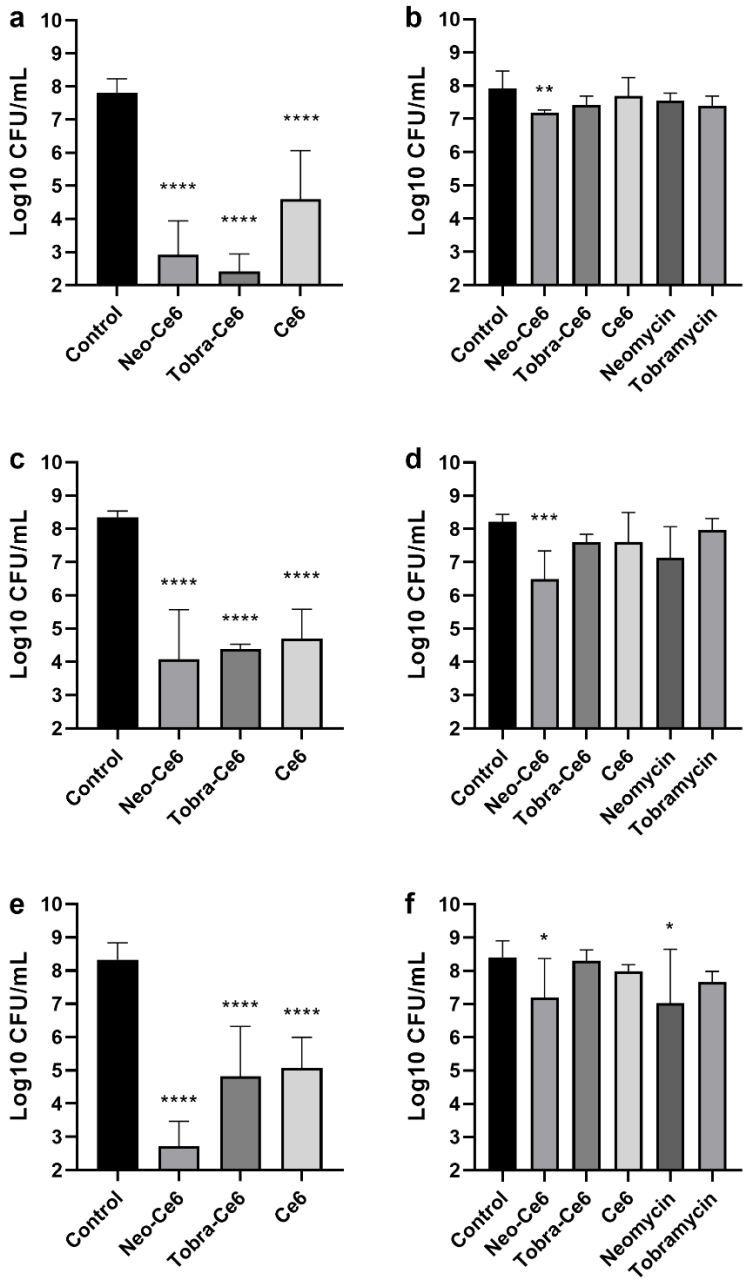

Figure 3: Log10 CFU/ml in *S. aureus* species, with or without irradiation. In A and B, *S. aureus* Mu50 with and without irradiation respectively, in C and D, *S. aureus* Newman with and without irradiation respectively and in E and F, *S. aureus* USA300 with and without irradiation respectively. Irradiated samples received 5 J/mm².

As described earlier, Gram-negative species are usually more resilient to aPDT than Gram-positive but we did have successful killing in most of our Gram-negative strains. For example, *A. baumannii* DSM30011 CFUs were under the detection limit in irradiated samples with Neo-Ce6 (Figure 4A). *E. coli* MG1655 mutants containing kanamycin-resistance cassettes also showed low survival following aPDT (Supplementary Figure S4). Survival was also close to the detection limit for non-irradiated samples (Figure 4B). Irradiated samples in Gram-positive *B. subtilis* 168 were also close to the detection limit (Figure 4C).

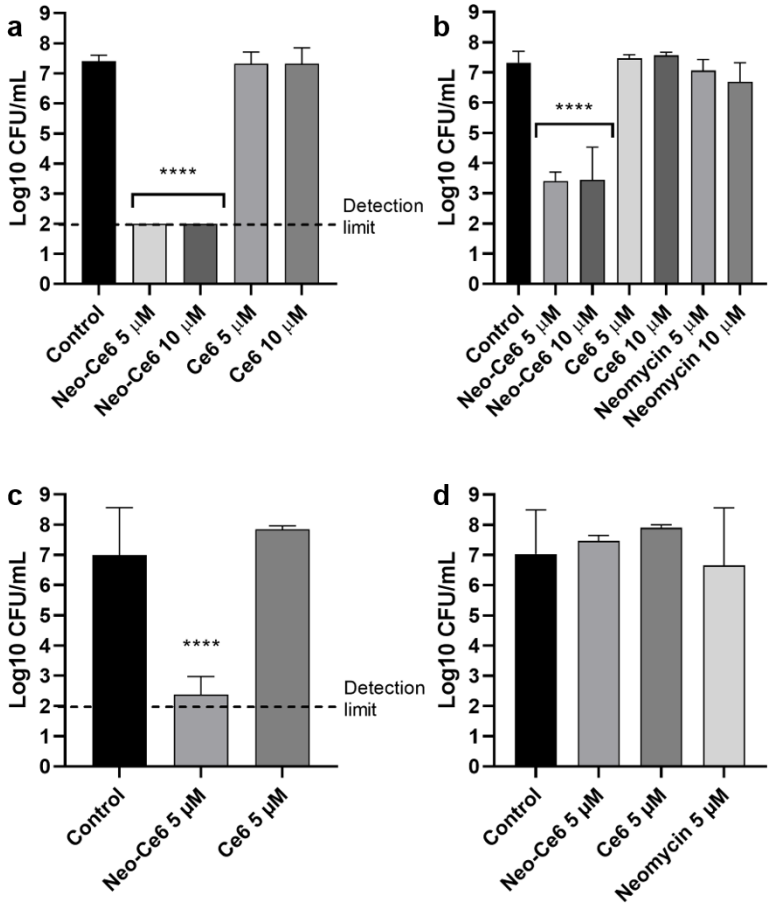

Figure 4: Log10 CFU/ml in Gram-negative and Gram-positive species following aPDT with Neo-Ce6. In A and B, *A. baumannii* DSM3001 with and without irradiation respectively, and in C and D, *B. subtilis* 168 with and without irradiation. Irradiated samples received a total of 168 mJ/mm².

Clinically relevant species *P. aeruginosa* PA14 and *P. aeruginosa* PAO1 were also used in aPDT. Survival dropped 3.8 and 2.6 log10 CFU/mL for irradiated *P. aeruginosa* PA14 cells treated with 10 µM of Neo-Ce6 and Tobra-Ce6, respectively (Figure 5A). In *P. aeruginosa* PAO1, Neo-Ce6 showed a similar drop as in PA14 (3.6 log10 CFU/mL), while Tobra-Ce6 had slightly more effect (3.5 log10 CFU/mL) (Figure 5C). This is also seen in tobramycin alone, which led to a drop of survival of about 2.3 log10 CFU/mL (Figure 5D). However, irradiated samples treated with Tobra-Ce6 remain significantly lower than samples incubated with tobramycin alone ($p = 0.046$).

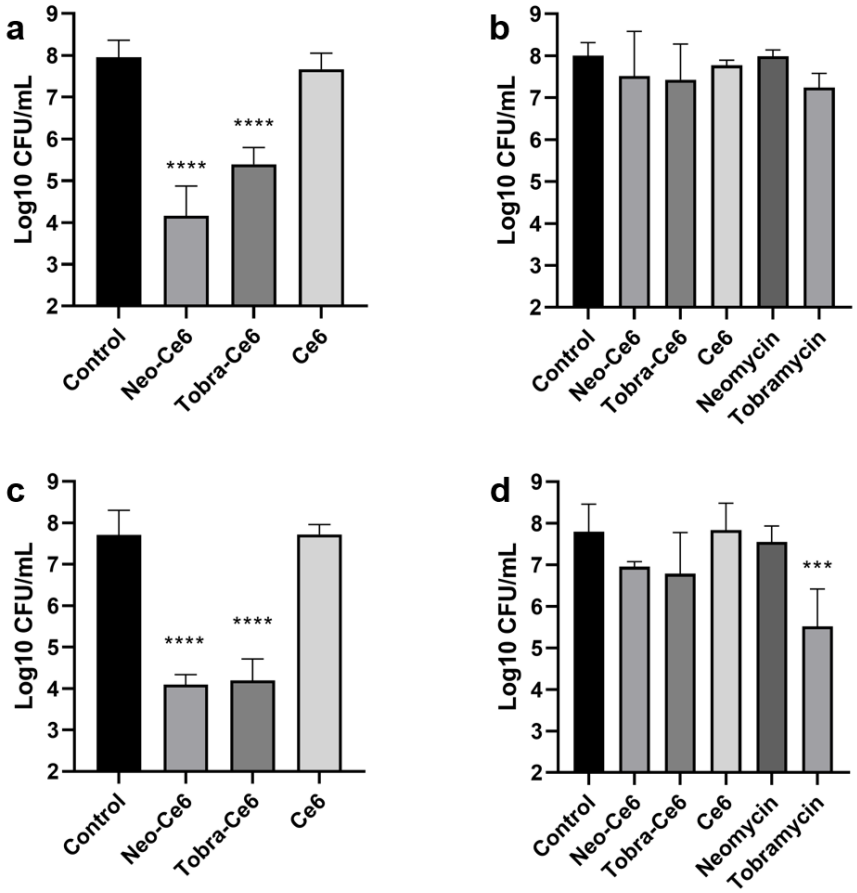

Figure 5: Log10 CFU/mL in *P. aeruginosa* species, with or without irradiation. In A and B, *P. aeruginosa* PA14 with and without irradiation, respectively, and in C and D, *P. aeruginosa* PAO1 with and without irradiation, respectively. Irradiated samples received 5 J/mm².

4.4 aPDT on Biofilm Cells

Biofilm cells were more resistant to aPDT than planktonic cells. A good example is *A. baumannii* DSM30011. Planktonic cells were under the detection limit (Figures 4A, 4B) while the cells found in the biofilm showed higher survival rate to both Neo-Ce6 and Tobra-Ce6 (Table 2).

This resilience was also witnessed in *S. aureus* and *P. aeruginosa* species (Table 2). Neo-Ce6 showed the most effect against *S. aureus* Mu50 and *P. aeruginosa* PAO1 biofilm cells, reducing bacterial load by about 1.9 log10 CFU/mL, while Tobra-Ce6 led to a drop of 1.7 log10 CFU/mL in *P. aeruginosa* PA14. No significant difference is seen between irradiated and non-irradiated samples for *S. aureus* Newman, while there is slightly less survival in irradiated samples in *S. aureus* Mu50. Irradiation did lead to significantly lower survival in *P. aeruginosa* PAO1 biofilm cells treated with Neo-Ce6, but all other results in *P. aeruginosa* PAO1 and PA14 strains are not significantly different than those obtained for non-irradiated samples.

Table 2: aPDT results for biofilm cells expressed in drop in the log10 CFU/mL compared to controls. Bold results show that the survival was significantly lower than the control following one-way ANOVA.

	+ irradiation			**- irradiation**		
	Neo-Ce6	Tobra-Ce6	Ce6	Neo-Ce6	Tobra-Ce6	Ce6	Neo
A. baumannii DSM30011	**2.3**	**4.17**	0.71	1.79	1.58	0.45	1.33
P. aeruginosa PA14	**1.38**	**1.69**	0.60	**0.83**	**0.85**	0.29	0.01
P. aeruginosa PAO1	**1.97**	**1.25**	0.25	**1.03**	**0.79**	0.28	0.28
S. aureus USA300	**0.80**	0.14	**0.73**	0.18	0.28	0.33	0.16
S. aureus Mu50	**1.92**	**1.32**	0.36	**0.74**	0.37	-0.005	0.18
S. aureus Newman	1.15	**1.36**	0.57	0.23	0.49	-0.19	-0.07

0.25	-0.02	0.26	0.39	**0.79**	0.93	Tobra	

4.5 aPDT on Persister Cells

Antibacterial PDT did lead to persister death in most tested species. Some species, like *P. aeruginosa* PA14 persister cells did show more resilience however. In Gram-negative *A. baumannii* DSM30011 and Gram-positive species *S. aureus* USA300 and Newman, aPDT against persister cells often led to CFU being under the detection limit.

Persister plateau and AG concentration varied from one specie to another. In *S. aureus* USA300, a stable plateau was obtained following 6 hours of incubation with 2 mM of neomycin. The resulting persister cells were close to or under the detection limit after aPDT with Neo-Ce6 and Tobra-Ce6 at 10 µM (Figure 6A). Ce6 alone also resulted in some killing as shown in Figure 6A. Neomycin alone resulted in no significant drop in survival, as expected. This control is crucial to make sure that a persister state has been achieved. CFUs were also lowered in samples that were not irradiated, showing that the synergistic penetration of the compounds may lead to an effect of neomycin even in cells in a persister state. As there are no significant differences between irradiated and non-irradiated samples, however, the production of singlet oxygen may not be the factor leading to cell death.

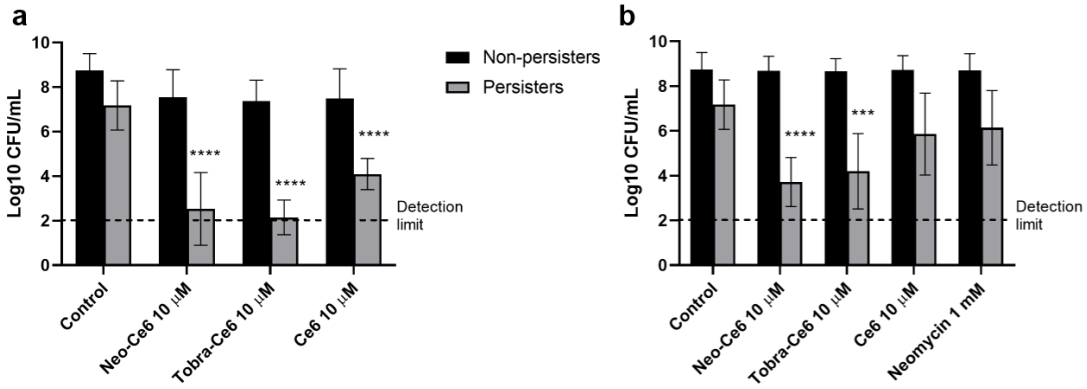

Figure 6: Log10 CFU/mL in *S. aureus* USA300 persister cells following aPDT with Neo-Ce6 and Tobra-Ce6. With (A) or without (B) irradiation. Samples received a total of 5 J/mm². Statistics were done using 2way ANOVA, comparing the mean of each column to the mean of the control for individual categories.

In *S. aureus* Newman, cells were treated for 24 hours with 1 mM of neomycin. Survival for irradiated persister cells treated with Neo-Ce6 and Tobra-Ce6 is significantly lower than in cells treated with Ce6 alone (Figure 7A). Although this synergy does exist, like in *S. aureus* USA300, there is no significant difference in survival for irradiated and non-irradiated samples, except for Ce6.

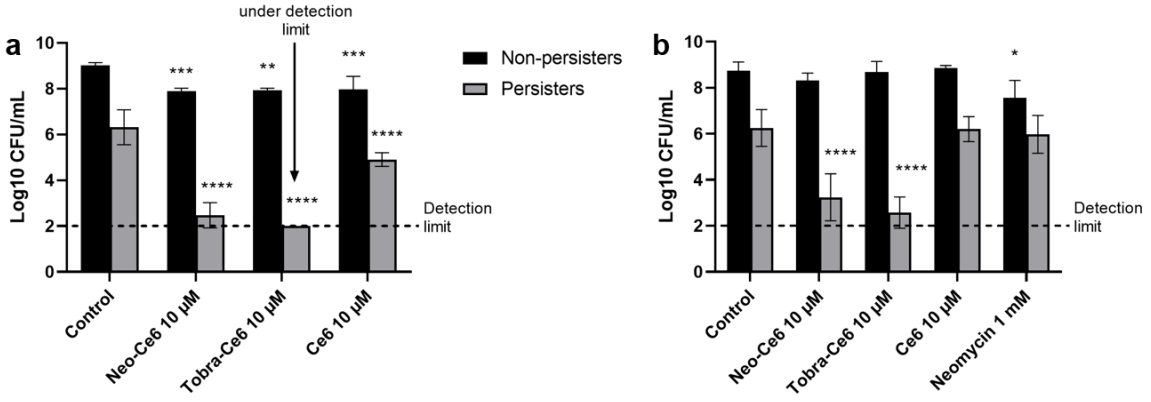

Figure 7: Log10 CFU/mL in *S. aureus* Newman persister cells following aPDT with Neo-Ce6 and Tobra-Ce6. With (A) or without (B) irradiation. Samples received a total of 5 J/mm². Statistics were done using 2way ANOVA, comparing the mean of each column to the mean of the control for individual categories.

Difference in irradiated and non-irradiated samples was found in Gram-negative bacteria *A. baumannii* DSM30011 where Neo-Ce6 leads to CFUs close to the detection limit (Figure 8A). Persister cells were obtained after incubation with 200 µM of neomycin for 24 hours. Treatment in aPDT led to a drop of 3.5 and 1.8 log10 CFU/mL for Neo-Ce6 and Tobra-Ce6, while non-irradiated samples incubated with Neo-Ce6 only showed a 1.4 log10 CFU/mL difference with the control (Figure 8B).

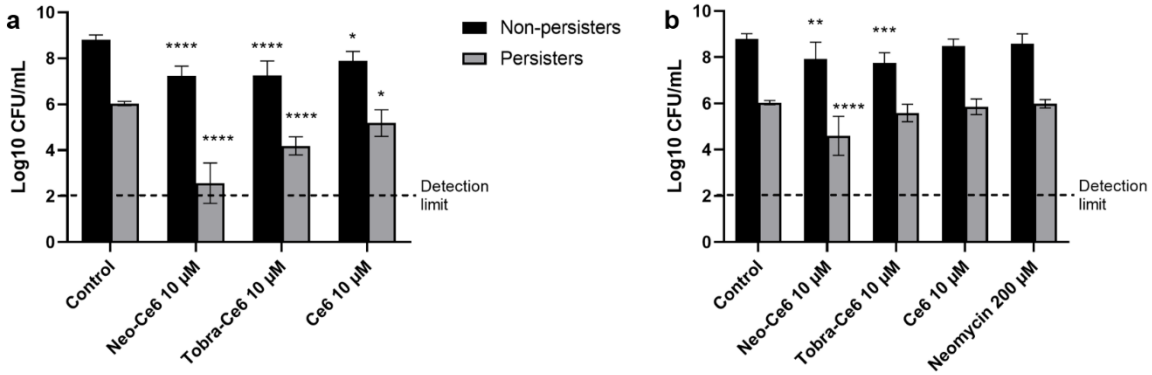

Figure 8: Log10 CFU/mL in *A. baumannii* DSM30011 non-persister and persister cells following aPDT with Neo-Ce6 and Tobra-Ce6. With (A) or without (B) irradiation. Samples received a total of 5 J/mm². Statistics were done using 2way ANOVA, comparing the mean of each column to the mean of the control for individual categories.

In *P. aeruginosa* PA14, persister cells were obtained by treating with 1 mM of tobramycin for 24 hours. The effect of aPDT was not as impactful (Figures 9A, 9B), but there was a slight drop of 1.6 and 1.1 log10 CFU/mL for Neo-Ce6 and Tobra-Ce6, respectively.

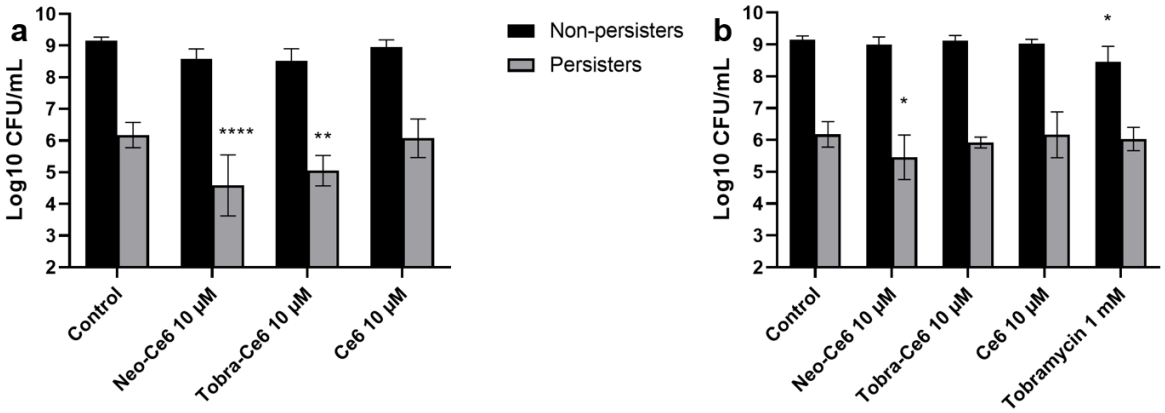

Figure 9: Log10 CFU/mL in *P. aeruginosa* PA14 non-persister and persister cells following aPDT with Neo-Ce6 and Tobra-Ce6. With (A) or without (B) irradiation. Samples received a total of 5 J/mm². Statistics were done using 2way ANOVA, comparing the mean of each column to the mean of the control for individual categories.

5. Discussion

The rise of drug resistance in microbes puts the health system at risk worldwide and many scientists are worried we could go back to the pre-antibiotic era (Laxminarayan *et al.*, 2016; Renwick *et al.*, 2016). Many alternatives are being investigated like antibodies, bacteriophages, probiotics and others. Antibacterial photodynamic therapy (aPDT) is one of those alternatives, however less investigated. Although its use is limited due to the need of both a light source and oxygen, promising results, the reduction of virulence factors in surviving bacteria and the low risk for generating resistance within bacteria have increased interest in aPDT (Tseng *et al.*, 2017; Wainwright *et al.*, 2017).

We conjugated aminoglycosides to photosensitizers to evaluate their combined effect on several ESKAPE pathogens with a focus on persister and multidrug-resistant cells. To our knowledge, research surrounding the effect of aPDT on persister cells is quite scarce.

Three compounds were created: Neo-MB, Neo-Ce6 and Tobra-Ce6. Analysis of the singlet oxygen production showed that the conjugation of neomycin and MB led to a decrease in yield. For Neo-Ce6 and Tobra-Ce6, singlet oxygen production was higher than that of Ce6 alone. Ce6 is poorly soluble in water which can lead to self-quenching and sub-optimal therapeutic efficacy (Jeong *et al.*, 2011). Thanks to the aminoglycoside moiety, Neo-Ce6 and Tobra-Ce6 are highly soluble which could positively influence singlet oxygen formation. It could also be hypothesized that the addition of an aminoglycoside adds stability to the Ce6 molecule and that the triplet state is maintained for a longer time, generating more singlet oxygen. Stabilizing PSs to create more singlet oxygen is already explored in literature, although most of the methods include adding heavy atoms in the structure, like in Rose

Bengal and squaraines or using a molecular symmetry-controlling strategy to fine-tune the excited state dynamics (Wang *et al.*, 2020).

Antibacterial PDT on different types of cells from diverse species led to mixed observations. Globally, Neo-Ce6 did seem to be more efficient than Tobra-Ce6. aPDT with the compounds on planktonic cells resulted in a significant drop in survival for all strains and MICs with Neo-Ce6 did show synergy against a few clinically relevant species like pathogenic yeast *C. albicans* SC5314 and virulent *S. aureus* strains. A disinfecting effect, characterized as a 5 log10 CFU drop in survival (Boyce and Pittet, 2002), was observed against *S. aureus* Mu50, *S. aureus* USA and *A. baumannii* DSM30011 for Neo-Ce6 and against *S. aureus* Mu50 for Tobra-Ce6. Interestingly, *S. aureus* Mu50 a strain resistant to AG did show resistance to both neomycin and tobramycin while being highly sensitive to aPDT with Neo-Ce6 and Tobra-Ce6.

For some species, aPDT led to no significant difference between survival of the cells treated with the conjugates when compared to irradiated Ce6. This was mainly observed in *S. aureus* species, like *S. aureus* Newman planktonic cells and *S. aureus* USA300 persister cells. As Ce6 is known to penetrate Gram-positive species such as *S. aureus*, this is not surprising (Winkler *et al.*, 2016). For conjugates, because CFUs were often close or under the detection limit, it remained difficult to evaluate their additive effect but synergy was witnessed for MICs. It was also observed that survival between irradiated and non-irradiated samples was sometimes not significantly different. Examples include *A. baumannii* DSM30011 planktonic cells and *P. aeruginosa* PA14 biofilm cells indicating that the main damage does not come from singlet oxygen production by Ce6, but rather to the linked aminoglycoside. Higher uptake through synergy is present though as aminoglycosides alone do not lead to the same drop in survival.

Biofilm cells were more resilient than planktonic cells. We speculate that a few factors may lead to reduced killing when comparing to planktonic cells. First, the lack of oxygen at the core of biofilms may hinder singlet oxygen production (Gad *et al.*, 2004; Walters *et al.*, 2003). This was witnessed in a few species where irradiated planktonic cells showed lower survival than non-irradiated samples, while biofilm cell CFUs were the same for irradiated and non-irradiated samples. The effect of the conjugate was therefore only related to the linked aminoglycoside and not to singlet oxygen production. The conjugates may also adhere to the matrix, which lowers the concentration that truly reaches the cells imbedded in the biofilm. Poor uptake in biofilms and difficulties reaching lower matrix layers are problems that have been reported in literature (Gad *et al.*, 2004). These limitations seem to be less of a concern when using cationic PSs (Sharma *et al.*, 2008 ; Zanin *et al.*, 2005). Lastly, it is hypothesized that biofilm cells are in a persister state (Waters *et al.*, 2016; Lewis, 2001). However, results against a few species, including *S. aureus* Newman and *S. aureus* USA300 do show that the compounds are efficient against persister cells while biofilm cells are resilient to aPDT.

The reduced effect of our compounds on biofilms therefore seems to be mainly linked to oxygen deprivation. Indeed, when aPDT was done by using “pulsing”, survival was slightly lower. This technique was used to allow oxygen renewal between irradiation periods.

As for persister cells, results were interesting in *A. baumannii* DSM30011, *S. aureus* Newman and *S. aureus* USA300. When comparing to the survival of planktonic cells and biofilm cells of the same species, those results lead to a few questions. Obviously, as cell density is lowered in persister samples due to aminoglycoside pressure, this could impact singlet oxygen stability and efficiency (Maisch *et al.*, 2007). However, most of the strains show mortality in their non-irradiated samples as well. Due to these results, it seems the persister death is rather linked to synergy in uptake and a double-effect from linked molecules than singlet oxygen alone.

There is also a discrepancy between planktonic and persister cells in the *P. aeruginosa* PA14. Although *P. aeruginosa* PA14 reached a stable plateau at 24 hours, aPDT had almost no effect against the persister cells. In 2016, a team did find *P. aeruginosa* subpopulations that showed a persister state following aPDT with MB (Forte Giacobone *et al.*, 2016). Their results suggest that *P. aeruginosa* could produce aPDT-specific persisters with no cross-tolerance to antibiotics. However, following study by the same team does show that the experiment is also applicable in the other way, meaning that treatment with ofloxacin followed by aPDT with MB did lead to decreased survival (Oppezzo and Forte Giacobone, 2018). Thus, increased resilience in *P. aeruginosa* PA14 could be explained by environmental stress promoting a reduction of non-specific porin proteins in exchange for more nutrient-specific porins (Tamber and Hancock, 2003).

6. Conclusion

We successfully linked Ce6 to aminoglycosides, leading to an increased production of singlet oxygen for Neo-Ce6 and Tobra-Ce6. Both molecules showed synergy in some strains and led to decreased survival in clinically relevant species like *P. aeruginosa* and *S. aureus*. Although biofilm cells survived aPDT, persister cells in *A. baumannii* DSM30011, *S. aureus* Newman and *S. aureus* USA300 were highly sensitive. As persister cells are quite problematic in hospital settings, further studies on these conjugates will be done to assess their possible use to disinfect equipment linked to persister infections like prosthesis and catheters.

7. Conflict of interest

The authors declare that the research was conducted in the absence of any commercial or financial relationships that could be construed as a potential conflict of interest.

8. Author contributions

MC, SY and DF conceived and designed the project. MC selected the photosensitizers and bacterial strains, designed and performed the experiments, analysed the data and wrote the manuscript. DF produced the Neo-Ce6 and Neo-MB conjugates and participated to the manuscript. MPH produced the Tobra-Ce6 conjugate. SY built a LED device, designed experiments and participated to the manuscript. All authors reviewed and approved the final version of the manuscript.

9. Funding

This work was supported by the Centre National de la Recherche Scientifique (CNRS) to D.F. and S.Y. M.C was supported by a PhD fellowship from the French Ministère de l'Enseignement Supérieur et de la Recherche (MESR).

10. Acknowledgments

We thank Christian Forestier and Sophie Bachellier-Bassi for providing the necessary bacterial strains.

11. References

Alkasir, R., Ma, Y., Liu, F., Li, J., Lv, N., Xue, Y., ... & Zhu, B. (2018). Characterization and transcriptome analysis of Acinetobacter baumannii persister cells. *Microbial Drug Resistance*, *24*(10), 1466-1474.

Allison, K. R., Brynildsen, M. P., & Collins, J. J. (2011). Metabolite-enabled eradication of bacterial persisters by aminoglycosides. *Nature*, *473*(7346), 216-220.

Bertolini, G., Rossi, F., Valduga, G., Jori, G., & Van Lier, J. (1990). Photosensitizing activity of water- and lipid-soluble phthalocyanines on Escherichia coli. *FEMS microbiology letters*, *71*(1-2), 149-155.

Bigger, J. W. (1944). Treatment of staphylococcal infections with penicillin. *Lancet, 244.* 497-500

Boyce, J. M., & Pittet, D. (2002). Guideline for hand hygiene in health-care settings: recommendations of the Healthcare Infection Control Practices Advisory Committee and the HICPAC/SHEA/APIC/IDSA Hand Hygiene Task Force. *Infection Control & Hospital Epidemiology*, *23*(S12), S3-S40.

Bryers, J. D. (2008). Medical biofilms. *Biotechnology and bioengineering*, *100*(1), 1-18.

Calixto, G. M. F., de Annunzio, S. R., Victorelli, F. D., Frade, M. L., Ferreira, P. S., Chorilli, M., & Fontana, C. R. (2019). Chitosan-based drug delivery systems for optimization of photodynamic therapy: A review. *AAPS PharmSciTech*, *20*(7), 1-17.

Cassini, A., Högberg, L. D., Plachouras, D., Quattrocchi, A., Hoxha, A., Simonsen, G. S., ... & Hopkins, S. (2019). Attributable deaths and disability-adjusted life-years caused by infections with antibiotic-resistant bacteria in the EU and the European Economic Area in 2015: a population-level modelling analysis. *The Lancet infectious diseases*, *19*(1), 56-66.

Cohen, N. R., Lobritz, M. A., & Collins, J. J. (2013). Microbial persistence and the road to drug resistance. *Cell host & microbe*, *13*(6), 632-642.

Conlon, Brian P., et al. "Activated ClpP kills persisters and eradicates a chronic biofilm infection." *Nature* 503.7476 (2013): 365-370.

Czaplewski, L., Bax, R., Clokie, M., Dawson, M., Fairhead, H., Fischetti, V. A., ... & Rex, J. H. (2016). Alternatives to antibiotics—a pipeline portfolio review. *The Lancet infectious diseases*, *16*(2), 239-251.

Dahl, T. A., Midden, W. R., & Hartman, P. E. (1989). Comparison of killing of gram-negative and gram-positive bacteria by pure singlet oxygen. *Journal of bacteriology*, *171*(4), 2188-2194.

St. Denis, T. G., Dai, T., Izikson, L., Astrakas, C., Anderson, R. R., Hamblin, M. R., & Tegos, G. P. (2011). All you need is light: antimicrobial photoinactivation as an evolving and emerging discovery strategy against infectious disease. *Virulence*, *2*(6), 509-520.

Doern, C. D. (2014). When does 2 plus 2 equal 5? A review of antimicrobial synergy testing. *Journal of clinical microbiology*, *52*(12), 4124-4128.

Dougherty, T. J., Gomer, C. J., Henderson, B. W., Jori, G., Kessel, D., Korbelik, M., ... & Peng, Q. (1998). Photodynamic therapy. *JNCI: Journal of the national cancer institute*, *90*(12), 889-905.

Fila, G., Kawiak, A. and Grinholc, M.S., 2017. Blue light treatment of Pseudomonas aeruginosa: Strong bactericidal activity, synergism with antibiotics and inactivation of virulence factors. *Virulence*, *8*(6), pp.938-958.

Forte Giacobone, A. F., Ruiz Gale, M. F., Hogert, E. N., & Oppezzo, O. J. (2016). A possible phenomenon of persistence in Pseudomonas aeruginosa treated with methylene blue and red light. *Photochemistry and Photobiology*, *92*(5), 702-707.

Gad, F., Zahra, T., Hasan, T., & Hamblin, M. R. (2004). Effects of growth phase and extracellular slime on photodynamic inactivation of gram-positive pathogenic bacteria. *Antimicrobial agents and chemotherapy*, *48*(6), 2173-2178.

Grant, S. S., & Hung, D. T. (2013). Persistent bacterial infections, antibiotic tolerance, and the oxidative stress response. *Virulence*, *4*(4), 273-283.

Helaine, S., Cheverton, A. M., Watson, K. G., Faure, L. M., Matthews, S. A., & Holden, D. W. (2014). Internalization of Salmonella by macrophages induces formation of nonreplicating persisters. *Science*, *343*(6167), 204-208.

Hobby, G. L., Meyer, K., & Chaffee, E. (1942). Observations on the Mechanism of Action of Penicillin. *Proceedings of the Society for Experimental Biology and Medicine*, *50*(2), 281-285.

Jeong, H., Huh, M., Lee, S. J., Koo, H., Kwon, I. C., Jeong, S. Y., & Kim, K. (2011). Photosensitizer-conjugated human serum albumin nanoparticles for effective photodynamic therapy. *Theranostics*, *1*, 230.

Khadem, J., Veloso, A. A. Jr, Tolentino, F., Hasan, T. and Hamblin, M.R. (1999). Photodynamic tissue adhesion with chlorin e6 protein conjugates. Investigative Ophthalmology & Visual Science, 40 (13), 3132-3137.

Kim, W., Zhu, W., Hendricks, G. L., Van Tyne, D., Steele, A. D., Keohane, C. E., ... & Mylonakis, E. (2018). A new class of synthetic retinoid antibiotics effective against bacterial persisters. *Nature*, *556*(7699), 103-107.

Laxminarayan, R., Matsoso, P., Pant, S., Brower, C., Røttingen, J. A., Klugman, K., & Davies, S. (2016). Access to effective antimicrobials: a worldwide challenge. *The Lancet*, *387*(10014), 168-175.

Lebeaux, D., Leflon-Guibout, V., Ghigo, J. M., & Beloin, C. (2015). In vitro activity of gentamicin, vancomycin or amikacin combined with EDTA or l-arginine as lock therapy against a wide spectrum of biofilm-forming clinical strains isolated from catheter-related infections. *Journal of Antimicrobial Chemotherapy*, *70*(6), 1704-1712.

Lewis, K. I. M. (2001). Riddle of biofilm resistance. *Antimicrobial agents and chemotherapy*, *45*(4), 999-1007.

Lewis, K. (2010). Persister cells. *Annual review of microbiology*, *64*, 357-372.

Macdonald, I. J., & Dougherty, T. J. (2001). Basic principles of photodynamic therapy. *Journal of Porphyrins and Phthalocyanines*, *5*(02), 105-129.

Maisch, T., Baier, J., Franz, B., Maier, M., Landthaler, M., Szeimies, R. M., & Bäumler, W. (2007). The role of singlet oxygen and oxygen concentration in photodynamic inactivation of bacteria. *Proceedings of the National Academy of Sciences*, *104*(17), 7223-7228.

Martens, E., & Demain, A. L. (2017). The antibiotic resistance crisis, with a focus on the United States. *The Journal of antibiotics*, *70*(5), 520-526.

Miethke, M., Pieroni, M., Weber, T., Brönstrup, M., Hammann, P., Halby, L., ... & Müller, R. (2021). Towards the sustainable discovery and development of new antibiotics. *Nature Reviews Chemistry*, *5*(10), 726-749.

Nikaido, H., & Vaara, M. (1985). Molecular basis of bacterial outer membrane permeability. *Microbiological reviews*, *49*(1), 1-32.

Nitzan, Y., Wexler, H. M., & Finegold, S. M. (1994). Inactivation of anaerobic bacteria by various photosensitized porphyrins or by hemin. *Current microbiology*, *29*(3), 125-131.

Nordmann, P., Poirel, L., Toleman, M. A., & Walsh, T. R. (2011). Does broad-spectrum β-lactam resistance due to NDM-1 herald the end of the antibiotic era for treatment of infections caused by Gram-negative bacteria?. *Journal of antimicrobial chemotherapy*, *66*(4), 689-692.

Oppezzo, O. J., & Forte Giacobone, A. F. (2018). Lethal effect of photodynamic treatment on persister bacteria. *Photochemistry and photobiology*, *94*(1), 186-189.

Renwick, M. J., Simpkin, V., Mossialos, E., & World Health Organization. (2016). *Targeting innovation in antibiotic drug discovery and development: The need for a One Health–One Europe–One World Framework*. World Health Organization. Regional Office for Europe.

Rice, L. B. (2008). Federal funding for the study of antimicrobial resistance in nosocomial pathogens: no ESKAPE. *The Journal of infectious diseases*, *197*(8), 1079-1081.

Sabeti Azad, M., Okuda, M., Cyrenne, M., Bourge, M., Heck, M. P., Yoshizawa, S., & Fourmy, D. (2020). Fluorescent aminoglycoside antibiotics and methods for accurately monitoring uptake by bacteria. *ACS Infectious Diseases*, *6*(5), 1008-1017.

Sabeti Azad, M. (2019) Accumulation of a bactericidal antibiotic by tolerant bacteria and insights into bacterial persistence. Thesis, University Paris-Saclay.

Shah, D., Zhang, Z., Khodursky, A. B., Kaldalu, N., Kurg, K., & Lewis, K. (2006). Persisters: a distinct physiological state of E. coli. *BMC microbiology*, *6*(1), 1-9.

Sharma, M., Visai, L., Bragheri, F., Cristiani, I., Gupta, P. K., & Speziale, P. (2008). Toluidine blue-mediated photodynamic effects on staphylococcal biofilms. *Antimicrobial agents and chemotherapy*, *52*(1), 299-305.

Singh, R., Ray, P., Das, A., & Sharma, M. (2010). Penetration of antibiotics through Staphylococcus aureus and Staphylococcus epidermidis biofilms. *Journal of antimicrobial chemotherapy*, *65*(9), 1955-1958.

Soukos, N. S., Hamblin, M. R., & Hasan, T. (1997). The effect of charge on cellular uptake and phototoxicity of polylysine Chlorine6Conjugates. *Photochemistry and photobiology*, *65*(4), 723-729.

F Sperandio, F., Huang, Y. Y., & R Hamblin, M. (2013). Antimicrobial photodynamic therapy to kill Gram-negative bacteria. *Recent patents on anti-infective drug discovery*, *8*(2), 108-120.

Straight, R. C., & Spikes, J. D. (1985). Photosensitized oxidation of biomolecules. *Singlet O2*, *4*(91), 143.

Tamber, S., & Hancock, R. E. (2003). On the mechanism of solute uptake in Pseudomonas. *Frontiers in Bioscience-Landmark*, *8*(6), 472-483.

Tseng, S. P., Hung, W. C., Chen, H. J., Lin, Y. T., Jiang, H. S., Chiu, H. C., ... & Tsai, J. C. (2017). Effects of toluidine blue O (TBO)-photodynamic inactivation on community-associated methicillin-

resistant Staphylococcus aureus isolates. *Journal of Microbiology, Immunology and Infection*, *50*(1), 46-54.

Verstraeten, N., Knapen, W., Fauvart, M., & Michiels, J. (2016). A historical perspective on bacterial persistence. *Bacterial Persistence*, 3-13.

Wainwright, M., Maisch, T., Nonell, S., Plaetzer, K., Almeida, A., Tegos, G. P., & Hamblin, M. R. (2017). Photoantimicrobials—are we afraid of the light?. *The Lancet Infectious Diseases*, *17*(2), e49-e55.

Wang, X., Song, Y., Pan, G., Han, W., Wang, B., Cui, L., ... & Tian, W. (2020). Exploiting radical-pair intersystem crossing for maximizing singlet oxygen quantum yields in pure organic fluorescent photosensitizers. *Chemical science*, *11*(40), 10921-10927.

Waters, E. M., Rowe, S. E., O'Gara, J. P., & Conlon, B. P. (2016). Convergence of Staphylococcus aureus persister and biofilm research: can biofilms be defined as communities of adherent persister cells?. *PLoS pathogens*, *12*(12), e1006012.

Walters III, M. C., Roe, F., Bugnicourt, A., Franklin, M. J., & Stewart, P. S. (2003). Contributions of antibiotic penetration, oxygen limitation, and low metabolic activity to tolerance of Pseudomonas aeruginosa biofilms to ciprofloxacin and tobramycin. *Antimicrobial agents and chemotherapy*, *47*(1), 317-323.

Winkler, K., Simon, C., Finke, M., Bleses, K., Birke, M., Szentmáry, N., ... & Bischoff, M. (2016). Photodynamic inactivation of multidrug-resistant Staphylococcus aureus by chlorin e6 and red light (λ= 670 nm). *Journal of Photochemistry and Photobiology B: Biology*, *162*, 340-347.

Wozniak, A., & Grinholc, M. (2018). Combined antimicrobial activity of photodynamic inactivation and antimicrobials–state of the art. *Frontiers in Microbiology*, *9*, 930.

Zanin, I. C. J., Goncalves, R. B., Junior, A. B., Hope, C. K., & Pratten, J. (2005). Susceptibility of Streptococcus mutans biofilms to photodynamic therapy: an in vitro study. *Journal of antimicrobial chemotherapy*, *56*(2), 324-330.

Supplementary Material

1. Supplementary Data

Supplementary Material should be uploaded separately on submission. Please include any supplementary data, figures and/or tables. All supplementary files are deposited to FigShare for permanent storage and receive a DOI.

Supplementary material is not typeset so please ensure that all information is clearly presented, the appropriate caption is included in the file and not in the manuscript, and that the style conforms to the rest of the article. To avoid discrepancies between the published article and the supplementary material, please do not add the title, author list, affiliations or correspondence in the supplementary files.

Procedure synthesis Tobramycin-neoCe6

Commercially available tobramycin was protected to NHBoc tobramycin **1** by reacting the five amino groups with Boc groups. Then the primary alcohol of **1** was selectively transformed to sulfonate leaving group **2**. Its substitution reaction with sodium azide afforded azide **3**. Reduction of **3** with H_2 and Pd/C was unsuccessful and conducted with a complicated mixture of products while the mild azide reduction using Staudinger conditions (PPh_3, H_2O) successfully afforded desired amineTobramycin **4**.
Finally, amine **4** was reacted with Ce-6-NHS ester and the NHBoc protections were cleaved to yield Tobramycin Ce-6.

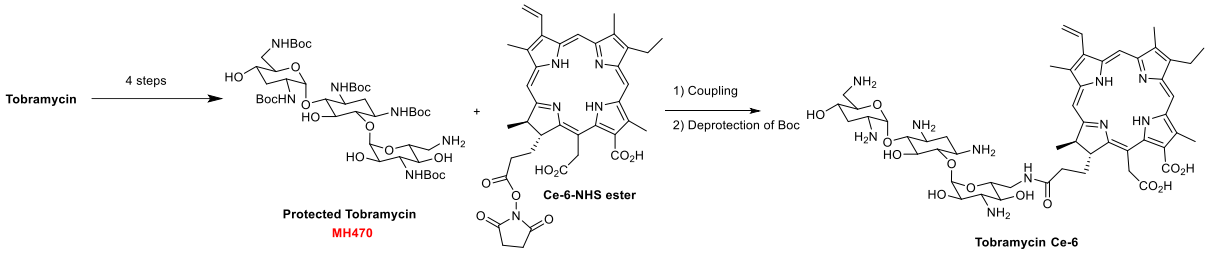

Detailed procedure :

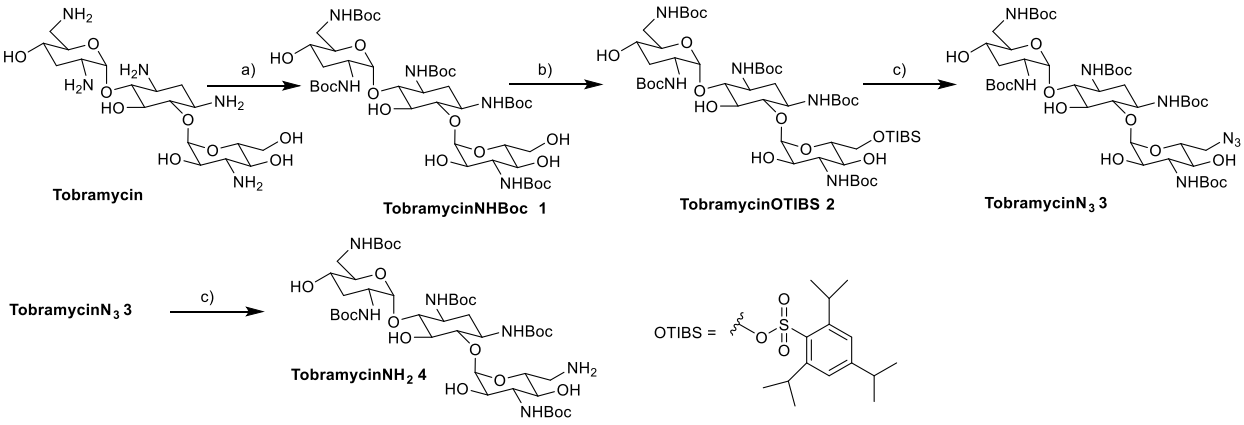

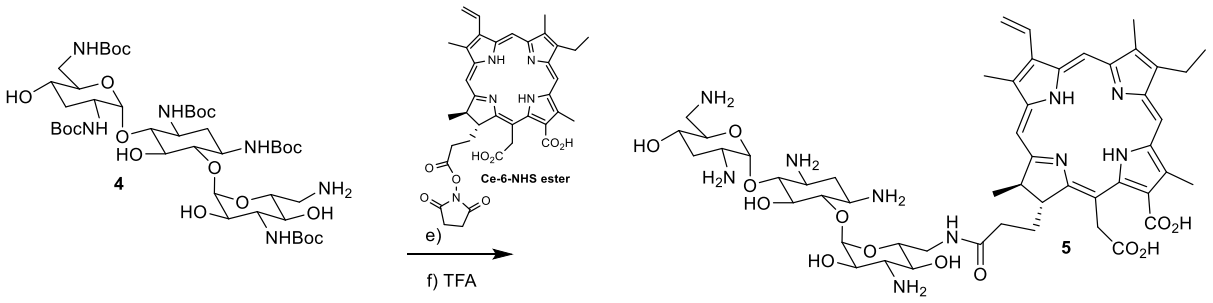

a) Boc_2O, DMSO/H_2O, 60°C 12h, 88% yield
b) TIBSCl, Py, 69%
c) NaN_3, DMF/H_2O, 46%
d) PPh_3, H_2O, THF 69%
e) Ce 6 NHS ester (synthesized), DIEA, DMF
f) TFA, CH_2Cl_2/H_2O

Supporting Infos

Compounds **1**, **2**, and **3** were synthesized following methods described in the literature (Bioorg. Med. Chem. 1999, 7, 1361-1371; Angew. Chem. Int. Ed. 2012, 51, 5652-5656, ChemMedChem 2012, 7, 1237-1244; with minor modifications and were fully characterized (^{1}H, ^{13}C NMR and HRMS are reported). A new method of synthesis is reported to prepare compound **4** from **3** and data are in agreement with literature (ChemMedChem 2014, 9, 2164-2171).

NMR Data and Analysis :

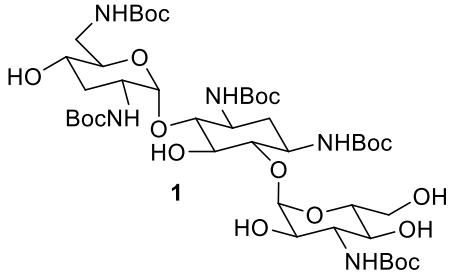

Synthesis of TobramycinNHBoc 1 To a solution of commercially available tobramycin (1 g, 2.1 mmol) in DMSO/H_2O (24 mL/4 mL) was added di-*tert*-butyl dicarbonate (2.6 g, 11,8 mmol, 5.5 eq.). The resulting mixture was heated at 60° C for 5 h and at room temperature for 2 h. Then 30% aqueous ammonia (10 ml) was added dropwise and the mixture was stirred for 30 min allowing the formation of a white precipitate. This solid was isolated by filtration, washed with H_2O (2 x 50 mL) and dried in vacuo to yield tobramycineNHBoc **1** (1.8 g, 88% yield).). ^{1}H NMR (400 MHz, CD_3OD) δ = 5.11 (br, 1H), 5.08 (br, 1H), 3.94 (d, 1H, J = 8 Hz), 3.80-3.77 (m, 1H), 3.72 (t, 2H, J = 8 Hz), 3.63-3.61 (m, 3H), 3.48-3.36 (m, 9H), 2.16-2.10 (m, 1H), 2.08- 1.95 (m, 1H), 1.66 (q, 1H, J = 12 Hz), 1;46 (bs, 45H). ^{13}C NMR (100 MHz, CD_3OD) δ = 159.7, 159.2, 158.1, 157.8, 157.6, 84.1, 81.1,

80.9, 80.6, 80.2, 80.0, 77.1, 74.8, 73.5, 72.1, 69.7, 66.4, 62.3, 57.7, 51.5; 50.9; 44.4, 42.1, 36.1, 34.4, 28.9; LCMS (ESI+): m/z calculated for $[C_{43}H_{77}N_5O_{19}]^+$: 968, found $[M+H]^+$ = 969.

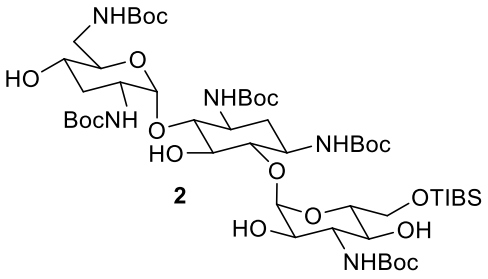

Synthesis of tobramycinOTIBS 2 To a solution of tobramycinNHBoc **1** (1 g, 1.03 mmol) in pyridine (10 mL) was added 2,4,6-triisopropylbenzenesulfonyl chloride (1.56 g, 2.17 mmol, 5 eq.). The reaction was stirred at room temperature for 12 h. Then HCl 1 N was added (3 mL) followed by H_2O (10 mL) and AcOEt (10 mL). The organic layer was separated, washed with H_2O, then dried over Na_2SO_4 and concentrated under vacuum. The crude residue was purified by silicagel chromatography (CH_2Cl_2/MeOH (9.5/0.5)) to afford tobramycinOTIBS **2** (880 mg, 69 % yield); ^{1}H NMR (400 MHz, CD_3OD) δ = 5.06-5.05 (br, 2H), 4.41 (d, 1H, J = 8 Hz), 4.18 (d, 1H, J = 8 Hz), 4.17-4.11 (m, 3H), 3.59 (t, 1H, J = 8 Hz), 3.50-3.40 (m, 12H), 2.95 (hex, J = 8 Hz, 3H), 2.12-2.03 (m, 2H), 1.68 (q, J = 12 Hz, 1H), 1.46-1.40 (m, 45H), 1.25 (m, 18H). ^{13}C NMR (100 MHz, CD_3OD) δ = 159.5, 157.8, 155.4, 152.4, 130.8, 130.1, 129.3, 126.4, 125.1, 80.8, 80.4, 76.7, 73.5, 72.1, 71.7, 69.1, 66.6, 57.14, 41.9, 35.6, 30.9, 28.8, 25.3, 23.8; HRMS (ESI+): m/z calculated for $[C_{58}H_{100}N_5O_{21}S_1+1\ H^+]^+$: 1234,6632, found $[M+H]^+$ = 1234,6636.

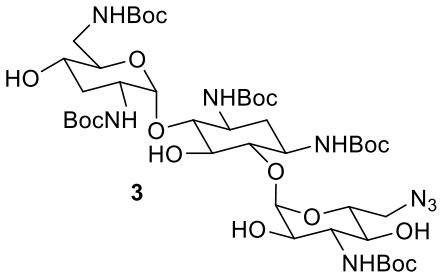

Synthesis of tobramycinN3 3 To a solution of tobramycinOTIBS **2** (228 mg, 0.19 mmol) in DMF (2 mL) was added sodium azide (97 mg, 1.5 mmol, 8 eq) and the solution was heated at 65°C for 24 h. After cooling to room temperature, CH_3CN (3 ml) was added and the excess of salts was filtred on P4 filter and discarded. The yellowish solution was concentrated under vacuum and purified by silicagel column chromatography (CH_2Cl_2/MeOH 95/5) to yield 140 mg of tobramycinN3 **3** (140 mg, 76% yield). ^{1}H NMR (400 MHz, CD_3OD) δ = 5.10-5.07 (bs, 2H), 4.16 (d, 1H, J = 8 Hz), 4.16 (dd, 1H, J = 4; 8 Hz), 4.17-4.11 (m, 3H), 3.71 (t, 1H, J = 8 Hz), 3.66-3.50 (m, 4H), 3.49-3.36 (m, 11H), 2.95 (hex, J = 12 Hz, 3H), 2.12-2.06 (m, 1H), 2.05-1.98 (m, 1H), 1.66 (q, J = 12Hz, 1H), 1.44 (bs, 45H); ^{13}C NMR (100 MHz, CD_3OD) δ = 159.5, 159.4, 157.9, 157.8, 99.6, 83.3, 82.8, 80.9, 80.4, 80.2,

76.9, 73.5, 71.9, 70.3, 66.4, 66.6, 57.1, 52.7, 51.2, 41.9, 35.9, 34.0, 30.7, 28.9; HRMS (ESI+) : m/z calculated for $[C_{43}H_{76}N_8O_{18}+1H^+]^+$: 994.5434, found $[M+H]^+$ = 994.5440.

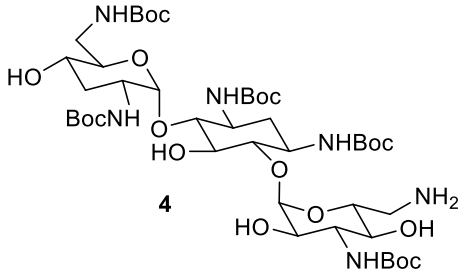

Synthesis of tobramycinNH_2 4 To a solution of tobramycinN3 **3** (15 mg, 0.016 mmol) in THF (1mL) was added triphenylphosphine (8 mg, 0.032 mmol, 2 eq.) and the solution was stirred for 30 min before to add H_2O (0.1 mL). The mixture was stirred for 1 hour at room temperature and then concentrated under vacuum. The crude was purified on silicagel column chromatography (CH_2Cl_2/MeOH 9/1) to afford tobramycinNH_2 **4** (10 mg, 69% yield). ^{1}H NMR (400 MHz, CD_3OD) 5.11 (bs, 2H), 4.04-3.94 (m, 2H), 3.69 (t, 1H, J = 8 Hz), 3.65-3.38 (m, 11H), 3.18 (t, J = 8 Hz, 1H), 3.10-3.04 (m, 1H), 2.80-2.72 (m, 1H), 2.14-1.96 (m, 2H), 1.64 (q, J = 12Hz, 1H), 1.45 (bs, 45H); ^{13}C NMR (100 MHz, CD_3OD) δ = 159.4, 159.2, 158.0, 157.8, 99.6, 99.2, 83.8, 80.9, 80.4, 80.2, 79.9, 76.9, 73.7, 72.3, 67.5, 66.5, 54.5, 51.5, 50.9, 43.5, 42.0, 36.0, 34.1, 28.9; HRMS (ESI+) : m/z calculated for $[C_{43}H_{78}N_6O_{18}+1H^+]^+$: 968,5529 found $[M+H]^+$ = 968.5565.

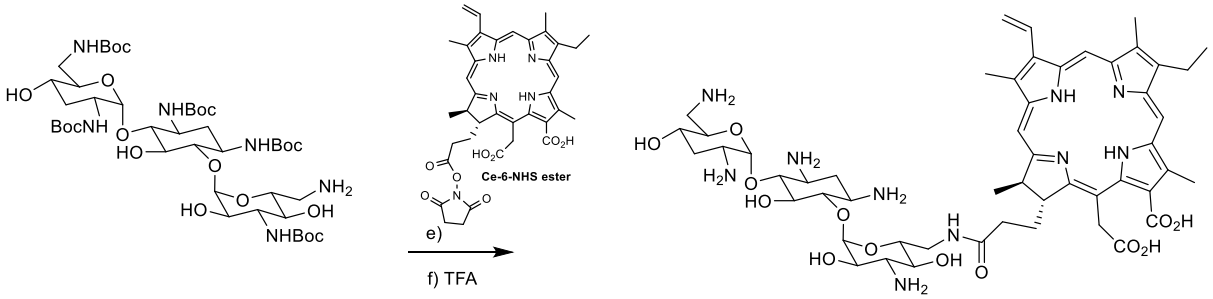

a) Boc_2O, DMSO/H_2O, 60°C 12h, 88% yield
b) TIBSCl, Py, 69%
c) NaN_3, DMF/H_2O, 46%
d) PPh_3, H_2O,THF 69%
e) Ce 6 NHS ester (synthesized), DIEA, DMF
f) TFA, CH_2Cl_2/H_2O

Synthesis of Ce-6- NHS

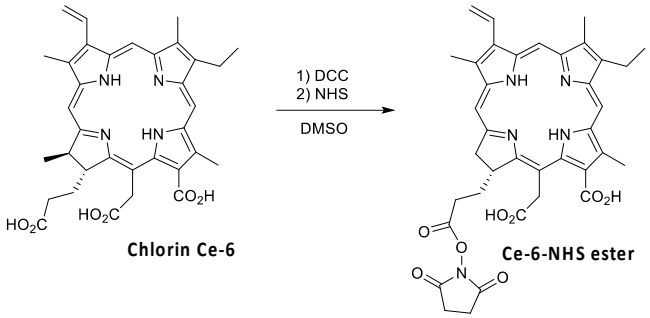

2. Supplementary Figures and Tables

For more information on Supplementary Material and for details on the different file types accepted, please see here. Figures, tables, and images will be published under a Creative Commons CC-BY licence and permission must be obtained for use of copyrighted material from other sources (including re-published/adapted/modified/partial figures and images from the internet). It is the responsibility of the authors to acquire the licenses, to follow any citation instructions requested by third-party rights holders, and cover any supplementary charges.

2.1 Supplementary Figures

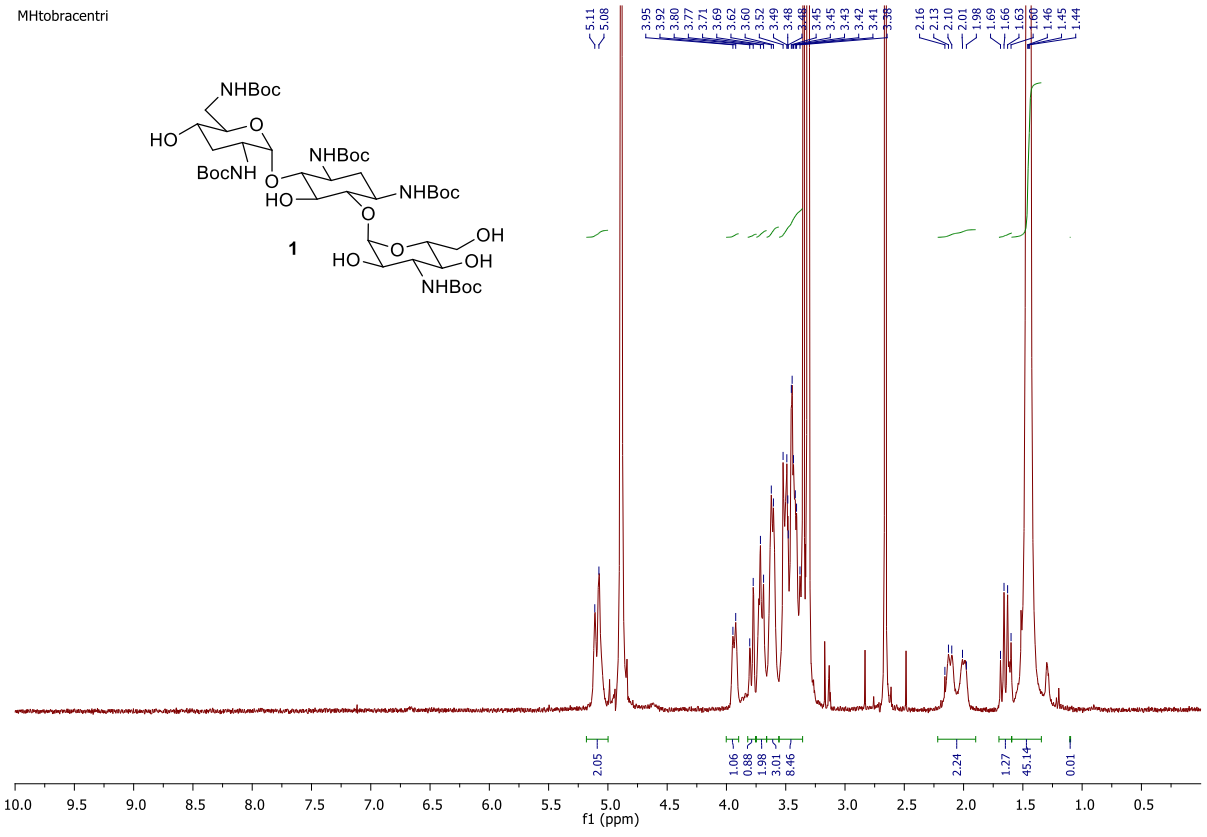

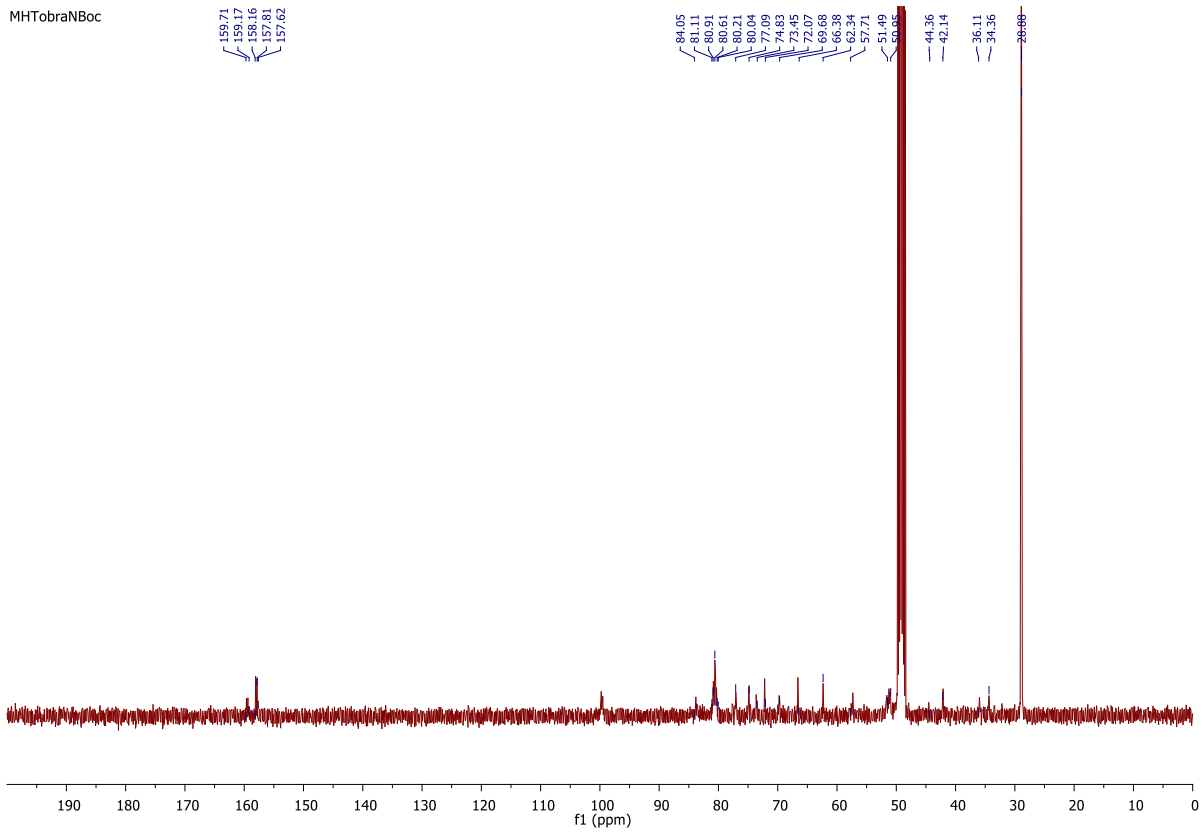
MHTobraNBoc
159.71
159.17
158.16
157.81
157.62
84.05
81.11
80.91
80.61
80.21
80.04
77.09
74.83
73.45
72.07
69.68
66.38
62.34
57.71
51.49
50.95
44.36
42.14
36.11
34.36
28.88
190
180
170
160
150
140
130
120
110
100
90
80
70
60
50
40
30
20
10
0
f1 (ppm)

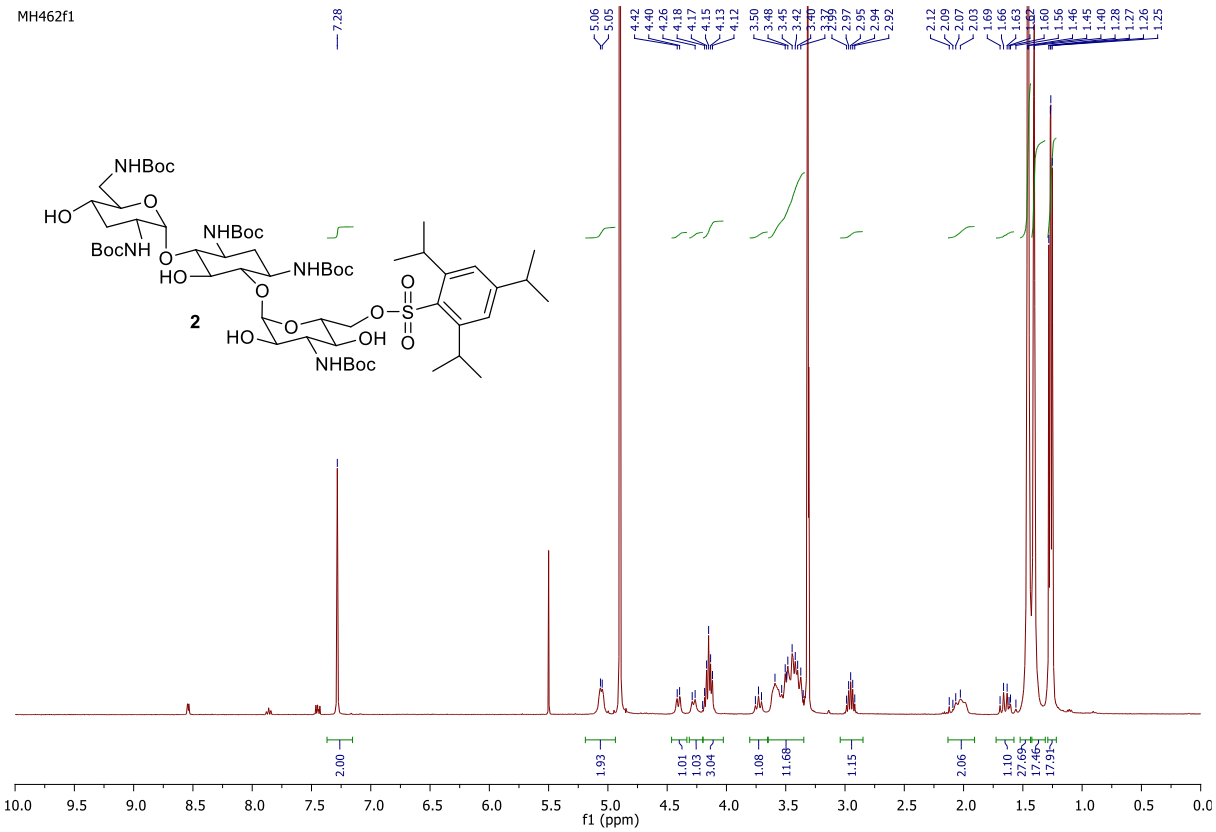
MH462f1
NHBoc
HO
O
BocNH
NHBoc
O
HO
NHBoc
O
2
O
HO
O
OH
O
S
O
NHBoc
f1 (ppm)

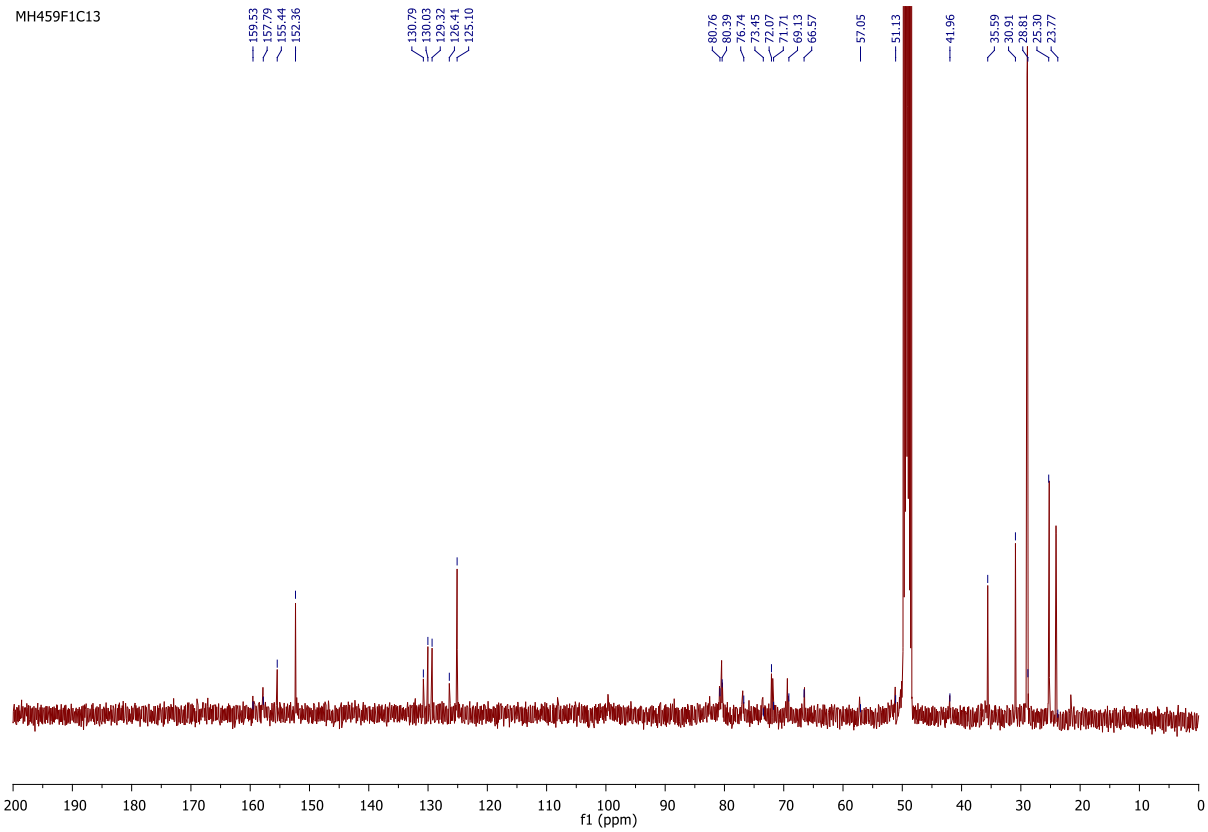
MH459F1C13
159.53
157.79
155.44
152.36
130.79
130.03
129.32
126.41
125.10
80.76
80.39
76.74
73.45
72.07
71.71
69.13
66.57
57.05
51.13
41.96
35.59
30.91
28.81
25.30
23.77
200
190
180
170
160
150
140
130
120
110
100
90
80
70
60
50
40
30
20
10
0
f1 (ppm)

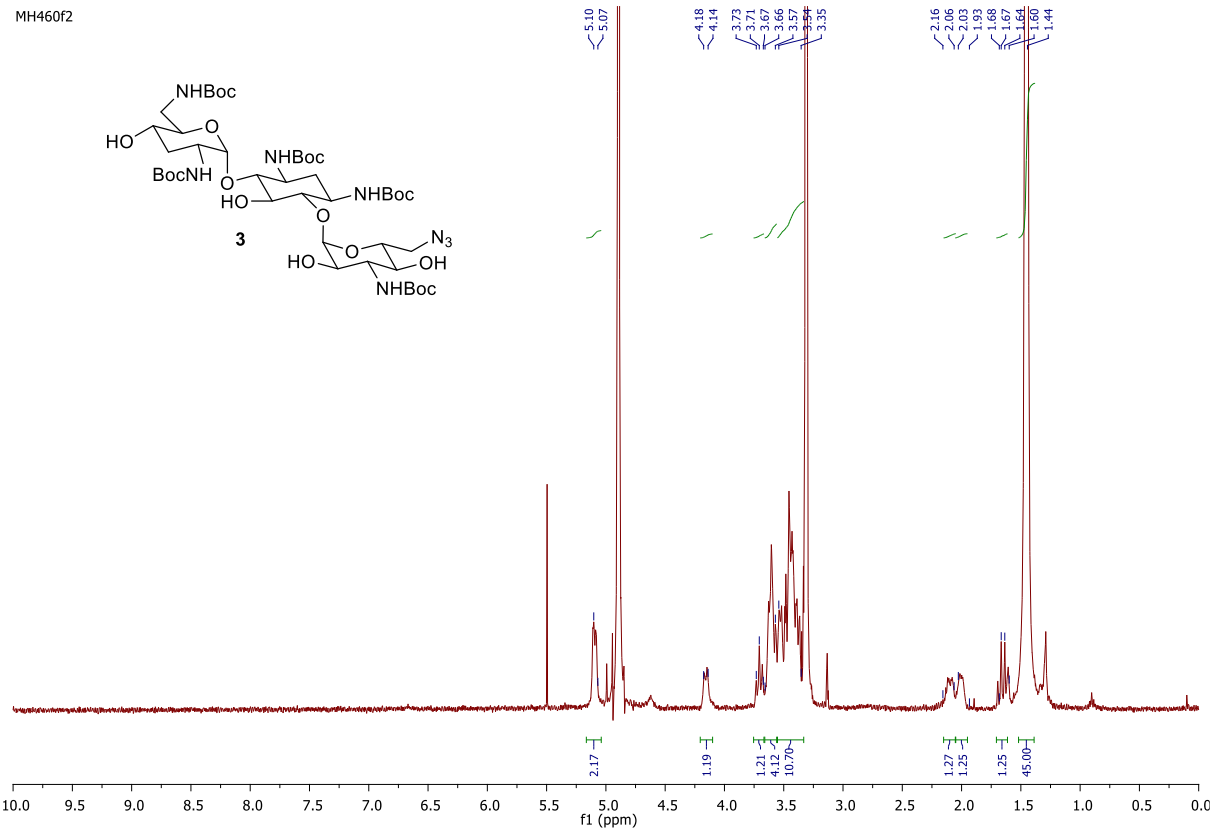
MH460f2
NHBoc
HO
O
BocNH
NHBoc
O
HO
NHBoc
O
3
O
N3
HO
OH
NHBoc
5.10
5.07
4.18
4.14
3.73
3.71
3.67
3.66
3.57
3.54
3.35
2.16
2.06
2.03
1.93
1.68
1.67
1.64
1.60
1.44
2.17
1.19
1.21
4.12
10.70
1.27
1.25
1.25
45.00
10.0
9.5
9.0
8.5
8.0
7.5
7.0
6.5
6.0
5.5
5.0
4.5
4.0
3.5
3.0
2.5
2.0
1.5
1.0
0.5
0.0
f1 (ppm)

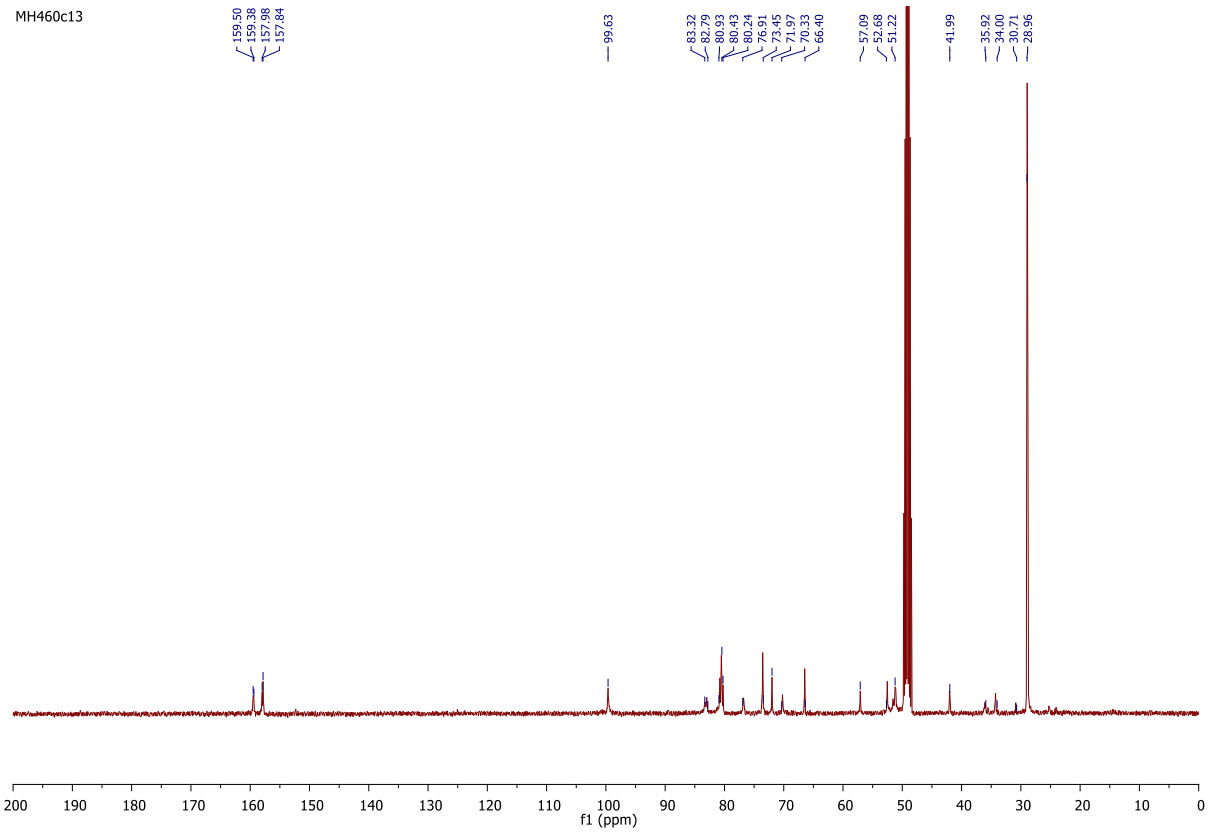
MH460c13
159.50
159.38
157.98
157.84
99.63
83.32
82.79
80.93
80.43
80.24
76.91
73.45
71.97
70.33
66.40
57.09
52.68
51.22
41.99
35.92
34.00
30.71
28.96
200
190
180
170
160
150
140
130
120
110
100
90
80
70
60
50
40
30
20
10
0
f1 (ppm)

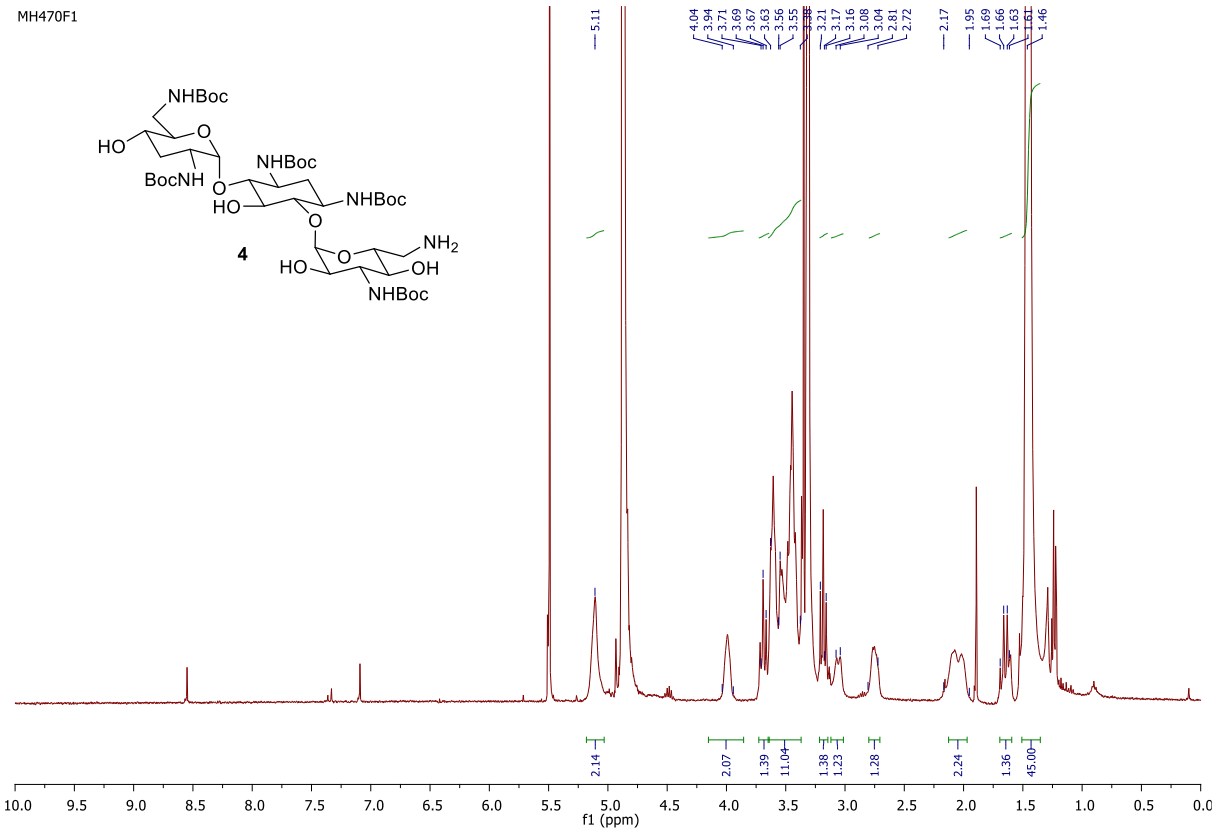
MH470F1
NHBoc
HO
O
BocNH
NHBoc
O
HO
NHBoc
O
4
NH2
O
HO
OH
NHBoc
5.11
4.04
3.94
3.71
3.69
3.67
3.63
3.56
3.55
3.38
3.21
3.17
3.16
3.08
3.04
2.81
2.72
2.17
1.95
1.69
1.66
1.63
1.61
1.46
2.14
2.07
1.39
11.04
1.38
1.23
1.28
2.24
1.36
45.00
10.0
9.5
9.0
8.5
8.0
7.5
7.0
6.5
6.0
5.5
5.0
4.5
4.0
3.5
3.0
2.5
2.0
1.5
1.0
0.5
0.0
f1 (ppm)

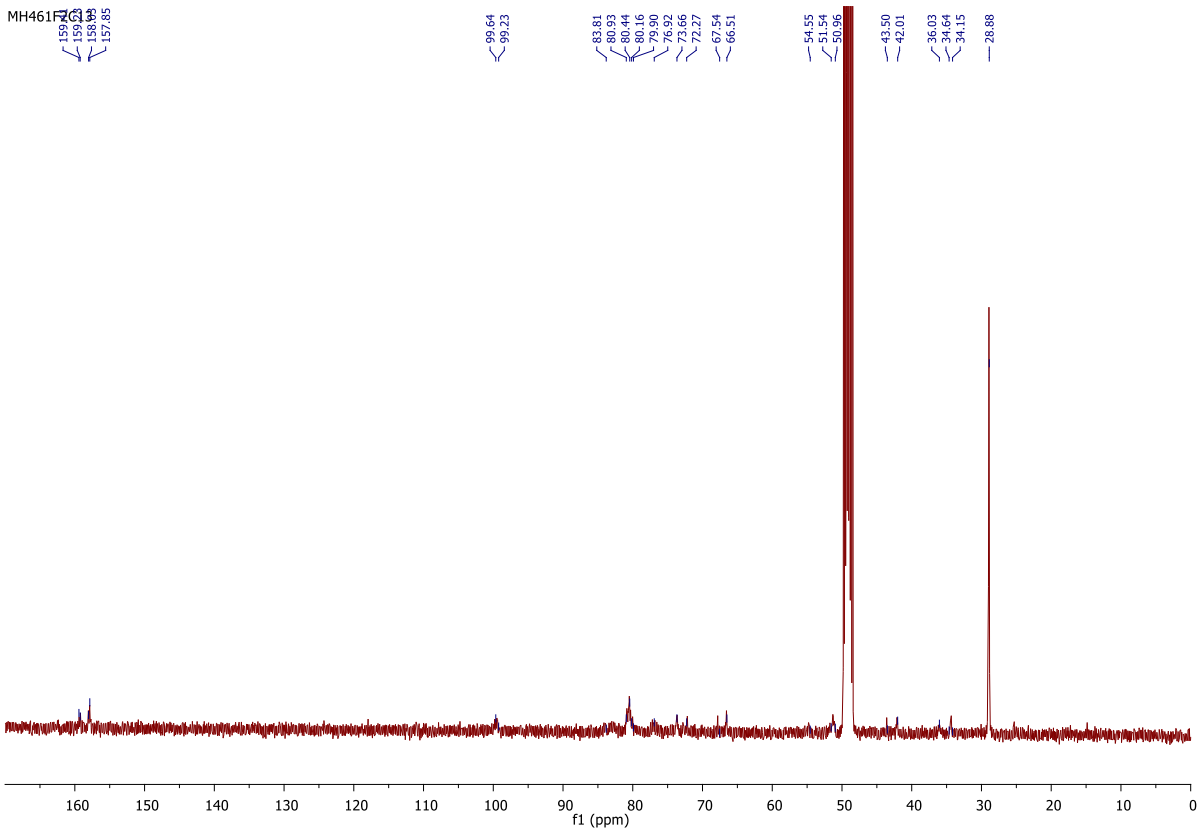

Supplementary Figure S1. NMR data for the characterization of the products in the synthesis of tobramycin-Ce6.

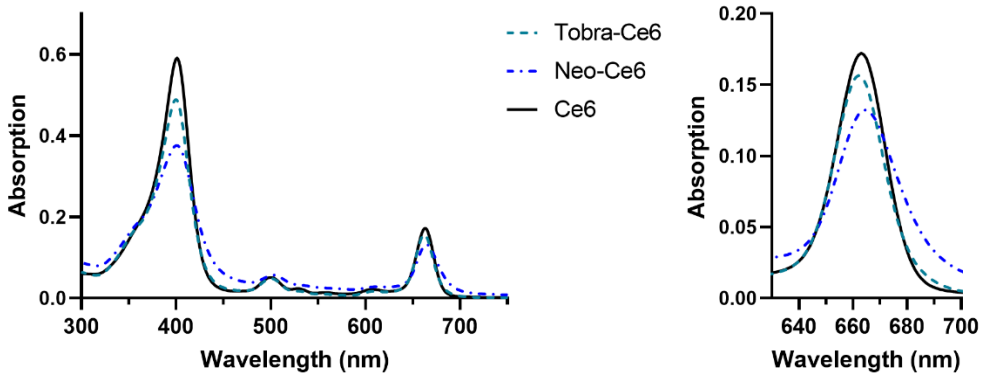

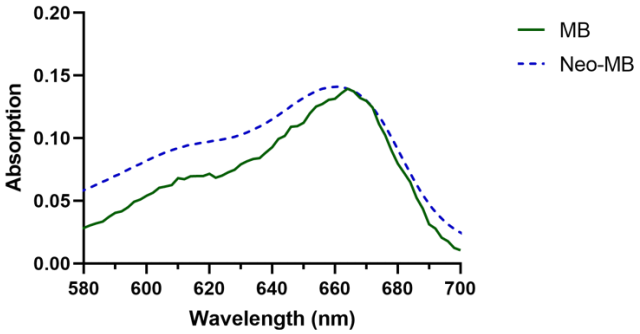

Supplementary Figure S2. Absorption of Ce6 (3.1 μM), Neo-Ce6 (2.4 μM) and Tobra-Ce6 (2.8 μM). Absorption of MB and Neo-MB at 5 μM.

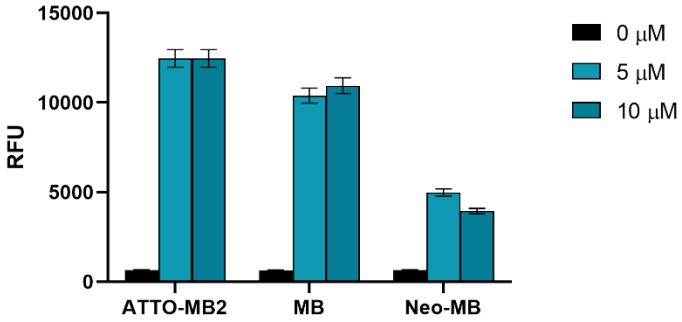

Supplementary Figure S3. Neo-MB has impaired singlet oxygen production. Fluorescence measured using the SOSGR kit after a 15-minute illumination with the prototype (665 nm). Total energy received: 84 mJ/mm^2.

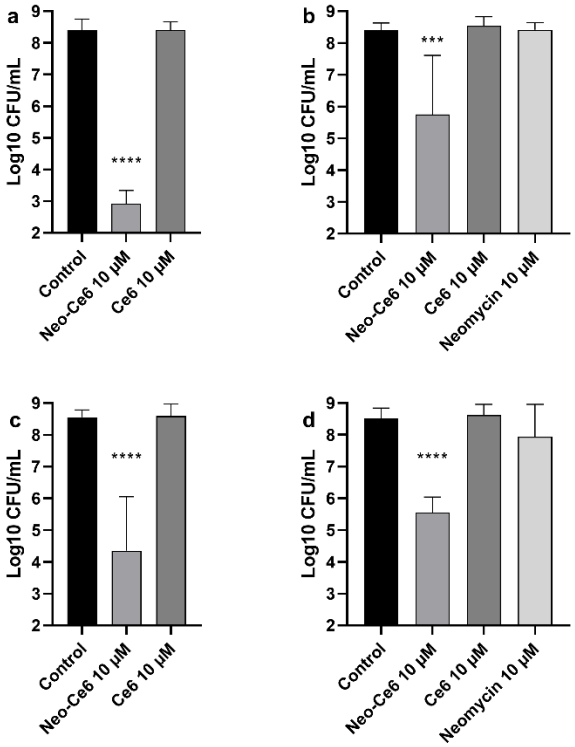

Figure S4: Log10 CFU/ml in *E. coli* kanamycin resistant mutants following aPDT with Neo-Ce6. In a and b, *E. coli* KanR with and without irradiation respectively, in c and d, *E. coli* pET-29 with and without irradiation. Irradiated samples received a total of 168 mJ/mm^2.

REFERENCES

Abraham, E.P. and Chain, E., 1940. An enzyme from bacteria able to destroy penicillin. *Nature*, *146*(3713), pp.837-837.

Abrahamse, H. and Hamblin, M.R., 2016. New photosensitizers for photodynamic therapy. Biochemical Journal, 473(4), pp.347-364.

Ackroyd, R., Kelty, C., Brown, N. and Reed, M., 2001. The history of photodetection and photodynamic therapy. *Photochemistry and photobiology*, *74*(5), pp.656-669.

Afif, H., Allali, N., Couturier, M. and Van Melderen, L., 2001. The ratio between CcdA and CcdB modulates the transcriptional repression of the ccd poison–antidote system. *Molecular microbiology*, *41*(1), pp.73-82.

Aggen, J.B., Armstrong, E.S., Goldblum, A.A., Dozzo, P., Linsell, M.S., Gliedt, M.J., Hildebrandt, D.J., Feeney, L.A., Kubo, A., Matias, R.D. and Lopez, S., 2010. Synthesis and spectrum of the neoglycoside ACHN-490. Antimicrobial agents and chemotherapy, 54(11), pp.4636-4642.

Aires, J.R., Köhler, T., Nikaido, H. and Plésiat, P., 1999. Involvement of an active efflux system in the natural resistance of Pseudomonas aeruginosa to aminoglycosides. *Antimicrobial agents and chemotherapy*, *43*(11), pp.2624-2628.

Aires, J.R. and Nikaido, H., 2005. Aminoglycosides are captured from both periplasm and cytoplasm by the AcrD multidrug efflux transporter of Escherichia coli. *Journal of Bacteriology*, *187*(6), pp.1923-1929.

Alam, S.T., Le, T.A.N., Park, J.S., Kwon, H.C. and Kang, K., 2019. Antimicrobial Biophotonic Treatment of Ampicillin-Resistant Pseudomonas aeruginosa with Hypericin and Ampicillin Cotreatment Followed by Orange Light. Pharmaceutics, 11(12), p.641.

Alkasir, R., Ma, Y., Liu, F., Li, J., Lv, N., Xue, Y., Hu, Y. and Zhu, B., 2018. Characterization and transcriptome analysis of Acinetobacter baumannii persister cells. Microbial Drug Resistance, 24(10), pp.1466-1474.

Allen, P.J., Naghski, J. and Hoover, S.R., 1944. Decomposition of guayule resins by microorganisms. *Journal of bacteriology*, *47*(6), pp.559-572.

Allison, K.R., Brynildsen, M.P. and Collins, J.J., 2011. Metabolite-enabled eradication of bacterial persisters by aminoglycosides. *Nature*, *473*(7346), pp.216-220.

Allison, R.R. and Sibata, C.H., 2010. Oncologic photodynamic therapy photosensitizers: a clinical review. Photodiagnosis and photodynamic therapy, 7(2), pp.61-75.

Al Sheikh, Y.A., Marie, M.A.M., John, J., Krishnappa, L.G. and Dabwab, K.H.M., 2014. Prevalence of 16S rRNA methylase genes among β-lactamase-producing Enterobacteriaceae clinical isolates in Saudi Arabia. *Libyan Journal of Medicine*, *9*(1), p.24432.

Alves, E., Costa, L., Carvalho, C.M., Tomé, J.P., Faustino, M.A., Neves, M.G., Tomé, A.C., Cavaleiro, J.A., Cunha, Â. and Almeida, A., 2009. Charge effect on the photoinactivation of Gram-negative and Gram-positive bacteria by cationic meso-substituted porphyrins. *BMC microbiology*, *9*(1), pp.1-13.

Alves, E., Faustino, M.A., Neves, M.G., Cunha, A., Tome, J. and Almeida, A., 2014. An insight on bacterial cellular targets of photodynamic inactivation. *Future medicinal chemistry*, *6*(2), pp.141-164.

Avent, M.L., Rogers, B.A., Cheng, A.C. and Paterson, D.L., 2011. Current use of aminoglycosides: indications, pharmacokinetics and monitoring for toxicity. Internal medicine journal, 41(6), pp.441-449.

Azevedo, M.M., Lisboa, C., Cobrado, L., Pina-Vaz, C. and Rodrigues, A., 2020. Hard-to-heal wounds, biofilm and wound healing: an intricate interrelationship. British Journal of Nursing, 29(5), pp.S6-S13.

Azzouzi, A.R., Lebdai, S., Benzaghou, F. and Stief, C., 2015. Vascular-targeted photodynamic therapy with TOOKAD® Soluble in localized prostate cancer: standardization of the procedure. World journal of urology, 33(7), pp.937-944.

Baba, T., Bae, T., Schneewind, O., Takeuchi, F. and Hiramatsu, K., 2008. Genome sequence of Staphylococcus aureus strain Newman and comparative analysis of staphylococcal genomes: polymorphism and evolution of two major pathogenicity islands. *Journal of bacteriology*, *190*(1), pp.300-310.

Bafna, J.A., Sans-Serramitjana, E., Acosta-Gutiérrez, S., Bodrenko, I.V., Hörömpöli, D., Berscheid, A., Brötz-Oesterhelt, H., Winterhalter, M. and Ceccarelli, M., 2020. Kanamycin uptake into Escherichia coli is facilitated by OmpF and OmpC porin channels located in the outer membrane. *ACS infectious diseases*, *6*(7), pp.1855-1865.

Balaban, N.Q., Merrin, J., Chait, R., Kowalik, L. and Leibler, S., 2004. Bacterial persistence as a phenotypic switch. *Science*, *305*(5690), pp.1622-1625.

Balata, M.L., Andrade, L.P.D., Santos, D.B.N., Cavalcanti, A.N., Tunes, U.D.R., Ribeiro, E.D.P. and Bittencourt, S., 2013. Photodynamic therapy associated with full-mouth ultrasonic debridement in the treatment of severe chronic periodontitis: a randomized-controlled clinical trial. Journal of Applied Oral Science, 21(2), pp.208-214.

Balestrino, D., Ghigo, J.M., Charbonnel, N., Haagensen, J.A. and Forestier, C., 2008. The characterization of functions involved in the establishment and maturation of Klebsiella pneumoniae in vitro biofilm reveals dual roles for surface exopolysaccharides. *Environmental microbiology*, *10*(3), pp.685-701.

Barclay, W.R., 1953. Distribution and excretion of radioactive isoniazid in tuberculous patients. J Am Med Assn, 151, pp.1384-1388.

Barth Jr, V.C., Rodrigues, B.Á., Bonatto, G.D., Gallo, S.W., Pagnussatti, V.E., Ferreira, C.A.S. and de Oliveira, S.D., 2013. Heterogeneous persister cells formation in Acinetobacter baumannii. *PLoS One*, *8*(12), p.e84361.

Battersby, A.R., 2000. Tetrapyrroles: the pigments of life. Natural product reports, 17(6), pp.507-526.

Beauclerk, A.A. and Cundliffe, E., 1987. Sites of action of two ribosomal RNA methylases responsible for resistance to aminoglycosides. *Journal of molecular biology*, *193*(4), pp.661-671.

Bernard, P., Kézdy, K.E., Van Melderen, L., Steyaert, J., Wyns, L., Pato, M.L., Higgins, P.N. and Couturier, M., 1993. The F plasmid CcdB protein induces efficient ATP-dependent DNA cleavage by gyrase. *Journal of molecular biology*, *234*(3), pp.534-541.

Bigger, J.W., 1944. Treatment of staphylococcal infections with penicillin. Lancet 244:497–500

Blanchard, C., Brooks, L., Beckley, A., Colquhoun, J., Dewhurst, S. and Dunman, P.M., 2016. Neomycin sulfate improves the antimicrobial activity of mupirocin-based antibacterial ointments. Antimicrobial agents and chemotherapy, 60(2), pp.862-872.

Boles, B.R. and Horswill, A.R., 2008. Agr-mediated dispersal of Staphylococcus aureus biofilms. PLoS pathogens, 4(4).

Boyce, J.M. and Pittet, D., 2002. Guideline for hand hygiene in health-care settings: recommendations of the Healthcare Infection Control Practices Advisory Committee and the HICPAC/SHEA/APIC/IDSA Hand Hygiene Task Force. *Infection Control & Hospital Epidemiology*, *23*(S12), pp.S3-S40.

Branda, S.S., Chu, F., Kearns, D.B., Losick, R. and Kolter, R., 2006. A major protein component of the Bacillus subtilis biofilm matrix. Molecular microbiology, 59(4), pp.1229-1238.

Briandet, R., Herry, J.M. and Bellon-Fontaine, M.N., 2001. Determination of the van der Waals, electron donor and electron acceptor surface tension components of static Gram-positive microbial biofilms. Colloids and Surfaces B: Biointerfaces, 21(4), pp.299-310.

Bryan, L.E. and Van den Elzen, H.M., 1976. Streptomycin accumulation in susceptible and resistant strains of Escherichia coli and Pseudomonas aeruginosa. Antimicrobial agents and chemotherapy, 9(6), pp.928-938.

Bryers, J.D., 2008. Medical biofilms. Biotechnology and bioengineering, 100(1), pp.1-18.

Burmølle, M., Webb, J.S., Rao, D., Hansen, L.H., Sørensen, S.J. and Kjelleberg, S., 2006. Enhanced biofilm formation and increased resistance to antimicrobial agents and bacterial invasion are caused by synergistic interactions in multispecies biofilms. *Applied and environmental microbiology*, *72*(6), pp.3916-3923.

Bush, K., 2013. Proliferation and significance of clinically relevant β-lactamases. *Annals of the New York Academy of Sciences*, *1277*(1), pp.84-90.

Cahan, R., Swissa, N., Gellerman, G. and Nitzan, Y., 2010. Photosensitizer–antibiotic conjugates: A novel class of antibacterial molecules. *Photochemistry and photobiology*, *86*(2), pp.418-425.

Caires, C.S., Leal, C.R., Ramos, C.A., Bogo, D., Lima, A.R., Arruda, E.J., Oliveira, S.L., Caires, A.R. and Nascimento, V.A., 2017. Photoinactivation effect of eosin methylene blue and chlorophyllin sodium-copper against Staphylococcus aureus and Escherichia coli. Lasers in medical science, 32(5), pp.1081-1088.

Calixto, G.M.F., de Annunzio, S.R., Victorelli, F.D., Frade, M.L., Ferreira, P.S., Chorilli, M. and Fontana, C.R., 2019. Chitosan-based drug delivery systems for optimization of photodynamic therapy: A review. *AAPS PharmSciTech*, *20*(7), pp.1-17.

Camilli, A. and Bassler, B.L., 2006. Bacterial small-molecule signaling pathways. Science, 311(5764), pp.1113-1116.

Campbell, E.A., Korzheva, N., Mustaev, A., Murakami, K., Nair, S., Goldfarb, A. and Darst, S.A., 2001. Structural mechanism for rifampicin inhibition of bacterial RNA polymerase. *Cell*, *104*(6), pp.901-912.

Carpenter, B., Situ, X., Scholle, F., Bartelmess, J., Weare, W. and Ghiladi, R., 2015. Antiviral, antifungal and antibacterial activities of a BODIPY-based photosensitizer. Molecules, 20(6), pp.10604-10621.

Cassini, A., Högberg, L.D., Plachouras, D., Quattrocchi, A., Hoxha, A., Simonsen, G.S., Colomb-Cotinat, M., Kretzschmar, M.E., Devleesschauwer, B., Cecchini, M. and Ouakrim, D.A., 2019. Attributable deaths and disability-adjusted life-years caused by infections with antibiotic-resistant bacteria in the EU and the European Economic Area in 2015: a population-level modelling analysis. The Lancet infectious diseases, 19(1), pp.56-66.

Cataudella, I., Sneppen, K., Gerdes, K. and Mitarai, N., 2013. Conditional cooperativity of toxin-antitoxin regulation can mediate bistability between growth and dormancy. PLoS computational biology, 9(8).

Chambers, H.F. and DeLeo, F.R., 2009. Waves of resistance: Staphylococcus aureus in the antibiotic era. *Nature Reviews Microbiology*, *7*(9), pp.629-641.

Chan, W.M., Lim, T.H., Pece, A., Silva, R. and Yoshimura, N., 2010. Verteporfin PDT for non-standard indications—a review of current literature. Graefe's Archive for Clinical and Experimental Ophthalmology, 248(5), pp.613-626.

Chapman, M.R., Robinson, L.S., Pinkner, J.S., Roth, R., Heuser, J., Hammar, M., Normark, S. and Hultgren, S.J., 2002. Role of Escherichia coli curli operons in directing amyloid fiber formation. Science, 295(5556), pp.851-855.

Chen, S., Kong, E.C.T., Lee, J. and Zhu, S., 2012. Resistance to Tobramycin in Pseudomonas aeruginosa PA14 and PA14 ΔpelB Co-culture Biofilm through Antibiotic Sequestering. *Journal of Experimental Microbiology and Immunology (JEMI) Vol*, *16*, pp.49-53.

Chen, Y., Zheng, W., Li, Y., Zhong, J., Ji, J. and Shen, P., 2008. Apoptosis induced by methylene-blue-mediated photodynamic therapy in melanomas and the involvement of mitochondrial dysfunction revealed by proteomics. Cancer science, 99(10), pp.2019-2027.

Chowdhury, N., Wood, T.L., Martínez-Vázquez, M., García-Contreras, R. and Wood, T.K., 2016. DNA-crosslinker cisplatin eradicates bacterial persister cells. Biotechnology and bioengineering, 113(9), pp.1984-1992.

Christensen, S.K., Mikkelsen, M., Pedersen, K. and Gerdes, K., 2001. RelE, a global inhibitor of translation, is activated during nutritional stress. Proceedings of the National Academy of Sciences, 98(25), pp.14328-14333.

Cieplik, F., Deng, D., Crielaard, W., Buchalla, W., Hellwig, E., Al-Ahmad, A. and Maisch, T., 2018. Antimicrobial photodynamic therapy–what we know and what we don't. *Critical Reviews in Microbiology*, *44*(5), pp.571-589.

Cieplik, F., Späth, A., Regensburger, J., Gollmer, A., Tabenski, L., Hiller, K.A., Bäumler, W., Maisch, T. and Schmalz, G., 2013. Photodynamic biofilm inactivation by SAPYR—an exclusive singlet oxygen photosensitizer. Free Radical Biology and Medicine, 65, pp.477-487.

Cirz, R.T., O'Neill, B.M., Hammond, J.A., Head, S.R. and Romesberg, F.E., 2006. Defining the Pseudomonas aeruginosa SOS response and its role in the global response to the antibiotic ciprofloxacin. Journal of bacteriology, 188(20), pp.7101-7110.

Coates, A., Hu, Y., Bax, R. and Page, C., 2002. The future challenges facing the development of new antimicrobial drugs. Nature reviews Drug discovery, 1(11), pp.895-910.

Cohen, N.R., Lobritz, M.A. and Collins, J.J., 2013. Microbial persistence and the road to drug resistance. Cell host & microbe, 13(6), pp.632-642.

Coleman, S.R., Blimkie, T., Falsafi, R. and Hancock, R.E., 2020. Multidrug adaptive resistance of Pseudomonas aeruginosa swarming cells. *Antimicrobial agents and chemotherapy*, *64*(3), pp.e01999-19.

Colvin, K.M., Irie, Y., Tart, C.S., Urbano, R., Whitney, J.C., Ryder, C., Howell, P.L., Wozniak, D.J. and Parsek, M.R., 2012. The Pel and Psl polysaccharides provide Pseudomonas aeruginosa structural redundancy within the biofilm matrix. Environmental microbiology, 14(8), pp.1913-1928.

Conlon, B.P., Nakayasu, E.S., Fleck, L.E., LaFleur, M.D., Isabella, V.M., Coleman, K., Leonard, S.N., Smith, R.D., Adkins, J.N. and Lewis, K., 2013. Activated ClpP kills persisters and eradicates a chronic biofilm infection. Nature, 503(7476), pp.365-370.

Conlon, B.P., Nakayasu, E.S., Fleck, L.E., LaFleur, M.D., Isabella, V.M., Coleman, K., Leonard, S.N., Smith, R.D., Adkins, J.N. and Lewis, K., 2013. Killing persister cells and eradicating a biofilm infection by activating the ClpP protease. Nature, 503(7476), p.365.

Conlon, B.P., Rowe, S.E. and Lewis, K., 2015. Persister cells in biofilm associated infections. In Biofilm-based healthcare-associated infections (pp. 1-9). Springer, Cham.

Conlon, B.P., Rowe, S.E., Gandt, A.B., Nuxoll, A.S., Donegan, N.P., Zalis, E.A., Clair, G., Adkins, J.N., Cheung, A.L. and Lewis, K., 2016. Persister formation in Staphylococcus aureus is associated with ATP depletion. Nature microbiology, 1(5), pp.1-7.

Connell, S.R., Tracz, D.M., Nierhaus, K.H. and Taylor, D.E., 2003. Ribosomal protection proteins and their mechanism of tetracycline resistance. *Antimicrobial agents and chemotherapy*, *47*(12), pp.3675-3681.

Correia, F.F., D'Onofrio, A., Rejtar, T., Li, L., Karger, B.L., Makarova, K., Koonin, E.V. and Lewis, K., 2006. Kinase activity of overexpressed HipA is required for growth arrest and multidrug tolerance in Escherichia coli. Journal of bacteriology, 188(24), pp.8360-8367.

Costa, A.C.B.P., Rasteiro, V.M.C., Pereira, C.A., Rossoni, R.D., Junqueira, J.C. and Jorge, A.O.C., 2012. The effects of rose bengal-and erythrosine-mediated photodynamic therapy on Candida albicans. Mycoses, 55(1), pp.56-63.

Cruz-Muñiz, M.Y., López-Jacome, L.E., Hernández-Durán, M., Franco-Cendejas, R., Licona-Limón, P., Ramos-Balderas, J.L., Martinéz-Vázquez, M., Belmont-Díaz, J.A., Wood, T.K. and García-Contreras, R., 2017. Repurposing the anticancer drug mitomycin C for the treatment of persistent Acinetobacter baumannii infections. International journal of antimicrobial agents, 49(1), pp.88-92.

Čunderlíková, B., Gangeskar, L. and Moan, J., 1999. Acid–base properties of chlorin e6: relation to cellular uptake. *Journal of Photochemistry and Photobiology B: Biology*, *53*(1-3), pp.81-90.

Cundliffe, E., 1989. How antibiotic-producing organisms avoid suicide. *Annual review of microbiology*, *43*(1), pp.207-233.

Czaplewski, L., Bax, R., Clokie, M., Dawson, M., Fairhead, H., Fischetti, V.A., Foster, S., Gilmore, B.F., Hancock, R.E., Harper, D. and Henderson, I.R., 2016. Alternatives to antibiotics—a pipeline portfolio review. *The Lancet infectious diseases*, *16*(2), pp.239-251.

Dahl, T.A., Midden, W.R. and Hartman, P.E., 1989. Comparison of killing of gram-negative and gram-positive bacteria by pure singlet oxygen. Journal of bacteriology, 171(4), pp.2188-2194.

Dahl, T.A., Midden, W.R. and Hartman, P.E., 1988. Pure exogenous singlet oxygen: nonmutagenicity in bacteria. Mutation Research/Fundamental and Molecular Mechanisms of Mutagenesis, 201(1), pp.127-136.

Dahl, T., Robert Middenand, W. and Hartman, P., 1987. Pure singlet oxygen cytotoxicity for bacteria. Photochemistry and photobiology, 46(3), pp.345-352.

Dai, C.F., Mangiardi, D., Cotanche, D.A. and Steyger, P.S., 2006. Uptake of fluorescent gentamicin by vertebrate sensory cells in vivo. Hearing research, 213(1-2), pp.64-78.

Datta, A., Dube, A., Jain, B., Tiwari, A. and Gupta, P.K., 2002. The Effect of pH and Surfactant on the Aggregation Behavior of Chlorin p6: A Fluorescence Spectroscopic Study¶. *Photochemistry and photobiology*, *75*(5), pp.488-494.

Davis, B.D., 1987. Mechanism of bactericidal action of aminoglycosides. Microbiological reviews, 51(3), p.341.

Davis, B.D., Chen, L.L. and Tai, P.C., 1986. Misread protein creates membrane channels: an essential step in the bactericidal action of aminoglycosides. Proceedings of the National Academy of Sciences, 83(16), pp.6164-6168.

Debbia, E.A., Roveta, S., Schito, A.M., Gualco, L. and Marchese, A., 2001. Antibiotic persistence: the role of spontaneous DNA repair response. Microbial Drug Resistance, 7(4), pp.335-342.

De Jonge, N., Garcia-Pino, A., Buts, L., Haesaerts, S., Charlier, D., Zangger, K., Wyns, L., De Greve, H. and Loris, R., 2009. Rejuvenation of CcdB-poisoned gyrase by an intrinsically disordered protein domain. Molecular cell, 35(2), pp.154-163.

Demidova, T.N. and Hamblin, M.R., 2005. Photodynamic inactivation of Bacillus spores, mediated by phenothiazinium dyes. *Applied and environmental microbiology*, *71*(11), pp.6918-6925.

Deng, X., Tang, S., Wu, Q., Tian, J., Riley, W.W. and Chen, Z., 2016. Inactivation of Vibrio parahaemolyticus by antimicrobial photodynamic technology using methylene blue. Journal of the Science of Food and Agriculture, 96(5), pp.1601-1608.

De Groote, V.N., Verstraeten, N., Fauvart, M., Kint, C.I., Verbeeck, A.M., Beullens, S., Cornelis, P. and Michiels, J., 2009. Novel persistence genes in Pseudomonas aeruginosa identified by high-throughput screening. FEMS microbiology letters, 297(1), pp.73-79.

Dienemann, C., Bøggild, A., Winther, K.S., Gerdes, K. and Brodersen, D.E., 2011. Crystal structure of the VapBC toxin–antitoxin complex from Shigella flexneri reveals a hetero-octameric DNA-binding assembly. Journal of molecular biology, 414(5), pp.713-722.

Diep, B.A., Gill, S.R., Chang, R.F., Phan, T.H., Chen, J.H., Davidson, M.G., Lin, F., Lin, J., Carleton, H.A., Mongodin, E.F. and Sensabaugh, G.F., 2006. Complete genome sequence of USA300, an epidemic clone of community-acquired meticillin-resistant Staphylococcus aureus. *The Lancet*, *367*(9512), pp.731-739.

Diggle, S.P., Stacey, R.E., Dodd, C., Cámara, M., Williams, P. and Winzer, K., 2006. The galactophilic lectin, LecA, contributes to biofilm development in Pseudomonas aeruginosa. Environmental microbiology, 8(6), pp.1095-1104.

Doern, C.D., 2014. When does 2 plus 2 equal 5? A review of antimicrobial synergy testing. *Journal of clinical microbiology*, *52*(12), pp.4124-4128.

Doménech-Sánchez, A., Martínez-Martínez, L., Hernández-Allés, S., del Carmen Conejo, M., Pascual, Á., Tomás, J.M., Albertí, S. and Benedí, V.J., 2003. Role of Klebsiella pneumoniae OmpK35 porin in antimicrobial resistance. *Antimicrobial agents and chemotherapy*, *47*(10), pp.3332-3335.

Dönhöfer, A., Franckenberg, S., Wickles, S., Berninghausen, O., Beckmann, R. and Wilson, D.N., 2012. Structural basis for TetM-mediated tetracycline resistance. *Proceedings of the National Academy of Sciences*, *109*(42), pp.16900-16905.

Donlan, R.M., 2001. Biofilms and device-associated infections. Emerging infectious diseases, 7(2), p.277.

Dörr, T., Lewis, K. and Vulić, M., 2009. SOS response induces persistence to fluoroquinolones in Escherichia coli. PLoS genetics, 5(12), p.e1000760.

Dörr, T., Vulić, M. and Lewis, K., 2010. Ciprofloxacin causes persister formation by inducing the TisB toxin in Escherichia coli. PLoS biology, 8(2), p.e1000317.

Dovigo, L.N., Carmello, J.C., Carvalho, M.T., Mima, E.G., Vergani, C.E., Bagnato, V.S. and Pavarina, A.C., 2013. Photodynamic inactivation of clinical isolates of Candida using Photodithazine®. *Biofouling*, *29*(9), pp.1057-1067.

Dysart, J.S. and Patterson, M.S., 2005. Characterization of Photofrin photobleaching for singlet oxygen dose estimation during photodynamic therapy of MLL cells in vitro. Physics in Medicine & Biology, 50(11), p.2597.

Ehrenberg, B., Malik, Z. and Nitzan, Y., 1985. Fluorescence spectral changes of hematoporphyrin derivative upon binding to lipid vesicles, Staphylococcus aureus and Escherichia coli cells. *Photochemistry and photobiology*, *41*(4), pp.429-435.

Epe, B., Hegler, J. and Wild, D., 1989. Singlet oxygen as an ultimately reactive species in Salmonella typhimurium DNA damage induced by methylene blue/visible light. Carcinogenesis, 10(11), pp.2019-2024.

Ettinger, A., Miklauz, M.M., Bihm, D.J., Maldonado-Codina, G. and Goodrich, R.P., 2012. Preparation of cryoprecipitate from riboflavin and UV light-treated plasma. Transfusion and Apheresis Science, 46(2), pp.153-158.

Falghoush, A., Beyenal, H., Besser, T.E., Omsland, A. and Call, D.R., 2017. Osmotic compounds enhance antibiotic efficacy against Acinetobacter baumannii biofilm communities. Appl. Environ. Microbiol., 83(19), pp.e01297-17.

Favre-Bonte, S., Joly, B. and Forestier, C., 1999. Consequences of reduction of Klebsiella pneumoniae capsule expression on interactions of this bacterium with epithelial cells. *Infection and immunity*, *67*(2), pp.554-561.

Fernandez, J.M., Bilgin, M.D. and Grossweiner, L.I., 1997. Singlet oxygen generation by photodynamic agents. *Journal of Photochemistry and Photobiology B: Biology*, *37*(1-2), pp.131-140.

Fischer, R.S., Zhao, G. and Jensen, R.A., 1991. Cloning, sequencing, and expression of the P-protein gene (pheA) of Pseudomonas stutzeri in Escherichia coli: implications for evolutionary relationships in phenylalanine biosynthesis. Microbiology, 137(6), pp.1293-1301.

Flensburg, J. and Sköld, O., 1987. Massive overproduction of dihydrofolate reductase in bacteria as a response to the use of trimethoprim. *European journal of biochemistry*, *162*(3), pp.473-476.

Floss, H.G. and Yu, T.W., 2005. Rifamycin mode of action, resistance, and biosynthesis. *Chemical reviews*, *105*(2), pp.621-632.

Foggiato, A.A., Silva, D.F. and Castro, R.C.F.R., 2018. Effect of photodynamic therapy on surface decontamination in clinical orthodontic instruments. Photodiagnosis and photodynamic therapy, 24, pp.123-128.

Foote, C.S., 1976. Photosensitized oxidation and singlet oxygen: consequences in biological systems, in W.A. Pryor (ed.), Free Radicals in Biology, Vol. II, Academic Press, New York, pp. 59-134.

Forte Giacobone, A.F., Ruiz Gale, M.F., Hogert, E.N. and Oppezzo, O.J., 2016. A possible phenomenon of persistence in Pseudomonas aeruginosa treated with methylene blue and red light. *Photochemistry and Photobiology*, *92*(5), pp.702-707.

Foulds, J.O.H.N. and Chai, T.J., 1978. New major outer membrane proteins found in an Escherichia coli tolF mutant resistant to bacteriophage TuIb. Journal of bacteriology, 133(3), pp.1478-1483.

Fourmy, D., Recht, M.I., Blanchard, S.C. and Puglisi, J.D., 1996. Structure of the A site of Escherichia coli 16S ribosomal RNA complexed with an aminoglycoside antibiotic. Science, 274(5291), pp.1367-1371.

Fourmy, D., Yoshizawa, S. and Puglisi, J.D., 1998. Paromomycin binding induces a local conformational change in the A-site of 16 S rRNA. Journal of molecular biology, 277(2), pp.333-345.

Foxman, B., 1990. Recurring urinary tract infection: incidence and risk factors. American journal of public health, 80(3), pp.331-333.

Friedmann, T. and Brown, D.M., 1978. Base-specific reactions useful for DNA sequencing: Methylene blue–sensitized photooxidation of guanine and osmium tetraoxide modification of thymine. Nucleic acids research, 5(2), pp.615-622.

Gad, F., Zahra, T., Hasan, T. and Hamblin, M.R., 2004. Effects of growth phase and extracellular slime on photodynamic inactivation of gram-positive pathogenic bacteria. *Antimicrobial agents and chemotherapy*, *48*(6), pp.2173-2178.

Gaimster, H. and Summers, D., 2015. Regulation of Indole Signalling during the Transition of E. coli from Exponential to Stationary Phase. PloS one, 10(9).

Garcia-Pino, A., Balasubramanian, S., Wyns, L., Gazit, E., De Greve, H., Magnuson, R.D., Charlier, D., van Nuland, N.A. and Loris, R., 2010. Allostery and intrinsic disorder mediate transcription regulation by conditional cooperativity. Cell, 142(1), pp.101-111.

Gavrish, E., Sit, C.S., Cao, S., Kandror, O., Spoering, A., Peoples, A., Ling, L., Fetterman, A., Hughes, D., Bissell, A. and Torrey, H., 2014. Lassomycin, a ribosomally synthesized cyclic peptide, kills Mycobacterium tuberculosis by targeting the ATP-dependent protease ClpC1P1P2. Chemistry & biology, 21(4), pp.509-518.

Gefen, O., Gabay, C., Mumcuoglu, M., Engel, G. and Balaban, N.Q., 2008. Single-cell protein induction dynamics reveals a period of vulnerability to antibiotics in persister bacteria. Proceedings of the National Academy of Sciences, 105(16), pp.6145-6149.

Gelens, L., Hill, L., Vandervelde, A., Danckaert, J. and Loris, R., 2013. A general model for toxin-antitoxin module dynamics can explain persister cell formation in E. coli. PLoS computational biology, 9(8).

Germain, E., Castro-Roa, D., Zenkin, N. and Gerdes, K., 2013. Molecular mechanism of bacterial persistence by HipA. Molecular cell, 52(2), pp.248-254.

Germain, E., Roghanian, M., Gerdes, K. and Maisonneuve, E., 2015. Stochastic induction of persister cells by HipA through (p) ppGpp-mediated activation of mRNA endonucleases. Proceedings of the National Academy of Sciences, 112(16), pp.5171-5176.

Gilleland, L.B., Gilleland, H.E., Gibson, J.A. and Champlin, F.R., 1989. Adaptive resistance to aminoglycoside antibiotics in Pseudomonas aeruginosa. *Journal of medical microbiology*, *29*(1), pp.41-50.

Gollmer, A., Felgenträger, A., Bäumler, W., Maisch, T. and Späth, A., 2015. A novel set of symmetric methylene blue derivatives exhibits effective bacteria photokilling—a structure—response study. *Photochemical & photobiological sciences*, *14*(2), pp.335-351.

Gomez, J.E. and McKinney, J.D., 2004. M. tuberculosis persistence, latency, and drug tolerance. Tuberculosis, 84(1-2), pp.29-44.

Gouterman, M., 1961. Spectra of porphyrins. *Journal of Molecular Spectroscopy*, *6*, pp.138-163.

Graindorge, D., Martineau, S., Machon, C., Arnoux, P., Guitton, J., Francesconi, S., Frochot, C., Sage, E. and Girard, P.M., 2015. Singlet oxygen-mediated oxidation during UVA radiation alters the dynamic of genomic DNA replication. PLoS One, 10(10), p.e0140645.

Grant, S.S. and Hung, D.T., 2013. Persistent bacterial infections, antibiotic tolerance, and the oxidative stress response. Virulence, 4(4), pp.273-283.

Green, R. and Noller, H.F., 1997. Ribosomes and translation. Annual review of biochemistry, 66(1), pp.679-716.

Hage, R., Ferreira, J., Bagnato, V.S., Vollet-Filho, J.D. and Plapler, H., 2012. Pharmacokinetics of photogem using fluorescence spectroscopy in dimethylhydrazine-induced murine colorectal carcinoma. International Journal of Photoenergy, 2012.

Hall, J.W., Yang, J., Guo, H. and Ji, Y., 2017. The Staphylococcus aureus AirSR two-component system mediates reactive oxygen species resistance via transcriptional regulation of staphyloxanthin production. *Infection and immunity*, *85*(2), pp.e00838-16.

Hamblin, M.R. and Hasan, T., 2004. Photodynamic therapy: a new antimicrobial approach to infectious disease?. Photochemical & Photobiological Sciences, 3(5), pp.436-450.

Hancock, R.E. and Brinkman, F.S., 2002. Function of Pseudomonas porins in uptake and efflux. *Annual Reviews in Microbiology*, *56*(1), pp.17-38.

Hansen, S., Lewis, K. and Vulić, M., 2008. Role of global regulators and nucleotide metabolism in antibiotic tolerance in Escherichia coli. Antimicrobial agents and chemotherapy, 52(8), pp.2718-2726.

Harriott, M.M. and Noverr, M.C., 2009. Candida albicans and Staphylococcus aureus form polymicrobial biofilms: effects on antimicrobial resistance. Antimicrobial agents and chemotherapy, 53(9), pp.3914-3922.

Harriott, M.M. and Noverr, M.C., 2011. Importance of Candida–bacterial polymicrobial biofilms in disease. *Trends in microbiology*, *19*(11), pp.557-563.

Hasdemir, U.O., Chevalier, J., Nordmann, P. and Pagès, J.M., 2004. Detection and prevalence of active drug efflux mechanism in various multidrug-resistant Klebsiella pneumoniae strains from Turkey. *Journal of clinical microbiology*, *42*(6), pp.2701-2706.

Hayes, F. and Van Melderen, L., 2011. Toxins-antitoxins: diversity, evolution and function. Critical reviews in biochemistry and molecular biology, 46(5), pp.386-408.

Heidary, N. and Cohen, D.E., 2005. Hypersensitivity reactions to vaccine components. Dermatitis, 16(3), pp.115-120.

He, J., Baldini, R.L., Déziel, E., Saucier, M., Zhang, Q., Liberati, N.T., Lee, D., Urbach, J., Goodman, H.M. and Rahme, L.G., 2004. The broad host range pathogen Pseudomonas aeruginosa strain PA14 carries two pathogenicity islands harboring plant and animal virulence genes. *Proceedings of the National Academy of Sciences*, *101*(8), pp.2530-2535.

Hinkeldey, B., Schmitt, A. and Jung, G., 2008. Comparative photostability studies of BODIPY and fluorescein dyes by using fluorescence correlation spectroscopy. ChemPhysChem, 9(14), pp.2019-2027.

Hiramatsu, K., Ito, T., Tsubakishita, S., Sasaki, T., Takeuchi, F., Morimoto, Y., Katayama, Y., Matsuo, M., Kuwahara-Arai, K., Hishinuma, T. and Baba, T., 2013. Genomic basis for methicillin resistance in Staphylococcus aureus. *Infection & chemotherapy*, *45*(2), pp.117-136.

Hobby, G.L., Meyer, K. and Chaffee, E., 1942. Observations on the Mechanism of Action of Penicillin. Proceedings of the Society for Experimental Biology and Medicine, 50(2), pp.281-285.

Hogan, S., Zapotoczna, M., Stevens, N.T., Humphreys, H., O'Gara, J.P. and O'Neill, E., 2016. In vitro approach for identification of the most effective agents for antimicrobial lock therapy in the treatment of intravascular catheter-related infections caused by Staphylococcus aureus. Antimicrobial agents and chemotherapy, 60(5), pp.2923-2931.

Hollingshead, S. and Vapnek, D., 1985. Nucleotide sequence analysis of a gene encoding a streptomycin/spectinomycin adenyltransferase. *Plasmid*, *13*(1), pp.17-30.

Hollmann, B., Perkins, M., Walsh, D. Biofilms and their role in pathogenesis. British Society for Immunology.

Hollmann, B., Perkins, M., Chauhan, V.M., Aylott, J.W. and Hardie, K.R., 2021. Fluorescent nanosensors reveal dynamic pH gradients during biofilm formation. *npj Biofilms and Microbiomes*, *7*(1), pp.1-13.

Holloway, B.W., 1975. Genetic organization of Pseudomonas. *Genetics and biochemistry of Pseudomonas*, pp.133-161.

Hunstad, D.A. and Justice, S.S., 2010. Intracellular lifestyles and immune evasion strategies of uropathogenic Escherichia coli. Annual review of microbiology, 64, pp.203-221.

Huntosova, V. and Stroffekova, K., 2016. Hypericin in the dark: foe or ally in photodynamic therapy?. Cancers, 8(10), p.93.

Ilina, K., MacCuaig, W.M., Laramie, M., Jeouty, J.N., McNally, L.R. and Henary, M., 2019. Squaraine Dyes: Molecular Design for Different Applications and Remaining Challenges. Bioconjugate chemistry.

Iscla, I., Wray, R., Wei, S., Posner, B. and Blount, P., 2014. Streptomycin potency is dependent on MscL channel expression. *Nature communications*, *5*(1), pp.1-7.

Jeon, Y.M., Lee, H.S., Jeong, D., Oh, H.K., Ra, K.H. and Lee, M.Y., 2015. Antimicrobial photodynamic therapy using chlorin e6 with halogen light for acne bacteria-induced inflammation. Life sciences, 124, pp.56-63.

Jeong, H., Huh, M., Lee, S.J., Koo, H., Kwon, I.C., Jeong, S.Y. and Kim, K., 2011. Photosensitizer-conjugated human serum albumin nanoparticles for effective photodynamic therapy. *Theranostics*, *1*, p.230.

Jiafeng, L., Fu, X. and Chang, Z., 2015. Hypoionic shock treatment enables aminoglycosides antibiotics to eradicate bacterial persisters. Scientific reports, 5, p.14247.

Jiang, M., Karasawa, T. and Steyger, P.S., 2017. Aminoglycoside-induced cochleotoxicity: a review. Frontiers in cellular neuroscience, 11, p.308.

Jindal, S., Yang, L., Day, P.J. and Kell, D.B., 2019. Involvement of multiple influx and efflux transporters in the accumulation of cationic fluorescent dyes by Escherichia coli. *BMC microbiology*, *19*(1), pp.1-16.

Jõers, A., Kaldalu, N. and Tenson, T., 2010. The frequency of persisters in Escherichia coli reflects the kinetics of awakening from dormancy. Journal of bacteriology, 192(13), pp.3379-3384.

Jones, T., Federspiel, N.A., Chibana, H., Dungan, J., Kalman, S., Magee, B.B., Newport, G., Thorstenson, Y.R., Agabian, N., Magee, P.T. and Davis, R.W., 2004. The diploid genome sequence of Candida albicans. *Proceedings of the National Academy of Sciences*, *101*(19), pp.7329-7334.

Kamkaew, A., Lim, S.H., Lee, H.B., Kiew, L.V., Chung, L.Y. and Burgess, K., 2013. BODIPY dyes in photodynamic therapy. Chemical Society Reviews, 42(1), pp.77-88.

Karatan, E. and Watnick, P., 2009. Signals, regulatory networks, and materials that build and break bacterial biofilms. Microbiol. Mol. Biol. Rev., 73(2), pp.310-347.

Karlowsky, J.A., Zelenitsky, S.A. and Zhanel, G.G., 1997. Aminoglycoside adaptive resistance. *Pharmacotherapy: The Journal of Human Pharmacology and Drug Therapy*, *17*(3), pp.549-555.

Karygianni, L., Ruf, S., Follo, M., Hellwig, E., Bucher, M., Anderson, A.C., Vach, K. and Al-Ahmad, A., 2014. Novel broad-spectrum antimicrobial photoinactivation of in situ oral biofilms by visible light plus water-filtered infrared A. Appl. Environ. Microbiol., 80(23), pp.7324-7336.

Kashiwagi, K., Tsuhako, M.H., Sakata, K., Saisho, T., Igarashi, A., Pinto da Costa, S.O. and Igarashi, K., 1998. Relationship between spontaneous aminoglycoside resistance in Escherichia coli and a decrease in oligopeptide binding protein. *Journal of bacteriology*, *180*(20), pp.5484-5488.

Kaspy, I., Rotem, E., Weiss, N., Ronin, I., Balaban, N.Q. and Glaser, G., 2013. HipA-mediated antibiotic persistence via phosphorylation of the glutamyl-tRNA-synthetase. Nature communications, 4, p.3001.

Katayama, Y., Sekine, M., Hishinuma, T., Aiba, Y. and Hiramatsu, K., 2016. Complete reconstitution of the vancomycin-intermediate Staphylococcus aureus phenotype of strain Mu50 in vancomycin-susceptible S. aureus. *Antimicrobial agents and chemotherapy*, *60*(6), pp.3730-3742.

Kell, D.B., 2015. What would be the observable consequences if phospholipid bilayer diffusion of drugs into cells is negligible?. *Trends in pharmacological sciences*, *36*(1), pp.15-21.

Kell, D.B., Dobson, P.D., Bilsland, E. and Oliver, S.G., 2013. The promiscuous binding of pharmaceutical drugs and their transporter-mediated uptake into cells: what we (need to) know and how we can do so. *Drug discovery today*, *18*(5-6), pp.218-239.

Kell, D.B. and Oliver, S.G., 2014. How drugs get into cells: tested and testable predictions to help discriminate between transporter-mediated uptake and lipoidal bilayer diffusion. *Frontiers in Pharmacology*, *5*, p.231.

Keren, I., Shah, D., Spoering, A., Kaldalu, N. and Lewis, K., 2004. Specialized persister cells and the mechanism of multidrug tolerance in Escherichia coli. Journal of bacteriology, 186(24), pp.8172-8180.

Khadem, J., Veloso, A.A., Tolentino, F., Hasan, T. and Hamblin, M.R., 1999. Photodynamic tissue adhesion with chlorin e6 protein conjugates. Investigative ophthalmology & visual science, 40(13), pp.3132-3137.

Kim, W., Conery, A.L., Rajamuthiah, R., Fuchs, B.B., Ausubel, F.M. and Mylonakis, E., 2015. Identification of an antimicrobial agent effective against methicillin-resistant Staphylococcus aureus persisters using a fluorescence-based screening strategy. PLoS One, 10(6).

Koeva, M., Gutu, A.D., Hebert, W., Wager, J.D., Yonker, L.M., O'Toole, G.A., Ausubel, F.M., Moskowitz, S.M. and Joseph-McCarthy, D., 2017. An antipersister strategy for treatment of chronic Pseudomonas aeruginosa infections. Antimicrobial agents and chemotherapy, 61(12), pp.e00987-17.

Kohanski, M.A., DePristo, M.A. and Collins, J.J., 2010. Sublethal antibiotic treatment leads to multidrug resistance via radical-induced mutagenesis. Molecular cell, 37(3), pp.311-320.

Koronakis, V., 2003. TolC–the bacterial exit duct for proteins and drugs. *FEBS letters*, *555*(1), pp.66-71.

Krause, D.O., Little, A.C., Dowd, S.E. and Bernstein, C.N., 2011. Complete genome sequence of adherent invasive Escherichia coli UM146 isolated from Ileal Crohn's disease biopsy tissue. *Journal of bacteriology*, *193*(2), pp.583-583.

Krause, K.M., Serio, A.W., Kane, T.R. and Connolly, L.E., 2016. Aminoglycosides: an overview. Cold Spring Harbor perspectives in medicine, 6(6), p.a027029.

Kresge, N., Simoni, R.D. and Hill, R.L., 2004. Selman Waksman: the father of antibiotics. Journal of Biological Chemistry, 279(48), pp.e7-e7.

Krinsky, N.I., 1974. Singlet excited oxygen as a mediator of the antibacterial action of leukocytes. Science, 186(4161), pp.363-365.

Kuimova, M.K., Yahioglu, G. and Ogilby, P.R., 2009. Singlet oxygen in a cell: spatially dependent lifetimes and quenching rate constants. *Journal of the American Chemical Society*, *131*(1), pp.332-340.

Kunst, F., Ogasawara, N., Moszer, I., Albertini, A.M., Alloni, G.O., Azevedo, V., Bertero, M.G., Bessières, P., Bolotin, A., Borchert, S. and Borriss, R., 1997. The complete genome sequence of the gram-positive bacterium Bacillus subtilis. *Nature*, *390*(6657), pp.249-256.

Kuroda, M., Ohta, T., Uchiyama, I., Baba, T., Yuzawa, H., Kobayashi, I., Cui, L., Oguchi, A., Aoki, K.I., Nagai, Y. and Lian, J., 2001. Whole genome sequencing of meticillin-resistant Staphylococcus aureus. *The Lancet*, *357*(9264), pp.1225-1240.

Kwan, B.W., Chowdhury, N. and Wood, T.K., 2015. Combatting bacterial infections by killing persister cells with mitomycin C. Environmental microbiology, 17(11), pp.4406-4414.

Landman, D., Kelly, P., Bäcker, M., Babu, E., Shah, N., Bratu, S. and Quale, J., 2011. Antimicrobial activity of a novel aminoglycoside, ACHN-490, against Acinetobacter baumannii and Pseudomonas aeruginosa from New York City. Journal of Antimicrobial Chemotherapy, 66(2), pp.332-334.

Latasa, C., Solano, C., Penadés, J.R. and Lasa, I., 2006. Biofilm-associated proteins. Comptes rendus biologies, 329(11), pp.849-857.

Laursen, B.S., Sørensen, H.P., Mortensen, K.K. and Sperling-Petersen, H.U., 2005. Initiation of protein synthesis in bacteria. Microbiol. Mol. Biol. Rev., 69(1), pp.101-123.

Laxminarayan, R., Matsoso, P., Pant, S., Brower, C., Røttingen, J.A., Klugman, K. and Davies, S., 2016. Access to effective antimicrobials: a worldwide challenge. *The Lancet*, *387*(10014), pp.168-175.

Lebeaux, D., Chauhan, A., Létoffé, S., Fischer, F., de Reuse, H., Beloin, C. and Ghigo, J.M., 2014. pH-mediated potentiation of aminoglycosides kills bacterial persisters and eradicates in vivo biofilms. The Journal of infectious diseases, 210(9), pp.1357-1366.

Lebeaux, D., Leflon-Guibout, V., Ghigo, J.M. and Beloin, C., 2015. In vitro activity of gentamicin, vancomycin or amikacin combined with EDTA or l-arginine as lock therapy against a wide spectrum of biofilm-forming clinical strains isolated from catheter-related infections. Journal of Antimicrobial Chemotherapy, 70(6), pp.1704-1712.

Leclercq, R., 2002. Mechanisms of resistance to macrolides and lincosamides: nature of the resistance elements and their clinical implications. *Clinical Infectious Diseases*, *34*(4), pp.482-492.

Ledo, E. and Ledo, A., 2000. Phototherapy, photochemotherapy, and photodynamic therapy: unapproved uses or indications. Clinics in dermatology, 18(1), pp.77-86.

Lee, D.G., Urbach, J.M., Wu, G., Liberati, N.T., Feinbaum, R.L., Miyata, S., Diggins, L.T., He, J., Saucier, M., Déziel, E. and Friedman, L., 2006. Genomic analysis reveals that Pseudomonas aeruginosa virulence is combinatorial. *Genome biology*, *7*(10), pp.1-14.

Lee, H.H., Molla, M.N., Cantor, C.R. and Collins, J.J., 2010. Bacterial charity work leads to population-wide resistance. Nature, 467(7311), pp.82-85.

Leite, D.P.V., Paolillo, F.R., Parmesano, T.N., Fontana, C.R. and Bagnato, V.S., 2014. Effects of photodynamic therapy with blue light and curcumin as mouth rinse for oral disinfection: a randomized controlled trial. Photomedicine and laser surgery, 32(11), pp.627-632.

Lerner, A.M., Cone, L., Jansen, W., Reyes, M., Blair, D., Wright, G. and Lorber, R., 1983. Randomised, controlled trial of the comparative efficacy, auditory toxicity, and nephrotoxicity of tobramycin and netilmicin. *The Lancet*, *321*(8334), pp.1123-1126.

Levin, B.R. and Rozen, D.E., 2006. Non-inherited antibiotic resistance. Nature Reviews Microbiology, 4(7), pp.556-562.

Lewis, K., 2010. Persister cells. Annual review of microbiology, 64, pp.357-372.

Lewis, K., 2001. Riddle of biofilm resistance. Antimicrobial agents and chemotherapy, 45(4), pp.999-1007.

Liebens, V., Defraine, V., Knapen, W., Swings, T., Beullens, S., Corbau, R., Marchand, A., Chaltin, P., Fauvart, M. and Michiels, J., 2017. Identification of 1-((2, 4-Dichlorophenethyl) Amino)-3-Phenoxypropan-2-ol, a novel antibacterial compound active against persisters of Pseudomonas aeruginosa. Antimicrobial agents and chemotherapy, 61(9), pp.e00836-17.

Lin, J.F., Li, J., Gopal, A., Munshi, T., Chu, Y.W., Wang, J.X., Liu, T.T., Shi, B., Chen, X. and Yan, L., 2019. Synthesis of photo-excited Chlorin e6 conjugated silica nanoparticles for enhanced anti-bacterial efficiency to overcome methicillin-resistant Staphylococcus aureus. Chemical Communications, 55(18), pp.2656-2659.

Lister, P.D., Wolter, D.J. and Hanson, N.D., 2009. Antibacterial-resistant Pseudomonas aeruginosa: clinical impact and complex regulation of chromosomally encoded resistance mechanisms. *Clinical microbiology reviews*, *22*(4), pp.582-610.

Li, W., Atkinson, G.C., Thakor, N.S., Allas, Ü., Lu, C.C., Chan, K.Y., Tenson, T., Schulten, K., Wilson, K.S., Hauryliuk, V. and Frank, J., 2013. Mechanism of tetracycline resistance by ribosomal protection protein Tet (O). *Nature communications*, *4*(1), pp.1-8.

López, D., Vlamakis, H. and Kolter, R., 2010. Biofilms. Cold Spring Harbor perspectives in biology, 2(7), p.a000398.

López-Chicón, P., Gulías, Ò., Nonell, S. and Agut, M., 2016. In vitro antimicrobial photodynamic therapy against trichophyton mentagrophytes using new methylene blue as the photosensitizer. Actas Dermo-Sifiliográficas (English Edition), 107(9), pp.765-770.

Lu, C., Sun, F., Liu, Y., Xiao, Y., Qiu, Y., Mu, H. and Duan, J., 2019. Versatile Chlorin e6-based magnetic polydopamine nanoparticles for effectively capturing and killing MRSA. Carbohydrate Polymers, 218, pp.289-298.

Luksiene, Z., 2003. Photodynamic therapy: mechanism of action and ways to improve the efficiency of treatment. Medicina, 39(12), pp.1137-1150.

Lv, B., Zeng, Y., Zhang, H., Li, Z., Xu, Z., Wang, Y., Gao, Y., Chen, Y. and Fu, X., 2022. Mechanosensitive Channels Mediate Hypoionic Shock-Induced Aminoglycoside Potentiation against Bacterial Persisters by Enhancing Antibiotic Uptake. *Antimicrobial Agents and Chemotherapy*, *66*(2), pp.e01125-21.

Lyczak, J.B., Cannon, C.L. and Pier, G.B., 2002. Lung infections associated with cystic fibrosis. Clinical microbiology reviews, 15(2), pp.194-222.

Macdonald, I.J. and Dougherty, T.J., 2001. Basic principles of photodynamic therapy. Journal of Porphyrins and Phthalocyanines, 5(02), pp.105-129.

Ma, D., Cook, D.N., Hearst, J.E. and Nikaido, H., 1994. Efflux pumps and drug resistance in gram-negative bacteria. *Trends in microbiology*, *2*(12), pp.489-493.

Madsen, J.S., Burmølle, M., Hansen, L.H. and Sørensen, S.J., 2012. The interconnection between biofilm formation and horizontal gene transfer. *FEMS Immunology & Medical Microbiology*, *65*(2), pp.183-195.

Magnet, S. and Blanchard, J.S., 2005. Molecular insights into aminoglycoside action and resistance. *Chemical reviews*, *105*(2), pp.477-498.

Magnet, S., Courvalin, P. and Lambert, T., 2001. Resistance-nodulation-cell division-type efflux pump involved in aminoglycoside resistance in Acinetobacter baumannii strain BM4454. *Antimicrobial agents and chemotherapy*, *45*(12), pp.3375-3380.

Magnuson, R. and Yarmolinsky, M.B., 1998. Corepression of the P1 addiction operon by Phd and Doc. Journal of bacteriology, 180(23), pp.6342-6351.

Mahamoud, A., Chevalier, J., Alibert-Franco, S., Kern, W.V. and Pagès, J.M., 2007. Antibiotic efflux pumps in Gram-negative bacteria: the inhibitor response strategy. Journal of Antimicrobial Chemotherapy, 59(6), pp.1223-1229.

Maisch, T., Baier, J., Franz, B., Maier, M., Landthaler, M., Szeimies, R.M. and Bäumler, W., 2007. The role of singlet oxygen and oxygen concentration in photodynamic inactivation of bacteria. Proceedings of the National Academy of Sciences, 104(17), pp.7223-7228.

Maisch, T., Eichner, A., Späth, A., Gollmer, A., König, B., Regensburger, J. and Bäumler, W., 2014. Fast and effective photodynamic inactivation of multiresistant bacteria by cationic riboflavin derivatives. PloS one, 9(12), p.e111792.

Maisch, T., Szeimies, R.M., Jori, G. and Abels, C., 2004. Antibacterial photodynamic therapy in dermatology. Photochemical & Photobiological Sciences, 3(10), pp.907-917.

Maisonneuve, E. and Gerdes, K., 2014. Molecular mechanisms underlying bacterial persisters. Cell, 157(3), pp.539-548.

Maisonneuve, E., Castro-Camargo, M. and Gerdes, K., 2013. RETRACTED:(p) ppGpp controls bacterial persistence by stochastic induction of toxin-antitoxin activity.

Malik, Z., Ladan, H. and Nitzan, Y., 1992. Photodynamic inactivation of Gram-negative bacteria: problems and possible solutions. Journal of Photochemistry and Photobiology B: Biology, 14(3), pp.262-266.

Mannucci, E., Genovese, S., Monami, M., Navalesi, G., Dotta, F., Anichini, R., Romagnoli, F. and Gensini, G., 2014. Photodynamic topical antimicrobial therapy for infected foot ulcers in patients with diabetes: a randomized, double-blind, placebo-controlled study—the DANTE (Diabetic ulcer Antimicrobial New Topical treatment Evaluation) study. Acta diabetologica, 51(3), pp.435-440.

Manoil, D., Filieri, A., Schrenzel, J. and Bouillaguet, S., 2016. Rose bengal uptake by E. faecalis and F. nucleatum and light-mediated antibacterial activity measured by flow cytometry. Journal of Photochemistry and Photobiology B: Biology, 162, pp.258-265.

Martin, W.J., Gardner, M. and Washington, J.A., 1972. In vitro antimicrobial susceptibility of anaerobic bacteria isolated from clinical specimens. Antimicrobial Agents and Chemotherapy, 1(2), pp.148-158.

McMurry, L., Petrucci, R.E. and Levy, S.B., 1980. Active efflux of tetracycline encoded by four genetically different tetracycline resistance determinants in Escherichia coli. *Proceedings of the national academy of sciences*, *77*(7), pp.3974-3977.

Mestres, J., Gregori-Puigjané, E., Valverde, S. and Solé, R.V., 2009. The topology of drug–target interaction networks: implicit dependence on drug properties and target families. *Molecular BioSystems*, *5*(9), pp.1051-1057.

Michiels, J. and Fauvart, M. eds., 2016. Bacterial persistence: Methods and protocols. Humana Press.

Michiels, J.E., Van den Bergh, B., Verstraeten, N., Fauvart, M. and Michiels, J., 2016. In vitro emergence of high persistence upon periodic aminoglycoside challenge in the ESKAPE pathogens. Antimicrobial agents and chemotherapy, 60(8), pp.4630-4637.

Mikkelsen, N.E., Brännvall, M., Virtanen, A. and Kirsebom, L.A., 1999. Inhibition of RNase P RNA cleavage by aminoglycosides. Proceedings of the National Academy of Sciences, 96(11), pp.6155-6160.

Mima, T., Joshi, S., Gomez-Escalada, M. and Schweizer, H.P., 2007. Identification and characterization of TriABC-OpmH, a triclosan efflux pump of Pseudomonas aeruginosa requiring two membrane fusion proteins. *Journal of bacteriology*, *189*(21), pp.7600-7609.

Minnock, A., Vernon, D.I., Schofield, J., Griffiths, J., Parish, J.H. and Brown, S.B., 1996. Photoinactivation of bacteria. Use of a cationic water-soluble zinc phthalocyanine to photoinactivate both gram-negative and gram-positive bacteria. *Journal of Photochemistry and Photobiology B: Biology*, *32*(3), pp.159-164.

Mitchell, G., Lafrance, M., Boulanger, S., Séguin, D.L., Guay, I., Gattuso, M., Marsault, É., Bouarab, K. and Malouin, F., 2012. Tomatidine acts in synergy with aminoglycoside antibiotics against multiresistant Staphylococcus aureus and prevents virulence gene expression. *Journal of antimicrobial chemotherapy*, *67*(3), pp.559-568.

Miyaue, S., Suzuki, E., Komiyama, Y., Kondo, Y., Morikawa, M. and Maeda, S., 2018. Bacterial memory of persisters: bacterial persister cells can retain their phenotype for days or weeks after withdrawal from colony–biofilm culture. Frontiers in microbiology, 9, p.1396.

Mlynek, K.D., Callahan, M.T., Shimkevitch, A.V., Farmer, J.T., Endres, J.L., Marchand, M., Bayles, K.W., Horswill, A.R. and Kaplan, J.B., 2016. Effects of low-dose amoxicillin on Staphylococcus aureus USA300 biofilms. Antimicrobial agents and chemotherapy, 60(5), pp.2639-2651.

Moan, J., Berg, K., Kvam, E., Western, A., Malik, Z., Rück, A. and Schneckenburger, H., 2007, September. Intracellular localization of photosensitizers. In Ciba Foundation Symposium 146-Photosensitizing Compounds: Their Chemistry, Biology and Clinical Use: Photosensitizing Compounds: Their Chemistry, Biology and Clinical Use: Ciba Foundation Symposium 146 (pp. 95-111). Chichester, UK: John Wiley & Sons, Ltd..

Moan, J. and Boye, E., 1981. Photodynamic effect on DNA and cell survival of human cells sensitized by hematoporphyrin. *Photobiochemistry and Photobiophysics*, *2*(4-5), pp.301-307.

Möker, N., Dean, C.R. and Tao, J., 2010. Pseudomonas aeruginosa increases formation of multidrug-tolerant persister cells in response to quorum-sensing signaling molecules. Journal of bacteriology, 192(7), pp.1946-1955.

Monack, D.M., Mueller, A. and Falkow, S., 2004. Persistent bacterial infections: the interface of the pathogen and the host immune system. Nature Reviews Microbiology, 2(9), pp.747-765.

Morita, Y., Tomida, J. and Kawamura, Y., 2012. MexXY multidrug efflux system of Pseudomonas aeruginosa. *Frontiers in microbiology*, *3*, p.408.

Morones-Ramirez, J.R., Winkler, J.A., Spina, C.S. and Collins, J.J., 2013. Silver enhances antibiotic activity against gram-negative bacteria. Science translational medicine, 5(190), pp.190ra81-190ra81.

Moyed, H.S. and Bertrand, K.P., 1983. hipA, a newly recognized gene of Escherichia coli K-12 that affects frequency of persistence after inhibition of murein synthesis. Journal of bacteriology, 155(2), pp.768-775.

Mroz, P., Huang, Y.Y., Szokalska, A., Zhiyentayev, T., Janjua, S., Nifli, A.P., Sherwood, M.E., Ruzié, C., Borbas, K.E., Fan, D. and Krayer, M., 2010. Stable synthetic bacteriochlorins overcome the resistance of melanoma to photodynamic therapy. The FASEB journal, 24(9), pp.3160-3170.

Mulcahy, L.R., Burns, J.L., Lory, S. and Lewis, K., 2010. Emergence of Pseudomonas aeruginosa strains producing high levels of persister cells in patients with cystic fibrosis. *Journal of bacteriology*, *192*(23), pp.6191-6199.

Munita, J.M. and Arias, C.A., 2016. Mechanisms of antibiotic resistance. *Virulence mechanisms of bacterial pathogens*, pp.481-511.

Munita, J.M., Mishra, N.N., Alvarez, D., Tran, T.T., Diaz, L., Panesso, D., Reyes, J., Murray, B.E., Adachi, J.A., Bayer, A.S. and Arias, C.A., 2014. Failure of high-dose daptomycin for bacteremia caused by daptomycin-susceptible Enterococcus faecium harboring LiaSR substitutions. *Clinical Infectious Diseases*, *59*(9), pp.1277-1280.

Munita, J.M., Tran, T.T., Diaz, L., Panesso, D., Reyes, J., Murray, B.E. and Arias, C.A., 2013. A liaF codon deletion abolishes daptomycin bactericidal activity against vancomycin-resistant Enterococcus faecalis. *Antimicrobial agents and chemotherapy*, *57*(6), pp.2831-2833.

Murphy, E., 1985. Nucleotide sequence of a spectinomycin adenyltransferase AAD (9) determinant from Staphylococcus aureus and its relationship to AAD (3 ″)(9). *Molecular and General Genetics MGG*, *200*(1), pp.33-39.

Nagata, J.Y., Hioka, N., Kimura, E., Batistela, V.R., Terada, R.S.S., Graciano, A.X., Baesso, M.L. and Hayacibara, M.F., 2012. Antibacterial photodynamic therapy for dental caries: evaluation of the photosensitizers used and light source properties. *Photodiagnosis and photodynamic therapy*, *9*(2), pp.122-131.

Nakonechny, F., Barel, M., David, A., Koretz, S., Litvak, B., Ragozin, E., Etinger, A., Livne, O., Pinhasi, Y., Gellerman, G. and Nisnevitch, M., 2019. Dark Antibacterial Activity of Rose Bengal. International journal of molecular sciences, 20(13), p.3196.

Neu, H.C., 1976. Tobramycin: an overview. *The journal of infectious diseases*, pp.S3-S19.

Nikaido, H., 2003. Molecular basis of bacterial outer membrane permeability revisited. *Microbiol. Mol. Biol. Rev.*, *67*(4), pp.593-656.

Niepa, T.H., Gilbert, J.L. and Ren, D., 2012. Controlling Pseudomonas aeruginosa persister cells by weak electrochemical currents and synergistic effects with tobramycin. Biomaterials, 33(30), pp.7356-7365.

Ni, S., Li, B., Chen, F., Wei, H., Mao, F., Liu, Y., Xu, Y., Qiu, X., Li, X., Liu, W. and Hu, L., 2018. Novel staphyloxanthin inhibitors with improved potency against multidrug resistant Staphylococcus aureus. *ACS medicinal chemistry letters*, *9*(3), pp.233-237.

Nitzan, Y. and Ashkenazi, H., 1999. Photoinactivation of Deinococcus radiodurans: an unusual Gram-positive microorganism. *Photochemistry and photobiology*, *69*(4), pp.505-510.

Nitzan, Y., Gutterman, M., Malik, Z. and Ehrenberg, B., 1992. Inactivation of gram-negative bacteria by photosensitized porphyrins. Photochemistry and photobiology, 55(1), pp.89-96.

Nitzan, Y., Wexler, H.M. and Finegold, S.M., 1994. Inactivation of anaerobic bacteria by various photosensitized porphyrins or by hemin. Current microbiology, 29(3), pp.125-131.

Nomura, A., Stemmermann, G.N., Chyou, P.H., Perez-Perez, G.I. and Blaser, M.J., 1994. Helicobacter pylori infection and the risk for duodenal and gastric ulceration. Annals of internal medicine, 120(12), pp.977-981.

Nostro, A., Cellini, L., Di Giulio, M., D'Arrigo, M., Marino, A., Blanco, A.R., Favaloro, A., Cutroneo, G. and Bisignano, G., 2012. Effect of alkaline pH on staphylococcal biofilm formation. *Apmis*, *120*(9), pp.733-742.

Nyman, E.S. and Hynninen, P.H., 2004. Research advances in the use of tetrapyrrolic photosensitizers for photodynamic therapy. *Journal of Photochemistry and Photobiology B: Biology*, *73*(1-2), pp.1-28.

O'Gara, J.P., 2007. ica and beyond: biofilm mechanisms and regulation in Staphylococcus epidermidis and Staphylococcus aureus. FEMS microbiology letters, 270(2), pp.179-188.

OhUigin, C., McConnell, D.J., Kelly, J.M. and van der Putten, W.J., 1987. Methylene blue photosensitised strand cleavage of DNA: effects of dye binding and oxygen. Nucleic acids research, 15(18), pp.7411-7427.

Okamoto, S. and Suzuki, Y., 1965. Chloramphenicol-, dihydrostreptomycin-and kanamycin-inactivating enzymes from multiple drug-resistant Escherichia coli carrying episome 'R'. *Nature*, *208*(5017), pp.1301-1303.

O'Neill, J., 2018. Tackling drug-resistant infections globally: Final report and recommendations. 2016. HM Government and Welcome Trust: UK.

Oppezzo, O.J. and Forte Giacobone, A.F., 2018. Lethal effect of photodynamic treatment on persister bacteria. *Photochemistry and photobiology*, *94*(1), pp.186-189.

Orman, M.A. and Brynildsen, M.P., 2016. Persister formation in Escherichia coli can be inhibited by treatment with nitric oxide. Free Radical Biology and Medicine, 93, pp.145-154.

Orman, M.A. and Brynildsen, M.P., 2013. Dormancy is not necessary or sufficient for bacterial persistence. Antimicrobial agents and chemotherapy, 57(7), pp.3230-3239.

Ormond, A.B. and Freeman, H.S., 2013. Dye sensitizers for photodynamic therapy. Materials, 6(3), pp.817-840.

O'Shea, R. and Moser, H.E., 2008. Physicochemical properties of antibacterial compounds: implications for drug discovery. *Journal of medicinal chemistry*, *51*(10), pp.2871-2878.

O'Toole, G.A. and Kolter, R., 1998. Flagellar and twitching motility are necessary for Pseudomonas aeruginosa biofilm development. Molecular microbiology, 30(2), pp.295-304.

O'Toole, G., Kaplan, H.B. and Kolter, R., 2000. Biofilm formation as microbial development. Annual Reviews in Microbiology, 54(1), pp.49-79.

Ounissi, H., Derlot, E., Carlier, C. and Courvalin, P., 1990. Gene homogeneity for aminoglycoside-modifying enzymes in gram-positive cocci. *Antimicrobial agents and chemotherapy*, *34*(11), pp.2164-2168.

Overgaard, M., Borch, J., Jørgensen, M.G. and Gerdes, K., 2008. Messenger RNA interferase RelE controls relBE transcription by conditional cooperativity. Molecular microbiology, 69(4), pp.841-857.

Page, R. and Peti, W., 2016. Toxin-antitoxin systems in bacterial growth arrest and persistence. *Nature chemical biology*, *12*(4), p.208.

Pandey, D.P. and Gerdes, K., 2005. Toxin–antitoxin loci are highly abundant in free-living but lost from host-associated prokaryotes. *Nucleic acids research*, *33*(3), pp.966-976.

Panzarini, E., Inguscio, V., Fimia, G.M. and Dini, L., 2014. Rose Bengal acetate photodynamic therapy (RBAc-PDT) induces exposure and release of damage-associated molecular patterns (DAMPs) in human HeLa cells. PloS one, 9(8), p.e105778.

Parasuraman, P., Anju, V.T., Lal, S.S., Sharan, A., Busi, S., Kaviyarasu, K., Arshad, M., Dawoud, T.M. and Syed, A., 2019. Synthesis and antimicrobial photodynamic effect of methylene blue conjugated carbon nanotubes on E. coli and S. aureus. Photochemical & Photobiological Sciences, 18(2), pp.563-576.

Parasuraman, P., R Y, T., Shaji, C., Sharan, A., Bahkali, A.H., Al-Harthi, H.F., Syed, A., Anju, V.T., Dyavaiah, M. and Siddhardha, B., 2020. Biogenic silver nanoparticles decorated with methylene blue potentiated the photodynamic inactivation of Pseudomonas aeruginosa and Staphylococcus aureus. *Pharmaceutics*, *12*(8), p.709.

Pedersen, K., Zavialov, A.V., Pavlov, M.Y., Elf, J., Gerdes, K. and Ehrenberg, M., 2003. The bacterial toxin RelE displays codon-specific cleavage of mRNAs in the ribosomal A site. *Cell*, *112*(1), pp.131-140.

Peng, B., Su, Y.B., Li, H., Han, Y., Guo, C., Tian, Y.M. and Peng, X.X., 2015. Exogenous alanine and/or glucose plus kanamycin kills antibiotic-resistant bacteria. Cell metabolism, 21(2), pp.249-262.

Pereira, N.M., Feitosa, L.S., Navarro, R.S., Kozusny-Andreani, D.I. and Carvalho, N.M.P., 2018. Use of photodynamic inactivation for in vitro reduction of prevalent bacteria in Fournier's Gangrene. International braz j urol, 44(1), pp.150-155.

Piddock, L.J., 2006. Clinically relevant chromosomally encoded multidrug resistance efflux pumps in bacteria. *Clinical microbiology reviews*, *19*(2), pp.382-402.

Pimentel, M., Saad, R.J., Long, M.D. and Rao, S.S., 2020. ACG Clinical Guideline: Small Intestinal Bacterial Overgrowth. American Journal of Gastroenterology, 115(2), pp.165-178.

Pinto, J.G., de Souza Martins, J.F., Pereira, A.H.C., Mittmann, J., Raniero, L.J. and Ferreira-Strixino, J., 2017. Evaluation of methylene blue as photosensitizer in promastigotes of Leishmania major and Leishmania braziliensis. Photodiagnosis and photodynamic therapy, 18, pp.325-330.

Plenagl, N., Seitz, B.S., Duse, L., Pinnapireddy, S.R., Jedelska, J., Brüßler, J. and Bakowsky, U., 2019. Hypericin inclusion complexes encapsulated in liposomes for antimicrobial photodynamic therapy. International journal of pharmaceutics, 570, p.118666.

Poole, K., 2005. Aminoglycoside resistance in Pseudomonas aeruginosa. *Antimicrobial agents and Chemotherapy*, *49*(2), pp.479-487.

Poole, K., 2005. Efflux-mediated antimicrobial resistance. *Journal of Antimicrobial Chemotherapy*, *56*(1), pp.20-51.

Prajapati, J.D., Kleinekathöfer, U. and Winterhalter, M., 2021. How to enter a bacterium: bacterial porins and the permeation of antibiotics. *Chemical Reviews*, *121*(9), pp.5158-5192.

Proctor, R.A., Von Eiff, C., Kahl, B.C., Becker, K., McNamara, P., Herrmann, M. and Peters, G., 2006. Small colony variants: a pathogenic form of bacteria that facilitates persistent and recurrent infections. Nature Reviews Microbiology, 4(4), pp.295-305.

Pushpan, S.K., Venkatraman, S., Anand, V.G., Sankar, J., Parmeswaran, D., Ganesan, S. and Chandrashekar, T.K., 2002. Porphyrins in photodynamic therapy-a search for ideal photosensitizers. Current Medicinal Chemistry-Anti-Cancer Agents, 2(2), pp.187-207.

Quinn, J.P., Dudek, E.J., DiVincenzo, C.A., Lucks, D.A. and Lerner, S.A., 1986. Emergence of resistance to imipenem during therapy for Pseudomonas aeruginosa infections. *Journal of Infectious Diseases*, *154*(2), pp.289-294.

Quiocho, F.A., 1986. Carbohydrate-binding proteins: tertiary structures and protein-sugar interactions. *Annual review of biochemistry*, *55*, pp.287-315.

Ramaiah, D., Eckert, I., Arun, K.T., Weidenfeller, L. and Epe, B., 2004. Squaraine Dyes for Photodynamic Therapy: Mechanism of Cytotoxicity and DNA Damage Induced by Halogenated Squaraine Dyes Plus Light (> 600 nm)¶. Photochemistry and photobiology, 79(1), pp.99-104.

Ramirez, M.S. and Tolmasky, M.E., 2010. Aminoglycoside modifying enzymes. Drug Resistance Updates, 13(6), pp.151-171

Ramsey, B.W., Pepe, M.S., Quan, J.M., Otto, K.L., Montgomery, A.B., Williams-Warren, J., Vasiljev-K, M., Borowitz, D., Bowman, C.M., Marshall, B.C. and Marshall, S., 1999. Intermittent administration of inhaled tobramycin in patients with cystic fibrosis. *New England Journal of Medicine*, *340*(1), pp.23-30.

Ranieri, M.R., Whitchurch, C.B. and Burrows, L.L., 2018. Mechanisms of biofilm stimulation by subinhibitory concentrations of antimicrobials. Current opinion in microbiology, 45, pp.164-169.

Ren, H., He, X., Zou, X., Wang, G., Li, S. and Wu, Y., 2015. Gradual increase in antibiotic concentration affects persistence of Klebsiella pneumoniae. *Journal of Antimicrobial Chemotherapy*, *70*(12), pp.3267-3272.

Renwick, M.J., Simpkin, V., Mossialos, E. and World Health Organization, 2016. *Targeting innovation in antibiotic drug discovery and development: The need for a One Health–One Europe–One World Framework*. World Health Organization. Regional Office for Europe.

Review on Antimicrobial Resistance, 2014. Antimicrobial Resistance: Tackling a crisis for the health and wealth of nations. Review on Antimicrobial Resistance.

Ribeiro, A.P.D., Andrade, M.C., Bagnato, V.S., Vergani, C.E., Primo, F.L., Tedesco, A.C. and Pavarina, A.C., 2015. Antimicrobial photodynamic therapy against pathogenic bacterial suspensions and biofilms using chloro-aluminum phthalocyanine encapsulated in nanoemulsions. *Lasers in medical science*, *30*(2), pp.549-559.

Richter, P., Krüger, M., Prasad, B., Gastiger, S., Bodenschatz, M., Wieder, F., Burkovski, A., Geißdörfer, W., Lebert, M. and Strauch, S.M., 2019. Using colistin as a trojan horse: Inactivation of Gram-negative bacteria with chlorophyllin. Antibiotics, 8(4), p.158.

Rodríguez-Cerdeira, C., Martínez-Herrera, E., Fabbrocini, G., Sanchez-Blanco, B., López-Barcenas, A., El-Samahy, M., Juárez-Durán, E.R. and González-Cespón, J.L., 2021. New Applications of Photodynamic Therapy in the Management of Candidiasis. *Journal of Fungi*, *7*(12), p.1025.

Roelandts, R., 2002. The history of phototherapy: something new under the sun?. Journal of the American Academy of Dermatology, 46(6), pp.926-930.

Romero, D., Aguilar, C., Losick, R. and Kolter, R., 2010. Amyloid fibers provide structural integrity to Bacillus subtilis biofilms. Proceedings of the National Academy of Sciences, 107(5), pp.2230-2234.

Rosenberg, E.Y., Ma, D. and Nikaido, H., 2000. AcrD of Escherichia coli is an aminoglycoside efflux pump. *Journal of bacteriology*, *182*(6), pp.1754-1756.

Rotem, E., Loinger, A., Ronin, I., Levin-Reisman, I., Gabay, C., Shoresh, N., Biham, O. and Balaban, N.Q., 2010. Regulation of phenotypic variability by a threshold-based mechanism underlies bacterial persistence. Proceedings of the National Academy of Sciences, 107(28), pp.12541-12546.

Saavedra, R., Rocha, L.B., Dąbrowski, J.M. and Arnaut, L.G., 2014. Modulation of biodistribution, pharmacokinetics, and photosensitivity with the delivery vehicle of a bacteriochlorin photosensitizer for photodynamic therapy. ChemMedChem, 9(2), pp.390-398.

Sabeti Azad, M., Okuda, M., Cyrenne, M., Bourge, M., Heck, M.P., Yoshizawa, S. and Fourmy, D., 2020. Fluorescent aminoglycoside antibiotics and methods for accurately monitoring uptake by bacteria. ACS Infectious Diseases.

Sader, H.S., Rhomberg, P.R., Farrell, D.J. and Jones, R.N., 2015. Arbekacin activity against contemporary clinical bacteria isolated from patients hospitalized with pneumonia. Antimicrobial agents and chemotherapy, 59(6), pp.3263-3270.

Salauze, D. and Davies, J., 1990. Mécanismes moléculaires de la bactéridie: aminosides. Bactéricidie. Maloine, Paris, France, pp.23-34.

Salvatore, S., Salvatore, S., Cattoni, E., Siesto, G., Serati, M., Sorice, P. and Torella, M., 2011. Urinary tract infections in women. European journal of obstetrics & gynecology and reproductive biology, 156(2), pp.131-136.

Satoskar, R.R., Shah, S.J. and Shenoy, S.G., 1986. Evaluation of anti-inflammatory property of curcumin (diferuloyl methane) in patients with postoperative inflammation. International journal of clinical pharmacology, therapy, and toxicology, 24(12), pp.651-654.

Sawicki, G.S., Signorovitch, J.E., Zhang, J., Latremouille-Viau, D., von Wartburg, M., Wu, E.Q. and Shi, L., 2012. Reduced mortality in cystic fibrosis patients treated with tobramycin inhalation solution. *Pediatric pulmonology*, *47*(1), pp.44-52.

Schumacher, M.A., Balani, P., Min, J., Chinnam, N.B., Hansen, S., Vulić, M., Lewis, K. and Brennan, R.G., 2015. HipBA–promoter structures reveal the basis of heritable multidrug tolerance. Nature, 524(7563), pp.59-64.

Schureck, M.A., Maehigashi, T., Miles, S.J., Marquez, J., Cho, S.E., Erdman, R. and Dunham, C.M., 2014. Structure of the Proteus vulgaris HigB-(HigA) 2-HigB toxin-antitoxin complex. Journal of Biological Chemistry, 289(2), pp.1060-1070.

Segado, M. and Reguero, M., 2011. Mechanism of the photochemical process of singlet oxygen production by phenalenone. Physical Chemistry Chemical Physics, 13(9), pp.4138-4148.

Serio, A.W., Keepers, T., Andrews, L. and Krause, K.M., 2018. Aminoglycoside Revival: Review of a Historically Important Class of Antimicrobials Undergoing Rejuvenation. EcoSal Plus, 8(1).

Shafeekh, K.M., Soumya, M.S., Rahim, M.A., Abraham, A. and Das, S., 2014. Synthesis and Characterization of Near-Infrared Absorbing Water Soluble Squaraines and Study of their Photodynamic Effects in DLA Live Cells. Photochemistry and photobiology, 90(3), pp.585-595.

Shah, D., Zhang, Z., Khodursky, A.B., Kaldalu, N., Kurg, K. and Lewis, K., 2006. Persisters: a distinct physiological state of E. coli. BMC microbiology, 6(1), p.53.

Shan, Y., Lazinski, D., Rowe, S., Camilli, A. and Lewis, K., 2015. Genetic basis of persister tolerance to aminoglycosides in Escherichia coli. MBio, 6(2), pp.e00078-15.

Shaw, K.J., Rather, P.N., Hare, R.S. and Miller, G.H., 1993. Molecular genetics of aminoglycoside resistance genes and familial relationships of the aminoglycoside-modifying enzymes. *Microbiology and Molecular Biology Reviews*, *57*(1), pp.138-163.

Shteinberg, M. and Elborn, J.S., 2015. Use of inhaled tobramycin in cystic fibrosis. Advances in therapy, 32(1), pp.1-9.

Singh, R., Ray, P., Das, A. and Sharma, M., 2010. Penetration of antibiotics through Staphylococcus aureus and Staphylococcus epidermidis biofilms. Journal of antimicrobial chemotherapy, 65(9), pp.1955-1958.

Sorlozano, A., Jimenez-Pacheco, A., del Castillo, J.D.D.L., Sampedro, A., Martinez-Brocal, A., Miranda-Casas, C., Navarro-Marí, J.M. and Gutiérrez-Fernández, J., 2014. Evolution of the resistance to antibiotics of bacteria involved in urinary tract infections: a 7-year surveillance study. American journal of infection control, 42(10), pp.1033-1038.

Soupene, E., Van Heeswijk, W.C., Plumbridge, J., Stewart, V., Bertenthal, D., Lee, H., Prasad, G., Paliy, O., Charernnoppakul, P. and Kustu, S., 2003. Physiological studies of Escherichia coli strain MG1655: growth defects and apparent cross-regulation of gene expression. *Journal of bacteriology*, *185*(18), pp.5611-5626.

F Sperandio, F., Huang, Y.Y. and R Hamblin, M., 2013. Antimicrobial photodynamic therapy to kill Gram-negative bacteria. *Recent patents on anti-infective drug discovery*, *8*(2), pp.108-120.

Starkey, M., Lepine, F., Maura, D., Bandyopadhaya, A., Lesic, B., He, J., Kitao, T., Righi, V., Milot, S., Tzika, A. and Rahme, L., 2014. Identification of anti-virulence compounds that disrupt quorum-sensing regulated acute and persistent pathogenicity. PLoS pathogens, 10(8).

Stewart, P.S. and Costerton, J.W., 2001. Antibiotic resistance of bacteria in biofilms. The lancet, 358(9276), pp.135-138.

Stewart, P.S., Davison, W.M. and Steenbergen, J.N., 2009. Daptomycin rapidly penetrates a Staphylococcus epidermidis biofilm. Antimicrobial agents and chemotherapy, 53(8), pp.3505-3507.

Stewart, P.S., Davison, W.M. and Steenbergen, J.N., 2009. Daptomycin rapidly penetrates a Staphylococcus epidermidis biofilm. Antimicrobial agents and chemotherapy, 53(8), pp.3505-3507.

Straight, R.C. and Spikes, J.D., 1985. Photosensitized oxidation of biomolecules. Singlet O2, 4(91), p.143.

Stratton, C.W., 2005. Molecular mechanisms of action for antimicrobial agents: general principles and mechanisms for selected classes of antibiotics. Antibiotics in laboratory medicine, pp.547-549.

Su, Y.B., Peng, B., Li, H., Cheng, Z.X., Zhang, T.T., Zhu, J.X., Li, D., Li, M.Y., Ye, J.Z., Du, C.C. and Zhang, S., 2018. Pyruvate cycle increases aminoglycoside efficacy and provides respiratory energy in bacteria. Proceedings of the National Academy of Sciences, 115(7), pp.E1578-E1587.

Sultana, S.T., Call, D.R. and Beyenal, H., 2016. Eradication of Pseudomonas aeruginosa biofilms and persister cells using an electrochemical scaffold and enhanced antibiotic susceptibility. NPJ biofilms and microbiomes, 2(1), pp.1-8.Hu, Y., Shamaei-Tousi, A., Liu, Y. and Coates, A., 2010. A new approach for the discovery of antibiotics by targeting non-multiplying bacteria: a novel topical antibiotic for staphylococcal infections. PLoS One, 5(7).

Sulavik, M.C., Houseweart, C., Cramer, C., Jiwani, N., Murgolo, N., Greene, J., DiDomenico, B., Shaw, K.J., Miller, G.H., Hare, R. and Shimer, G., 2001. Antibiotic susceptibility profiles of Escherichia coli strains lacking multidrug efflux pump genes. *Antimicrobial agents and chemotherapy*, *45*(4), pp.1126-1136.

Sun, H., Yang, Y., Xue, T. and Sun, B., 2013. Modulation of cell wall synthesis and susceptibility to vancomycin by the two-component system AirSR in Staphylococcus aureus NCTC8325. *BMC microbiology*, *13*(1), pp.1-10.

Sun, X., Wang, L., Lynch, C.D., Sun, X., Li, X., Qi, M., Ma, C., Li, C., Dong, B., Zhou, Y. and Xu, H.H., 2019. Nanoparticles having amphiphilic silane containing Chlorin e6 with strong anti-biofilm activity against periodontitis-related pathogens. Journal of dentistry, 81, pp.70-84.

Taber, H.W., Mueller, J.P., Miller, P.F. and Arrow, A.S., 1987. Bacterial uptake of aminoglycoside antibiotics. Microbiological reviews, 51(4), p.439.

Tamber, S. and Hancock, R.E., 2003. On the mechanism of solute uptake in Pseudomonas. *Frontiers in Bioscience-Landmark*, *8*(6), pp.472-483.

Taylor, S.D. and Palmer, M., 2016. The action mechanism of daptomycin. *Bioorganic & medicinal chemistry*, *24*(24), pp.6253-6268.

Thomas, C.M. and Nielsen, K.M., 2005. Mechanisms of, and barriers to, horizontal gene transfer between bacteria. *Nature reviews microbiology*, *3*(9), p.711.

Tichaczek-Goska, D., Wojnicz, D., Symonowicz, K., Ziółkowski, P. and Hendrich, A.B., 2019. Photodynamic enhancement of the activity of antibiotics used in urinary tract infections. Lasers in medical science, pp.1-7.

Tielker, D., Hacker, S., Loris, R., Strathmann, M., Wingender, J., Wilhelm, S., Rosenau, F. and Jaeger, K.E., 2005. Pseudomonas aeruginosa lectin LecB is located in the outer membrane and is involved in biofilm formation. Microbiology, 151(5), pp.1313-1323.

To, W.P., Zou, T., Sun, R.W.Y. and Che, C.M., 2013. Light-induced catalytic and cytotoxic properties of phosphorescent transition metal compounds with a d8 electronic configuration. Philosophical Transactions of the Royal Society A: Mathematical, Physical and Engineering Sciences, 371(1995), p.20120126.

Tré-Hardy, M., Nagant, C., El Manssouri, N., Vanderbist, F., Traore, H., Vaneechoutte, M. and Dehaye, J.P., 2010. Efficacy of the Combination of Tobramycin and a Macrolide in an I n V itro Pseudomonas aeruginosa Mature Biofilm Model. *Antimicrobial agents and chemotherapy*, *54*(10), pp.4409-4415.

Tseng, S.P., Hung, W.C., Chen, H.J., Lin, Y.T., Jiang, H.S., Chiu, H.C., Hsueh, P.R., Teng, L.J. and Tsai, J.C., 2017. Effects of toluidine blue O (TBO)-photodynamic inactivation on community-associated methicillin-resistant Staphylococcus aureus isolates. Journal of Microbiology, Immunology and Infection, 50(1), pp.46-54.

Uppu, D.S., Konai, M.M., Sarkar, P., Samaddar, S., Fensterseifer, I.C., Farias-Junior, C., Krishnamoorthy, P., Shome, B.R., Franco, O.L. and Haldar, J., 2017. Membrane-active macromolecules kill antibiotic-tolerant bacteria and potentiate antibiotics towards Gram-negative bacteria. PLoS One, 12(8).

Usuda, J., Kato, H., Okunaka, T., Furukawa, K., Tsutsui, H., Yamada, K., Suga, Y., Honda, H., Nagatsuka, Y., Ohira, T. and Tsuboi, M., 2006. Photodynamic therapy (PDT) for lung cancers. Journal of Thoracic Oncology, 1(5), pp.489-493.

Usuda, J., Kato, H., Okunaka, T., Furukawa, K., Honda, H., Suga, Y., Hirata, T., Ohira, T., Tsuboi, M. and Hirano, T., 2006. Photodynamic therapy using Laserphyrin for centrally located early stage lung cancer. Journal of Clinical Oncology, 24(18_suppl), pp.7229-7229.

Vaca, C.E., Wilhelm, J. and Harms-Ringdahl, M., 1988. Interaction of lipid peroxidation products with DNA. A review. Mutation Research/Reviews in Genetic Toxicology, 195(2), pp.137-149.

Valduga, G., Bertoloni, G., Reddi, E. and Jori, G., 1993. Effect of extracellularly generated singlet oxygen on Gram-positive and Gram-negative bacteria. Journal of Photochemistry and Photobiology B: Biology, 21(1), pp.81-86.

Vallet, I., Olson, J.W., Lory, S., Lazdunski, A. and Filloux, A., 2001. The chaperone/usher pathways of Pseudomonas aeruginosa: identification of fimbrial gene clusters (cup) and their involvement in biofilm formation. Proceedings of the National Academy of Sciences, 98(12), pp.6911-6916.

van der Lee, R., Lang, B., Kruse, K., Gsponer, J., de Groot, N.S., Huynen, M.A., Matouschek, A., Fuxreiter, M. and Babu, M.M., 2014. Intrinsically disordered segments affect protein half-life in the cell and during evolution. Cell reports, 8(6), pp.1832-1844.

Vega, N.M., Allison, K.R., Khalil, A.S. and Collins, J.J., 2012. Signaling-mediated bacterial persister formation. Nature chemical biology, 8(5), pp.431-433.

Ventola, C.L., 2015. The antibiotic resistance crisis: part 1: causes and threats. Pharmacy and therapeutics, 40(4), p.277.

Verstraeten, N., Knapen, W., Fauvart, M. and Michiels, J., 2016. A historical perspective on bacterial persistence. In Bacterial Persistence (pp. 3-13). Humana Press, New York, NY.

Verstraeten, N., Knapen, W.J., Kint, C.I., Liebens, V., Van den Bergh, B., Dewachter, L., Michiels, J.E., Fu, Q., David, C.C., Fierro, A.C. and Marchal, K., 2015. Obg and membrane depolarization are part of a microbial bet-hedging strategy that leads to antibiotic tolerance. Molecular cell, 59(1), pp.9-21.

Wachino, J.I. and Arakawa, Y., 2012. Exogenously acquired 16S rRNA methyltransferases found in aminoglycoside-resistant pathogenic Gram-negative bacteria: an update. *Drug Resistance Updates*, *15*(3), pp.133-148.

Wachino, J.I., Shibayama, K., Kurokawa, H., Kimura, K., Yamane, K., Suzuki, S., Shibata, N., Ike, Y. and Arakawa, Y., 2007. Novel plasmid-mediated 16S rRNA m1A1408 methyltransferase, NpmA, found in a clinically isolated Escherichia coli strain resistant to

structurally diverse aminoglycosides. *Antimicrobial agents and chemotherapy*, *51*(12), pp.4401-4409.

Wagner, A., Denzer, U.W., Neureiter, D., Kiesslich, T., Puespoeck, A., Rauws, E.A., Emmanuel, K., Degenhardt, N., Frick, U., Beuers, U. and Lohse, A.W., 2015. Temoporfin improves efficacy of photodynamic therapy in advanced biliary tract carcinoma: A multicenter prospective phase II study. Hepatology, 62(5), pp.1456-1465.

Wainwright, M. and Crossley, K.B., 2002. Methylene blue-a therapeutic dye for all seasons?. Journal of chemotherapy, 14(5), pp.431-443.

Wainwright, M., Maisch, T., Nonell, S., Plaetzer, K., Almeida, A., Tegos, G.P. and Hamblin, M.R., 2017. Photoantimicrobials—are we afraid of the light?. *The Lancet Infectious Diseases*, *17*(2), pp.e49-e55.

Waksman, S.A. and Lechevalier, H.A., 1949. Neomycin, a new antibiotic active against streptomycin-resistant bacteria, including tuberculosis organisms. Science, 109(2830), pp.305-307.

Walters III, M.C., Roe, F., Bugnicourt, A., Franklin, M.J. and Stewart, P.S., 2003. Contributions of antibiotic penetration, oxygen limitation, and low metabolic activity to tolerance of Pseudomonas aeruginosa biofilms to ciprofloxacin and tobramycin. *Antimicrobial agents and chemotherapy*, *47*(1), pp.317-323.

Wang, X., Song, Y., Pan, G., Han, W., Wang, B., Cui, L., Ma, H., An, Z., Xie, Z., Xu, B. and Tian, W., 2020. Exploiting radical-pair intersystem crossing for maximizing singlet oxygen quantum yields in pure organic fluorescent photosensitizers. *Chemical science*, *11*(40), pp.10921-10927.

Wang, Y.Y., Ryu, A.R., Jin, S., Jeon, Y.M. and Lee, M.Y., 2017. Chlorin e6-mediated photodynamic therapy suppresses P. acnes-induced inflammatory response via NFκB and MAPKs signaling pathway. PLoS One, 12(1), p.e0170599.

Waters, E.M., Rowe, S.E., O'Gara, J.P. and Conlon, B.P., 2016. Convergence of Staphylococcus aureus persister and biofilm research: can biofilms be defined as communities of adherent persister cells?. PLoS pathogens, 12(12).

Weisblum, B., 1995. Erythromycin resistance by ribosome modification. *Antimicrobial agents and chemotherapy*, *39*(3), p.577.

Wexselblatt, E., Oppenheimer-Shaanan, Y., Kaspy, I., London, N., Schueler-Furman, O., Yavin, E., Glaser, G., Katzhendler, J. and Ben-Yehuda, S., 2012. Relacin, a novel antibacterial agent targeting the stringent response. PLoS pathogens, 8(9).

Whitchurch, C.B., Tolker-Nielsen, T., Ragas, P.C. and Mattick, J.S., 2002. Extracellular DNA required for bacterial biofilm formation. Science, 295(5559), pp.1487-1487.

Wiehlmann, L., Wagner, G., Cramer, N., Siebert, B., Gudowius, P., Morales, G., Köhler, T., Van Delden, C., Weinel, C., Slickers, P. and Tümmler, B., 2007. Population structure of Pseudomonas aeruginosa. *Proceedings of the national academy of sciences*, *104*(19), pp.8101-8106.

Wilson, B.C. and Patterson, M.S., 2008. The physics, biophysics and technology of photodynamic therapy. *Physics in Medicine & Biology*, *53*(9), p.R61.

Wilson, D.N., 2014. Ribosome-targeting antibiotics and mechanisms of bacterial resistance. Nature Reviews Microbiology, 12(1), pp.35-48.

Winkler, K., Simon, C., Finke, M., Bleses, K., Birke, M., Szentmáry, N., Hüttenberger, D., Eppig, T., Stachon, T., Langenbucher, A. and Foth, H.J., 2016. Photodynamic inactivation of multidrug-resistant Staphylococcus aureus by chlorin e6 and red light (λ= 670 nm). Journal of Photochemistry and Photobiology B: Biology, 162, pp.340-347.

Wiuff, C., Zappala, R.M., Regoes, R.R., Garner, K.N., Baquero, F. and Levin, B.R., 2005. Phenotypic tolerance: antibiotic enrichment of noninherited resistance in bacterial populations. Antimicrobial agents and chemotherapy, 49(4), pp.1483-1494.

Woodruff, H.B., 2014. Selman A. Waksman, winner of the 1952 Nobel Prize for physiology or medicine. Appl. Environ. Microbiol., 80(1), pp.2-8.

World Health Organization, 2014. Antimicrobial resistance global report on surveillance: 2014 summary (No. WHO/HSE/PED/AIP/2014.2). World Health Organization.

Wotherspoon, A.C., Ortiz-Hidalgo, C., Falzon, M.R. and Isaacson, P.G., 1991. Helicobacter pylori-associated gastritis and primary B-cell gastric lymphoma. The Lancet, 338(8776), pp.1175-1176.

Wozniak, D.J., Wyckoff, T.J., Starkey, M., Keyser, R., Azadi, P., O'Toole, G.A. and Parsek, M.R., 2003. Alginate is not a significant component of the extracellular polysaccharide matrix of PA14 and PAO1 Pseudomonas aeruginosa biofilms. Proceedings of the National Academy of Sciences, 100(13), pp.7907-7912.

Wray, R., Iscla, I., Gao, Y., Li, H., Wang, J. and Blount, P., 2016. Dihydrostreptomycin directly binds to, modulates, and passes through the MscL channel pore. *PLoS biology*, *14*(6), p.e1002473.

Wright, K.J., Seed, P.C. and Hultgren, S.J., 2007. Development of intracellular bacterial communities of uropathogenic Escherichia coli depends on type 1 pili. Cellular microbiology, 9(9), pp.2230-2241.

Wu, J., Mou, H., Xue, C., Leung, A.W., Xu, C. and Tang, Q.J., 2016. Photodynamic effect of curcumin on Vibrio parahaemolyticus. Photodiagnosis and photodynamic therapy, 15, pp.34-39.

Wu, M.F., Deichelbohrer, M., Tschernig, T., Laschke, M.W., Szentmáry, N., Hüttenberger, D., Foth, H.J., Seitz, B. and Bischoff, M., 2017. Chlorin e6 mediated photodynamic inactivation for multidrug resistant Pseudomonas aeruginosa keratitis in mice in vivo. Scientific reports, 7, p.44537.

Wu, Y., Vulić, M., Keren, I. and Lewis, K., 2012. Role of oxidative stress in persister tolerance. Antimicrobial agents and chemotherapy, 56(9), pp.4922-4926.

Yamaguchi, Y. and Inouye, M., 2011. Regulation of growth and death in Escherichia coli by toxin–antitoxin systems. Nature Reviews Microbiology, 9(11), pp.779-790.

Yang, G., Trylska, J., Tor, Y. and McCammon, J.A., 2006. Binding of aminoglycosidic antibiotics to the oligonucleotide A-site model and 30S ribosomal subunit: Poisson− Boltzmann model, thermal denaturation, and fluorescence studies. *Journal of medicinal chemistry*, *49*(18), pp.5478-5490.

Yokoyama, K., Doi, Y., Yamane, K., Kurokawa, H., Shibata, N., Shibayama, K., Yagi, T., Kato, H. and Arakawa, Y., 2003. Acquisition of 16S rRNA methylase gene in Pseudomonas aeruginosa. *The lancet*, *362*(9399), pp.1888-1893.

Xie, J., Talaska, A.E. and Schacht, J., 2011. New developments in aminoglycoside therapy and ototoxicity. Hearing research, 281(1-2), pp.28-37.

Yin, R. and R Hamblin, M., 2015. Antimicrobial photosensitizers: drug discovery under the spotlight. Current medicinal chemistry, 22(18), pp.2159-2185.

Zanin, I.C.J., Goncalves, R.B., Junior, A.B., Hope, C.K. and Pratten, J., 2005. Susceptibility of Streptococcus mutans biofilms to photodynamic therapy: an in vitro study. *Journal of antimicrobial chemotherapy*, *56*(2), pp.324-330.

Zapotoczna, M., McCarthy, H., Rudkin, J.K., O'Gara, J.P. and O'Neill, E., 2015. An essential role for coagulase in Staphylococcus aureus biofilm development reveals new therapeutic possibilities for device-related infections. The Journal of infectious diseases, 212(12), pp.1883-1893.

Zhang, Y., Yew, W.W. and Barer, M.R., 2012. Targeting persisters for tuberculosis control. *Antimicrobial agents and chemotherapy*, *56*(5), pp.2223-2230.

Zhao, X. and Drlica, K., 2014. Reactive oxygen species and the bacterial response to lethal stress. Current opinion in microbiology, 21, pp.1-6.

Zhao, Y., Lv, B., Sun, F., Liu, J., Wang, Y., Gao, Y., Qi, F., Chang, Z. and Fu, X., 2020. Rapid Freezing Enables Aminoglycosides To Eradicate Bacterial Persisters via Enhancing Mechanosensitive Channel MscL-Mediated Antibiotic Uptake. Mbio, 11(1).

Zheng, Z. and Stewart, P.S., 2002. Penetration of rifampin through Staphylococcus epidermidis biofilms. Antimicrobial agents and chemotherapy, 46(3), pp.900-903.

Zimcik, P. and Miletin, M., 2008. Photodynamic therapy. Dyes and pigments: new research, pp.1-62.

Zug, K.A., Warshaw, E.M., Fowler Jr, J.F., Maibach, H.I., Belsito, D.L., Pratt, M.D., Sasseville, D., Storrs, F.J., Taylor, J.S., Mathias, T.C. and DeLeo, V.A., 2009. Patch-test results of the North American contact dermatitis group 2005-2006. Dermatitis, 20(3), pp.149-160.